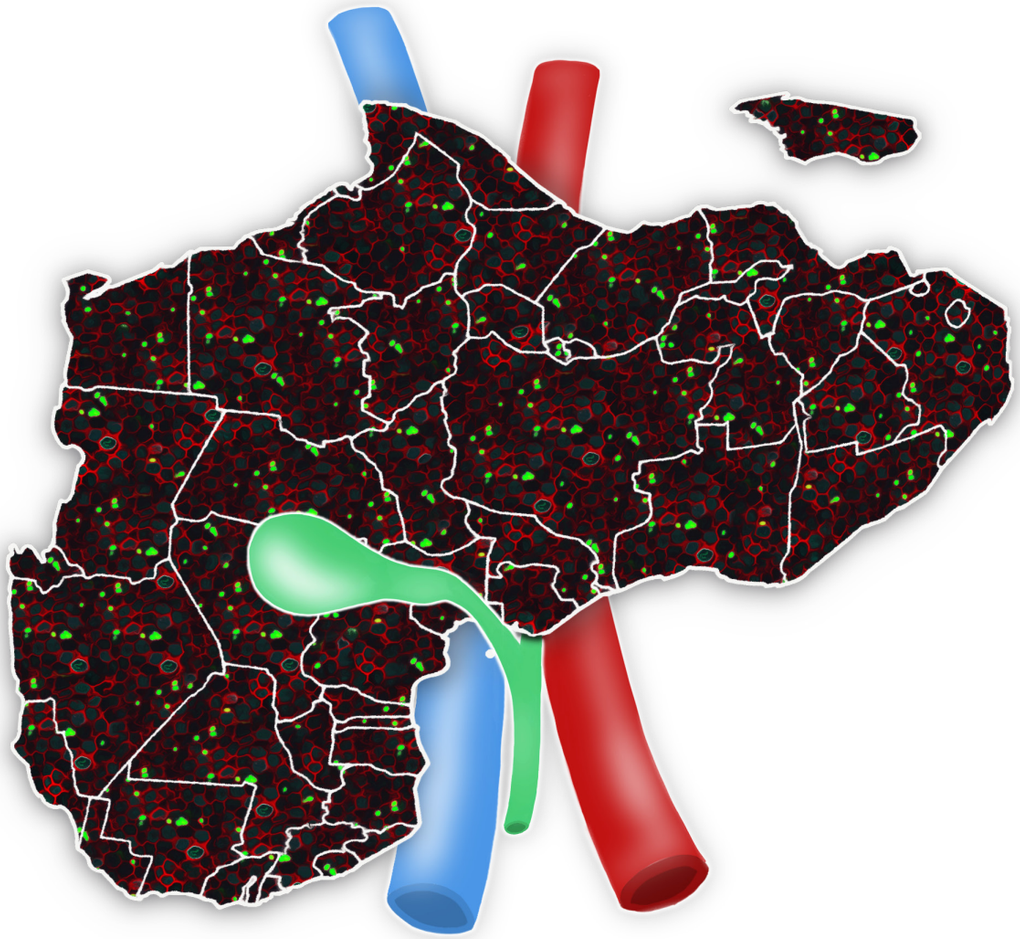

Edna Filipa Pais Soares

β-GLUCAN-BASED ADJUVANTS FOR HEPATITIS B VACCINATION: PARTICULATE DESIGN FOR PROPHYLACTIC AND THERAPEUTIC NEEDS

Tese de doutoramento em Ciências Farmacêuticas, ramo de Tecnologia Farmacêutica, orientada por Professora Doutora Olga Maria Fernandes Borges Ribeiro e por Doutor Henrique Manuel dos Santos Faneca e apresentada à Faculdade de Farmácia da Universidade de Coimbra

Março/2018

· U C ·

Universidade de Coimbra

Front Cover Image

The image represents the hepatitis B current needs combined with the possible solution found in the present thesis. The shape of the African continent was used both as a representation of developing countries and also because of its resemblance to the shape of a liver, in the perspective presented. The shape of Africa was filled with a laser scanning confocal microscopy image of the β-glucan particles produced in this thesis (GPs, in green) following uptake by RAW 264.7 murine macrophages (cell membrane in red and cell nucleus in blue).

Imagem da Capa

A imagem representa uma combinação das necessidades da hepatite B com uma possível solução encontrada na presente tese. A forma do continente Africano foi usada tanto como uma representação dos países em vias de desenvolvimento como por se assemelhar com a forma de um fígado, na perspetiva apresentada. A forma de África foi preenchida com uma imagem de microscopia confocal de varrimento a laser de partículas de β-glucano produzidas nesta tese (GPs, a verde) após internalização na linha de macrófagos de murganhos RAW 264.7 (membrana celular a vermelho e núcleo a azul).

Edna Filipa Pais Soares

β-GLUCAN-BASED ADJUVANTS FOR HEPATITIS B VACCINATION: PARTICULATE DESIGN FOR PROPHYLACTIC AND THERAPEUTIC NEEDS

ADJUVANTES À BASE DE β-GLUCANO APLICADOS À VACINAÇÃO CONTRA A HEPATITE B: DESENHO DE FORMAS PARTICULADAS PARA SUPRIR AS NECESSIDADES PROFILÁTICAS E TERAPÊUTICAS

Candidature thesis for doctoral degree in Pharmaceutical Sciences, branch of Pharmaceutical Technology, submitted to the Faculty of Pharmacy of the University of Coimbra

Tese de candidatura ao grau de doutor em Ciências Farmacêuticas, ramo de Tecnologia Farmacêutica, apresentada à Faculdade de Farmácia da Universidade de Coimbra

• U C •

FFUC FACULDADE DE FARMÁCIA
UNIVERSIDADE DE COIMBRA

The research work presented in this thesis was performed at the Laboratory of Pharmaceutical Technology, Faculty of Pharmacy, University of Coimbra and at the Center for Neuroscience and Cell Biology, University of Coimbra, under the scientific supervision of Professora Olga Maria Fernandes Borges Ribeiro and co-supervision of Doutor Henrique Manuel dos Santos Faneca and at the Laboratory of Gastroenterology and Hepatology, Erasmus University Medical Center of Rotterdam, under the scientific supervision of Professor André Boonstra.

O trabalho de investigação apresentado nesta tese foi efetuado no Laboratório de Tecnologia Farmacêutica da Faculdade de Farmácia da Universidade de Coimbra, sob a orientação científica da Professora Doutora Olga Maria Fernandes Borges Ribeiro e co-orientação do Doutor Henrique Manuel dos Santos Faneca e no Laboratório de Gastroenterologia e Hepatologia do Centro Médico Universitário Erasmus de Roterdão, sob a orientação científica do Professor Doutor André Boonstra.

Financial support was given by the European Regional Development Fund (ERDF), through the Centro 2020 Regional Operational Programme under project CENTRO-01-0145-FEDER-000008:BrainHealth 2020, and through the COMPETE 2020 - Operational Programme for Competitiveness and Internationalisation and Portuguese national funds via FCT – Foundation for Scicence and Technology, I.P., under the projects PROSAFE/0001/2016 and POCI-01-0145-FEDER-007440 (UID/NEU/04539/2013), and PhD fellowship DFRH - SFRH/BD/96167/2013.

Foi financiado por fundos da European Regional Development Fund (ERDF), através do Centro 2020 Regional Operational Programme com o projecto CENTRO-01-0145-FEDER-000008:BrainHealth 2020, e através do COMPETE 2020 - Operational Programme for Competitiveness and Internationalisation e fundos nacionais via FCT – Fundação para a Ciência e Tecnologia, I.P., com os projetos PROSAFE/0001/2016 e POCI-01-0145-FEDER-007440 (UID/NEU/04539/2013), e bolsa de doutoramento DFRH - SFRH/BD/96167/2013.

“Don't Say Hi If You Don't Have Time For a Nice Goodbye”

Noiserv

À minha avó Lucy

Acknowledgements / Agradecimentos

Quatro anos se passaram! Várias pessoas se cruzaram! Resta-me agradecer aos que me ajudaram!

Professora Olga, obrigada pela sua dedicada e incansável orientação de todo o trabalho apresentado nesta tese! Agradeço-lhe acima de tudo a oportunidade e também todos os ensinamentos proporcionados no decorrer desta jornada!

Doutor Henrique, obrigada pelo seu apoio e dedicação na co-orientação do trabalho desenvolvido!

André Boonstra, thank you for accepting me in your lab and providing me that great experience. The way you lead your group inspired me!

Doutor Frederico e Doutor Flávio, obrigada por terem despertado em mim o interesse pela ciência. Desta vez, não colaboraram na tese, mas, são sem dúvida responsáveis pela sua existência.

NANOLAB, obrigada por me terem aceite nesta "instituição", sem grandes burocracias! Tive só de comprar uns fones, não é Sandra? Obrigada por me terem feito sentir anormalmente normal! Obrigada por se terem mostrado uma amostra não representativa da população. Obrigada por terem abraçado a minha loucura. Obrigada por terem aceite o meu sentido crítico! Tanto no lab, como nos restaurantes! Obrigada por me terem ensinado "nanocenas". Obrigada por tudo o que aconteceu nos bastidores d'*Uma aventura na FFUC*! Obrigada pela amizade! **Filipa, Dulce e Sandra**, muito obrigada! Mesmo! Já dizia Fernando Pessoa, e com razão, "o valor das coisas não está no tempo que elas duram, mas na intensidade com que elas acontecem".

João, Patrícia, Mariana e Alana, obrigada pela amizade e companheirismo tanto no lab como nos petiscos fora dele. Um agradecimento especial à **Patrícia** pela deteção de gralhas madrugada dentro.

Rose, obrigada pelo apoio e ajuda prestada na colaboração de parte do trabalho desenvolvido.

Dina e Daniela, obrigada pela ajuda prestada sempre que tive de vos ocupar o lab.

Anthonie, thank you for your kindness help and friendship! I really liked to work with you! Thank you for making me ride my bike at 7 am! Thank you for those 20 ELISAs in one day! Respect bro!

Dona Gina, obrigada pelo seu constante apoio ao laboratório de Tecnologia Farmacêutica da Faculdade de Farmácia. "Viste a Dona Gina?", "Já perguntaste à Dona Gina?", "A Dona Gina não sabe?" é que mais se ouve por lá.

Luísa Cortes, Isabel Dantas, Isabel Nunes, Margarida Caldeira e Cândida Mendes, obrigada pelo apoio técnico dos trabalhos realizados no Centro de Neurociências e Biologia Celular da Universidade de Coimbra.

Doutora Ana Donato, obrigada pela disponibilidade e ajuda nos trabalhos realizados no Laboratório de Análises Clínicas da Faculdade de Farmácia.

Mónica Zuzarte, obrigada pelo apoio técnico na aquisição de imagens de TEM no IBILI.

Marlene, Susana e João, obrigada pela amizade e por me terem acolhido tão prontamente sem me julgar, exceto o João, que demorou mais um pouco!

Maria, obrigada pela amizade, ainda que o primeiro impacto te tenha feito duvidar. Obrigada por perceberes que dizer a verdade não é ser má pessoa, muito pelo contrário! Obrigada por me teres proporcionado o "test-drive" da maternidade, sem a chatice das fraldas! Eu nem sempre sei o que é certo ou errado, mas fico mesmo contente que tenhas interesse na minha opinião!

Mauro e Mariana, obrigada pela amizade e companhia. Principalmente por me terem ouvido (muito!) no último ano!

Bicker, Joanita, Daniela, Carla, Ana Fortuna, Samantha, Cristina, Hélito e Débora, obrigada pelo companheirismo no primeiro piso da FFUC (pelas escadas… pelo elevador é o quarto!) e pelos momentos de convívio fora dele.

Gertina, Kim, Paula, Gulce, Petra, Patrick, Jan, Shanta, Gijs, Thomas, Noé, Lauke, Jun, thank you all for your great kindness in welcoming me. And, of course, thanks to all the volunteers for blood collection and nurses from ERASMUS MC.

Sara, obrigada por me dares tantos motivos para gozar contigo! Obrigada por deixares pouco por dizer! Obrigada pelas pausas para "fumar um pensativo cigarro", como dizem os poetas, essenciais no decorrer desta jornada!

Amigos de Coimbra: Cati, Abel, Hugo, Sílvia e Ricardo, obrigada pelos momentos fora do lab, não menos importantes na manutenção da ameaçada sanidade mental.

André, obrigada pela ajuda com os bonecos! Aqui tens a tua linha!

Mana, obrigada por justificares tão bem a minha existência como irmã mais velha. Ver-te lutar pelo que queres deixa-me com a sensação de dever cumprido!

Mãe e Pai, obrigada! Obrigada por tudo o que me deram! Sempre menos do que queriam e, muitas vezes, mais do que podiam! Obrigada principalmente pelo que não me deram! Não há maior riqueza do que a de lutar pelo que não temos! Obrigada por me terem ensinado isso tão bem! Obrigada por investirem em mim o que não puderam investir em vocês! Esta tese não é minha! É nossa!

Table of contents

List of abbreviations

AAL	*Aleuria aurantia* lectin
Abs	absorbance
Akt	Protein kinase B
AlgChiPs	Alginate coated chitosan particles
ALT	Alanine transferase
APC(s)	Antigen presenting cell(s)
AS	Adjuvant systems
ATCC	American type culture collection
AV	Combined with antiviral therapies
BAFF-R	B cell activating factor receptor
BSA	Bovine serum albumin
CARD9	Caspase-associated recruitment domain 9
cccDNA	Covalently closed circular DNA
CD	Cluster of differentiation
CHB	Chronic hepatitis B
ChiPs	Chitosan particles
CLR(s)	C-type lectin receptor(s)
CR3	Complement receptor 3
CTB	Cholera toxin B
CTL(s)	Cytotoxic T lymphocyte(s)
DAMP(s)	Damage associated molecular pattern(s)
DC(s)	Dendritic cell(s)
DLS	Dynamic light scattering
DMSO	Dimethylsulfoxide
DNA	Deoxyribonucleic acid
DTAF	5-([4,6-Dichlorotriazin-2-yl]amino) fluorescein hydrochloride

EASL	European association for the study of liver disease
ELISA	Enzyme-linked immunosorbent assay
ELS	Electrophoretic light scattering
EMA	European medicines agency
FA	Formaldehyde
FAE	Follicle associated epithelium
FBS	Fetal bovine serum
FDA	Food and drug administration
FITC	Fluorescein isothiocyanate
GALT	Gut associated lymphoid tissue
GC(s)	Germinal center(s)
GenChiPs	Chitosan particles with genipin crosslink
GenGluChiPs	β-glucan/chitosan particles with genipin crosslink
GluPol	PβAE/PDMAEMA polyplexes prepared in the presence of β-glucan
GPs	Glucan particles
GPsPol	PβAE/PDMAEMA polyplexes combined with GPs
GRAS	Generally recognized as safe
GSK	GlaxoSmithKline
HBcAg	Hepatitis B nucleocapsid/core protein antigen
HBeAg	Hepatitis B e antigen
HBIG	Hepatitis B immunoglobulin
HBsAg	Hepatitis B surface antigen
HBV	Hepatitis B virus
HBx	Hepatitis B regulatory X protein
HCC	Hepatocellular carcinoma
HCV	Hepatitis C virus
HIV	Human immunodeficiency virus
HP	Homing peptide
HPMCAS	Hydroxyl propyl methyl cellulose acetate succinate

HRP	Horseradish peroxidase
iC3	Third intracellular loop
IFN	Interferon
Ig	Immunoglobulin
IL	Interleukin
ILoop	Ileal loop
IM	Intramuscular
IN	Intranasal
IP	Intraperitoneal
iRNA	Interference RNA
ISCOM(s)	Immune stimulating complex(es)
IV	Intravenous
J	Joining
LacCer	Lactosylceramide receptor
LbL	Layer-by-layer
LC	Loading capacity
LE	Loading efficiency
LPS	Lipopolysaccharide
LSCM	Laser scanning confocal microscopy
M	Microfold
MALT	Mucosal associated lymphoid tissue
MAPK	Mitogen-activated protein kinase
MHC-I	Major histocompatibility complex molecules class I
MHC-II	Major histocompatibility complex molecules class II
MIP-2	Macrophage inflammatory protein 2
MLN(s)	Mesenteric lymph node(s)
MPL	Monophosphoryl lipid A
MTBCL	Mycobacterium TB cell lysate microspheres
MVA	Modified vaccinia virus

MyD88	Myeloid differentiation primary response 88
Mφ	Macrophages
NA(s)	Nucleos(t)ide analogue(s)
NAG	N-acetyl-β-D-glucosaminidase
NFAT	Nuclear factor of activated T cells
NF-κβ	Nuclear factor-κβ
NK	Natural killer
NLR(s)	NOD-like receptor(s)
NLRP3	NACHT, LRR and PYD domains-containing protein 3
NOD	Nucleotide-binding oligomerization domain
NTCP	Sodium taurocholate co-transporting polypeptide
OA	Oral administration
OD	Optical density
ON	Overnight
OND(s)	Oligodeoxynucleotide(s)
OPD	o-Phenylenediamine dihydrochloride
OVA	Ovalbumin
p	Pandemic
PAMP(s)	Pathogen associated molecular pattern(s)
PBS	Phosphate buffer saline
PBS-T	Phosphate buffer saline with 0.05 % Tween™20
PCL	Poly(ε-caprolactone)
PCV2	Porcine circovirus type 2
PDI	Polydispersity index
PDMAEMA	Poly[2-(dimethylamino)ethylmethacrylate]
PEG	Poly(ethylene glycol)
PEI	Poly(ethylenimine)
PEIPol	PEI-based polyplexes
PenStrep	Penicillin/streptomycin

pgRNA	Pregenomic RNA
PI	Propidium iodide
PI3K	Phosphoinositide 3-kinase
pIgR	Polymeric Ig receptor
PKC	Protein kinase C
PLA	Poly(lactic acid)
PLGA	Poly(lactic-co-glycolic acid)
Pol	PβAE/PDMAEMA polyplexes
poly (I:C)	Polyinosinic:polycytidylic acid
PolyMix	PβAE/PDMAEMA mixture
PP(s)	Peyer's patch(es)
pre-p	Pre-pandemic
PRR(s)	Pathogen recognition receptors
PβAE	Poly(β-amino ester)
rcDNA	Relaxed circular conformation
Ref.	References
RLR(s)	RIG-I-like Receptor(s)
RLU	Relative light units
RNA	Ribonucleic acid
ROS	Reactive oxygen species
RPMI	Roswell park memorial institute medium
RT	Reverse transcriptase
RT°	Room temperature
s	Seasonal
SC	Subcutaneous
Scav	Scavenger receptor
SED	Subepithelial dome
SEM	Standard error of the mean
sgRNA	Subgenomic RNA

sIgA	Secretory IgA
SIGN-R1	DC-specific intercellular adhesion molecule-3-grabbing non-integrin-related 1
Syk	Spleen tyrosine kinase
TBE	Tris-borate-EDTA buffer
TCR	T cell receptor
TEM	Transmission electron microscopy
Tfh	Follicular Th cells
TGF-β	Transforming growth factor-β
Th	Helper T cells
TIF	Liver interstitial fluid
TLR(s)	Toll-like receptor(s)
TMC	Trimethylated chitosan
TNF-α	Tumor necrosis factor-α
TRAF-6	TNF receptor associated factor 6
Treg	Regulatory helper T cells
tRNA	RNA from *torula* yeast
VLPs	Virus-like particles
WHO	World Health Organization
ZP	Zeta potential
β-hex	β-hexosaminidase

Abstract

The hepatitis B virus (HBV) killed 887 000 people in 2015. The World Health Organization (WHO) set the goal to eliminate HBV as a public health threat by 2030. The major hurdles include the high prevalence in developing countries due to limited vaccination coverage and mother-to-child transmission and, the ineffective HBV clearance from hepatocytes with currently available antivirals. Hence, therapeutic vaccines may stimulate both the neonate immature or the chronic hepatitis B exhausted immune systems, to either avoid HBV persistence or promote HBV clearance. Additionally, new vaccines can be designed to provide the antigen with increased stability to temperature variations, benefiting HBV vaccine coverage in developing countries, where the cold chain to vaccine transportation is not readily available. Thus, this thesis aimed to develop new powerful adjuvants to include in new vaccines to meet hepatitis B current needs. β-glucan particles were elected to mimic pathogen three-dimensional structure and chemical composition. The capacity to induce HBsAg-specific Th1 antiviral protection through several vaccination strategies was the main goal. Indeed, this was the first time that non-modified natural β-glucans were used as adjuvants for HBsAg.

The new formulations of HBsAg vaccines were tested through subcutaneous (SC) and oral routes, while plasmid DNA (pDNA) vaccines only through the SC route. Different β-glucan adjuvants were developed and included β-glucan particles (GPs), prepared from alkaline/acid treatment of *Saccharomyces cerevisiae*, β-glucan/chitosan particles (GenGluChiPs), prepared by a precipitation technique followed by genipin crosslink and, polyplexes prepared by pDNA complexation with cationic PβAE and PDMAEMA polymers (Pol) in the presence of β-glucan (GluPol) or combined with GPs (GPsPol). Notably, GenGluChiPs were produced by a new precipitation technique to combine two polymers that do not interact with each other. GPs were tested in all vaccination schedules while GenGluChiPs only for HBsAg SC vaccination and GluPol only for pDNA SC vaccination. Additionally, chitosan particles were developed for comparison purposes either by precipitation/coacervation (ChiPs) or precipitation followed by genipin crosslink (GenChiPs). Both were positively charged and had a mean diameter near 900 nm.

GenGluChiPs, also positively charged, measured approximately 1.3 µm. On the other side, alginate coated ChiPs (AlgChiPs), used for oral vaccination, were negatively charged and had a mean diameter close to 1.5 µm. GPs were electrically neutral and measured between 2 µm and 4 µm. Pol and GluPol were highly positive with a mean diameter of 180 nm.

Regarding the oral vaccination study (Chapter 2), although both AlgChiPs and GPs were efficiently internalized by intestinal Peyer's patches, the oral vaccination schedule resulted in 60 % mice seroconversion, easily surpassed by a SC priming prior the oral boosts. The presence of HBsAg-specific IgA on mucosal surfaces and IFN-γ in the liver were the major advantages found. Interestingly, *in vitro* studies showed that only ChiPs were able to induce mast cell activation, evaluated by cell degranulation and β-hexosaminidase release. Concerning pDNA vaccination study (Chapter 3), although the excellent Pol transfection results, further enhanced by the combination with GPs (GPsPol) in fibroblast and macrophage cell lines, the SC vaccination either with Pol, GluPol or GPsPol resulted in only 40 % seroconversion and low antibody titers.

The mechanistic study with GenChiPs, GenGluChiPs and GPs showed that the increased TNF-α secretion from mice spleen cells was associated to β-glucan (GenGluChiPs and GPs), while RANTES secretion was associated to chitosan (GenChiPs and GenGluChiPs), suggesting an immunological advantage of the newly developed GenGluChiPs. However, in the human monocyte study, the TNF-α production was consistently observed for all the particles. The mice immunization study with HBsAg to validate GenGluChiPs adjuvant (Chapter 4) showed high serum anti-HBsAg IgG, mostly subtype IgG1 followed by IgG3. No signs of cell-mediated immunity were found after two vaccine doses. However, in another study with three vaccine doses (Chapter 5), the GPs adjuvant induced a strong and varied HBsAg-specific cell-mediated immunity observed by the secretion of cytokines related with Th1, Th2, Th17, Th22 and Treg-biased immune responses. For the first time, these studies allowed the validation of GPs as great adjuvant to include in HBsAg vaccines, also revealing a therapeutic value against viral infections.

Overall, the work herein developed and described represents an important contribution to the knowledge of both β-glucan and chitosan/β-glucan particle adjuvant mechanisms, with a great impact for future studies.

Keywords: polymeric particles, adjuvants, vaccines, β-glucan, chitosan, oral vaccine, DNA vaccine, hepatitis B virus, hepatitis B antigen.

Resumo

O vírus da hepatite B (HBV) originou 887 000 mortes em 2015. A Organização Mundial de Saúde (OMS) estabeleceu o objetivo de eliminar o HBV como uma ameaça de saúde pública até 2030. Os principais problemas incluem a elevada prevalência nos países em vias de desenvolvimento devido à ineficiente cobertura de vacinação e elevada transmissão mãe-filho, e a dificuldade em eliminar o HBV dos hepatócitos com as terapias antivirais disponíveis. A nova geração de vacinas deverá ter em conta tanto o sistema imunitário imaturo dos recém-nascidos como a exaustão do sistema imunitário dos portadores crónicos. Além disso, novas vacinas podem promover a estabilidade do antigénio perante variações de temperatura, frequente nos países em vias de desenvolvimento, onde cadeias de transporte adequadas são ainda escassas. Nesse sentido, esta tese teve como objetivo desenvolver novos e poderosos adjuvantes para incluir em novas vacinas, de modo a ir ao encontro das necessidades de controlo da hepatite B. Partículas à base de β-glucano foram selecionadas por simularem as propriedades químicas e tridimensionais dos patogénios. O objetivo principal foi desenvolver uma vacina com a capacidade de induzir uma resposta celular específica para o HBsAg, e para isso foram desenvolvidas e testadas várias estratégias. Curiosamente, esta foi a primeira vez que β-glucanos naturais não modificados foram usados como adjuvante para o HBsAg.

Vacinas com o HBsAg foram testadas pelas vias subcutânea (SC) e oral, e vacinas com o plasmídeo (pDNA) foram testadas pela via SC. Foram desenvolvidos vários adjuvantes compostos por β-glucano, tais como partículas de β-glucano (GPs) preparadas por tratamento ácido/alcalino da *Saccharomyces cerevisiae*, partículas de β-glucano/chitosano (GenGluChiPs) produzidas por um método de precipitação/reticulação com genipina e poliplexos preparados por complexação do pDNA com os polímeros catiónicos PβAE e PDMAEMA (Pol) na presença de β-glucano (GluPol) ou posteriormente combinados com as GPs (GPsPol). Notavelmente, as GenGluChiPs foram produzidas por um método inovador para a combinação de dois polímeros que não interagem entre si. As GPs foram testadas em todas as estratégias de vacinação, enquanto que as

GenGluChiPs foram apenas testadas pela via SC com o HBsAg e os GluPol pela via SC com o pDNA. Partículas de quitosano foram desenvolvidas tanto por precipitação (ChiPs) como por precipitação/reticulação (GenChiPs), como termo de comparação. Ambas apresentaram carga positiva e um diâmetro médio de 900 nm. As GenGluChiPs, também positivas, mediam cerca de 1,3 µm. Por outro lado, ChiPs revestidas com alginato (AlgChiPs) para vacinação oral apresentaram carga negativa e um tamanho médio de 1,5 µm. As GPs, neutras, possuíam um tamanho entre 2 µm e 4 µm. Os Pol e os GluPol apresentaram uma carga fortemente positiva e um diâmetro médio de 180 nm.

Quanto ao estudo de vacinação oral (Capítulo 2), apesar de as AlgChiPs e as GPs terem sido internalizadas pelas placas de Peyer do intestino de murganhos, três doses pela via oral resultaram em apenas 60 % de eficácia, enquanto que a presença de um priming pela via SC levou a 100 % de eficácia. O mais interessante, não observado pela via SC, foi a indução de anti-HBsAg IgA nas mucosas e aumento de IFN-γ no fígado. Curiosamente, apenas as ChiPs ativaram uma linha celular de mastócitos, verificado pela desgranulação e libertação de β-hexosaminidase. Quanto ao estudo de vacinação com o pDNA (Capítulo 3), apesar da excelente transfecção dos Pol, aumentada na presença de GPs (GPsPol) em fibroblastos e em macrófagos, a vacinação pela via SC resultou em apenas 40 % de eficácia e baixos títulos de anticorpos para todas as formulações (Pol, GluPol e GPsPol).

Nos estudos mecanísticos, o aumento da secreção de TNF-α em células do baço de murganhos foi associada com o β-glucano (GenGluChiPs and GPs) e a secreção de RANTES com o quitosano (GenChiPs e GenGluChiPs), sugerindo uma vantagem para as GenGluChiPs aqui desenvolvidas. Por outro lado, o aumento da produção de TNF-α em monócitos humanos, foi observada após a incubação com os três tipos de partículas. A vacinação pela via SC para a validação da GenGluChiPs como adjuvante (Capítulo 4) levou ao aumento de IgG específica para o HBsAg no soro de murganhos, maioritariamente do subtipo IgG1 e também IgG3. As duas doses da vacina mostraram-se ineficazes na indução da resposta celular. Por outro lado, num segundo estudo com três doses da vacina (Capítulo 5), apenas as GPs levaram numa elevada e ampla secreção de citocinas relacionadas com respostas Th1, Th2, Th17, Th22 e Treg, específica para o HBsAg. Pela

primeira vez, este estudo consagrou o valor de incluir as GPs em vacinas com o HBsAg, bem como o seu potencial terapêutico para estas infeções virais.

No geral, o trabalho desenvolvido providenciou uma importante contribuição para o conhecimento do mecanismo adjuvante de partículas de β-glucano e β-glucano/quitosano, relevante para estudos futuros.

Palavras-chave: partículas poliméricas, adjuvantes, vacinas, β-glucano, quitosano, vacina oral, vacina de DNA, vírus da hepatite B, antigénio da hepatite B.

CHAPTER 1

GENERAL INTRODUCTION

1.1. Hepatitis B is still a global health problem!

Hepatitis B is a liver infection caused by the hepatitis B virus (HBV) that resulted in 887 000 deaths in 2015 [1]. HBV infection might either be spontaneously cleared or evolve into a chronic infection, most likely to happen when virus exposure occurs early in life [2, 3]. Regardless of the introduction of an effective vaccine in the 80's and the resultant decrease in HBV incidence and prevalence, the World Health Organization (WHO) estimated that 257 million people (3.5 % of global population) are currently living with chronic hepatitis B (CHB) [1, 4, 5]. In fact, although the worldwide HBV prevalence has declined modestly, the total number of people infected has increased consequent to population growth [5]. To date, as no effective treatment is available, once HBV is chronically established it is incurable. CHB individuals are usually asymptomatic until they age and develop severe related complications [1, 3]. It was estimated that 15 % to 25 % of individuals with persistent infection die of cirrhosis or hepatocellular carcinoma (HCC) [6]. HBV is currently considered as the most carcinogenic factor after tobacco and a possible link with gastric cancer has also been documented [7]. Therefore, hepatitis B is a global health burden that needs an urgent and global response.

1.2. HBV infection and disease – immune exhaustion

HBV is a non-cytopathic member of the *Hepadnaviridae* family of viruses. The observed liver damage is usually mediated by the immunological response of the host to the virus [8]. The virus has a partially double-stranded DNA genome in a relaxed circular conformation (rcDNA) that encodes a total of seven proteins: the non-structural precore protein also known as secreted e-antigen (hepatitis B e-antigen – HBeAg), the nucleocapsid/core protein (HBcAg), three envelope proteins, structurally and functionally divided, collectively known as surface antigens (HBsAg), the regulatory X protein (HBx) and a DNA polymerase [8]. These proteins constitute the 42 nm HBV viral particle, composed by an inner nucleocapsid surrounding the viral genome and a polymerase enclosed by a lipoprotein envelope containing surface proteins.

HBV life cycle begins when bloodstream circulating HBV reaches the liver and enters hepatocytes via the sodium taurocholate co-transporting polypeptide (NTCP) receptor, specific to human and non-human primates [9, 10]. Then, the rcDNA containing

nucleocapsid is released into the cytoplasm and transported to the nucleus for repair and formation of the covalently closed circular DNA (cccDNA) minichromossome [8]. The cccDNA serves as the template for the transcription viral RNAs: the subgenomic RNA (sgRNA) that will be translated into HBsAg and HBx proteins, and the pregenomic RNA (pgRNA) that might be either translated into HBcAg, HBeAg and DNA polymerase proteins or encapsidated together with the DNA polymerase for reverse transcription to new rcDNA [11]. Nucleocapsids are either re-imported to the nucleus for ongoing viral replication or enveloped and secreted as new virions that will infect other hepatocytes. HBsAg and HBeAg are formed and secreted over and above the production of fully formed virions. Both are not infectious but secreted HBsAg may have immunogenic properties favoring infectivity and secreted HBeAg is associated with high viral load and used as a serological marker for active infection and replication [12, 13].

The outcome of HBV infection varies according to the age at infection. Immunocompetent adults exposed to HBV most frequently develop acute self-limited infection, resulting in infected hepatocytes clearance, temporary liver injury and subsequent life-long sterilizing immunity. Contrasting, nearly all newborns perinatally infected or half of the children infected in the first five years of life would develop CHB [1, 14]. The virus takes advantage of the developing immune system of young children, still learning to recognize and tolerate itself, which might temporarily accept HBV as self, allowing viral persistence [14]. Chronic HBV infection is categorized into four distinct clinical phases associated with varying degrees of immune activation and consequent liver injury, traditionally defined by serum HBeAg, HBV DNA and alanine transferase (ALT) levels [4, 15, 16]. The first phase, the immune tolerant phase, occurs early after infection and it is HBeAg-positive characterized by high viremia (serum HBV DNA) and negligible immune activation or liver injury. The second phase, the immune active phase, is when the immune system recognizes HBV infection eliciting HBeAg seroconversion and a strong CD8+ T cell response resulting in viral suppression and marked liver injury, typically HBeAg-positive, high HBV DNA and ALT levels. The third phase, the inactive carrier or HBeAg negative phase, is characterized by low HBV DNA and normal ALT levels, mild inflammation and fibrosis. The fourth phase, the HBeAg-negative chronic hepatitis phase, occurs as HBV may periodically reactivate resulting in sporadic flares of serum HBV DNA

and ALT elevations and active inflammation. HBsAg secretion occurs from the first to the fourth phase but serum levels are highest during the immune tolerant phase and lowest during the inactive carrier phase, a parameter that may help in determining the phase of infection, particularly for HBeAg-negative individuals [15]. In later stages of chronic infection, as a result of persistence of viral antigens and their prolonged presentation to the immune system, HBV-specific CD8+ and CD4+ T cells are quantitatively, functionally and metabolically impaired, especially in patients with high viral load [16]. These exhausted T cells are ultimately unable to express effector mechanisms critical to control or eliminate the pathogen. Dysfunction of potential antiviral effector cells (e.g. Kupffer cells, Natural Killer (NK) cells and dendritic cells (DCs)) has also been associated with chronicity [15, 16]. On the other hand, B cells seem to be functionally intact, secreting antibodies against HBsAg, correlated to clinical protective immunity likely contributing to viremia control [16].

1.3. HBV eradication: is it a mission possible?

The world has expressed its alarm about the global response to HBV infection in 2015, when the General Assembly of the United Nations called the international community for the elimination of hepatitis B as a public health threat. To accomplish that, starting from the 2015 worldwide baseline described in the WHO Global Hepatitis Report 2017, the world needs to reduce new infections by 90 % and mortality by 65 %, by the year of 2030 [1]. Interruption of transmission routes is the most effective way to reduce infection, contributing to the suppression of the pathogen reservoir [4]. Vaccination arises as a great victory of public health that circumvented a variety of infectious diseases. It is amongst the most cost-effective measures to prevent mortality, second only to clean water [17]. However, the implementation of global vaccination coverage is a difficult task, mostly for low-income regions. HBV available prophylactic interventions and the concern of developing countries toward eradication will be further discussed below (sections 1.3.1 and 1.3.1.1). While effective global vaccination is not feasible and millions of CHB carriers still exist, the search for an effective treatment must be pursued. Although HBV has been discovered for more than half a century, a cure for CHB remains a challenging task. Effective HBV clearance is the major concern and the possible help of immunomodulatory

agents to achieve the WHO 2030 eradication goal are better discussed below (sections 1.3.2, 1.3.2.1 and 1.4).

Recently Food and Drug Administration (FDA) approved new therapies for hepatitis C (HCV) achieving remarkable 90 % to 99 % cure rates which proves that it is possible to achieve an effective cure for diseases that were thought incurable only a decade ago. FDA approved the first once-daily pill (Harvoni®) that doesn't require interferon (IFN) or ribavirin (old-fashioned treatments associated with concerning side-effects and a sustained HCV eradication in only 40 % to 50 % of the cases) in 2014, the first drug for the treatment of all HCV genotypes (Epclusa®) in 2015, and the first drug to treat all HVC strains in just 8 weeks (Mavyret®) in 2017. The fact that from 1989 to 2014 all the available treatments included IFN and ribavirin, and during the last 4 years several other drugs were approved with improved outcomes, encourages the research on HBV therapies and makes us believe that HBV eradication is a mission possible. The question now is not if, but how and when it will be possible!?

1.3.1. Available prophylactic interventions

Although the clear difficulties in achieving complete hepatitis B eradication, there is great evidence of feasibility. In the late 18th century, Edward Jenner took the first step in that direction as the pioneer of the world's first vaccine [18]. In fact, human disease smallpox and livestock disease rinderpest, two infectious diseases, have already been eliminated in human history through successful vaccination campaigns, while other diseases such as measles and polio are close to elimination. Vaccination has this altruistic side called herd immunity, that will ultimately lead to pathogens elimination, when 60 % to 90 % of the population is vaccinated resulting in a very low likelihood to find another naïve host to spread [19]. Indeed, two recombinant HBV vaccines with an excellent safety profile are available since the 80's: Recombivax HB® from Merck & Co, Inc (West Point, PA, USA) and Engerix-B® from GlaxoSmithKline (GSK) Biologicals (Rixensart, Belgium). Three intramuscular doses are required to induce protective antibodies in more than 95 % of infants and children, persisting by 60 years in 75 % [20]. Hepatitis B universal childhood vaccination programs recommended by the WHO since 1992 contributed to dramatically reduce HBV prevalence, reaching a current global coverage of 84 %. The

world now has the tools to prevent HBV, they just have to be appropriately implemented. Unfortunately, that is not the case of low-income countries [1].

1.3.1.1. The concern of developing countries

Developing countries, still unable to implement effective vaccination programs, are the major concern for hepatitis B elimination [21]. Accordingly, 68 % of total HBV chronic carriers are from African and Western Pacific regions, where political and socio-economic problems difficult healthcare support [1, 21]. The price of medicines and diagnosis are the key drivers that influence the feasibility of elimination plans and universal health coverage [1]. Additionally, vaccines are highly sensitive to temperature variations due to their biological origin that can lead to their inactivation. For effective vaccine maintenance, cold storage is required from the production to the delivery, often not assured in developing countries [22]. In these countries, most of the infected individuals are undiagnosed and untreated at risk of developing cirrhosis, liver failure and HCC resulting in high mortality [3, 21]. Disturbingly, more than 80 % of HCC cases occur in eastern Asia and sub-Saharan Africa, with approximately 40 % occurring before the age of 40 in the latter region [23]. Health care costs with CHB individuals are considerably high, increasing the socio-economic impact of HBV infection [24]. Deaths are increasing and will continue to do so unless effective treatment strategies are implemented [1].

Mother-to-child transmission predominant in hyperendemic areas and accounts for the major portion of HBV infections, associated with increased risk for chronicity and consequently HCC [2]. Preventing perinatal and early postnatal HBV transmission is a key component to reach the WHO 2030 goal of eradication [1, 2]. For that, all infants should receive the first dose of hepatitis B vaccine ideally 24 h after birth, which may take more than a generation, as nowadays it only happens in 39 % of the cases [1, 2]. Concomitant strategies might include immunoprophylaxis to the newborn children from infected mothers to fill the gap between birth and development of antigenemia, despite of being post-exposure [2, 25]. Neonatal vaccination requires dedicated strategies to overcome immune immaturity and immunoregulatory mechanisms [26]. The combination of hepatitis B immunoglobulin (HBIG) prophylaxis with hepatitis B vaccination starting at birth can reduce the rate of mother-to-child transmission by 90 % [2, 4, 25]. However,

concerns related to supply, safety and cost make it difficult. Additionally, a 10 % to 30 % failure rate has been reported in infants born from high viral load mothers [27]. Although not routinely recommended and the absence of data of long-term safety for children, antiviral therapy during the third semester and early weeks post-partum is being evaluated to complement HBIG to diminish transmission from those mothers [28]. Moreover, promising newly developed adjuvants and vaccination strategies have proven to improve neonatal responses in preclinical or *in vitro* models and include toll-like receptors (TLRs) and C-type lectin receptors (CLRs) agonists (section 6.1.2.2) to elicit Th1 antiviral protection in human newborns [26].

1.3.2. Available therapeutic interventions

Current antiviral therapies can efficiently suppress viral replication and reduce liver inflammation but permanent HBV clearance is rare as they have no direct effect on hepatic cccDNA reservoir [8, 29]. Consequently, long-term therapy is needed and cccDNA persistence leads to frequent viral relapses observed after treatment cessation [11]. The European Association for the Study of Liver Disease (EASL) recommends two main therapeutic strategies for chronic HBV infection: treatment for a limited period with PEGylated IFN-α or a nucleos(t)ide analogue (NA) such as entecavir or tenofovir, or long-term treatment with a NA. Both have been associated with decreased risk of HCC and HBV-related mortality, especially following several years of continued treatment [30]. NAs effectively suppress the production of new virions, reducing HBV replication through the inhibition of viral reverse transcription. This in turn results in viremia reduction to undetectable levels and ALT normalization. The first line therapy entecavir and tenofovir have low risk of drug resistance, are administered orally and have negligible adverse effects [15]. However, virologic relapse even after HBV DNA has become undetectable is frequent after NAs cessation, HBsAg loss is rarely achieved and the requirement of lifelong therapy increases the cost and the risk of long-term toxicity [31]. The main advantage of IFN-α treatment is the dual effect on the direct suppression of viral replication and the indirect enhancement of host immunity against the virus, achieving higher rates of HBeAg and HBsAg loss compared to NAs [32]. Thus, IFN-α is associated with a more durable response. Enhanced pgRNA encapsidation inhibition and cccDNA degradation have also been reported following a combination therapy with polymerase

inhibitors when compared to the monotherapy [33]. However, IFN-α therapy has low applicability as it can achieve sustained off-treatment control only in a minority of patients and it is often associated with systemic side-effects, making it contraindicated for patients with decompensated cirrhosis and autoimmune illnesses [34]. This is the major drawback of this treatment.

1.3.2.1. The concern of HBV clearance – cues from acute infection

Incoming virions and recycling of encapsidated rcDNA from the cytoplasm provide a constant cccDNA source, the hallmark of infection establishment, that together with the long half-life are the main reason that difficult HBV clearance [4, 8, 11, 15]. cccDNA elimination is the Achilles' heel of the search for an effective treatment [4, 8, 11, 15]. Detailed understanding of what determines spontaneously viral clearance in acute HBV infection can unveil the path for effective treatments. The fact that adult infection typically leads to HBV control, whereas perinatal infection frequently results in chronicity, strongly suggests the contribution of immune maturation [16]. The CD8+ T cell immune responses are thought to be the main determinants, as weak responses have been associated to the ones who failed to eradicate HBV infection and strong cytotoxic T lymphocyte (CTL) responses have been detected in patients with acute viral infection [35]. Several other immune impairments have been associated to CHB when compared to acute viral control: weak innate proinflammatory responses and cytokine activation; impaired IFN-γ production by NK cells and consequently reduced IFN-γ-induced non-cytolytic HBV clearance by specific CD8+ T cells; and, impaired expression of IFN-stimulated genes (ISGs) encoding intracellular or secreted effector proteins with antiviral properties [15, 16, 36]. This dichotomy of the specific immune response elicited in self-limited HBV versus CHB makes it possible to hypothesize that the restoration of anti-HBV immunity in CHB patients could lead to a functional cure [37]. The term "functional cure", defined by Block *et al*. [38], is achieved when the patient returns to a state of health equivalent to that of a person who has recovered spontaneously from HBV infection, and has a similar likelihood of developing cirrhosis or HCC. The clinical outcome mimicking the natural resolution of infection would include sustained off-drug suppression of virologic markers to undetectable levels (serum HBsAg, HBeAg and viral DNA) and the normalization of liver function (serum ALT levels) [38]. Nevertheless, it is known that low

amounts of cccDNA molecules can persist in some hepatocytes of patients recovering from acute HBV infection for decades, raising the hope that not the entire intrahepatic cccDNA reservoir needs to be eliminated to gain immunological control and resolve the infection [11].

1.4. The need for new immunomodulatory therapies for hepatitis B

The unsatisfactory results of the latest generation of antiviral drugs demonstrate that additional strategies are needed to achieve a functional cure [15, 38, 39]. As described before, the immune system can clear HBV and establish long-term control over the virus in 5 % to 10 % of the patients. For that to happen in CHB individuals, it will certainly be necessary to provide sufficient help to boost their exhausted and dysregulated immune system [40]. Immunomodulatory agents arise as a promising strategy that can be specifically designed for that. Immune-based therapies have the additional advantage to be suitable for young patients at early stages of liver disease (immune tolerant phase) when T cell function is still preserved, contrasting to current antiviral therapies only recommended for patients with cirrhosis, decompensated liver disease or high viremia [36, 41, 42]. This would, theoretically, have a greater impact on reducing the risk of HCC and ultimately death, the main goal of any successful therapy [42].

Most authors recognize T cell function restoration as the best immunotherapeutic approach for controlled destruction of persisting HBV-producing hepatocytes [4, 11, 15, 29, 36]. In fact, there is a correlation between HBV-specific T cell responses and viral replication control [40]. Consistently, CD8+ T cells targeting all HBV proteins with cytolytic and non-cytolytic cytokine-mediated (e.g. IFN-α, IFN-γ and tumor necrosis factor (TNF)-α) effector functions were identified to inhibit HBV replication and contribute to cccDNA destabilization [11]. Additionally, killing infected cells may also induce compensatory proliferation of HBV-infected hepatocytes, frequently impaired in CHB, leading to cccDNA dilution among the daughter cells [11]. Interestingly, HBV-specific NK cells have the capacity not only to destroy the cccDNA in sporadic non-proliferating hepatocytes but also induce neighboring hepatocytes proliferation [16]. Therefore, they can be a useful target as well. As functional restoration highly depends on the quantity and quality of

exhausted T cells, the adoptive transference of new HBV-specific T cells is discussed as a possibility, with obvious difficulties for clinical implementation, unless new technology and methods progress rapidly on the way to large-scale production of engineered T cells [36]. Actually, most of recent research advances that provide some hope to achieve a functional CHB cure, extensively reviewed by others [15, 37, 40, 43] and outlined in figure 1.1, include several immunomodulatory approaches with multiple targets to restore HBV-specific and non-specific immunity: 1) blockade of immunosuppressive pathways; 2) recovery of exhausted adaptive immunity; 3) stimulation of innate immunity; and 4) therapeutic vaccination. There is significant evidence that therapeutically manipulating innate immunity can have a strong antiviral effect, as it is known that the induction of innate proinflammatory responses and cytokine activation are weak in chronic HBV infection. The stimulation of the innate immune system can have an antiviral effect beyond simply the production of cytokines with direct antiviral activity, like the currently available IFN-α mediated effect. Moreover, targeting innate immune cells, such as the Kupffer cells (specialized macrophages of the liver), can modulate the inflammatory/anti-inflammatory intrahepatic environment through the localized production of antiviral and inflammatory cytokines [40]. Current strategies to target the innate immune cells use synthetic drugs that activate pathogen recognition receptors (PRRs), namely TLRs (e.g. TLR7) [40]. The PRRs activation will stimulate the production of antiviral/inflammatory cytokines other than IFNs, associated with the induction of ISGs that alone does not correlate with viral control. TNF-α, IL-6 and IL-12, all potentially induced by PRRs agonists, have anti-HBV activity and may be more important for viral control because of their impact on the environment and adaptive immunity [40]. Adaptive immunity has been the primary focus of immune-based therapies, aimed to overcome the established HBV-specific T cell exhaustion, restoring the level of the HBV-specific T cell populations and anti-HBs antibodies that define disease resolution [40, 43]. Therefore, providing the correct stimulus to promote orchestrated innate and adaptive immune responses will be necessary to provide a global antiviral activity able to sense and control the infection though multiple cytokine production and activation of T, NK and B cells [15, 35, 40, 43].

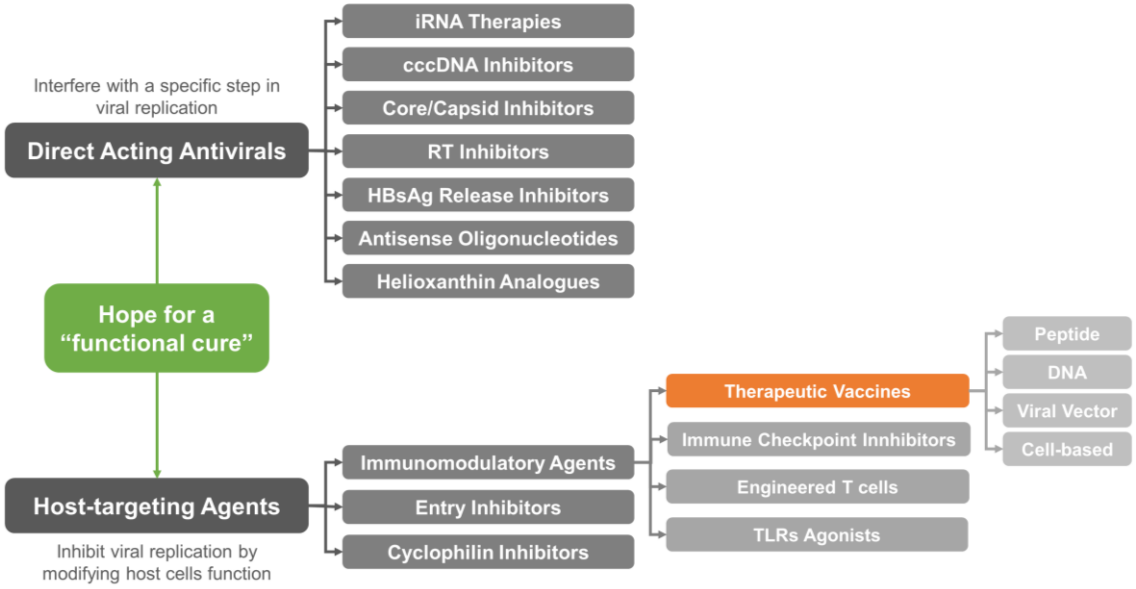

Figure 1.1. Current investigational agents under development for chronic hepatitis B (CHB) functional cure. The therapeutic agents under development could be divided in two categories: 1) direct acting antivirals and 2) host-targeting agents. It is currently accepted that a functional cure is likely to come in the form of combination of two or more therapies including agents from both categories. Therefore, therapeutic vaccines will be the main focus of the present thesis, due to the possibility to combine a multitude of agents in the vaccine formulation. *cccDNA, covalently closed circular DNA; iRNA, interference RNA; RT, reverse transcriptase, TLRs, Toll-like receptors.* Adapted from [43].

1.4.1. Therapeutic vaccination

A major effort has been centered on therapeutic vaccination. Therapeutic vaccines employing new technology and new immunomodulatory drugs can bring together the best for HBV clearance. If the appropriate delivery system is chosen, a variety of effector molecules (Figure 1.1) can be coupled and targeted to the right cells or tissues, providing the capacity to elicit simultaneously adaptive (antigen – e.g. HBsAg) and innate (adjuvant – e.g. TLR agonists) immunity with additional blockade effect of immunosuppressive pathways (e.g. coupling checkpoint inhibitors). As Gehring said in a recent review of HBV new treatments to reach functional cure, vaccines with new adjuvants and delivery methods may still require combination with checkpoint blockade for maximum T cell stimulation or innate immunomodulators to drive vaccine-induced T cells to the liver [40]. Indeed, it is currently accepted that a functional cure is likely to come in the form of combination of two or more therapies, mostly combining direct antiviral agents with host

targeting agents (Figure 1.1), synergistically amplifying the therapeutic effect [15, 37-39, 43]. In that regard, vaccine formulations have been tested in combination with antiviral therapies. Several strategies have been evaluated in clinical trials with discouraging results, mostly including classical prophylactic vaccines, regardless of combination with antiviral therapy (Table 1.1) [44-48]. The demonstrated limited effect of those trials helps to understand the challenge of boosting anti-HBV immunity and at the same time provided some evidence of what may be effective. Contrasting from DNA vaccination, most recombinant antigens were relatively weak at inducing T cell immunity (Table 1.1) [44-53], suggesting that significant humoral anti-HBs response might not be sufficient to induce HBV clearance and the inclusion of potent adjuvants to increase and modulate the vaccine potency might be needed [40]. New vaccine developments that evolve as a second generation of HBV therapeutic candidates are now under clinical evaluation, and mainly include adjuvanted formulations with recombinant antigens or DNA vaccination (section 1.6.1.1) with a few additional approaches (Table 1.1).

As evidenced by the lack of a licensed therapeutic vaccine for chronic HBV infection, none of the strategies have been consistently successful yet, although some have reached phase III clinical trials [54, 55]. Thus, there remains the challenge for researchers to improve the current approaches or develop a new highly efficient and safe therapeutic vaccine. Potential adverse effects including severe liver inflammation as a result from the hyper-responsiveness of the T cell cytotoxicity activity in the liver infected cells need to be carefully managed [36].

Table 1.1. Summary of HBV therapeutic vaccine clinical trials.

Candidate	Type	Composition	AV	Year	Ref.
GenHevacB® or Recombivax®	Recombinant	HBsAg, alum	-	1999, 2001,	[44, 46, 48]
CY-1989	Lipopeptide	Tetanus 830 CD4, HBc18-27 CD8 epitope	-	1999	[56]
Hepacare®	Recombinant	HBs, PreS2, PreS1, alum	-	2002	[50]
Engerix-B®	Recombinant	HBsAg, alum	+	2002	[45]
Gamma-HB®	Recombinant	HBsAg	+	2005	[47]
pCMV-S2.S	DNA	S, PreS	-	2004, 2006	[57, 58]
HB-100 and IL-12N222L	DNA	S, PreS, Core, Pol, IL-12	+	2006	[59]
HBsAg/AS02B	Recombinant	HBsAg, AS02B adjuvant	-	2007	[53]
Antigen-antibody complex (YIC)	Recombinant	HBsAg, HBIG immune complex, alum	-	2008, 2013	[55, 60]
Sci-B-Vac	Recombinant	HBs, PreS2, PreS1	+	2009	[49]
Autologous DCs	Cellular Therapy	Autologous DCs, CD8+ T cell epitopes	-/+	2010	[61]
TG1050	DNA, Viral Vector	Recombinant MVA encoding HBs (MVA.HBs)	+	2011	[62]
pS2.S and pFP (hIL-2 and hIFN-γ)	DNA	PreS, IL-2, IFN-γ	+	2012	[63]
INO-9112 and/or INO-1800	DNA	IL12 and/or HBsAg and consensus sequence of HBcAg	+	2012	[64, 65]
DV-601	Recombinant	HBsAg, HBcAg, ISCOMATRIX® adjuvant	+	2011, 2013	[51, 52]
HerberNasvac®	Recombinant	HBsAg, HBcAg	-/+	2013	[54, 66-68]
Tarmogen®	Yeast	Heat-inactivated yeast expressing HBx, HBsAg, HBcAg	-	2014	[69-71]
pCMV-S2.S	DNA	S, PreS	+	2015	[72]
HB-110	DNA	HBs, PreS1 HBc, HBp IL-12	+	2015	[73]
HepTCell (FP-02.2)	Recombinant	Nine peptides of HBV, CD4+ and CD8+ T cell epitopes	+	2015	[74]

AV, combined with antiviral therapies; DCs, dendritic cells; HBV, hepatitis B virus; MVA, modified vaccinia virus Ankara; Ref., reference. Adapted from [37, 40].

1.5. Key players of immune defense: an overview

Immunity has both a less and a more specific arm. Danger signals usually activate the innate immunity, a quick first line of defense, to stimulate and mobilize antiviral activities of innate immune cells (granulocytes, monocytes, eosinophils, macrophages, DCs, mast cells and NK cells) that usually involve the ingestion of extracellular particulate materials by phagocytosis. Innate immune cells express PRRs that recognize pathogen associated molecular patterns (PAMPs) present on microorganisms and damage associated molecular patterns (DMAPs) released from affected cells, leading to the activation of transcription factors and expression of cytokines (section 1.6.1.2.2) [75]. When these mechanisms fail to prevent the spread of an invading pathogen, a more specific and versatile line of defense needs to be initiated: the adaptive immune system.

Additional components, like epithelial cell barriers, complement system, antimicrobial peptides and other soluble factor are also part of the innate immune system. Major adaptive immune cells include antibody secreting B cells and effector T cells that ultimately promote viral clearance. An adaptive immune response is slower to develop but establishes an immunological memory ensuring a more rapid and effective immune response on a subsequent exposure to the same pathogen. To note that both innate and adaptive immune systems do not operate independently, they rather function as a highly interactive and synergistic system more effective than either branch by itself. Additionally, some innate cells were recently recognized to show memory-like behavior, suggesting that that innate immunity can also display adaptive characteristics [76]. Overall, two major groups of cells are involved in the generation of an effective and specific immune response: antigen presenting cells (APCs) and lymphocytes.

1.5.1. Antigen presenting cells and T cell interactions

Although macrophages and B cells are important APCs, DCs are recognized as the professional ones and represent the main link between innate and adaptive immunity [77]. Coherently, immature DCs reside in peripheral tissues and serve as sentinels for foreign antigens and microbial pathogens. Following vaccine capture and antigen processing, these antigen-capturing cells undergo maturation and migrate to the draining lymph nodes for T cell presentation, illustrated in figure 1.2. As DCs mature, they evolve

for processing and transporting antigens to the cell surface. This mechanism coincides with increased expression of costimulatory molecules (e.g. CD40, CD80 and CD86) and release cytokines that will amplify T cell receptor (TCR) signaling and promote T cells activation and polarization. DCs are capable to process both endogenous and exogenous antigens and present them to naïve T cells in the context of major histocompatibility complex molecules class I (MHC-I) or class II (MHC-II), eliciting antigen-specific CD8+ or CD4+ T cell differentiation, respectively [77, 78].

1.5.1.1. Helper T cell differentiation

Typically, exogenous processed antigens are presented in the context of MHC-II molecules and result in helper T (Th) cell differentiation. These CD4+ T cells secrete cytokines that provide help to other cells of the immune system. Depending on the activation mechanism and the surrounding cytokine milieu naïve CD4+ T cells can differentiate into different subsets that have unique cytokine profile and functional properties. Since the discovery of the Th1/Th2 dichotomy, several additional Th subsets were discovered and include Th17 cells, regulatory T cells (Treg) and most recently Th9 cells, Th22 cells and follicular Th cells (Tfh) (Figure 1.2) [79, 80]. Th1 cells are primarily associated with cell-mediated immunity particularly important against intracellular pathogens. These cells are mainly characterized by IFN-γ and TNF-α secretion that will activate CD8+ T cells and macrophages to kill both the pathogen and infected cells. IFN-γ is a potent proinflammatory cytokine linked with increased phagocytosis and antigen presentations, B cells stimulation to secrete immunoglobulin G2 (IgG2) or IgG3 subclasses of IgG antibodies, generally associated to opsonization and virus neutralization. Th2 cells lineage are associated with host defense against extracellular parasites. It is responsible for the production of IL-4, IL-5 and IL-13 and the co-stimulation of B cells to originate short-lived plasma cells inducing a strong humoral immune response characterized by IgG1 and IgE production. Activated B cells can also differentiate into memory B cells that represent the specific immunologic memory maintenance after vaccination, able to induce a rapid specific immune response following a further pathogen exposition, preventing the establishment of infection [81]. Th17 subset comprises potent inflammatory mediators involved in host defense against infectious diseases, particularly at mucosal sites. The secretion of IL-17, IL-21 and IL-22, responsible for neutrophil

recruitment and B cell functions enhancement, is the major contributor. Although strongly associated with immunopathology, mainly serious inflammatory and autoimmune reactions, IL-17 has been recently considered a chief orchestrator of immunity. It is shown to have only modest activity on its own, but has a synergistic action with other factors such as the IFN-γ , serving as an important adjunct to Th1 responses [82]. Conversely, Th17 cell lineage is negatively regulated by Th1 and Th2 cytokines.

1.5.1.2. Cytotoxic T cell differentiation

On the other side, endogenously produced viral proteins or exogenous antigens processed by a phenomenon called cross-presentation are presented in the context of MHC-I molecules and result in CTLs differentiation [77]. These CD8+ T cells are mainly involved in the clearance of intracellular pathogens as they can recognize and destroy infected cells. Antigen cross-presentation is a process mainly carried out by DCs and believed to be vital for immunity against viruses that do not readily infect APCs. It is highly dependent on DCs maturation stimuli, influenced by the internalization route, the pathway of endocytic trafficking and the simultaneous activation through PRRs [83].

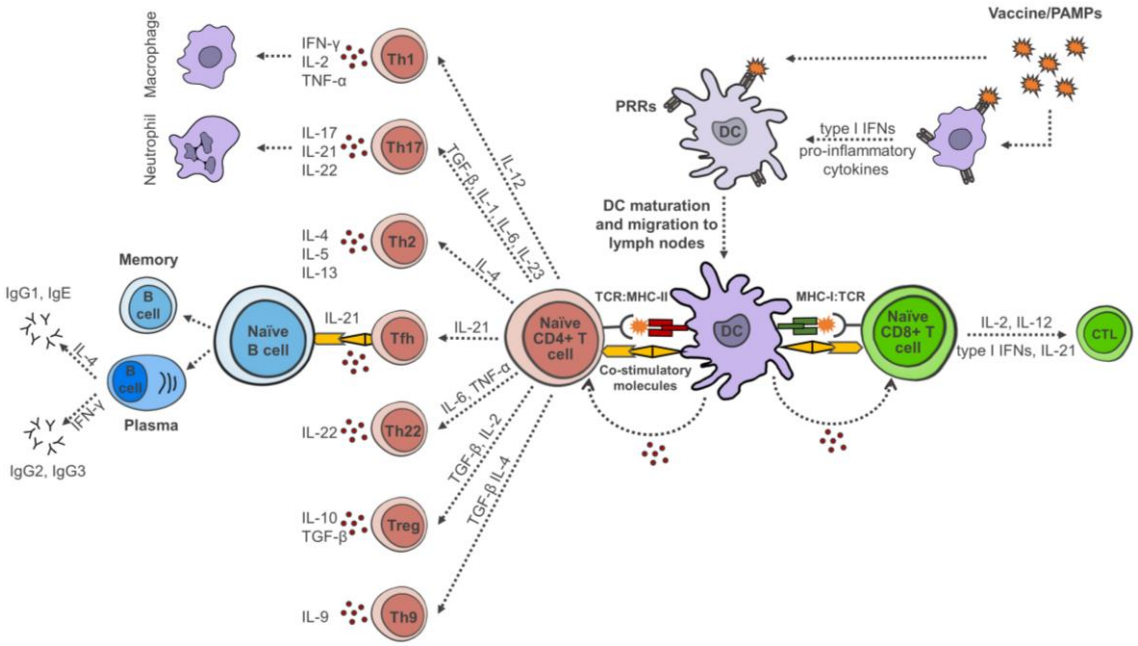

Figure 1.2. Adaptive immune response to vaccines/PAMPs. Vaccines may contain pathogen-associated molecular patterns (PAMPs) as adjuvants. These PAMPs are directly detected by pattern-recognition receptors (PRRs) expressed by dendritic cells (DCs), leading to DCs activation, maturation and migration to the lymph nodes. PRRs are also expressed by macrophages that may cooperate in the activation and orientation of the DC response through the release of cytokines. In the lymph nodes, activated DCs may present the antigen to T cells, providing co-stimulatory signals and cytokine-mediated stimulation for CD4+ and CD8+ T cells differentiation via MHC-II and MHC-I, respectively. Depending on the cytokine milieu, CD4+ T cells may differentiate into different T helper (Th) cell subtypes, such as Th1, Th2, Th9, Th17, Th22, Treg or Tfh cells. In turn, these subsets release distinct cytokines that mediate different functions, such as B cell isotype switching following B cell activation by Tfh cells. CD8+ T cells differentiate into memory and effector CD8+ T cells (CTLs). Adapted from [75].

1.6. Vaccine design for viral infections

Acquired immunity for a specific disease organism can result from either an actual infection or a preventive inoculation. Indeed, vaccination is one of the great victories of public health, efficiently circumventing a variety of infectious diseases. It is amongst the most cost-effective measures to prevent mortality, second only to clean water [17]. Since Edward Jenner developed the first vaccine candidate in the 18th century great advances have been made. The field has moved from expensive traditional vaccines (inactivated or live-attenuated pathogens), with major problems related to safety issues and adverse host reactions, to extremely safer options [84]. Advancing technology and the desire for harmless and cost-effective alternatives led to development of subunit vaccines that

contain a protective antigen of the pathogen that can be expressed by an attenuated bacterial or virus vector (recombinant vaccines) or encoded by DNA or RNA (DNA or RNA vaccines). Subunit vaccines in general were poorly immunogenic and required the addition of immunostimulatory agents to induce strong and long-lasting protective immune responses [19, 84, 85]. Although the success to generate strong antibody responses useful for a prophylactic application, the lack of robust antigen specific T cell responses makes their use for therapeutic interventions of viral infections deceptive. Modern vaccinology still has some challenges to solve and their applicability for incurable viral infections such as the hepatitis B remains a great challenge (sections 1.3.2.1 and 1.4) [37, 40, 84].

T cell function restoration is commonly recognized as the best immunotherapeutic approach for a functional HBV cure (section 1.4). Thus, the induction of cell-mediated immunity (based on the action of T cells) is vital in vaccine design for viral infections, often ineffective without the activation of innate immunity [78]. Thus, and for the reasons explained in section 1.5.1, DCs are key targets to modulate the vaccine elicited immune response. Specifically, DCs activation to induce antigen specific CD8+ T cells differentiation is a crucial factor for controlled destruction of persisting HBV-producing hepatocytes [77, 78]. As explained in sections 1.5.1.1 and 1.5.1.2, two immune events often promote CTLs differentiation: antigen presentation in the context of MHC-I or polyfunctional CD4+ T cells differentiation resulting in cytokine and antibody secretion that will favor cell mediated immunity and virus neutralization and opsonization (Th1-biased response). Design vaccines that mimic pathogen properties, categorizing the microbial features responsible for immunity is a promising approach to promote that [19, 84, 85].

1.6.1. Mimicking pathogens

In fact, traditional live attenuated or inactivated whole-cell vaccines usually do not require additional immunostimulatory components since they contain some naturally occurring adjuvants such as nucleic acids, lipids and cell membrane components [86]. The repetitive surface molecule organization, the particulate nature and the ability to stimulate both innate and adaptive immune responses are some of the key parameters

responsible for their superb immunogenicity. These parameters may serve as the paradigms to successful development of safe and potent modern vaccines that may embrace DNA vaccines and the development and selection of novel vaccine adjuvants, primarily acting via DCs activation [87-90].

1.6.1.1. DNA vaccines

The immune response following DNA vaccination suggests that it follows a complex pathway mimicking natural viral infections. The use of DNA as the immunogen will lead to uptake and expression/translation of the transgene using the host cell's replication machinery [91] linked with MHC-I presentation and CTLs differentiation in addition to humoral immunity [77, 87, 89, 91]. Once DNA plasmid (pDNA) is administered through common routes (e.g. subcutaneous (SC), intravenous (IV), nasal or intramuscular (IM)) the two main cell types that become transfected are myocytes and APCs, great targets to trigger and modulate immunity. Additionally, as DNA vaccines are unable to induce antivector immunity (as recombinant vaccines can do), they have theoretically unlimited boosting potential and are therefore a recognized CHB therapeutic candidate [91-93] already tested in some clinical trials (Table 1.1). Other advantages include the low cost of production, transport and storage as DNA vaccines are highly stable and do not require refrigeration. Cold storage is necessary for current available recombinant vaccines to remain antigenically active, a struggle in developing countries where hepatitis B is a major problem [21, 88, 89]. Nevertheless, poor transfection, transient antigen expression and immunological tolerance are the main hurdles of current DNA vaccines research seeking *in vivo* immunogenicity and efficacy [87, 92, 94].

A variety of non-viral DNA delivery vehicles have been investigated including physical (e.g. 'gene guns', electroporation) and chemical (e.g. cationic molecules) approaches. Complexation with cationic polymers to condense pDNA and deliver it to target cells is highly promising and may shape the future of DNA vaccination [92, 94]. Improving cellular internalization, endosomal escape and enhancing their delivery to cell nucleus are some of the main advantages conferred [95]. Synthetic polymers that have gained some attention include poly(β-amino ester) (PβAE) [94, 96] and poly[2-(dimethylamino)ethylmethacrylate] (PDMAEMA) [94, 97]. In addition, particles based on

PβAEs were recently characterized for their intrinsic immunogenicity, activating DCs, antigen presentation and enhancing T cell proliferation [98]. PDMAEMA-based polyplexes were also previously considered a potential delivery vehicle for the HBsAg-encoding DNA vaccination [99]. Heterologous prime-boost regimens have also provided significant contributions to DNA vaccine immunogenicity. Again, vaccine targeting to APCs is also a possibility to overcome such limitations [100]. Codelivery with adjuvants can also enhance vaccine-induced immunity. Therefore, there remains the opportunity for DNA vaccine design improvement to achieve viral clearance not achieved yet by the therapeutic DNA vaccines that entered clinical trials (Table 1.1).

1.6.1.2. Development of new adjuvants

The word adjuvant comes from the Latin word *adiuvare*, which means to help. Adjuvants were first described by Gaston Ramon in 1920s [101] and consist of substances capable of enhancing, modulating or prologing antigen-specific immune responses. To sensitize the immune system against infectious agents and induce long-lasting memory response, vaccine adjuvants usually have some characteristic properties extensively reviewed by others and summarized in table 1.2 [22, 90, 102]. Adjuvants have diverse modes of action and are therefore divided into delivery systems and immunomodulators. Antigens and adjuvants are usually formulated for enhanced presentation by APCs as emulsions or particulate delivery systems such as liposomes, virosomes, immune stimulating complexes (ISCOMs), virus-like particles (VLPs) and polymeric particles. Immunomodulators comprise any substance that activates, suppresses or changes immune responses and generally enhance vaccine efficacy primarily by stimulating innate immunity. They can modulate cytokine and chemokine secretion and include TLRs ligands, CpG oligodeoxynucleotides (ONDs), galactosylceramides and bacterial toxins among others. Nevertheless, this division is not static since some particulate delivery systems such as liposomes and polymeric particles also have intrinsic immunomodulatory properties.

Table 1.2. Adjuvant characteristic properties.

• Elevate antigen processing and presentation by APCs
• Induce cell-mediated immunity (like CTLs)
• Facilitate mucosal responses (protecting the antigen from the harsh GI tract)
• Increase antigen potency (enabling dose sparing)
• Ensure a rapid response
• Induce long-lasting adaptive immune responses
• Induce antigen-specific clonal expansion
• Induce broad and high specific antibody production
• Good immunomodulatory capacity
• Induce secretion of cytokines that control T and B cell responses
• Function as effective innate immune signals
• Make vaccine more cost effective (less doses required)
• Enhance vaccine efficacy in infants, elderly and immunocompromised people
• Facilitate continuous antigen release (depot effect)

APCs, antigen presenting cells; CTLs, cytotoxic T lymphocytes; GI, gastrointestinal tract. Adapted from [102].

Despite the great advance in the field, few adjuvants are currently licensed for human use (Table 1.3) mainly associated with the toxic properties of the adjuvant material [22, 102, 103] and considerable increase in regulatory demands since the initial approval of aluminum salts (e.g. alum) [86]. Although aluminum salts are the most widely utilized adjuvant in human vaccines since 1926 [104], they are poor inducers of T cell responses and have some inherent complications including local reactions, augmentation of IgE antibody responses and the occurrence of granulomas [102, 105]. For human administrations, adjuvant choice is based on the balance between higher adjuvanticity and lesser side effects [22]. Furthermore, a new-generation of adjuvants is crucially awaited to create new vaccines or improve the existing ones with the capacity to stimulate both the innate and adaptive immunity to induce robust cell-mediated immune responses including Th cells and CTLs differentiation, with reduced toxicity [90, 102]. In that regard, the rapidly increasing knowledge on how the immune system interacts with pathogens means that there is increased understanding of the role of adjuvants and how the formulation of modern vaccines can be better tailored, contrasting from early

adjuvants that were used empirically. Depending on the mode of action, each adjuvant can have unique immunological properties (Table 1.2) and should be selected according to the target pathogen and the desired clinical outcome [102]. Nevertheless, many challenges are being experienced including preparation in suboptimal conditions, confinement in adjuvanticity, safety concerns and biological dissimilarity [22].

Table 1.3. Licensed adjuvants for human vaccines.

Adjuvant	Type	Trade name (disease)	Year
Alum	Mineral salt	Various	1926
MF59	Squalene-based oil-in-water emulsion	Fluad®, Optaflu® (s. influenza) Focetria™, Aflunov® (p. influenza)	1997
Virosomes	Liposome	Inflexal® (s. influenza) Epaxal® (hepatitis A)	2000
CTB	Non-toxic enterotoxin derivative	Dukoral® (cholera)	2004
AS04	Alum adsorbed MPL	Fendrix® (hepatitis B) Cervarix™ (human papilloma	2005
AS03	Squalene-based oil-in-water emulsion	Pandremix® (s., p. influenza) Prepandrix™ (pre-p. influenza)	2009
AS01	Combination of liposome, MPL and saponin QS-21	Mosquirix™ (malaria) Shingrix (herpes zoster)	2015

Adjuvants approved by the Food and Drug Administration (FDA) and/or the European Medicines Agency (EMA). MPL, monophosphoryl lipid A - TLR4 agonist; p., pandemic; pre-p., pre-pandemic; s., seasonal. Adapted from [102].

Therefore, careful and rational design is mandatory to succeed and in the next sub-section it will be explained why the combination of a particulate form and PAMPs comprise the most rational design of “pathogen-mimicking” adjuvants with the ability to enhance recognition and uptake by APCs, leading to enhanced immune responses with reduced side effects.

1.6.1.2.1. Particulate form

The importance of a particulate form is a consistent principle for enhanced immunity, mimicking the particulate nature of a pathogen. In fact, Gaston Ramon has already observed in the 1920's that horses injected with inactivated toxin and starch, breadcrumbs or tapioca induced local sterile abscesses resulting in increasing anti-sera production [101]. Consistently, particulate antigens are generally more immunogenic than soluble ones. For instance, VLPs particulate structure and size facilitate their uptake into APCs and efficient cross-presentation on MHC-I molecules, an additional advantage for therapeutic approaches for infectious diseases [106]. A perfect example is the HBsAg that can self-assemble into 22 nm VLP about 1000 times more immunogenic than non-assembled HBsAg [107]. Still, although HBsAg intrinsic immunogenicity it often requires the concomitant use of adjuvants for an efficient vaccination, like the commercially available vaccines that include aluminum hydroxide (Engerix-B®) or alum (Recombivax HB®).

Moreover, particulate materials often create a proinflammatory environment that recruit immune cells and prolong particle-cell interactions [108]. Beyond the adjuvant characteristic properties described in table 1.2 and the fact that they can act both as immunomodulators and delivery systems, particulate adjuvants have the potential to be specifically tailored in order to regulate the type of innate immune responses induced, offering significant opportunities in terms of designing systems with increased immune-mediated efficacy [108]. They permit size and surface properties control and the co-delivery of multiple molecules in the same structure (e.g. antigen, adjuvant, targeting molecules) enabling a local, simultaneous and possible synergistic effect usually valuable for the vaccine efficacy and potency [85, 109, 110]. In fact, the combination of two adjuvants in the same vaccine formulation can be highly beneficial to enhance, but mostly to modulate the type of immune response desired [111]. For instance, Adjuvant Systems (AS01, AS02 and AS03 – Table 1.3) from GSK are an example of successful adjuvants combination in the same formulation for enhanced immunogenicity and modulation of the immune response. Particularly for AS04, the addition of MPL to aluminum salts enhanced cell-mediated immunity to human papilloma virus (HPV) vaccine by rapidly triggering a local cytokine response favorable for APCs activation [112]. Most approaches

combine a delivery system with an immunopotentiator, because they have the potential to act synergistically to enhance antigen-specific immunity and increase vaccine safety, reducing the adjuvant-related side effects. The reduction of systemic distribution of the immunopotentiator preventing systemic cytokine-mediated inflammatory toxicity was demonstrated by Illyinskii *et al*. with the association of TLR agonists R848 and CpG ODN with polymeric nanoparticles [113]. Several particulate platforms have been explored and include VLPs, liposomes, ISCOMs, nanoemulsions and polymeric-based particles [22, 85].

These new adjuvants will be crucial in future clinical development of safer and more effective therapeutic vaccination against intracellular infections, such as the hepatitis B. Nanotechnology has been playing an important role in the design and development of those formulations, giving the appropriate features to particulate systems [19, 85], resulting in some successful achievements that already reached the market (e.g. emulsions and liposomes - Table 1.3).

1.6.1.2.2. PAMPs for PRRs targeting

The use of PRRs targeting PAMPs, present on microorganisms, able to control and shape the subsequent adaptive immune activities specific to the invading pathogen, is one of the most exciting areas of adjuvant development [90, 103]. PRRs are central to stimulate innate immunity and are considered key targets to drive the desired T cell responses. PRRs stimulation can promote DCs activation towards polyfunctional Th1 cells, T cell memory and CTL responses [85, 90, 103]. The generated immune response may differ depending on the PRRs activated that will be translated in a specific cytokine production with distinct T cell polarizing effects. TLRs, CLRs, nucleotide-binding oligomerization domain (NOD)-Like Receptors (NLRs) and RIG-I-Like Receptors (RLRs) are the four main groups of PRRs. In fact, most of the molecular adjuvants currently under evaluation are PRRs ligands, with the most extensively studied being TLRs agonists [109]. TLRs activation may induce the mitogen-activated protein kinase (MAPK), nuclear factor-(NF-κβ) or IFN regulatory factors pathways inducing the expression of cytokines that modulate adaptive immunity [114]. In that regard, several TLRs agonists have been evaluated for their adjuvant properties in vaccines for infectious diseases: 1) TLR-3 ligand polyinosinic:polycytidylic acid (poly (I:C)); 2) TLR4 ligands monophosphoryl lipid A (MPL)

(already licensed for use in human vaccines - Table 1.4) and lipopolysaccharide (LPS); 3) TLR-5 ligand flagellin; 4) TLR7/8 ligand imiquimod (already has FDA approval for use in actinic keratosis, external genital warts and recently superficial basal carcinoma - Aldara® topical cream); and 5) TLR9 ligand CpG ODNs [85]. LPS, also known as endotoxin, is a highly immunogenic component of the gram-negative bacteria's outer cell wall that can lead to septic shock or endotoxin tolerance, depending on the dose. CpG ODNs are known to induce the production of Th1 proinflammatory cytokines and increased innate and adaptive immune response, with effects ranging from increased antibody production, faster memory response, or a change in the cytokine profile of the vaccine leading to a stronger immune response. Single stranded RNA from infecting microorganisms stimulates TLR7 and TLR8 leading to the production of proinflammatory cytokines. However, the short half-life of RNA difficults the development of long lasting vaccine formulations [19].

1.6.1.3. Mucosal vaccination – oral delivery

Most infectious agents, like the HBV, enter the body through mucosal surfaces, the largest body areas that separate the external milieu from the internal sterile environment. Mucosal surfaces are physical barriers of epithelial and immune cells, representing the body's first line of defense, commonly referred to as mucosal associated lymphoid tissue (MALT). The MALT mainly comprises B and T cells, but APCs like DCs and macrophages also play a major role in mucosal immunity [115-117]. MALT immune organization usually enables to tolerate the continuous stimulation of a vast variety of commensal microorganisms and to initiate a specific immune response against the plethora of potential pathogens [116], thus being hopeful candidate sites for vaccination [118]. The most attractive feature of mucosal vaccines (e.g. oral, rectal, vaginal, nasal, pulmonary) is the provided double layer of protection characterized by antigen-specific antibody responses in the bloodstream and the local production and secretion of antigen-specific secretory IgA (sIgA), fundamental for virus neutralization and opsonization [119-123]. Additionally, safety, convenience of administration, lower risk of infection transmission, the non-requirement of trained personnel and simplified manufacturing, transporting and storing are among the major vantages compared to injectable vaccines [124], that can benefit HBV vaccination in developing countries. Despite the extensive

research regarding needle-free vaccination, it is such a demanding accomplishment owing to physical barriers (e.g. mucus, epithelium) and poor immunogenicity mostly related to degradation of vaccine materials in the harsh stomach environment, rich in enzymes or with a very low pH [119]. Indeed, few mucosal vaccines are currently licensed for human use and none of the options includes subunit antigens (Table 1.4). The induction of immune tolerance frequently occurs in the absence of potent adjuvants due to low soluble antigen adsorption to mucosal surfaces [121, 125].

Table 1.4. Licensed mucosal vaccines for human use.

Pathogen	Trade name	Route	Vaccine type
Influenza virus	FluMist®, Fluenz® Tetra, Nasovac-S®	Nasal	Live attenuated monovalent or not influenza virus
Poliovirus	Orimune®, OPV®, etc.	Oral	Live attenuated trivalent, bivalent and monovalent polioviruses
Rotavirus	Rotarix®, RotaTeq®	Oral	Live attenuated, monovalent or pentavalent rotaviruses
Vibrio cholerae	Dukoral®, Orochol®, Shanchol®	Oral	Inactivated V. cholera with or without CTB
Salmonella Typhi	Vivotif®	Oral	Live attenuated *S. Typhi*

Mucosal vaccines approved by the Food and Drug Administration (FDA) Agency and/or the European Medicines Agency (EMA). CTB, cholera toxin B; Adapted from [126].

A winning approach for mucosal vaccination is the oral delivery to the gut associated lymphoid tissue (GALT), mimicking pathogens entry pathways, such as the HBV [127-129]. Additionally, new drugs for HBV treatment are being developed for oral administration as they will be absorbed through the intestine and delivered to the liver via the portal vein. Specially, drugs that target PRRs will stimulate production of antiviral and environment modifying cytokines (e.g. IFN-α, IFN-γ, TNF-a, IL-6 and IL-12) both in the intestinal tract and in the liver [40]. The GALT is reviewed by Lamichhane as the "command center" for mucosal immunity [118]. It can be subdivided into two immunological distinct regions: 1) highly organized lymphoid tissues such as the Peyer's patches (PPs) that serve as inductive sites for antigen presentation; and 2) poorly organized regions constituted by diffusely distributed lymphoid and plasma cells that serve as effector sites for sIgA synthesis and T cell responses [130, 131].

1.6.1.3.1. Peyer's patches

PPs are referred to as "the immune sensors of the intestine" by Jung and coworkers [132] and consist of macroscopic lymphoid aggregates found in submucosa along the small intestine. PPs, and other lymphoid areas, are separated from the intestinal lumen by a single layer of columnar epithelial cells, known as the follicle associated epithelium (FAE). The subepithelial dome (SED) is located underneath and is a more diffuse area of B cells, T cells, macrophages and DCs. The follicular areas are mainly composed by germinal centers (GCs) containing proliferating B cells, follicular DCs and macrophages spaced by interfollicular T cell regions [132, 133]. PPs GCs exhibit unique conditions totally different from those in peripheral nodes with a special ability to start, expand and synchronize gut IgA B cell responses [134] (Figure 1.3). The most notable feature of PPs is the presence of microfold (M) cells, enterocytes specialized to take up antigens, particles and microorganisms from the intestinal lumen by vesicular transport, delivering them to the underlying mucosal immune system [132, 135-137]. Interestingly, at basal side, M cell plasma membrane is deeply invaginated to form a large sac-like structure ("M cell pocket"), where DCs and lymphocytes can move in and take up residence [137], providing the ability to start, expand and synchronize gut IgA B cell responses [134]. Additionally, M cells express IgA receptors on their apical plasma membrane and transport sIgA-bound antigens to PPs [122, 137].

1.6.1.3.2. Production of secretory IgA

The production of IgA directed against intestinal antigens depends on resident mucosal APCs, mostly DCs, that sample antigens at various mucosal sites and is illustrated in figure 1.3. Mucosal DCs can be located beneath the epithelial dome of PPs sampling antigens that penetrate the overlying epithelium, entering PPs interfollicular T cell zone to activate naïve T cells for CD4+ differentiation. Then, CD4+ T cells move to PPs B cell follicles of germinal centers (GCs) and secrete cytokines (e.g. IL-4, IL-5, IL-13 and transforming growth factor (TGF)-β) that promote IgA B cell class switch recombination. This can also occur in draining mesenteric lymph nodes (MLNs) following migration of DCs located in the lamina propria that direct sample antigens present at the apical surface of epithelial cells by extending their dendrites. Although these DCs can migrate to the MLNs, they do not penetrate further into the body. IgA+ B cells differentiate to IgA+ plasma cells

that will be translocated from lymphoid sites to the intestinal lamina propria (and other mucosal immune effector sites such as the upper respiratory tract and the female urogenital tract) where they terminally differentiate to secrete dimeric IgA, then transported across mucosal epithelial cell layer via a polymeric Ig receptor (pIgR), giving rise to the sIgA. sIgA differs from serum IgA by two additional features, the joining (J) chain and the secretory component [138]. The secretory component of sIgA among other functions protects the Ig from being degraded by proteolytic enzymes, so it can resist in the harsh mucosal environment [138]. Therefore, sIgA is a major immune effector at mucosal surfaces and acts via three mechanisms: 1) antigen excretion, through the binding of sIgA to antigens removing them from lamina propria; 2) immune exclusion, by sIgA interaction with antigens blocking their attachment to epithelial cells; and 3) intracellular antigen neutralization, by neutralizing and eventually removing the pathogenic antigens inside the cells (Figure 1.3) [126, 139].

1.6.1.3.3. Polymer-based particulate adjuvants

Surely, to obtain a good immune response, the key strategy is to protect antigens and enhance vaccine uptake by PPs, which can be obtained throughout antigen encapsulation in polymer-based particles [140]. Antigen encapsulation in polymeric particles can be an important tool to ensure that oral tolerance does not develop, reducing the rate of dilution and degradation of antigen, among other features enumerated in table 1.2. In fact, particulate antigens are generally more immunogenic at mucosal surfaces, where soluble antigens are more prone to induce mucosal tolerance [141, 142]. For all the reasons explained in upper sections, targeting the antigen to PPs will play a major role in the development of a rapid and potent immune response. Multiple studies demonstrated the ability of polymeric delivery systems to reach PPs, associated or not with M cell ligands (Table 1.5). In some cases, they generated long-lasting immunological memory, not only at the site of antigen exposure but also systemically or in other mucosal compartments due to antigen-sensitized precursor B and T cells dissemination [116, 121, 122, 131, 132, 143-152].

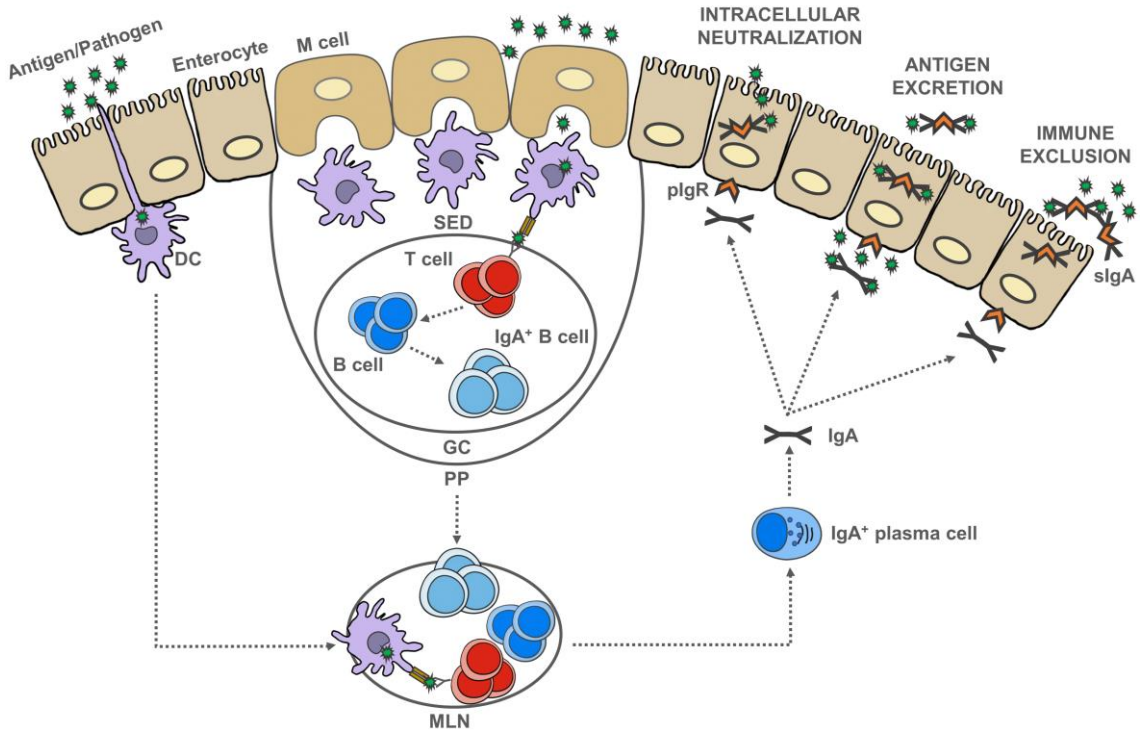

Figure 1.3. Gut-associated lymphoid tissue IgA production in response to antigens/pathogens. Dendritic cells (DCs) can sample antigens both located in the subepithelial dome (SED) of Peyer's patches (PPs) or in the lamina propria by extending their dendrites between the epithelial cells to reach the external milieu. Then, depending on the case, activated DCs can present the antigen locally on PPs germinal centre (GC) or migrate to the mesenteric lymph nodes (MLNs) where they induce B cells to differentiate into IgA+ plasma cells. IgA+ plasma cells home to the lamina propria and secrete dimeric IgA that is transcytosed across the mucosal epithelial cell layer via a polymeric Ig receptor (pIgR), giving rise to the secretory IgA (sIgA). IgA can protect mucosal surfaces by: 1) antigen excretion, through the binding of sIgA to antigens removing them from lamina propria; 2) immune exclusion, by sIgA interaction with antigens blocking their attachment to epithelial cells; and 3) intracellular antigen neutralization, by neutralizing and eventually removing the pathogenic antigens inside the cells. Adapted from [126, 139].

Once again, a combination of particle size and surface properties could directly influence interaction with the intestinal mucosa and consequently PPs uptake, better reviewed elsewhere [140]. However, general rules are difficult to draw due to the impossibility to evaluate one exclusive factor and not a multitude of parameters. In fact, polymeric particles with a wide range of size and various surface properties were successfully internalized by PPs, as shown in table 1.5.

Table 1.5. Peyer's patches uptake of immunogenic delivery systems in animal models.

Study Type	Delivery System	Size	Charge	M cell Ligand	Observations	Ref.
OA	Thiolated HPMCP particles	3.7 µm	---	M cell HP	Thiolation improved mucoadhesive properties; M cell HP improved antigen delivery to PPs.	[76]
ILoop/OA	Thiolated Eudragit® particles	1-10 µm	---	M cell HP	Thiolation resulted in higher residence time; M cell HP induced higher transcytosis to PPs through M cells.	[35]
OA	PLGA particles	166 nm	-20 mV	---	Effective PPs uptake.	[44]
OA	Guar gum particles	900 nm	---	---	Targeting potential to PPs.	[32]
In vitro/ex vivo	Polystyrene/BSA/ MTBCL microspheres	---	---	AAL	Lectin-coupled microspheres preferentially bind M cells.	[71]

Table 1.5. (Continued) Peyer's patches uptake of immunogenic delivery systems in animal models.

Study Type	Delivery System	Size	Charge	M cell Ligand	Observations	Ref.
ILoop	OVA-AlexaFluor loaded GPs	4 µm	-6 mV	---	Intraepithelial or intraluminal GPs localized in the SED region.	[50]
OA	HPMCAS + Eudragit® FS 30D particles	0.35 – 2 µm	+16 mV	AAL	Increased particulate uptake in PPs.	[37]
OA	HPMCAS + Eudragit® FS 30D + BSA particles	1.5 µm	+16 mV	AAL	Prolonged release.	[38]
ILoop	PLA particles	200 – 250 nm	-40 mV	---	Uptake exclusively through M cells; PLA interaction with SED B cells and DCs.	[40]
ILoop	Alginate coated chitosan particles	300 - 600 nm	-34 mV	---	Effective PPs uptake.	[36]

AAL, aleuria aurantia lectin; BSA, bovine serum albumin; DCs, dendritic cells; GPs, glucan particles; HP, homing peptide; HPMCAS, hydroxyl propyl methyl cellulose acetate succinate; ILoop, ileal loop; MTBCL, mycobacterium TB cell lysate microspheres; OA, oral administration. OVA, ovalbumin; PLA, poly(lactic acid); PLGA, poly(lactic-co-glycolide); PPs, Peyer's patches; Ref., references; SED, subepithelial dome. Adapted from [140].

Nevertheless, the literature points out some directions. Size is undoubtedly a key feature, as it will not only determine the efficiency of PPs uptake but also the internalization route through PPs epithelium: the transcellular pathway for smaller particles (<100 nm) and the paracellular pathway for larger particles (>100 nm) (Figure 1.4). Smaller particles (<500 nm) have good probability to be internalized by APCs and transported to the lymph nodes. Oppositely, bigger particles will be retained into PPs and so, mucosal and systemic specific immune responses will not be efficiently induced. In fact, IgA intestinal immune responses were found to be size dependent and favorable for smaller particles.

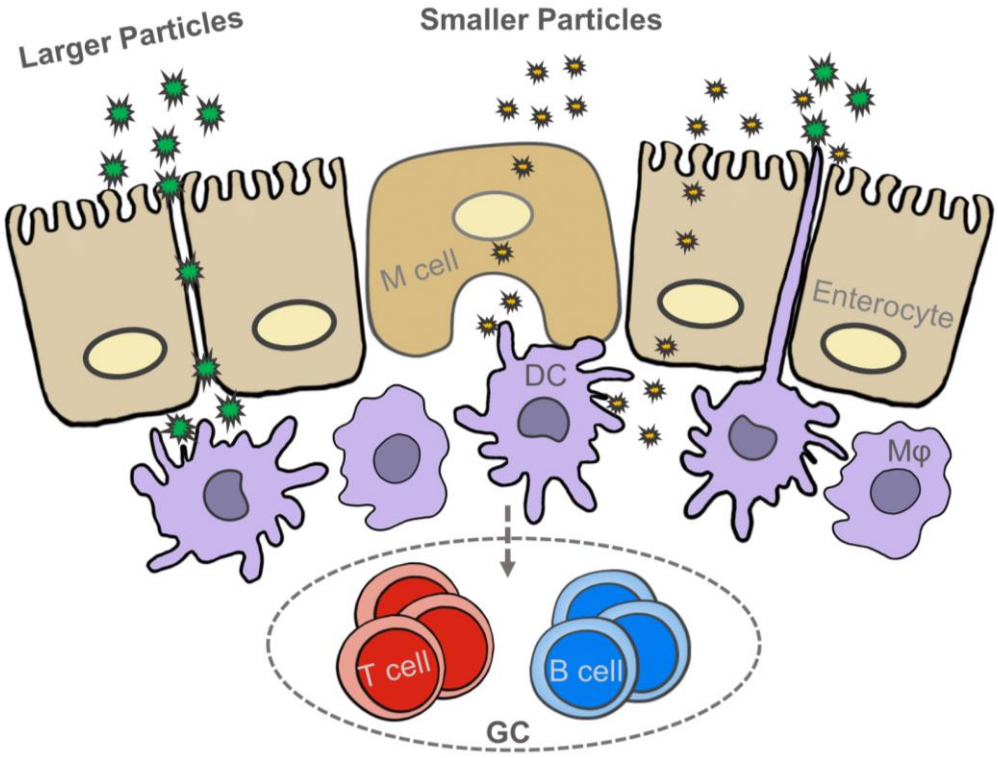

Figure 1.4. Size dependent uptake of orally administered particles in Peyer's patches. Two size-dependent uptake pathways through mouse PPs epithelium are illustrated: the transcellular pathway and the paracellular pathway. Smaller particles (<100 nm) are taken up by enterocytes (transcellular-E pathway) or M cells (transcellular-M pathway) to the subepithelial dome (SED) of PPs. Larger particles (>100 nm) appear to pass between enterocytes (paracellular-E pathway) and accumulate in the follicle associated epithelium (FAE) PPs region. *Adapted from [140].*

Regarding the optimal surface properties, the picture is not so clear, but a combination of moderate mucoadhesive properties to improve intestinal residence time, and the incorporation of M cell specific ligands for a targeted particulate delivery seems to be the

winning approach. Finally, it is also not clear if the particles should be positively charged. Positively charged particles interact with the mucosa sialic acid and thus their retention time is increased which can be a good feature on the nasal mucosa. However, on GALT, when the interaction is very strong, this can cause particle entrapment in the mucus and so particles would have difficulty to reach PPs. Summarizing, three main factors should be taken into account for particles design towards mucosal vaccine efficacy: 1) particle modification to increase interaction with the mucosa and enhance antigen bioavailability; 2) particles coating with specific targeting agents to increase M cells mediated uptake (e.g. lectins); and 3) include polymers that promote DCs activation and enhance innate and adaptive immunity following uptake [153]. The challenge remains to identify the best combination of adjuvants and/or targeting agents to promote optimal immune activation without the induction of adverse reactions.

1.7. Biodegradable polymer-based particles

Biodegradable polymers have a great potential in medicine simply because they can be degraded *in vivo* by enzymatic processes and the degradation products further eliminated by the normal metabolic pathways [109]. Thus, regarding the previously described and desired characteristics, biodegradable polymer-based particles arise as a great choice for the development of “pathogen-like” adjuvant candidates for vaccine formulations against infectious diseases. First, they display a particulate form. Second, they can be formulated using PAMPs in its composition. Third, bioactive molecules can be easily trapped in the particles by encapsulation to be released during particle degradation, or simply adsorbed on particle surface by electrostatic or hydrophobic interactions (e.g. immunomodulators, antigens, ligands for specific cells or tissues) [154]. Interestingly, the association of immunopotentiators with polymer-based vaccines can potentiate the immune effect and reduce its toxicity by directing the immunopotentiator to appropriate compartments (e.g. lymph nodes), enabling local immune responses rather than clearance to the bloodstream and the induction of a cytokine storm, as can occur with soluble adjuvants. Also, vaccine accumulation in lymph nodes will promote superior antigen-specific humoral immunity due to prolonged exposure to immune cells. Antigen formulation into polymeric nanoparticles allows the process of cross-presentation leading to the induction of cytotoxic immune responses, essential to fight

against intracellular pathogens (e.g. HBV) [109]. Additionally, biopolymers can enhance the shelf-life of antigens and display immunostimulatory properties improving antigenicity of conjugated antigens, highly influenced by the polymer chemistry, format, charge and fine balance between hydrophobicity and hydrophilicity [22, 109, 154].

Overall, particle size and surface composition are the main influencers of the outcome immune response. Several parameters can be controlled to tailor the desired particle size, recently reviewed as an intrinsic characteristic that affects the generation of long-last adaptive immunity, namely through the impact of particle size on the polymer half-life *in vivo* and the influence of that in the duration and type of the innate and adaptive immune responses generated [22, 108]. The effect of particle size on the immune response is not often consensual. Size-dependent immune responses are usually favorable for smaller particles directing to a more balanced Th1/Th2 immune responses [155]. Some authors associated particles with less than 1000 nm to a better uptake profile and an enhanced capacity to induce cell-mediated immunity [156, 157]. Even though, there is an ever-increasing obsession with the nanoscale, micro-sized particles also have many advantages as adjuvants. In fact, particulate vaccines typically within 0.1 μm and 10 μm range, resemble the dimensions of common bacteria and viruses, and are therefore recognized by the immune system [125]. Chitosan-based particles of 1 μm had favorable antigen delivery, upregulation of surface activation markers and cytokine release from macrophages when compared to similar 300 nm and 3 μm particles [158]. Surface composition is the other significant factor for immunomodulation. Hydrophobic domains of polymers are favorable for protein adsorption and APCs recruitment and activation [154]. Particle hydrophobicity was also demonstrated to initiate and enhance immune responses since many PRRs have evolved to recognize and react with hydrophobic molecular structures [159]. On the other side, hydrophilic moieties are also detrimental to determine polymer's adjuvant potential, preventing non-specific interactions of proteins with cells. That is why amphiphilic particles are referred by many authors as the best approach for vaccine delivery [160, 161]. A variety of other factors such as the surface chemistry are deeply involved and depend on the biopolymer used, or the use of targeting molecules for surface functionalization, such as PRRs agonists. It affects particle

charge, mainly determinant for mucosal vaccination where positively charged particles revealed improved immune responses than anionic particles [162].

Both synthetic and natural biodegradable polymers may be used. However, to date, the most popular biodegradable polymers used in vaccine applications include poly(epsilon-caprolactone) (PCL), poly(lactic acid) (PLA) or poly(lactic-co-glycolic acid) (PLGA), three synthetic polymers [19, 163]. PLGA is the most well studied and has been approved by the FDA for use as a drug delivery system since 1969. PLGA particles have been utilized to deliver a wide range of peptide antigens inducing potent immune responses [110]. One of the major drawbacks is the potential exposure of antigens to harsh organic solvents since the conventional antigen loading technique to PLGA particles involves the formation of single or double emulsions and solvent evaporation [110].

1.7.1. Natural occurring polymers – polysaccharides

Natural occurring polymers, in particular polysaccharides, have attracted attention in the mid 90's as promising platforms for antigen delivery, representing one of the main tendencies on the field of vaccine adjuvants for infectious diseases and cancer [85, 102, 103, 164]. Polysaccharides are a very diverse group of polymeric carbohydrate structures formed by long chains of monosaccharide units bound by glycosidic linkages and may differ in structure, conformation, length of the chain and the number of branches in it [165]. The natural and ubiquitous character of polysaccharides, together with their intrinsic biocompatibility, biodegradability and low reactogenicity justify their interest in the engineering of nanovaccines [85]. An advantage comparing to the synthetic polymers is that the technologies used to produce particulate systems rely on milder and simpler conditions, which minimize the use of solvents and high-energy sources, easy to scale-up and most importantly suitable for the association of labile biomolecules. These techniques usually rely on physicochemical processes such as ionic gelation, complexation and solvent displacement, among others [85].

Some polysaccharides are natural PAMPs found in the cell walls of bacteria or yeasts that activate PRRs, thus playing a vital role in both innate and adaptive immunity [75, 85, 90]. This is a characteristic that provides them intrinsic targeting abilities to APCs [85, 109] or PPs M cells that express a variety of immunosurveillance receptors on their

apical surface enabling them to be modulated through chemokines, interleukins, amines, TLRs activating molecules [166], highly benefic for a potential vaccine adjuvant candidate. As they are present in most of the whole pathogen-based vaccines, the stimulation of PRRs has been unwittingly used in vaccines for years [109]. Actually, most innate responses are directed against three classes of fungal cell wall conserved carbohydrate components: β-glucans, mannans, and chitin/chitosan [164]. In that regard, some authors have proposed the use of those polysaccharides for vaccine applications, with the caution that the natural origin of these materials is related to high variability that may lead to variable results concerning their adjuvant activity [85, 103]. The potential of these biomaterials for the vaccine adjuvant field deserves further attention. It is expected that the next few years will bring deeper knowledge in terms of mechanisms of action [85]. Therefore, and although the main focus of the present thesis is the β-glucan, the application of chitosan in the development of vaccine adjuvants will be also briefly described.

1.7.1.1. Chitosan

Chitosan is a copolymer of β-(1-4)-linked D-glucosamine (deacetylated unit) and N-acetyl-D-glucosamine (acetylated unit) monomers obtained by deacetylation of chitin present in the exoskeletons of crustaceans and cell walls of fungi (e.g. *Mucor* and *Cryptococcus*) or yeast spores (e.g. *Saccharomyces cerevisiae*). When more than 60 % of acetylated units are removed from chitin it is usually considered chitosan and, once solubized in acidic milieu, normally exhibits strong positive electrical charge [167]. The degree of deacetylation and, consequently, the number of amino groups, together with molecular weight are known factors that influence chitosan physical and biological properties [168]. Water-solubility (mostly aqueous acidic solutions with a pH ratio lower than 6.5) [169], allowing particle formulation and antigen encapsulation without the use of organic solvents, preserving antigens immunogenicity along with the strong affinity to negatively charged molecules represent the key to chitosan many talents [103, 110, 168-170]. Chitosan functional groups (amine and hydroxyl) allow facile chemical modification into chitosan derivatives (e.g. N-trimethyl-chitosan and carboxymethyl chitosan) to enhance solubility and mucoadhesivity [168, 171]. Chitosan intrinsic mucoadhesivity is conferred by the presence of amino groups that promote interaction with negatively

charged mucins facilitating adherence to mucosal membranes [171]. Additionally, chitosan is able to reversible open epithelial tight junctions promoting penetration through the mucosa [172, 173], an attractive feature for mucosal drug delivery [174, 175]. Indeed, chitosan was widely used for mucosal vaccination *in vivo* with some good results achieved (Table 1.6). For instance, feeding mice with porcine circovirus type 2 (PCV2) virus-like particles loaded into positively charged chitosan microparticles induced the proliferation of PCV2-specific splenic CD4+/CD8+ T-lymphocytes and the subsequent production of IFN-γ to levels comparable with those induced by an injectable commercial formulation [176]. It is also worth mentioning that chitosan is "generally recognized as safe" (GRAS) by the FDA.

Therefore, chitosan is the most described polysaccharide regarding polymeric particles for vaccine delivery of protein antigens [177, 178] and pDNA [179, 180], among other biomedical applications including tissue engineering and wound healing [181, 182]. Chitosan-based particles were developed for the first time in the 90s [183] and have been extensively studied ever since. Notably, although mainly used for formulation of delivery systems, chitosan-based formulations have been shown to enhance antigen uptake and presentation and to possess intrinsic immunomodulatory activities against pathogenic agents enhancing both cellular and humoral immune responses [164, 168, 170, 174, 184, 185], namely through the activation of the NRLP-3 inflammasome [186]. As an example, antigen-loaded chitosan particles significantly enhanced upregulation of surface activation markers MHC-I, MHC-II and costimulatory cytokines CD40, CD80, CD86, and CD54 and the release of proinflammatory cytokines (e.g. IL-1β, IL-6, TNF-α) as well as the proliferation of CD4+ and CD8+ T cells compared with soluble antigen [158]. Recently, Carroll *et al*. demonstrated that vaccination with chitosan as an adjuvant can promote DCs maturation by inducing type I IFNs and enhance antigen-specific Th1 and IgG2c responses [187]. Concerning HBV, preclinical studies using chitosan formulated in different types of particulate forms together with HBsAg have been extensively tested and are summarized in table 1.6. HBsAg-loaded chitosan particles already showed promising results highlighting increased serum anti-HBsAg IgG titers and the induction of IgG2c in comparison to HBsAg alone with and without co-association with immunostimulants such as CpG ODN [188-190]. Higher antigen-specific IFN-γ levels after

HBsAg recall in mice spleen cells were also reported [189]. The potential of a single-dose vaccination strategy after intraperitoneal (IP), IM or SC injection with an elicited immune response stronger and longer than the one elicited by Recombivax HB® given IP, was also shown [191]. The potential of chitosan for mucosal HBsAg vaccination was also studied, mostly through the nasal route (Table 1.6). For instance, trimethylated chitosan (TMC) derivative nanoparticles loaded with HBsAg given to mice intranasally induced higher nasal and serum antibody titers (IgG1 and IgG2a) than HBsAg alone or adsorbed onto aluminum [190]. Fewer studies evaluated the outcome following oral vaccination [145, 192, 193], mostly after particles coating with sodium alginate to provide increased stability in the acidic gastric lumen [145, 193], resulting in serum anti-HBsAg and mucosal secretions anti-HBsAg sIgA in most of the cases. Overall, chitosan is considered as one of the most advanced polymers in the regulatory path for the indication of vaccination, present in new nasal vaccine formulations against meningitis and norovirus [194-196] and in an IM vaccine hydrogel (ViscoGel) formulation against influenza that already reached clinical trials.

1.7.1.2. β-glucan

β-glucans are a group of β-D-glucose polysaccharides found in the cell walls of many organisms such as bacteria, yeasts and even some species of seaweed [197]. The most common forms are those comprising D-glucose units with β-1,3 type glycosidic bonds, from which yeast and fungal β-glucans usually contain β-1,6 side branches and cereal β-glucans contain both β-1,3 and β-1,4 backbone bonds. β-glucans have no charged functional groups and usually need to be modified to favor water solubility or to promote interaction with other molecules. Chemical alterations in the structure through derivatization may include sulfonylation, carboxymethylation, phosphorylation and acetylation, and may alter the biological activity [198]. Consistently, β-glucans from different sources are differential in their structure, branching frequency, location and length, molecular weight and shape, affecting both solubility and biological activity [199]. Additionally, the conformation also plays a crucial role on β-glucan biological activities [198]. Some β-glucans, such as the ones from *Saccharomyces cerevisiae*, *Ganoderma lucidum mycelium* and *Aureobasidium pullulans* are GRAS by the FDA and are used as food ingredients.

Table 1.6. Summary of preclinical studies using chitosan or glucan as an adjuvant for HBsAg.

Studies using chitosan with HBsAg						
Formulation	**Animal model**	**Antigen type**	**Antigen dose**	**Route**	**Immune events**	**Ref.**
Composite microspheres of alginate-chitosan-PLGA	Balb/C mice	Recombinant	10 µg	SC	Increased serum anti-HBsAg IgG to PLGA microspheres.	[200]
Chitosan particles	C57BL/6J mice	Recombinant	5 µg (2x)	SC	Increased serum anti-HBsAg IgG and IgG2c and mucosal secretions HBsAg-specific IgG; Increased HBsAg-specific IFN-γ in spleen cells.	[189]
Alginate coated or uncoated chitosan particles	BALB/c mice	Recombinant	10 µg (2x)	SC	Increased serum anti-HBsAg IgG and no signs of cell-mediated immunity. Increased IgG2a/IgG1 ratio and IFN-γ production after HBsAg recall in mice spleen cells (association with CpG ODN).	[188]
PLA microspheres with chitosan	BALB/c mice	Recombinant	1 µg (1x) 0.5 µg (1x)	SC	Increased serum anti-HBsAg IgG comparable to PLA microspheres alone.	[201]
PCL/chitosan particles	C57BL/6J mice	Recombinant	1.5 µg (2x)	SC	Higher anti-HBsAg IgG than commercially available vaccine; Higher IFN-γ and IL-17 in the spleen after HBsAg recall.	[202]
Chitosan and chitosan chloride coated PLA microspheres	BALB/c mice	Recombinant	4 µg (2x)	IP	Rapid anti-HBsAg IgG production and higher HBsAg-specific IL-2, IL-12, IFN-γ production by spleen cells compared to alum/HBsAg and PLA alone.	[203]

Table 1.6. (Continued) Summary of preclinical studies using chitosan or glucan as an adjuvant for HBsAg.

Studies using chitosan with HBsAg						
Formulation	**Animal model**	**Antigen type**	**Antigen dose**	**Route**	**Immune events**	**Ref.**
Chitosan particles	Wistar rats	Recombinant	2 µg	IM	Prolonged antigen release; Increased serum anti-HBsAg IgG.	[204]
Chitosan and γ-PGA nanogels	C57BL/6J mice	Recombinant	---	IM	Serum anti-HBsAg IgG; DCs maturation; HBsAg clearance and restored anti-HBsAg production after pAAV/HBV1.2 plasmid challenge; Increased IFN-γ+ CD8+ T cells in the spleen.	[205]
Chitosan particles	Balb/C mice	Recombinant	10 µg (2x), 10 or 20 µg (2x)	IM, IN	Increased serum anti-HBsAg IgG compared to conventional vaccine (9-fold higher).	[206]
Mannan and chitosan oligosaccharide-modified PLGA particles	Sprague Dawley Rats	Recombinant	20 µg (3x)	IN	Anti-HBsAg antibodies; Endogenous cytokine levels (IL-2 and IFN-γ) higher than SC HBsAg/alum.	[207]
Alginate coated chitosan particles	BALB/c mice	Recombinant	10 µg (3x)	IN	No serum IgG and no mucosal secretions IgA (only for association with CpG ODN); Higher IFN-γ production after HBsAg recall in mice spleen cells.	[208]
Chitosan or TMC coated PLGA particles	Balb/C mice	Recombinant	10 µg	IN	Increased mucin adsorption to TMC compared to chitosan coated particles; Increased serum anti-HBsAg IgG and mucosal secretions IgA for both (more pronounced for TMC).	[209]
PCL/chitosan particles	C57BL/6J mice	Recombinant	1.5, 5 or 10 µg (3x)	IN	Serum Anti-HBsAg IgG and mucosal secretions anti-HBsAg IgA (non-responder mice).	[210]

Table 1.6. (Continued) Summary of preclinical studies using chitosan or glucan as an adjuvant for HBsAg.

Studies using chitosan with HBsAg						
Formulation	**Animal model**	**Antigen type**	**Antigen dose**	**Route**	**Immune events**	**Ref.**
PCL/chitosan particles	C57BL/6J mice	Recombinant	1.5, 5 or 10 µg (3x)	IN	Serum Anti-HBsAg IgG and mucosal secretions anti-HBsAg IgA (non-responder mice).	[210]
Chitosan functionalized PLGA particles	Sprague Dawley Rats	Recombinant	20 µg (2x)	IN	Increased nasal residence time; Increased anti-HBsAg IgG and IL-2 and IFN-γ spleen production compared to PLGA (Th1/Th2).	[211]
Glycol chitosan and chitosan particles	BALB/c mice	Recombinant	10 µg (2x)	IN	Anti-HBsAg IgG similar to SC alum/HBsAg; Mucosal secretions anti-HBsAg IgA (not in SC alum/HBsAg)	[212]
Glycol chitosan and chitosan coated PLGA particles	BALB/c mice	Recombinant	10 µg	IN	Higher anti-HBsAg IgG, mucosal secretions sIgA and HBsAg-specific IL-2, IFN- γ and IL4 in spleen cells compared to PLGA (Th1/Th2).	[213]
TMC particles	BALB/c mice	Recombinant	10 µg (3x)	IN	Serum anti-HBsAg IgG and mucosal surfaces HBsAg-specific sIgA.	[214]
Chitosan and TMC particles	BALB/c mice	Recombinant	10 µg	IN	Higher serum anti-HBsAg IgG (also higher IgG2c) and mucosal secretions anti-HBsAg IgA for TMC.	[215]
Sodium alginate and VitB12–Chitosan coated LbL-Liposomes	BALB/c mice	Recombinant	5 µg	Oral	Higher anti-HBsAg IgG and mucosal secretions IgA compared to LBL-Lipo.	[193]

Table 1.6. (Continued) Summary of preclinical studies using chitosan or glucan as an adjuvant for HBsAg.

Studies using chitosan with HBsAg						
Formulation	**Animal model**	**Antigen type**	**Antigen dose**	**Route**	**Immune events**	**Ref.**
Alginate coated chitosan particles	BALB/c mice	Recombinant	10 µg (2x)	Oral	Higher values of the CD69 expression in CD4+ and CD8+ spleen T lymphocytes compared to HBsAg alone; Serum anti-HBsAg IgG and mucosal secretions anti-HBsAg sIgA (some non-responder mice).	[145]
Chitosan microspheres	Swiss rabbits	Recombinant	30 or 40 µg	Oral	Serum anti-HBsAg IgG.	[192]
Chitosan particles	---	Recombinant	---	---	Higher anti-HBsAg IgG compared to alum/HBsAg; Elevated numbers of BAFF-R+ B cells and CD138+ plasma cells; Increased Tfh cells.	[191]
PCL/chitosan particles	C57BL/6J mice	Recombinant and/or DNA	Recombinant: 1.5 µg (2x) DNA: 20 µg (2x)*(10 µg HBsAg)	SC SC + IN*	Increased anti-HBsAg IgG (mainly IgG1 – Th2); Increased HBsAg-specific IFN-γ and IL-17 in spleen cells.	[216]
Albumin-based chitosan particles	BALB/c mice	DNA	100 µg (14x)	Oral	Higher serum anti-HBsAg IgG and mucosal surfaces anti-HBsAg sIgA.	[217]
Chitosan particles	BALB/c mice	DNA	50 µg	IN	Lower serum anti-HBsAg IgG compared to pDNA or pDNA/alum; Increased mucosal secretions anti-HBsAg sIgA and increased endogenous IL-2 and IFN-γ in spleen compared to pDNA alone.	[218]

Table 1.6. (Continued) Summary of preclinical studies using chitosan or glucan as an adjuvant for HBsAg.

Studies using glucan with HBsAg						
Formulation	**Animal model**	**Antigen type**	**Antigen dose**	**Route**	**Immune events**	**Ref.**
Synthetic β-glucan oligosaccharide (β-glu6)	BALB/c mice	Recombinant	1 µg	IP	Enhanced Mϕ and DCs mobilization; Increased T and B cell activation in response to HBsAg; Enhanced HBsAg specific IL-4+ cells in the spleen (no effect on IFN-γ+ cells).	[219]
Curdlan sulfate	BALB/c mice	Recombinant	5 µg (3x)	SC	Increased serum anti-HBsAg IgG2a/IgG1 ratio compared to alum/HBsAg; Increased IFN-γ in spleen cells after HBsAg recall.	[220]
α-glucan	BALB/c mice	Recombinant	2 µg (2x)	IM	Increased anti-HBsAg IgG.	[221]

BAFF-R, B cell activating factor receptor; IM, intramuscular; IN, intranasal; IP, intraperitoneal; Mϕ, macrophages; PLA, poly(lactic acid); PLGA, poly(lactic-co-glycolide; SC, subcutaneous; TMC, trimethylated chitosan.

β-glucans have been reported to possess immunological, anti-tumor and anti-infection activities mostly relevant for vaccination purposes. Although the immunostimulatory properties were recognized long before the discovery of PPRs, stimulation of those receptors is the most recognized biological effect. β-glucans are PAMPs recognized by TLR2/6, Dectin-1, CR3 (complement receptor 3), scavenger (scav) and lactosylceramide (LacCer), triggering intracellular signaling activation followed by expression of immune-related molecules that regulate innate and adaptive immunity (Figure 1.5) [85, 222, 223]. CR3 activation, although not yet fully understood, leads to complement activation resulting in fungal opsonization and the generation of chemotaxins which can recruit inflammatory cells, followed by internalization of the structures [197]. On the other hand, signaling through Dectin-1, the most studied β-glucan receptor, mediates processes such as reactive oxygen species (ROS), cytokine production and pathogens internalization via phagocytosis [197, 224, 225]. Additionally, interaction mediated by CLRs (e.g. Dectin-1) is

known to facilitate further cross-presentation of the antigen in MHC-I [77]. Dectin-1 receptor is widely expressed by immune cells including monocytes, macrophages and DCs [226]. Thus, Dectin-1 recognition gives β-glucans interesting targeting capacities to enhance specific immune responses, through the modulation of both innate and adaptive immunity, usually promoting Th17 cell differentiation and cytotoxic T cell responses [227-229]. Indeed, several approaches have been successfully tested using β-glucans for Dectin-1 targeting. Dube *et al*. reported increased intracellular delivery of the encapsulated anti-tuberculosis drug and enhanced proinflammatory reaction after chitosan-coated PLGA particles functionalization with 1,3-β-glucan [230]. Targeting Dectin-1 receptor augmented and modulated the elicited immune response as demonstrated by Lipinski and coworkers [225]. A tricomponent mannan tetanus toxoid laminarin conjugate vaccine resulted in enhanced IgG antibody titers recognizing *candida albicans* and broad subclass distribution, comparing to the same formulation without the laminarin, after IP or SC administration. Moreover, these authors showed that this new conjugate antigen promoted receptor-based DCs uptake mediated by the interaction of laminarin with the Dectin-1 receptor, resulting in enhanced IL-6 and TGF-β production, known activators of Th17 cells. Concerning Dectin-1 activation, although both soluble and particulate β-glucans bind to the receptor, only the latter activates the downstream signaling [224], confirming the importance of a particulate form for an adjuvant. Coherently, TNF-α release, the hallmark of Dectin-1 activation, was only induced by a soluble β-1,3-glucan when it was covalently attached to the surface of polystyrene beads [231]. Additionally, β-glucan particle size may be critically important in orchestrating the nature of the immune response to fungi, influencing the secretion of cytokines from DCs. It was recently showed that large β-glucan-stimulated human DCs generate significantly more IL-1β, IL-6, and IL-23 compared to those stimulated with the smaller β-glucans [232].

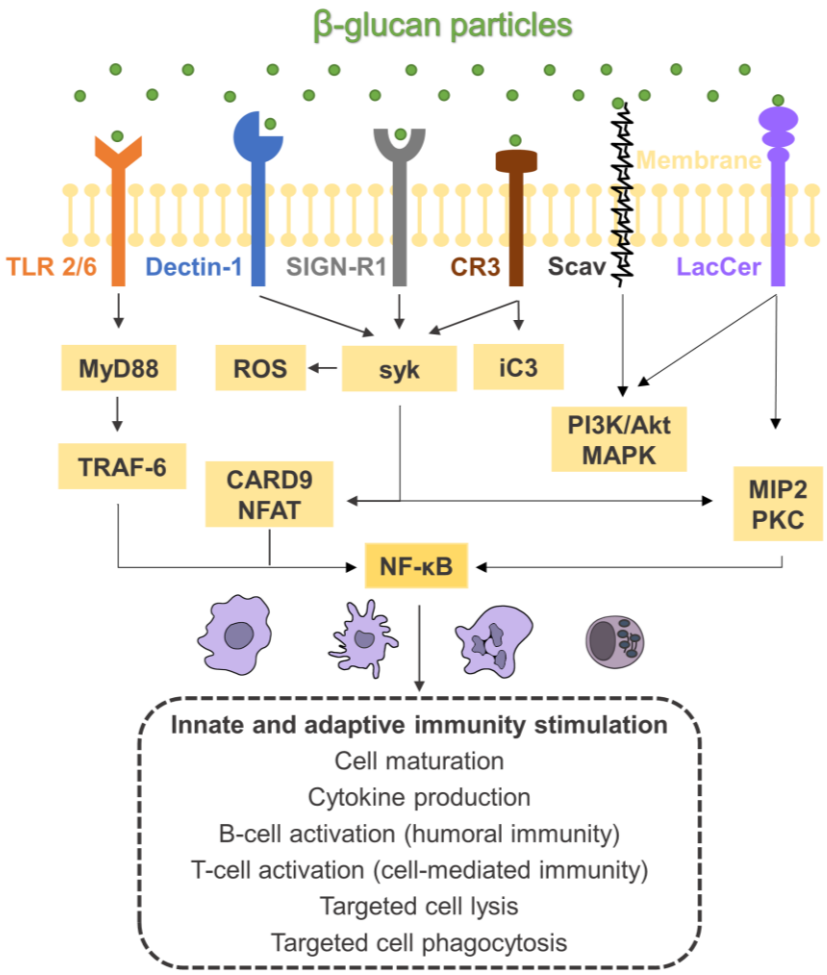

Figure 1.5. Receptor mediated immune cell activation by β-glucan particles. Particulate β-glucans can activate a variety of membrane receptors found in immune cells (e.g. macrophages, dendritic cells, natural killer cells and neutrophils) that commonly include TLR2/6, Dectin-1, CR3 (complement receptor 3), scavenger (scav), dendritic cell-specific intercellular adhesion molecule-3-grabbing non-integrin -related 1 (SIGN-R1); and lactosylceramide (LacCer). The activation of those receptors will trigger intracellular signaling activation followed by the expression of immune-related molecules (e.g. TNF-α), cell maturation, B and T cell activation, and targeted cells phagocytosis and lysis that collectively regulate both innate and adaptive immunity. *Akt, protein kinase B; CARD9, caspase-associated recruitment domain 9; iC3, third intracellular loop; MAPK, mitogen-activated protein kinase; MIP-2, macrophage inflammatory protein 2; MyD88, myeloid differentiation primary response 88; NFAT, nuclear factor of activated T-cells; NF-κβ, nuclear factor-κβ; PI3K, phosphoinositide 3-kinase; PKC, protein kinase C; ROS, reactive oxygen species; syk, spleen tyrosine kinase; TRAF-6, TNF receptor associated factor 6.* Adapted from [223].

Most research in terms of immunomodulatory properties has been done with β-1,3 or β-1,6-glucans such as curdlan (from *Alcaligenes faecalis*), laminarin (from *Laminaria digitata*), lentinan (from *Lentinus edodes*), pleuran (from *Pleurotus ostreatus*) and zymosan (from *Saccharomyces cerevisiae*) [164, 197]. Regarding HBV vaccination, few

studies (two, to be more specific) have tested the adjuvant effect of β-glucans for the HBsAg (Table 1.4). Co-administration of curdlan sulfate with HBsAg induced a shift toward a Th1-biased immune response following mice vaccination, demonstrated through IFN-γ increase after HBsAg recall and higher serum IgG2a/IgG1 ratio compared to alum [220]. The authors suggested the potential immunotherapeutic application for HBV. Others showed that the co-administration of a synthetic β-glucan oligosaccharide (β-glu6 – analogue of lentinan basic unit) with HBsAg enhanced mobilization and maturation of macrophages and DCs, increased HBsAg specific T and B cell responses in mice spleen cells after HBsAg recall. However, a Th2 biased immune response was detected based on serum IgG1/IgG2a ratio and the increase in IL-4-producing cells and not IFN-γ-producing cells [219]. The same authors have later reported that co-administration of β-glu6 with a DNA vaccine encoding HBcAg have promoted the recruitment and maturation of DCs, enhanced the activation of CD8+ and CD4+ T cells and increased the number of CD8+/IFN-γ+ in lymphoid and non-lymphoid tissue in vaccinated mice. Additionally, anti-HBcAg IgG and IgG2a antibody titers were also increased, suggesting that β-glu6 is a candidate adjuvant in DNA vaccination enhancing virus-specific CTLs and Th1-biased responses [233]. On the other side, the addition of yeast-derived β-glucan (dietary supplement) to recombinant hepatitis B vaccination (Genhevac-B®) showed no beneficial effect on antibody titers and seroconversion rate in chronic renal failure patients, that have impaired immune system [234]. Additionally, some studies show some evidence that β-glucans non-specific immune effects can be beneficial for CHB. Indeed, β-glucan containing dietary supplements (mushroom polysaccharide extracts) can play a role in the treatment of hepatitis B improving the efficacy of antiviral therapies [235] or normalizing liver functions of CHB patients [236]. Recently, it was reported that mushroom lectin stimulated innate immunity by activating TLR6 signaling of DCs and enhancing HBV-specific antibody levels and Tfh response that overcame HBV tolerance in transgenic mice, suggesting a therapeutic approach to break HBV tolerance [237]. Interestingly, β-glucans are also TLR6 agonists, possibly sharing these mechanisms. Lastly, it was demonstrated that daily oral administration of yeast-derived glucan particles (GPs) for 9 weeks to mice resulted in macrophages, DCs and effector T cells recruitment to the liver microenvironment accompanied by enhanced production of Th1 cytokines in liver

interstitial fluid (TIF) associated with GPs accumulation in the liver, a very promising result for further development of therapeutics against HBV [238].

1.7.1.2.1. Yeast-derived β-glucan particles

The use of the commonly designated glucan particles (GPs) as a particulate delivery system of a payload molecule, optionally, but typically including a payload trapping molecule was firstly described by Gary Ostroff [239] and extensively explored since then. GPs are highly purified hollow porous cell wall shells derived from *Saccharomyces cerevisiae* (baker's yeast) following a series of hot alkali and organic extractions, primarily composed of β-1,3-glucan free of mannans and proteins, containing some chitin and β-1,6-glucans. The extracted GPs are readily available, biodegradable, substantially spherical particles about 2-4 μm in diameter targeted to phagocytic cells, such as macrophages and cells of lymphoid tissue primarily due to their β-glucan content as an effective vaccine platform [239]. In fact, polymer-complexed cores can be constructed within the hollow GPs, enabling the delivery to DCs and macrophages of a wide variety of "payload" classes including proteins, siRNA, DNA, and other small molecules [228, 240-243]. The β-1,3-glucan outer shell provides a Dectin-1 mediated delivery and GPs were early designated as a macrophage targeted delivery system [240, 242, 244]. In addition, GPs stimulate macrophages to secrete cytokines such as TNF-α, monocyte chemotactic protein-1 (MCP-1), and IL-6 [245]. These proinflammatory cytokines can potentially link the activation of both innate and adaptive immunity. GPs have been used for macrophage-targeted delivery of a wide range of payloads (DNA, siRNA, protein, small molecules and nanoparticles) encapsulated inside the hollow GPs via core polyplex and layer-by-layer (LbL) synthetic strategies [228, 229, 240, 241, 243] or bound to the surface of chemically derivatized GPs [242]. Recently, macrophage targeting of gallium nanoparticles using GPs provides more efficient delivery of gallium and inhibition of human immunodeficiency virus (HIV) infection in macrophages compared to free gallium nanoparticles [246].

The potential adjuvant effect was extensively studied using ovalbumin (OVA) trapped with yeast RNA through electrostatic interactions within GPs following repeated SC administrations in mice [228, 229, 241] which showed robust and long-lasting antigen-

specific humoral and T cell responses were consistently observed. Specifically, GP-OVA induced secretion of Th1-associated IgG2c anti-OVA antibodies and induced strong humoral and Th1- and Th17-biased CD4+ T cell responses. In contrast, mice that received OVA admixed with alum predominantly exhibited IgG1 antibody responses [247], consistent with alum being a poor stimulator of T cell responses. In the regard of desired antigen sparing, submicron antigen doses still elicited vigorous Th1- and Th17-biased CD4+ T cell and antibody responses. Finally, it also demonstrated the function of GPs as both a delivery system and an adjuvant; as antibody and T cell responses are seen when GPs and OVA are admixed but are substantially greater when OVA is encapsulated within the GPs [229]. Additionally, the strong secretion of IFN-γ and IL-17 cytokines was further associated with protective immunity against the highly virulent strains *Cryptococcus neoformans* and *Criptococcus gatti* lethal challenge after SC vaccination with GPs-based vaccine [248]. Consistently, robust Th1 and Th17-biased CD4+ T cell recall responses were observed in the lungs of vaccinated and infected mice. GPs were also reported as a new DNA delivery technology based on the *in situ* LbL synthesis of a RNA/(Poly)ethylenimine (PEI) core followed by a DNA layer with a protective layer of PEI within hollow GPs, providing protection and facilitating oral and systemic receptor-targeted delivery of DNA payloads to phagocytic cells [243]. GPs were also suggested as good candidate for macrophage-targeted oral delivery protecting the encapsulated agent from enzymatic degradation [240, 244, 249, 250], suggesting an immunotherapeutic applicability. Orally administered GPs are ingested by gastrointestinal macrophages and then transported to spleen and bone marrow [251]. Moreover, GPs were recently seen as good candidates for mucosal antigen delivery [125, 249]. Oral administration of GP-OVA in mice stimulated spleen IL-17 expression significantly and increased OVA-specific IgA, sIgA and secretory component production in intestinal fluids [249]. However, systemic antibodies were only achieved after parenteral administrations [228, 229, 252, 253]. To date, no study was found testing GPs for oral vaccination with HBV antigens.

Consistently, heat-killed *Saccharomyces cerevisiae* genetically engineered to express antigens are undergoing clinical trials as immunotherapeutic vaccines for chronic infections such as HBV (Table 1.1) [69-71]. However, because yeast proteins, lipids, and nucleic acids are not eliminated, concerns regarding reactogenicity and autoimmunity

could limit the appeal of this platform as a preventive vaccine given to predominantly healthy people [164]. Stimulation of peripheral blood mononuclear cells (PBMCs) isolated from CHB patients or from HBV vaccine recipients with autologous DCs pulsed with Tarmogen® expressing HBV X-S-Core or a related product (S-Core) resulted in pronounced expansions of HBV-specific T cells possessing a cytolytic phenotype. These data indicate that X-S-Core-expressing yeast elicit functional adaptive immune responses and supports the ongoing evaluation of this therapeutic vaccine in patients with CHB to enhance the induction of HBV-specific T cell responses [69]. GlobeImmune's Tarmogen® immunotherapy platform consists of intact, heat-inactivated yeast containing a target protein. Those vaccines elicit immune-mediated killing of target cells expressing viral and cancer antigens *in vivo* via a CD8+ mediated mechanism. Tarmogens are not neutralized by host immune responses and can be administered repeatedly to boost antigen-specific immunity. Tarmogens are a versatile technology for the treatment of chronic hepatitis B and C and showed to be well tolerated and immunogenic in phase 1 and 2 clinical trials encompassing >600 subjects [254]. Overall, β-glucans intrinsic properties increased the interest of their use for vaccine development as better demonstrated elsewhere [85]. However, the real potential of β-glucans in this field has yet to be demonstrated.

1.8. Rationale behind the thesis

Regarding the hepatitis B disease, the WHO goal is to eliminate HBV as a public health threat by 2030. However, some major problems have been identified in the front line against HBV infection: 1) the high prevalence of HBV transmission in developing countries, mostly due to ineffective implantation of vaccination programs and mother-to-child transmission; and 2) the lack of an effective treatment, mostly due to the difficulty to reach HBV clearance with current antivirals. Therefore, and considering that immune responses are critically involved from infection to disease establishment, new immunomodulatory therapies must be developed to take the place of currently available ineffective therapies. With the support of vaccine technology, we hypothesized that the development of potent adjuvants may help both the neonate immature immune system and the exhausted CHB immune system seeking effective prophylaxis or therapy, respectively. Additionally, potent adjuvants may also help the development of effective DNA (with non-viral vectors) and oral vaccines, both associated with improved

formulation stability. Indeed, heat-stable and freeze-stable hepatitis B vaccines will aid to increase vaccine coverage in developing countries, where the cold chain transportation is not readily available. DNA vaccines are also associated with CTLs differentiation, advantageous for therapeutic purposes. Mimicking pathogen properties may be a requisite to polarize sustained HBsAg-specific immunity towards Th1 antiviral protection. In that regard, β-glucan was chosen to be the fundamental immunomodulatory constituent of the particulate adjuvant system (Figure 1.6). Additionally, chitosan was chosen to create blend β-glucan/chitosan particulate systems conferring additional immunostimulatory properties and the possibility to load bioactive molecules. Chitosan particles were also developed in the same conditions for comparison purposes, as the experience of our group suggests that strong cell-mediated immune responses are hard to achieve using chitosan particles (with approximately 400 nm) as an adjuvant for the HBsAg [188, 189]. Importantly, both, chitosan and β-glucans are generally recognized as safe (GRAS) by the FDA, an important notice as the long-term goal is to develop human vaccines.

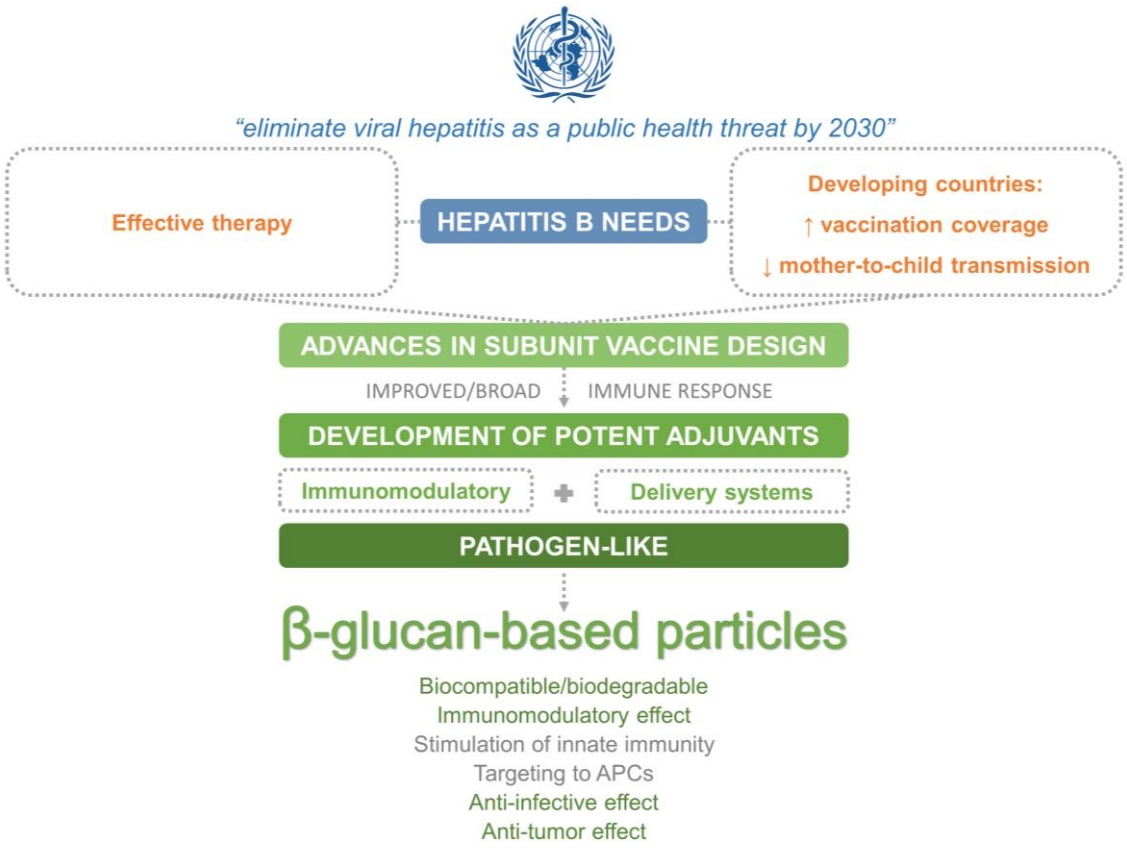

Figure 1.6. Rationale behind the thesis.

1.9. Aim and outline of the thesis

To meet the current needs of hepatitis B, the present thesis aimed to develop, characterize and evaluate the adjuvant effect of β-glucan-based particulate delivery systems for the HBsAg. A direct comparison with chitosan-based particulate delivery systems or no adjuvant was often done.

Chapter 2 describes both yeast-derived β-glucan and chitosan particle design for oral delivery of the HBsAg, including particle physicochemical characterization, *in vitro* stimulatory properties and internalization in immune cells, PPs uptake and *in vivo* evaluation of the potential adjuvant effect following oral vaccination.

Chapter 3 describes the use of a polymeric vector (1PDMAEMA:4PβAE) for pDNA condensation in the presence or not of β-glucan, including polyplex optimization and characterization, *in vitro* transfection activity and *in vivo* evaluation of the potential adjuvant effect following SC vaccination, using a pDNA encoding the HBsAg.

Chapter 4 describes the development of blend β-glucan/chitosan and chitosan particles, including particle physicochemical characterization, *in vitro* internalization in immune cells and *in vivo* evaluation of the potential adjuvant effect following SC vaccination.

Chapter 5 describes the use of the adjuvants developed in Chapter 4 and the yeast-derived β-glucan particles following a different vaccination schedule, including *in vitro* stimulatory properties and internalization in immune cells and *in vivo* evaluation of the potential adjuvant effect following SC vaccination.

Chapter 6 presents the general discussion and concluding remarks about the whole implication of the present thesis.

Chapter 7 contains all the references of the present thesis.

CHAPTER 2

ORAL HEPATITIS B VACCINE: CHITOSAN- OR β-GLUCAN-BASED DELIVERY SYSTEMS FOR EFFICIENT HBSAG VACCINATION FOLLOWING SUBCUTANEOUS PRIMING

Adapted from: Soares E, Jesus S and Borges O. Oral hepatitis B vaccine: chitosan or glucan based delivery systems for efficient HBsAg immunization following subcutaneous priming. International Journal of Pharmaceutics. 535 (1-2). 2017. DOI10.1016/j.ijpharm.2017.11.009.

Abstract

The World Health Organization (WHO) encourages "*the development of oral formulations to simplify their transport, storage and administration in poor countries"*, and to *"facilitate an effective immunization program to prevent sexually transmitted hepatitis B"*. Therefore, two distinct and promising delivery systems were developed: recombinant hepatitis B surface antigen (HBsAg) encapsulated into glucan particles (GPs) mainly composed of β-1,3-D-glucan and into alginate coated chitosan particles (AlgChiPs). *In vitro* preliminary studies showed that both could be internalized by peripheral blood mononuclear cells (PBMCs) and murine Peyer's patches (PPs), an imperative aspect regarding oral vaccination. Chitosan particles (ChiPs) have shown interesting immunostimulatory properties as mast cells activators. Vaccination studies reveal that three oral immunizations induced serum anti-HBsAg Immunoglobulin G (IgG) in 60 % of the animals and anti-HBsAg secretory IgA in faeces for both formulations. When a subcutaneous (SC) priming was done, followed by two oral boosts, all mice responded to the vaccine with higher serum anti-HBsAg IgG titers, besides mucosal protective immunity.

Keywords

Hepatitis B, oral vaccine, alginate coated chitosan particles, β-glucan particles.

Graphical Abstract

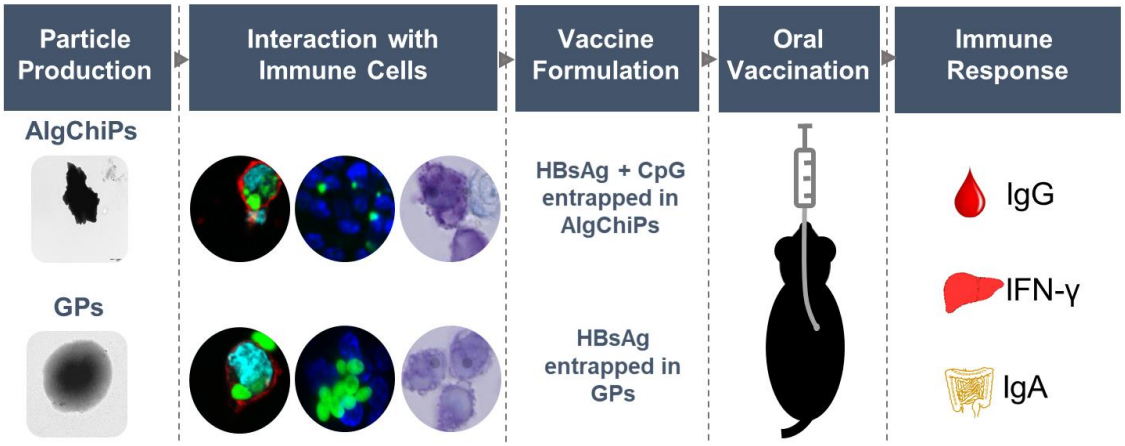

2.1. Introduction

The WHO estimates that 887 000 peopled died in 2015 related to the hepatitis B virus (HBV) [255], mostly from developing countries. The limited use of current licensed injectable HBV vaccines in those countries could be overcome by the development of stable oral formulations. Oral vaccines are seen as an economically feasible approach to mass vaccination regarding easier and safer administration and, theoretical better stability that would facilitate shipping and storage [124, 256]. Additionally, mucosal vaccination induces a double layer of immunity, both systemically and at mucosal surfaces through the generation of strong secretory IgA (sIgA) (resistant to protease and nuclease activity) associated with prolonged protection to viral infections [175]. This is mostly relevant for sexually transmitted HBV, the major route of dissemination in low endemic areas. Although no oral protein vaccine is currently approved, mainly due to oral tolerance or poor antigen immunogenicity/degradation in the gastrointestinal tract [257], antigen encapsulation in polymeric particles to improve antigen stability/bioavailability and to act as an adjuvant can be a vital tool to surpass all those hurdles [158, 175]. Indeed, some promising results for HBV oral vaccination have already been published using polymeric delivery systems [145, 258-260].

Therefore, the first aim of the present work was to prepare and evaluate for the first time, the outcome of β-glucan particles (GPs) as an adjuvant for HBsAg oral vaccination. The GPs are porous micrometer-sized shells derived from baker's yeast (*Saccharomyces cerevisiae*) cell walls [261]. The particles have the ability to target the loaded antigen to antigen presenting cells (APCs), as their β-1,3-D-glucan surface composition selectively binds to Dectin-1 receptor and Toll-like receptor (TLR)2, highly expressed on innate immune cell surface [250, 262, 263]. The potential of GPs for HBsAg oral vaccine delivery has never been evaluated, but the scientific literature suggests that they are an optimal oral vaccine platform for model antigens [125, 249, 264, 265], protecting the encapsulated agent from gastrointestinal conditions [249, 250, 264] and eliciting a robust humoral response in the intestine, characterized by the production of antigen specific sIgA [249]. Nevertheless, systemic immune responses were only elicited following parenteral administrations [228, 229, 252, 253]. On the other side, the second aim was to compare the GPs efficacy with a chitosan-based delivery system, as our

research group is widely experienced with chitosan-based particles and HBsAg vaccination through several routes [145, 184, 188, 189, 208, 210, 216, 266, 267]. Chitosan is a widely used hydrophilic polymer for particle preparation, allowing antigen encapsulation in an aqueous environment. It is a biodegradable polycationic polymer with interesting immunostimulatory and mucoadhesive properties, directing both cellular and humoral immune responses [170, 174], and therefore seen as a potential adjuvant for mucosal vaccines [175]. Chitosan-based particles mediated oral delivery is limited due to its solubility at the acidic pH of gastric lumen, leading, most probably, to the antigen release in the stomach. To provide the particles with greater stability, sodium alginate coating is frequently performed, as it is an acid insoluble polymer [148, 268]. A previous study from our group showed that oral vaccination with HBsAg loaded in alginate coated chitosan particles led to significant induction of anti-HBsAg IgA in the gut and systemic specific antibodies in less than 20 % of the mice. In the same study, when CpG oligodeoxynucleotide (ODN) loaded particles were added to the formulation, 40 % responder mice were observed [145]. In fact, combined use of protein antigens and CpG emerged as one of the innovative approaches for adjuvant development. Synthetic ODNs containing unmethylated CpG motifs trigger cells that express TLR9 to mount innate immune responses characterized by the activation and maturation of dendritic cells (DCs) and B cells differentiation into antibody-secreting plasma cells [269]. Therefore, in the present work we decided to improve the previous developed formulation, co-entrapping both the HBsAg and the CpG in the same particle. In fact, their temporal and physical proximity is an important requirement for an effective adjuvant effect [270], and can contribute to increase the low seroconversion rate observed before.

Prior oral vaccination studies, the ability of both delivery systems to be internalized by APCs and PPs, key mechanisms in the development of mucosal immune responses toward vaccine antigens, was evaluated. The capacity to activate mast cells, sentinels of infection strategically located close to host-environment interface such as mucosal tissues, directing immune modulation [271], was also tested.

2.2. Materials and methods

2.2.1. Materials

Chitosan (ChitoClear™ - 95 % DD and 8 cP viscosity measured in 1 % solution in 1 % acetic acid) was purchased from Primex BioChemicals AS (Avaldsnes, Norway) and purified as previously described [272]. A low molecular weight (18 kDa) pharmaceutical grade sodium alginate (MANUCOL LB® - 61 % mannuronic acid and 39 % guluronic acid) was kindly donated by ISP Technologies Inc. (Surrey, UK). Mauripan *Saccharomyces cerevisiae* was kindly donated by AB MAURI (Moita, Portugal). The HBsAg, subtype adw of approximately 25 kDa was acquired from Aldevron (Fargo, ND, USA). Buffy coats from healthy donors for PBMCs isolation were kindly given by IPST IP (Coimbra, PT). The HMC-1 cells were kindly provided by Dr Butterfield, Mayo Clinic (Rochester, MN, USA). The human epithelial colorectal adenocarcinoma cell line Caco-2 was acquired from American Type Culture Collection (ATCC) (Manassas, VA, USA). CpG ODN 1826 solution was acquired from InvivoGen (California, USA). Lymphoprep™ was acquired from Axis-Shield (Dundee, Scotland). Sodum azide, phenylmethylsulfonyl fluoride (PMSF), trypsin-EDTA, fetal bovine serum (FBS), trypsin, penicillin streptomycin (PenStrep), Image-iT™ LIVE Plasma Membrane and Nuclear Labeling Kit (Hoechst 33342 and Alexa Fluor® 594) was acquired from Life Technologies Corporation (Paisley, UK). N-Acetyl-β-D-Glucosaminidase (NAG), Iscove's Modified Dulbecco's Medium (IMDM), Dulbecco's modified eagle medium (DMEM), 5-([4,6-Dichlorotriazin-2-yl]amino) fluorescein hydrochloride (DTAF), Compound 48/80 (C48/80 - #021M4011V), *torula* yeast type IV (tRNA), 3-(4,5-Dimethylthiazol-2-yl)-2,5-Diphenyltetrazolium Bromide (MTT), bovine serum albumin (BSA) and o-Phenylenediamine dihydrochloride (OPD) were acquired from Sigma-Aldrich Corporation (St. Louis, MO, USA). Fluorescein isothiocyanate (FITC) was acquired from Santa Cruz Biotechnology (Santa Cruz, CA, USA). Goat anti-mouse HBsAg (ad/ay) horseradish peroxidase (HRP) was acquired from Meridian, Life Science®, Inc. (Memphis, TN, USA). IgG2c, IgG1 and IgG3 HRP were purchased to Rockland Immunochemicals Inc. (Limerick, PA, USA.). Murine interferon (IFN)-γ standard ABTS ELISA development kit was acquired from PeproTech (Rocky Hill, NJ, USA). Mouse IgA ELISA Quantitation Kit and IgG HRP were acquired from Bethyl Laboratories Inc. (Montgomery, TX, USA). Micro BCA assay kit was

obtained from Pierce Chemical Company (Rockford, IL, USA). All the other used reagents were of analytical grade.

2.2.2. Particle production

Chitosan-based particles (ChiPs) [273] and alginate coated ChiPs (AlgChiPs) were obtained using a preparation method similar to the previous studies from our group [148, 208], with some modifications. Briefly, chitosan was dissolved at a concentration of 0.1 % (w/v) in sodium acetate buffer 25 mM, pH 5.0 (1.36 g of sodium acetate anhydrous for 1 L of water and pH corrected using 1 M acetic acid solution). Particle formation was achieved after the addition of a sodium sulfate (0.625 % w/v) crosslink solution to the previous chitosan solution in a proportion of 1:1 (v/v), under vortex agitation. The resulting suspension maturated at room temperature (RT°) for 1 h and was further centrifuged for 25 min at 4500 x *g*. After that, the supernatant was discarded, and the pellet collected represented the ChiPs. ChiPs were resuspended in water and washed twice (centrifuging 25 min at 4500 x *g*) to remove exceeding compounds. AlgChiPs were obtained by mixing equal volumes of the ChiPs suspension and a sodium alginate solution (1 % w/v) in the acetate buffer pH 5.0, under magnetic stirring for 20 min. The suspension was finally centrifuged for 10 min at 461 x *g* and the supernatant was discarded. The pellet was further resuspended in Mili-Q water and washed twice (centrifuging 10 min at 461 x *g*) to remove the exceeding sodium alginate. Then, the pellet formed was resuspended in 2 mL of Mili-Q water and 60 µL of an 18 mM calcium chloride solution was added dropwise under vortex agitation, inducing gel formation as Ca^{2+} ions act as an alginate chain crosslink agent. To prepare the formulations for *in vivo* studies, the HBsAg was incubated with the crosslink solution (sodium sulfate – at 0.00055 % for SC formulations and at 0.004 % for oral formulations) prior ChiPs production. After that, HBsAg loaded ChiPs were incubated for 30 min with 2 mL of a CpG solution (at 0.0037 % for SC formulations and 0.002 % for oral formulations) to provide CpG adsorption to particle surface. At this point, HBsAg/CpG loaded ChiPs were ready for SC administrations (100 µL per animal at 2730 µg/mL ChiPs, 15 µg/mL HBsAg and 100 µg/mL CpG) or proceed to sodium alginate coating as described above (AlgChiPs) for oral administrations (300 µL per animal at 1667 µg/mL ChiPs, 67 µg/mL HBsAg and 33 µg/mL CpG).

GPs were produced from *Saccharomyces cerevisiae* by successive alkaline and acidic treatments which hydrolyses the outer cell wall and intracellular components as described by Soto and Ostroff [243] with minor modifications, resulting in hollow porous yeast cell walls mainly composed of β-glucans. Briefly, 20 g of *Saccharomyces cerevisiae* were suspended in 200 mL of NaOH 1 M and heating to 85 °C for 1 h, under rotational stirring. The insoluble material containing the yeast cell walls was collected by centrifugation at 2000 x *g* for 10 min. This procedure was repeated three times, with the third time just for 10 min. Then, the insoluble material was suspended in 200 mL of Mili-Q water and the pH brought to 4-5 with HCl and heated to 75 °C for 1 h. After that, the insoluble material was recovered again by centrifugation and washed three times in 200 mL of Mili-Q water, three times with 40 mL of isopropanol and twice with 40 mL of acetone and let dry at RT°. HBsAg loading in GPs was performed according to De Smet *et a*l. [249], with some modifications. Briefly, 6.5 mg or 3.5 mg of GPs were swollen with 65 µL or 49 µL of HBsAg in 0.9 % saline (0.395 µg/µL) for 2 h at 4 °C, allowing HBsAg diffusion into the hollow GPs cavity. GPs were frozen at -20 °C and lyophilized overnight (ON). Then, 65 µL or 35 µL of 25 mg/mL tRNA in TEN buffer (50 mM Tris-HCl, pH 8, 2 mM EDTA and 0.15 M NaCl) were added and incubated 30 min at 30 °C. After that, 260 µL or 140 µL of 10 mg/mL tRNA in TEN buffer were added and incubated 1 h at 30 °C. At the end, particles were then centrifuged (10 min at 2000 x *g*) to wash residual amounts of tRNA and suspended in Mili-Q water for SC (100 µl per animal at 2730 µg/mL GPs and 15 µg/mL HBsAg) or oral (300 µL per animal at 1667 µg/mL GPs and 67 µg/mL HBsAg) administrations.

For fluorescent particle preparation, GPs were labeled with DTAF, according to Huang *et al*. [274]. Briefly, 20 mg of GPs were suspended in borate buffer pH 10.8 (49.1 mL 0.1 M NaOH + 50.9 mL 0.05 M sodium tetraborate). Then, 20 mg of DTAF were dissolved in 500 µL of dimethyl sulfoxide (DMSO), added to the GPs suspension and incubated ON under magnetic stirring in the dark. After that, the GPs suspension was extensively washed by centrifugation (10 min, 2000 x *g*) until the supernatant was clear, to eliminate the exceeding DTAF. Chitosan was labeled with FITC, as previously described [210] and used to prepare both ChiPs and AlgChiPs. Chitosan was labeled by mixing 35 mL of dehydrated methanol containing 25 mg of FITC to 25 mL of a 1 % (w/v) chitosan in 0.1

M acetic acid. After 3 h of reaction in the dark at RT°, the FITC labeled chitosan was precipitated with 0.2 M NaOH until pH 10 and collected following centrifugation for 30 min at 4500 x *g*. The resultant pellet was washed three times with a mixture of methanol:water (70:30, v/v). The FITC-chitosan was resuspended in 15 mL of 0.1 M acetic acid, stirred ON, and was further dialyzed in the dark against 2.5 L of distilled water for 3 days before freeze-drying (FreezeZone 6, Labconco, Kansas City, MO, US).

2.2.3. HBsAg and CpG loading efficacy

The loading efficacy (LE) of HBsAg and CpG was calculated by an indirect way, quantifying the unbound HBsAg or CpG remaining in the supernatant as described before [208] and represented in Eq. 2.1. HBsAg was determined by a direct ELISA method. After an ON incubation, samples were washed five times with PBS-T (PBS (phosphate buffer saline pH 7.4) containing 0.05 % Tween™ 20) and blocked with 200 µL of 1 % BSA in PBS-T for 1 h at 37 °C. HBsAg was detected using the goat anti-HBsAg HRP (1:5000 dilution) in a 30 min incubation at 37 °C followed by extensively washing and substrate OPD solution (5 mg OPD to 10 mL citrate buffer and 10 µL H_2O_2) incubation for 10 min at RT° in the dark. Reaction was stopped with 1 M H_2SO_4 and absorbance was determined at 492 nm. CpG was quantified by the measurement of the optical density (OD) of the supernatants at 260 nm also by means of the Eq 2.1, using the supernatant of unloaded particles to eliminate background interference.

$$\text{LE (\%)} = \frac{\text{total}_{\text{HBsAg/CpG}}\ (\mu g/mL) - \text{free}_{\text{HBsAg/CpG}}\ \text{in supernatant}\ (\mu g/mL)}{\text{total}_{\text{HBsAg/CpG}}\ (\mu g/mL)} \times 100 \quad \text{(Eq. 2.1)}$$

2.2.4. Size, zeta potential and morphological analysis

Antigen loaded and unloaded particle size and zeta potential were measured using a Delsa^{TM} Nano C particle analyzer (Beckman Coulter, CA, USA) by dynamic light scattering (DLS) at 25 °C and backward scattering angle of 173° (presented as normalized intensity distribution) and electrophoretic light scattering (ELS) (calculated by Smoluchowski approximation), respectively. Transmission electron microscopy (TEM) of unloaded particles was performed placing the particle suspension in copper grids and analysed using a JEOL JEM 1400, 120 kV (JEOL, Peabody, MA, USA).

2.2.5. Uptake by peripheral blood mononuclear cells

Peripheral blood mononuclear cells (PBMCs) were obtained from healthy donors in heparinized syringes followed by serum depletion and isolated on a density gradient with Lymphoprep™, according to providers' guidance protocol, with minor modifications. The blood was diluted in 0.9 % saline solution in a proportion of 1:5. The tubes were centrifuged for 20 min at 1190 x *g* and 20 °C, and the mononuclear dense ring was carefully aspirated and diluted in PBS pH 7.4, at 37 °C, in a proportion of 1:10. Cell suspensions were washed through consecutive centrifugations (10 min, at 487 x *g* and 20 °C), until the supernatant was clear. After that, cells were suspended in Roswell park memorial institute medium (RPMI) 1640 supplemented with 1 % PenStrep and 10 % heat inactivated FBS and seeded in 24-wells plates at a concentration of $1x10^6$ cells/mL. After 2 h incubation, non-adherent cells were aspirated and washed twice with supplemented RPMI, and 1 mL of ice-cold PBS, was added to each well and incubated at 4 °C for 20 min. After incubation, the wells were washed again with 1 mL of ice-cold PBS, immediately replaced by 1 mL of supplemented RPMI at 37 °C and incubated ON. The uptake was performed following an incubation of 40 µL of a 500 µg/mL FITC labeled particles suspension for 4 h, after which cells were washed with 100 µL of PBS, detached with 100 µL of 5 x trypsin and inactivated by 100 µL of supplemented RPMI. Cells from 12 wells were pooled in the same tube, centrifuged for 20 min at 487 x *g* at 20 °C, and resuspended in 200 µL of ice-cold PBS for further cytometry analysis. Cells were split in two analysis tubes: one where 1 µL of 50 µg/mL PI solution was added and the other where 100 µL of 0.4 % trypan blue solution were added prior BD FACSCalibur Flow Cytometer analysis (BD Biosciences, San Jose, CA, USA). The fluorescence data for a population of 20000 lymphocytes was collected and the results processed by CellQuestModfit LT software. To observe PBMC particle uptake cells were seeded on glass coverslips in 12-well plates at a density of $1x10^6$ and incubated ON prior assay, performed as described above. After particle incubation, cells were washed three times with PBS and fixed with 4 % formaldehyde (FA) in PBS for 15 min at 37 °C. The nucleus and cell membrane were labeled using Image-iT™ LIVE Plasma Membrane and Nuclear Labeling Kit, according manufacturer's instructions. After labeling, cells were washed twice with PBS and the coverslips mounted in microscope slides with DAKO mounting medium.

Samples were examined under an inverted laser scanning confocal microscope (LSCM) (Zeiss LSM 510 META, Carl Zeiss, Oberkochen, Germany).

2.2.6. Mast cell activation

2.2.6.1. β-Hexosaminidase release

The β-Hexosaminidase (β-hex) release assay was performed as previously described [275]. The HMC-1 cells maintained in IMDM, were transferred to Tyrode's Buffer (NaCL – 3.94 g; KCl – 0.19 g; MgCl – 0.05 anhydrous; $CaCl_2$ – 0.1 g; Glucose – 0.5 g; BSA – 6.7 mL of 7.5 % solution; 10 mL Hepes 1M; to a final volume in Mili-Q water of 500 mL, pH 7.4 corrected with NaOH 1N) and plated in 96-well U bottom plates at a density of $5x10^5$ cells per well. Particles suspended in Tyrode's buffer were incubated with the cells for 45 min, to a final concentration of 500 and 1000 µg/mL. C48/80 was used as a positive control in three different concentrations: 20, 40 and 80 µg/mL. HMC-1 cells mixed with 0.5 % Triton™ X-100 and cells without any stimulus were used to measure total β-hex release and the basal release, respectively. Subsequently, 30 µL of supernatant from each well were incubated with 10 µL of NAG solution (1.3 mg/mL in 0.1 M citrate buffer) for 30 min at 37 °C. Then, 100 µL of carbonate buffer (pH 10) were added to induce a colour change prior OD reading at 405 nm in a microplate reader. β-hex release was measured using the following equation (Eq. 2.2):

$$\%\,\beta - hex\ release = \frac{(Sample\ \beta - hex\ release\ -\ cont\ \beta - hex\ release)}{(TritonX - 100\ \beta - hex\ release -\ \ cont\ \beta - hex\ release)}\ x\ 100 \quad \text{(Eq. 2.2)}$$

2.2.6.2. Degranulation

Granularity of HMC-1 cells after β-hex release assay was assessed using the toluidine blue dye. After the assay, performed on poly-L-lysine coated coverslips, cells were fixed cells with 4 % FA for 20 min, and stained with 1 mL of a toluidine blue solution (0.5 g toluidine blue in 30 mL of absolute ethanol) for 30 min. After staining, cells were washed repeatedly with PBS and mounted on slides for further microscopy visualization (Zeiss Axioskop 2 plus, Carl Zeiss AG, Germany).

2.2.6.3. Cell viability

After the β-hex release assay, the cell viability was either evaluated by an MTT assay or flow cytometry using propidium iodide (PI) as a probe for death cells. The MTT cytotoxicity assay was performed according to the manufacturer's protocol. The relative cell viability (%) related to control cells (without particles) was calculated by the following equation (Eq. 2.3):

$$\%\ Cell\ Viability = \frac{OD\ sample(540nm) - OD\ sample(630nm)}{OD\ control(540nm) - OD\ control(630nm)}\ x\ 100 \quad \text{(Eq. 2.3)}$$

For the flow cytometry analysis, the plates were centrifuged for 5 min at 600 x *g*, the cells washed with ice-cold PBS pH 7.4, centrifuged again and resuspended in a final volume of 300 µL. Cells were subsequently analysed following PI addition to the cell suspension (1 µL of 50 µg/mL) in a BD FACSCalibur Flow Cytometer (BD Biosciences, San Jose, CA, USA). The mean fluorescence data for a population of 20000 cells was recorded and the results processed by CellQuestModfit LT software and expressed as the % of FITC or PI positive cells.

2.2.7. *Ex vivo* internalization in Peyer's patches

Ex vivo PPs internalization studies were performed using FITC labeled AlgChiPs and DTAF labeled GPs. Mice were sacrificed by cervical dislocation and segments of jejunum (~3 cm, 1 PP per segment) were removed and placed into oxygenated (95 % O^2 and 5 % CO_2) Krebs-Ringer solution at 37 °C. Each intestinal loop, containing at least one PP, was filled with the particles at 1 mg/mL or the Krebs-Ringer solution as control, and incubated at 37 °C under orbital shaking, for 30 min. After that, PPs were excised and washed with ice-cold PBS, stained with 1 µM Hoechst 33342 for 15 min and examined by LSCM.

2.2.8. Mice vaccination

Seven-week old female C57BL/6 mice were obtained from Charles River Laboratories (Barcelona, Spain), acclimated for 1 week prior to the initiation of experiments and maintained in the local animal house facility, with free access to food and water, with 12 h light/dark cycle. Animal studies were approved (ORBEA_50_2013/27092013) and carried out in accordance with institutional ethical guidelines and with National (Dec. No. 113/2013) and International (2010/63/EU

Directive) legislation. Treatment groups included different formulations and vaccination schedules, described in table 2.1. A control group where no formulation was administered was also included in the study (Naïve, n=3). Mice were euthanized at day 42 by cervical dislocation. Formulations were administered in Mili-Q water and animals were fasted 4 h before each oral administration performed with a gavage-feeding needle.

Table 2.1. Treatment groups and vaccination schedule.

Group	**Dose 1 -** day 0			**Dose 2 -** day 14			**Dose 3 -** day 28		
	HBsAg	**Adjuvant**	**Route**	**HBsAg**	**Adjuvant**	**Route**	**HBsAg**	**Adjuvant**	**Route**
1 (n=5)	1.5 µg	10 µg CpG 273 µg ChiPs	SC	20 µg	10 µg CpG 500 µg AlgChiPs	Oral	20 µg	10 µg CpG 500 µg AlgChiPs	Oral
2 (n=7**)**	20 µg	10 µg CpG 500 µg AlgChiPs	Oral	20 µg	10 µg CpG 500 µg AlgChiPs	Oral	20 µg	10 µg CpG 500 µg AlgChiPs	Oral
3 (n=5)	1.5 µg	273 µg GPs	SC	20 µg	500 µg GPs	Oral	20 µg	500 µg GPs	Oral
4 (n=7)	20 µg	500 µg GPs	Oral	20 µg	500 µg GPs	Oral	20 µg	500 µg GPs	Oral

AlgChiPs, alginate coated chitosan particles; CpG, CpG oligodeoxynucleotide 1826; ChiPs, chitosan particles; GPs, β-glucan particles; HBsAg, hepatitis B surface antigen; SC, subcutaneous.

2.2.8.1. Blood collection

Blood samples were collected by submandibular venipuncture with an animal lancet to microcentrifuge tubes, 14 day after each immunization and immediately before the next boost. The blood coagulated over 6 h and was further centrifuged for 10 min at 4500 x *g*, for serum collection. The resultant supernatant was carefully transferred to another microcentrifuge tube and stored at −20 °C until further analysis.

2.2.8.1.1. Serum immunoglobulins

The determination of HBsAg-specific serum IgG titers was performed by ELISA as previously by our group [210]. Briefly, 100 µL of 1 µg/mL HBsAg in solution (50 mM sodium carbonate/bicarbonate, pH 9.6) were used for coating of high-binding 96-well plates (Nunc MaxiSorp™ flat-bottom, Thermo Fisher Scientific Inc., Waltham, MA, USA). After an ON incubation, plates were washed five times with PBS-T and blocked with 1 % BSA in PBS-T for 1 h at 37 °C. After washing, 100 µL of serial dilutions of serum samples, starting at 1:64, were added to the wells and incubated for 2 h at 37 °C. Following washing, 100 µL of HRP conjugated goat anti-mouse IgG (1:10000), IgG1 (1:20000), IgG2c (1:5000) and IgG3 (1:2500) antibody solutions in PBS-T were added and incubated for 30 min at 37 °C. After that, the detection was performed with 100 µL of a substrate OPD solution (5 mg OPD to 10 mL citrate buffer and 10 µL H_2O_2) incubation for 10 min at RT° in the dark. Reaction was stopped with 50 µL of 1 M H_2SO_4 and absorbance was determined at 492 nm. The serum IgG titers were presented as the end-point titer, which is the antilog of the last log 2 dilution for which the optical density (OD) was at least two-fold higher than the value of the naive sample equally diluted. The log 2 endpoint titers were used to normalize the data and equalize variability and then statistically analysed.

2.2.8.2. Mucosal secretions and faeces collection

Vaginal washings and faeces were collected at the end of the experiment (day 42) and treated as previously described [273]. Briefly, vaginal mucosa was collected using a micropipette by flushing in and out the vaginal cavity with 100 µL of ice-cold PBS (10 flushes per wash). 1 µL of 1 % sodium azide solution and 1 µL of 100 mM PMSF solution were added to each 100 µL of collected vaginal wash and incubated at RT° for 15 min. After that, it was centrifuged for 15 min at 3300 x *g*, and the supernatant collected and store at −80 °C until further analysis. Faeces were suspended in a proportion of 0.1 g to 1 mL of PBS and were treated equally.

2.2.8.2.1. Mucosal immunoglobulins

For mucosal samples, HBsAg-specific and total IgA were measured in concentrated vaginal and faeces samples using a mouse IgA ELISA Quantitation Kit, according to provider's instructions. Briefly, for HBsAg-specific IgA, the plate was coated with 100 µL of

1 µg/mL HBsAg in solution (50 mM sodium carbonate/bicarbonate, pH 9.6) and for total IgA, the plate was coated with 100 µL of the provided coating antibody and incubated at RT° for 1 h. The plate was washed five times with PBS-T and blocked with 200 µL of the provided blocking solution an incubated at RT° for 30 min. After plate washing, 100 µL of IgA standards or undiluted mucosal samples were added and incubated for 1 h at RT°. After washing, HRP conjugated IgA antibody (1:20000) was added and incubated for 1 h. Plates were washed and 100 µL of OPD substrate solution ware added and incubated for 15 min in the dark. The reaction was stopped with 50 µL of 1 M H_2SO_4 and absorbance was determined at 492 nm. Concentrations of total and anti-HBsAg mucosal IgA were extrapolated from absorbance values, using the calibration curves. Faeces IgA results are presented as the ratio between anti-HBsAg IgA and total IgA for each mouse and vaginal washings anti-HBsAg IgA is presented in pg/mL.

2.2.8.3. Liver tissue interstitial fluid IFN-γ

Tissue interstitial fluid (TIF) from liver was collected to ice-cold PBS as previously described [238]. Briefly, 0.25 g of 1-3 mm pieces of liver were suspended in 1 mL of ice-cold PBS and washed three times, centrifuging 3 min at 1000 x *g*, removing the supernatant. Samples were further centrifuged for 8 min at 2000 x *g* and then 30 min at 20000 x *g* at 4 °C. The resultant interstitial fluid was collect and stored at −80 °C until further analysis. Murine IFN-γ was evaluated using a standard ABTS ELISA development kit according to provider's instructions.

2.2.9. Statistical analysis

Results were expressed as mean ± standard error of the mean (SEM). Statistical analysis was performed by GraphPad Prism v 5.03 (GraphPad Software Inc., La Jolla, CA, USA). Comparisons between two samples were done using Student's t-test or ANOVA followed by a Tukey´s post-test for multiple comparisons test. A value of $p<0.05$ was considered statistically significant.

2.3. Results and discussion

2.3.1. Particle characterization

Particle characterization is an important task in particulate-based adjuvant vaccine formulations as their physicochemical properties might dictate their adjuvant activity. Size is a perfect example, and was recently reviewed as an intrinsic characteristic that affects the polymer half-life *in vivo* that, in turn, influences the duration of elicited innate and adaptive immune responses [108]. Even though there is an ever-increasing obsession with the nanoscale, micro-size particles also have many advantages as adjuvants. In fact, particulate vaccines typically within 0.1 µm and 10 µm range, resemble the dimensions of common bacteria and viruses and, are therefore recognized by the immune system [125]. Mean particle diameter and polydispersity index (PDI), zeta potential, HBsAg and CpG LE and empty particle morphology (TEM) are summarized in figure 2.1. The optimization of ChiPs prepared by a coacervation/precipitation technique, using sulphate ions as a crosslink agent, resulted in a mean diameter of 612.4 ± 8 nm (Figure 2.1A), confirmed in TEM images (Figure 2.1B). Low size PDI (0.18) and a positive surface charge in water (+18 ± 0.3 mV) were also correlated to those particles. When HBsAg was entrapped into ChiPs and CpG was subsequently adsorbed onto their surface, the mean size increased to 878 ± 39 nm ($p<0.001$) and the surface charge decreased to +12.7 ± 0.3 mV ($p<0.05$), due to the contribution of the negatively charged CpG phosphate groups. Coherently, sodium alginate coating (AlgChiPs) have resulted in a mean size of 1139 ± 39 nm with a higher PDI (0.44). A complete inversion of the zeta potential to negative values (−27.5 mV) was also observed. Additionally, the consecutively addition of calcium ions neutralized some charges and might induced some instability to the particle suspension. Therefore, the value of size measured may include the contribution of some agglomerates that can be observed on TEM images (Figure 2.1C). Particle size increased even more when the particles were loaded with HBsAg and CpG (1428 ± 24 nm, $p<0.001$), in agreement with previous reports of our research group [148, 188, 208]. Consistent with the literature, yeast-derived GPs had a mean diameter between 2-4 µm (3476 ± 176 nm, PDI 0.38) (Figure 2.1A), also confirmed by the TEM analysis (Figure 2.1D). A neutral zeta potential was also observed (−4.4 ± 0.9 mV), characteristic of β-glucans that have no charged functional groups. HBsAg loading into GPs did not change the overall physicochemical

properties, as it was entrapped inside the particle cavity. A high HBsAg LE was observed for both delivery systems: ChiPs polymer matrix (98.9 ± 0.4 %) and GPs cavity (98.8 ± 0.1 %). Concerning to CpG, the adsorption efficacy was 98.2 ± 0.3 %.

A

Particles	Size (nm)	PDI	Zeta Potential (mV)	HBsAg LE (%)	CpG LE (%)
ChiPs	612 ± 8	0.18 ± 0.02	18.0 ± 0.3	a	a
HBsAg and CpG loaded ChiPs	878 ± 39 ***	0.26 ± 0.01	12.7 ± 0.2 *	98.9 ± 0.4	98.2 ± 0.3
AlgChiPs	1139 ± 39	0.44 ± 0.01	-27.5 ± 0.9	a	a
HBsAg and CpG loaded AlgChiPs	1428 ± 34 ***	0.43 ± 0.01	-31.9 ± 0.8 *	b	b
GPs	3476 ± 176	0.38 ± 0.04	-4.4 ± 0.9	a	a
HBsAg loaded GPs	3087 ± 268	0.67 ± 0.03	-4.8 ± 1.7	98.8 ± 0.1	c

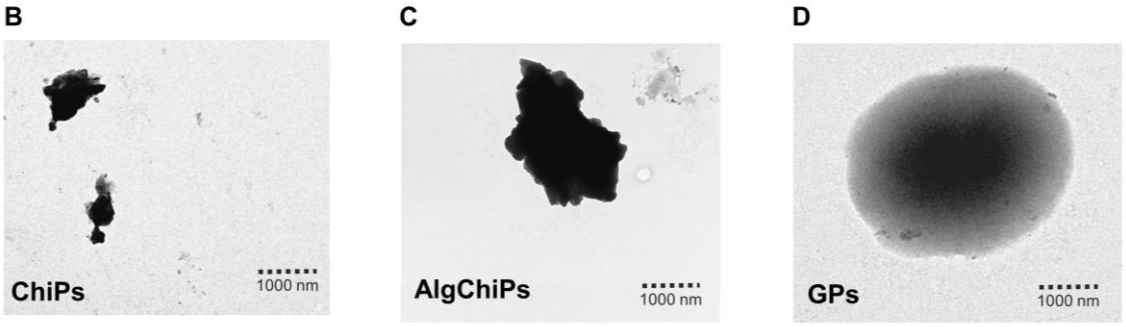

Figure 2.1. Particle physicochemical properties. (**A**) Mean particle size (nm), size distribution (polydispersity index (PDI)) and zeta potential mean value of empty and HBsAg/CpG loaded ChiPs, AlgChiPs and GPs measured in water. HBsAg and CpG loading efficacy (LE) is presented in % and evaluated for oral delivery formulations, that represent the highest amount of HBsAg loaded. Data (mean ± SEM) are representative of four independent replicates for size and zeta potential and three independent replicates for LE. Comparisons are made between empty and loaded particles. ** denotes statistical differences at p<0.05 and *** at p<0.001.* Representative TEM images of empty (**B**) ChiPs, (**C**) AlgChiPs and (**D**) GPs are depicted in the figure. *a, empty particles; b, HBsAg and CpG LE was measured in ChiPs; c, only HBsAg was loaded.*

2.3.2. ChiPs, AlgChiPs and GPs are efficiently internalized by peripheral blood mononuclear cells.

Any ideal vaccine delivery system should interact with APCs, like DCs and macrophages, that play major roles on mucosal immunity [117]. It is known that particulate adjuvants usually induce a local proinflammatory environment which results in immune cell recruitment, enabling prolonged particle/antigen-cell interactions [108]. Therefore, in our first experiment we intended to investigate the ability of ChiPs, AlgChiPs and GPs to be internalized by APCs precursors, like the PBMCs, which are recruited to

vaccine administration site. Monocyte-derived APCs are important players in the development of an adaptive immune response and, are therefore, a good target for vaccine design against infectious diseases [100]. In figure 2.2A, LSCM images confirmed that all particles (shown in green) were found inside the PBMCs, proving the effective uptake by those cells. Flow cytometry analysis (Figure 2.2B) revealed that more than 70 % of PBMCs exposed to ChiPs, AlgChiPs and GPs, produced a strong fluorescent signal, indicative of a high internalization rate, enabling the prediction of a biological effect of the loaded antigen namely through APCs activation and antigen presentation. The frequency of positive cells did not change in the presence of trypan blue (TB), used to quench extracellular fluorescence, which indicates that few or no particles were adsorbed on the cell surface. Despite the physicochemical differences between the particles, no significant differences were observed in thin study. In fact, the positive charge of chitosan-based particles might intermediate enhanced antigen uptake, activation and presentation by APCs, mainly due to the presence of amino-functionalized groups [158]. On the other side, the high cell internalization rate of GPs was expected as particulate β-glucans bind to Dectin-1 receptor, broadly expressed on populations of myeloid cells (monocytes/macrophages and neutrophils) [262], triggering phagocytosis. Therefore, GPs are widely reported as a selective delivery system to phagocytic cells [250, 263].

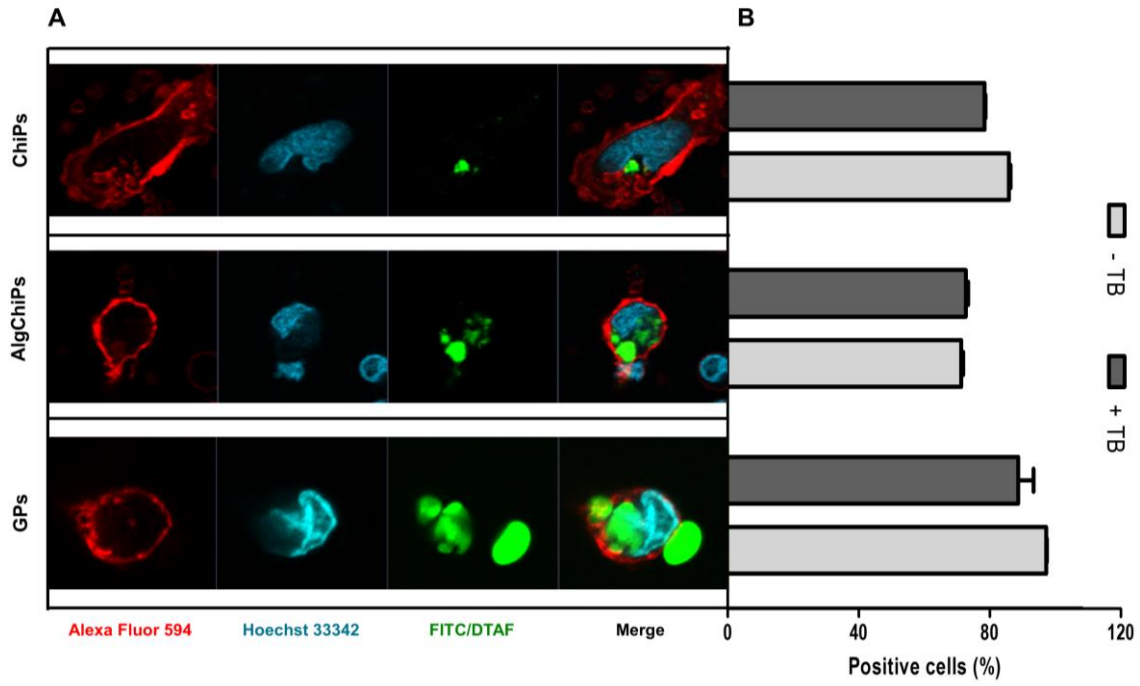

Figure 2.2. Particle internalization by peripheral blood mononuclear cells (PBMCs). FITC labeled ChiPs and AlgChiPs, and DTAF labeled GPs internalization in PBMCs was assessed after 4 h of incubation at a concentration of 200 µg/mL. (**A**) Confocal images of ChiPs, AlgChiPs and GPs (represented in green) internalization by PBMCs (Hoechst 33342 labeled nucleus in blue, and Alexa Fluor™ 594 labeled cell membrane in red). (**B**) Flow cytometry analysis expressed as the % of fluorescence positive cells. Trypan blue (TB) was used to quench extracellular fluorescence and thus assess only particle internalization and not particle adhesion to the cell membrane. Data (mean ± SEM) are representative of three independent assays of twelve replicates.

2.3.3. Only ChiPs are effective mast cell activators.

Other cells than APCs might modulate the mucosal immunity. A perfect example would be the mast cells, commonly recognized as the immune system sentinels' in the fight against pathogens due to their strategic location at host-environment interface [276]. In fact, mast cell activators are a class of highly effective vaccine adjuvants, capable to induce protective antigen-specific immune responses through needle-free routes [277]. Mast cell activation can help to link both innate and adaptive immunity through various mediators [276], as a result of granule exocytosis (degranulation) and consequent release of preformed granular particles, mainly composed of heparin and proteases, and some freely soluble molecules (e.g. histamine and β-hex) into the surroundings [271]. For that reason, we decided to study if the adjuvant mechanism of the developed delivery systems may occur through the activation of such cells. A mast cell degranulation screening assay, developed by Staats *et al*. [275], was perfomed and the results were

depicted in figure 2.3. In this assay, a solution of Compound 48/80 (C48/80) was used as a positive control and induced a β-hex release between 0.55 ± 0.4 % and 6.53 ± 0.13 %, corresponding to the lower and the highest concentrations, respectively. These values were comparable with those described by the authors, only slightly higher according to the higher time of exposure used in the present experiment. Figure 2.3B showed that only ChiPs induced mast cell activation at the concentrations of 500 μg/mL (β-hex release: 1.99 ± 0.08 %) and 1000 μg/mL (β-hex release: 9.55 ± 0.29 %). This result confirmed the previous report of our group where it was proved for the first time that chitosan-based particles were mast cell activators [278]. Interestingly, ChiPs coating with sodium alginate (AlgChiPs) diminished their capacity to act as mast cell activators. Another important observation was that the adjuvant mechanism of GPs seemed not to be related with mast cell activation. That conclusion was supported by another technique, where the analysis of microscopy images of toluidine blue stained HMC-1 cells confirmed that ChiPs effectively induced HMC-1 cell degranulation, revealed by the intense staining of the granules (Figure 2.3A). In contrast, the images of the cells incubated with both AlgChiPs and GPs were similar to the control cells. Size and shape of the possible activator-particle might be as important as its chemical composition. In fact, chitosan gels [279] were shown to induce rat mast cell activation, while chitosan oligosaccharides were found to significantly inhibit degranulation of the same cells [280]. ChiPs ability to activate HMC-1 cells but not AlgChiPs and GPs might be explained by the basic secretagogues mediated pathway, through which several molecules only sharing the cationic property (including C48/80) could activate these cells, probably acting at some non-selective membrane receptors or crossing the plasma membrane to directly activate Gi proteins [281]. Another question might be about cell viability. Consistently, Staats *et al*. [275] affirmed that they did not monitor cell viability in the screening for novel mast cell activators intentionally, because of the recent observations that alum, a US FDA approved vaccine adjuvant, involves cell death in its adjuvant mechanism of action. In fact, although all delivery systems have not induced significative mast cell cytotoxicity, ChiPs have induced higher cell death (25 %) compared to AlgChiPs (15 %) evaluated throughout the assay (PI - Figure 2.3C).

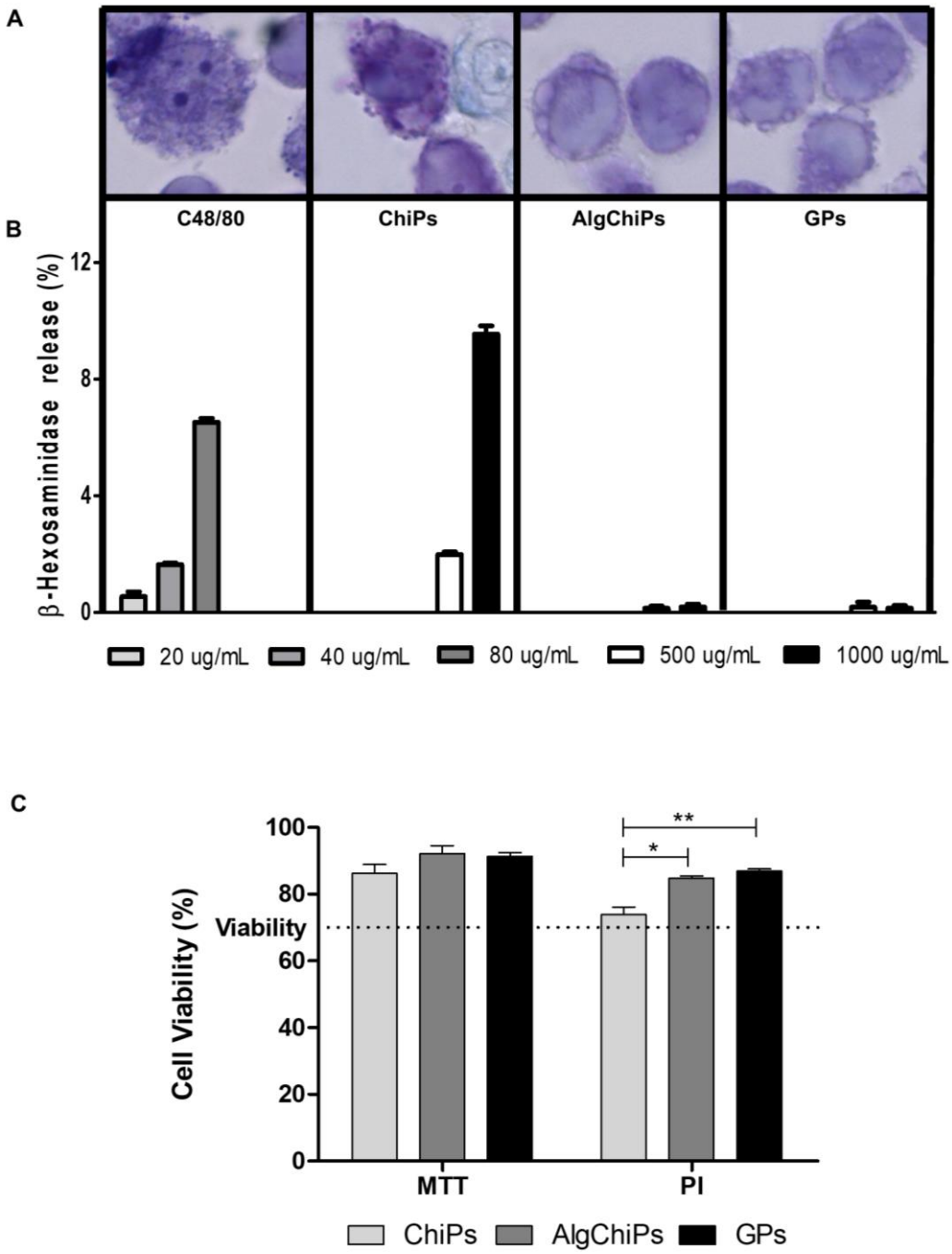

Figure 2.3. Particle induced mast cell activation. Mast cell activation was induced following particle incubation with HMC-1 mast cell line. (**A**) Microscopy images of toluidine blue stained cells after the β-hexosaminidase release assay. Degranulation of ChiPs exposed HMC-1 cells is comparable to the positive control Compound 48/80 (C48/80) and no degranulation of AlgChiPs or GPs exposed HMC-1 cells was comparable to the untreated cells. (**B**) For β-hexosaminidase release assay, cells were stimulated with 500 or 1000 µg/mL of ChiPs, AlgChiPs and GPs or the C48/80 at 20, 40 or 80 µg/mL, as a positive control. (**C**) Cell viability after β-hexosaminidase release assay evaluated either by an MTT assay or by flow cytometry using propidium iodide (PI). Data (mean ± SEM) are representative of three independent experiments performed in triplicate. ** denotes statistical differences at p<0.05 and ** at p<0.01.*

2.3.4. AlgChiPs and GPs are internalized by mice PPs.

Following the development of oral vaccine formulations, PPs are the spotlight for an effective mucosal immune response. They have the ability to transport luminal antigens either for the induction of immune tolerance or defence against pathogens, through an interplay between lymphoid follicles and follicle-associated epithelium immune cells [132]. Thus, it was mandatory to observe the internalization of both AlgChiPs and GPs into the PPs, as both particles should be the carriers of the antigen through the gastrointestinal tract. The assay was completed following an *ex vivo* incubation of fluorescently labeled particles with mice intestinal loops. LSCM images in figure 2.4 showed the presence of both FITC labeled AlgChiPs and DTAF labeled GPs (green spots) inside the PPs (not present in the control). The images were representative of an intermediate image of a z-scan starting from the surface to the bottom of a whole PP. In the case of AlgChiPs, those green dots may not be individual particles but agglomerates in agreement with a previous study [148]. For GPs, we could definitely see individualized particles. Particle physicochemical properties can affect PPs uptake, and although the literature shows a trend for the nanometer range, micrometer-sized particles cannot be excluded from the race for the optimal vehicle for efficient PPs uptake, as we showed in the present study and others have shown elsewhere [249, 282]. Actually, as said before, particulate vaccines resembling the dimensions of pathogens, are readily recognized by the immune system and internalized by PPs M cells [125]. Indeed, as extensively reviewed by Jung *et al*. [132] bacteria and viruses might enter and accumulate in the PPs through different mechanisms which is crucial for protective mucosal immune responses but also provides a route of entry for pathogenic agents.

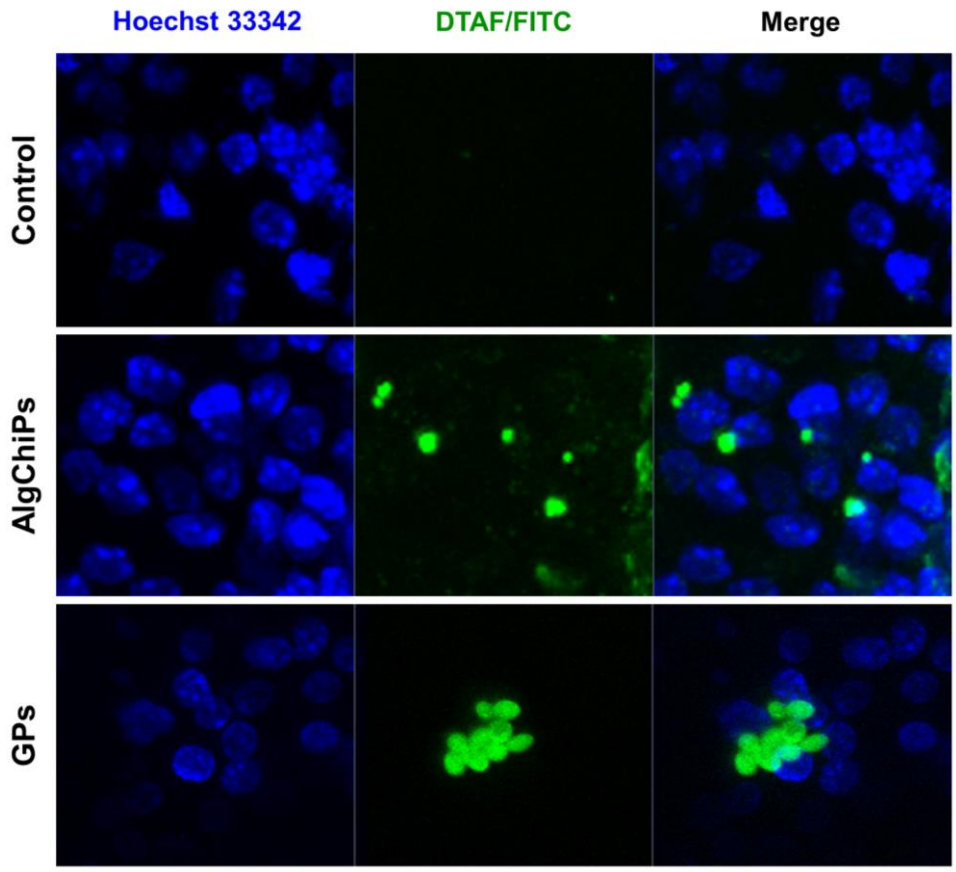

Figure 2.4. Particle internalization by mice Peyer's patches (PPs) *ex vivo*. Laser scanning confocal microscopy (LSCM) visualization of the whole PPs after excision from mice intestinal loops incubated with FITC labeled AlgChiPs or DTAF labeled GPs (green) for 30 min in oxygenated Krebs-Ringer solution, or only oxygenated Krebs-Ringer solution for Control PPs. Nucleus were stained with Hoechst 33342 (blue). The images represent a z-scan between the surface and the bottom of the PPs, and, thus, indicate that particles are inside the PPs but cannot confirm if they are inside de cells.

2.3.5. AlgChiPs and GPs effectively induce mucosal specific antibodies through the oral route, but systemic antibodies are only induced after a subcutaneous priming.

The greatest advantage of an hepatitis B oral vaccine is the potential to develop a double layer of immunity, mainly focused on the local production and secretion of antigen-specific sIgA, fundamental for virus neutralization and opsonization [122, 283]. Even though, this is a rather difficult task usually requiring high amounts of antigen and also good mucosal adjuvants to elicit effective immune responses [116]. Indeed, the main objective of the present study was to evaluate if both developed formulations (GPs and AlgChiPs) would be good mucosal adjuvants for the HBsAg, inducing both systemic and

mucosal immune responses. For that purpose, two vaccination schedules were tested: a SC priming followed by two oral boosts (Group 1 for ChiPs/AlgChiPs and Group 3 for GPs) and, three consecutive oral administrations (Group 2 for AlgChiPs and Group 4 for GPs), as it is shown in table 2.1. Figure 2.5A represented the serum anti-HBsAg immunoglobulin (IgG) titers evaluated. Three oral doses (day 0, 14 and 28) of either GPs or AlgChiPs formulations (groups 2 and 4, respectively) resulted in 4 out of 7 mice with anti-HBsAg IgG titers, corresponding to a 57 % of responders. To note that most of responder mice responded only after the third vaccine dose. Still, 1 out of 7 mice from group 2 responded right after the first oral dose, and the further two oral boosts lead to increased number responder mice, from 1 to 4 out of 7 mice (days 28 and 42). For group 4 (GPs vaccine), mice with significant antibody titers appeared only after the fully oral vaccination schedule, with similar titers as observed for group 2. One possible explanation to the later immune response elicited by group 4 is that larger particles seem to be retained in PPs following uptake, whereas smaller particles are subsequently disseminated to the mesenteric lymph nodes, blood circulation and spleen [125]. A recent study where HBsAg was entrapped in Pluronics® F127 stabilized poly-ε-caprolactone nanoparticles and administered through intramuscular, intradermal and oral route also revealed that an oral immunization might be as effective as the injectable route, but the increment of the antibody titers was more striking several weeks post administration [260]. This study also highlighted the efficacy of the developed novel adjuvant, generating significant antibody titers without booster dose. Therefore, we cannot exclude the possibility of a delayed and better immune response if the study had been prolonged in time, as the whole antibody titers were still in a growing phase. Even so, our results reporting low serum antibody titers following three oral immunizations with HBsAg loaded GPs are more encouraging than a previous study where five oral immunizations with ovalbumin (OVA) loaded GPs that did not induce serum antibodies at all [249]. All studies carried out so far using GPs as an adjuvant only achieved antigen specific serum IgGs following parenteral administrations [228, 229, 252, 253]. Although we can speculate slightly higher anti-HBsAg IgG for group 2 when compared to group 4, the results are not statistically different. Anyway, the overall outcome of three oral doses seemed to be favourable for AlgChiPs, also due to the early onset of responder mice. Indeed, as hypothesized, co-entrapping HBsAg and CpG into AlgChiPs resulted in increased percentage of responder

mice than our former approach where HBsAg and CpG were adsorbed on separate particles (40 % responder mice) [145]. This reinforces the theory that physical proximity of the antigen and the immunomodulator is an important requirement for an effective adjuvant effect [270]. Other encouraging results using chitosan particles for oral antigen delivery can be found in scientific literature, which means that we are on the right way to find a good oral vaccine adjuvant. The porcine circovirus type 2 (PCV2) virus-like particles, loaded in chitosan microparticles had successfully induced the proliferation of PCV2-specific splenic CD4+/CD8+ lymphocytes and the subsequent production of serum IFN-γ to levels comparable with those induced by an injectable commercial formulation, although the on the same study, a great amount of particles per dose (35 mg) have been used [176].

The results in figure 2.5A also showed that a SC priming followed by two oral boosts (groups 1 and 3), might overcome the difficulties of a fully oral schedule, resulting in 100 % responder mice. In detail, we can easily see the difference in the vaccination schedule for the same vaccine formulation with much higher antibody titers for groups 1 and 3 compared to groups 2 and 4, respectively (day 42, $p<0.05$). To note that antibodies were only detected in 1 out of 5 mice from group 3 (GPs) after the SC priming, but right after the 1st oral boost the number of responders increased to 100 %. Moreover, although only statistically relevant for group 1 ($p<0.01$) due to sole responder mice in group 3 (day 14), antibody titers increased after the first oral boost for both groups 1 and 3, representing either an effective consequence of the oral boost or a prolonged effect of the SC priming that may took longer to develop an immune response, probably due to slow antigen release. Similar vaccination schedules comprising an injectable priming followed by oral boosts [284, 285], in some cases only using the adjuvant for boosting [286], have been recently reported to elicit both systemic and mucosal immunity to HBsAg. For instance, the administration of selenium particles for 30 days prior conventional hepatitis B vaccination have induced a better immune response with a Th1 bias [286]. The immunogenicity of genetic modified plants to express HBsAg in maize, used as oral boosts following Recombivax® parenteral delivery, have also successfully induced increased systemic specific antibodies, achieved with extremely high doses of antigen, compared to the amounts used in the present study [284, 285, 287]. This

approach, in which an adjuvant is not used in boosting, although promisingly, has associated some hurdles related to ethical questions and non-uniformity of HBsAg doses.

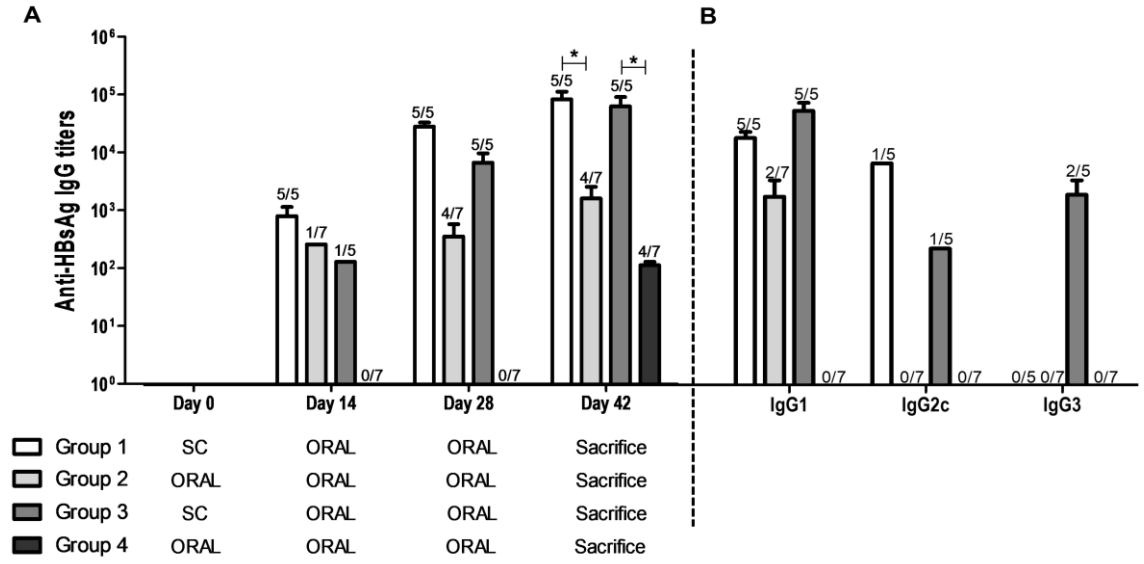

Figure 2.5. Elicited HBsAg-specific systemic immune response. (**A**) Serum anti-HBsAg total IgG titers of individual vaccinated mice, evaluated 14 days after each vaccine dose. (**B**) Anti-HBsAg IgG1, IgG2c and IgG3 subclasses analysed at the end of the experiment (day 42). Titers were defined as the highest plasma dilution resulting in an absorbance value twice higher than nonimmune plasma. Groups 1 and 2 include chitosan-based particles vaccinated mice (ChiPs and AlgChiPs) and groups 3 and 4 include β-glucan-based particles vaccinated mice (GPs). Data is expressed as mean ± SEM. ** denotes statistical differences at p<0.05.*

Figure 2.5B showed the serum subtype profile of anti-HBsAg IgG, evaluated at the end of the vaccination schedule. The results showed that IgG1 was the predominant antibody produced by groups 1 and 3, which is indicative of a Th2-biased immune response. As the IgG titers of groups vaccinated only through the oral route were low (groups 2 and 4), the IgG isotypes were barely detectable, with only two mice from group 2 exhibiting IgG1. CpG ODNs are characterized by the production of a Th1 response, boosting the generation of humoral and cellular vaccine-specific immunity [288]. However, only one mouse of group 1 had both an IgG2c/IgG1 immune response (ratio: 0.87), associated with a balanced Th1/Th2 profile. The improvement of previous formulation [145, 188, 208] with the strategy of adjuvant/antigen close and temporal proximity implemented in the present study led us to expect a greater extent of IgG2c production than observed. We believe that a strong interaction between chitosan and

CpG might hamper its ability to be released from the chitosan-based delivery system to interact with the intracellular TLR9 [289]. The GPs formulation stimulated the production of IgG2c and IgG 3 in some mice (Group 3), although in a lower extent than IgG1. This observation is in accordance with other studies with three SC doses of OVA loaded GPs [228, 229].

2.3.6. HBsAg-specific IgA is present in faeces from both AlgChiPs and GPs vaccinated mice.

To evaluate the ability of all formulations and vaccination schedules to elicit mucosal immune responses we measured the levels of IgA, in faecal material and vaginal washings at day 42 (Figure 2.6). Figure 2.6A showed anti-HBsAg IgA in the vaginal washings, only higher than the control for chitosan-based particles vaccinated mice, independent of the vaccination schedule (Groups 1 and 3). The results of IgA in the faeces are shown in figure 2.6B and, as expected based on previous oral vaccination studies with both AlgChiPs [145] and GPs [249], all groups had a specific IgA/total IgA ratio higher than the control, with some mice from group 4 evidencing a ten-fold increase. The objective of inducing antigen specific mucosal immunity with the developed formulations was successfully achieved, a characteristic not effectively induced by parenteral routes, as our group has demonstrated following SC administration of HBsAg and CpG chitosan-based formulation [188].

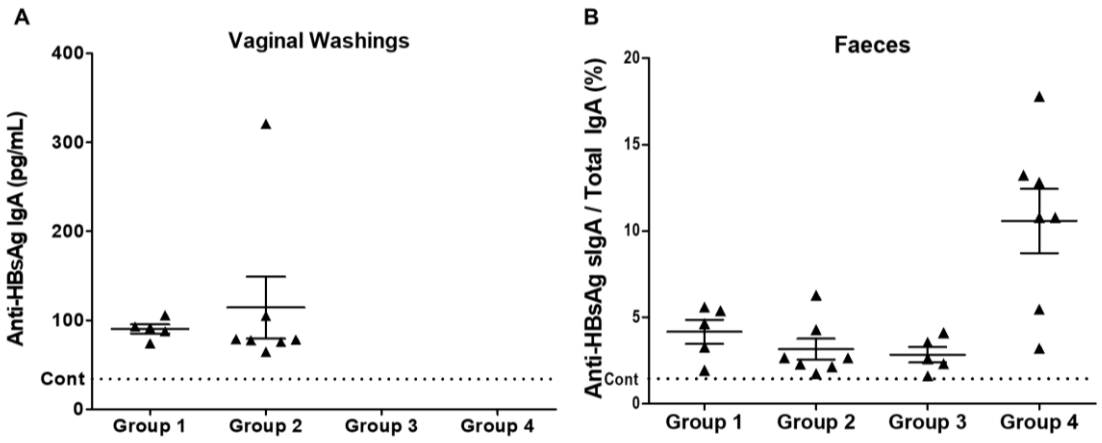

Figure 2.6. Elicited HBsAg-specific mucosal immune response. Anti-HBsAg IgA profile was evaluated both in (**A**) vaginal washings and (**B**) feaces of mice from all groups at the end of the experiment (day 42). In feaces the results are presented as the ratio between anti-HBsAg IgA and total IgA and in vaginal washings are presented as the concentration of anti-HBsAg IgA in pg/mL. Control (Naïve) values are presented as a dashed line on the graphs. Data are presented as mean ± SEM.

2.3.7. IFN-γ is increased in liver tissue interstitial fluid of GPs vaccinated mice.

Yu and colleagues [238] have demonstrated before that a daily oral administration of GPs for 9 weeks tend to accumulate in the liver of an HBV transfection mouse model. Furthermore, this GPs treatment resulted in recruitment of immune cells to the liver microenvironment which significantly enhanced the production of Th1 cytokines. Thus, we decided to investigate if our oral GPs administration schedules could alter the physiological state of the liver, concerning to cytokines environment, namely the IFN-γ levels, a cytokine produced by Th1 cells. In fact, results obtained from liver tissue interstitial fluid (TIF) shown in figure 2.7, the interface between circulating body fluids and intracellular fluids, revealed that IFN-γ production was significantly increased ($p<0.05$) compared to control group, for both groups 3 and 4, as a result of two or three GPs oral administrations, respectively. Our present results confirm the power and versatility of these yeast-derived GPs.

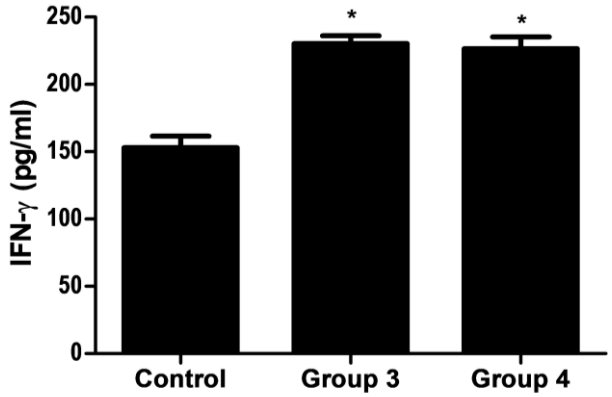

Figure 2.7. Mice liver tissue interstitial fluid (TIF) IFN-γ production. Livers from mice of groups 1, 3 and 4 were collected and liver TIF analysed for IFN-γ production. Data are presented as mean ± SEM. ** denotes statistical differences at p<0.05, related to the control group.*

2.3.8. Global impact for developing countries.

Universal vaccination may be required for global HBV eradication, however, it has not been introduced in many developing countries, or even in Japan [290]. Indeed, it may face several financial and logistical challenges, requiring proactive planning from the conception to the implementation [256]. Naturally, new vaccine designs and delivery systems need to be promoted, and there is where the present work fits into, promoting the development of an HBV oral vaccine. That would be the best strategy from a practical point of view, although the most difficult to achieve effectiveness. Mucosal immunity, evidenced by the presence of antigen specific IgA on mucosal surfaces, elicited by both AlgChiPs and GPs through the vaccination schedules tested is a proof of concept of the major advantage of mucosal vaccination, particularly relevant to prevent sexually transmitted HBV. Although the fully oral vaccination schedule was not effective in inducing a systemic immune response, the SC priming favourably reverted the poor effectiveness, particularly interesting for developing countries. Multidose injectable vaccines, as the commercial hepatits B vaccines, difficult the implementation of mass vaccination in those countries, mainly due the difficulty in maintaining an uninterrupted cold chain transportation/storage to not compromise the vaccine stability. One instead of three injectable doses would facilitate that process, as the theoretically better stability of the boosting oral formulations, as result of antigen protection by the delivery systems,

will not require cold chain transportation. When it comes to mass vaccination, the amount of cold chain transportation cargo does matter. There are also some difficulties in gathering the population as many times as the injectable vaccine doses required. The only one injectable dose would facilitate the vaccination procedure and also reduce the risk of infections related to syringes and needles reuse in these countries. The future perspectives of this work rely on some questions that remained unanswered, namely to understand if this vaccination schedule mediates a cellular immune response, as might be suggested by the immunomodulatory properties of both chitosan and β-glucan-based vaccine formulations, essential against intracellular pathogens.

2.4. Conclusion

Vaccination is the most effective intervention in modern medicine. The development of new mucosal formulations for underutilized vaccines could be the way towards vaccine-preventable diseases eradication. Antigen encapsulation in polymer-based particles is a primordial tool for effective vaccine delivery to mucosal sites. The appellative features of chitosan and β-glucan-based particles as delivery systems for oral vaccination as well as their interesting immunostimulatory properties made them eligible for future developments. This study highlights the need for a SC priming prior oral boosting to induce HBsAg seroconversion in all mice, as a fully oral vaccination schedule resulted only in 60 % efficacy for both AlgChiPs and GPs-based vaccines. This vaccination schedule with only one injectable dose may have a high translational potential for mass vaccination in developing countries, overcoming transport and storage difficulties and resulting in lower risk of infections related to injections.

CHAPTER 3

POLYMERIC NANOENGINEERED HBSAG DNA VACCINE DESIGNED IN COMBINATION WITH β-GLUCAN ADJUVANT

Abstract

The generation of antigen-specific immune responses following DNA vaccination has been hard to achieve, mainly related to the difficulty in finding an efficient vector to mediate the gene delivery. Antigen presenting cells (APCs) activation with the help of adjuvants can be a good strategy to improve transfection efficiency in immune cells and the consequent vaccine efficacy. In that regard, this study proposed the use of PDMAEMA:PβAE/DNA polyplexes (Pol) as the vehicle of a pDNA vaccine encoding the hepatitis B surface antigen (HBsAg), with some Pol designed in combination with a soluble (Glu) or a particulate (GPs) form of β-glucan as an additional adjuvant with the ability to activate APCs. Results showed that the Pol produced respecting a 16:1 polymer:DNA charge ratio, were positively charged (+41 mV) and had a mean size of 180 nm. These Pol resulted in enhanced transfection activity compared to the positive control for all formulations tested, with those in the presence of GPs showing even higher luciferase gene expression, both in COS-7 and RAW 264.7 cell lines. The developed formulations were then used to carry pDNA encoding the HBsAg (pCMV-S) in mice vaccination studies, resulting in a seroconversion rate of 40 %. This work showed the potential of this nanosystem together with GPs to enhance *in vitro* transfection capacity and to be further studied as a platform for DNA vaccine development.

Keywords

DNA vaccine, HBsAg, PDMAEMA, PβAE, β-glucan.

Graphical abstract

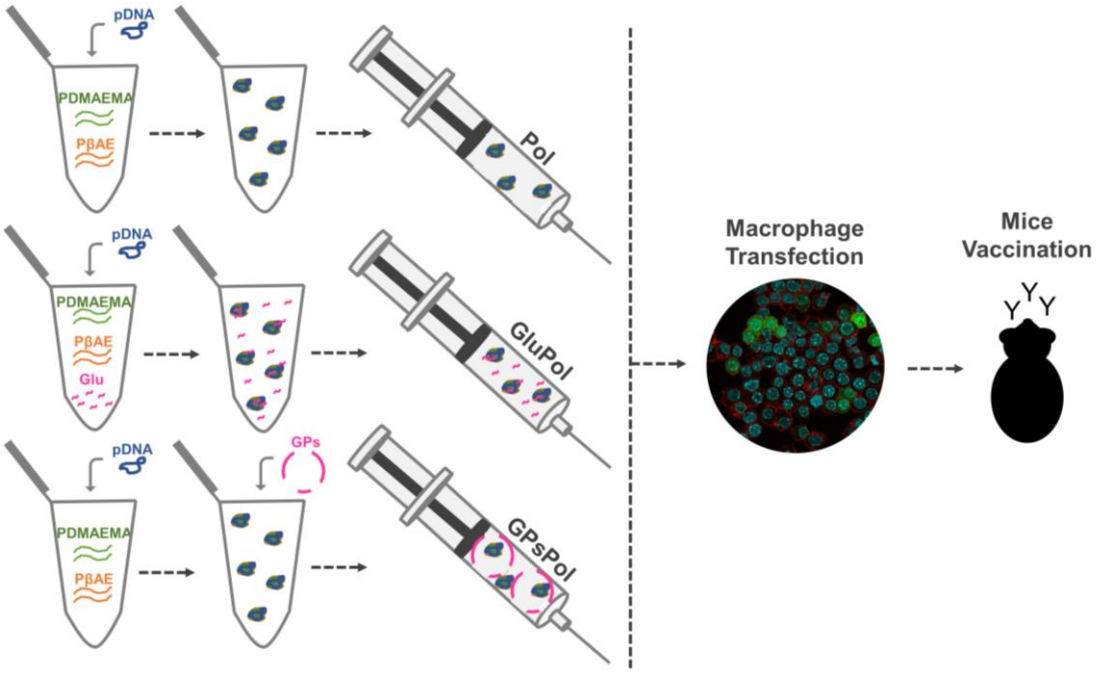

3.1. Introduction

Vaccination is one of the most effective strategies to prevent infectious diseases. The implementation of global vaccination programs for hepatitis B would prevent part of the 887 000 deaths observed in 2015, related to cirrhosis and hepatocellular carcinoma [291]. Common prophylactic vaccines generate strong antibody responses however, the induction of cell-mediated immunity is rarely observed. To counter that, we highlight the imperative role of DNA vaccines [87-89] and adjuvants [102, 292] in the induction of helper T cells (Th) and cytotoxic lymphocytes (CTLs), usually required to fight infectious diseases. DNA vaccines are a recognized therapeutic candidate for chronic hepatitis B [92, 93], associated with strong immune responses, as they induce antigen expression inside the host [87, 89]. Other advantages include the low cost of production and increased stability that would facilitate transport and storage in developing countries [88, 89], where hepatitis B is still a major problem [21]. Nevertheless, poor transfection, transient antigen expression and immunological tolerance are the main hurdles seeking *in vivo* immunogenicity and vaccine efficacy [87, 92, 94]. The inclusion of adjuvants that activate antigen presenting cells (APCs), such as macrophages and dendritic cells (DCs), can be a remarkable strategy to overcome such limitations, as they are important immune effectors to trigger adaptive immune responses and antigen cross-presentation [100].

A variety of non-viral delivery vehicles has been investigated including physical (e.g. 'gene guns', electroporation) and chemical (e.g. cationic molecules) approaches. Complexation with cationic polymers to condense plasmid DNA (pDNA) and deliver it to target cells is highly promising and may shape the future of DNA vaccination [92, 94]. Improving cellular internalization, endosomal escape and enhancing pDNA delivery to cell nucleus are the main advantages [95]. Synthetic polymers have gained some attention for that purpose and include poly(β-amino ester) (PβAE) [94, 96, 293] and poly[2-(dimethylamino)ethylmethacrylate] (PDMAEMA) [94, 97, 294]. In addition, particles based on PβAEs were recently characterized for their intrinsic immunogenicity, activating DCs, antigen presentation and enhancing T cell proliferation [98]. PDMAEMA-based polyplexes were also considered a potential delivery vehicle for the hepatitis B surface antigen (HBsAg)-encoding DNA vaccination [99]. Accordingly, the new and highly effective PDMAEMA:PβAE non-viral vector (Pol) previously developed by our group [295], emerged

as an optimal choice for the present work to study: 1) the use of these Pol as the vehicle for a pDNA vaccine encoding the HBsAg, and 2) to evaluate the effect β-glucan association as an additional adjuvant for enhanced vaccine efficacy. β-glucans interact with pathogen recognition receptors (PRRs), namely the Dectin-1 receptor, mostly present on APCs surface. Consistently, a β-glucan analogue and a particulate form of β-glucan have been successful associated to pDNA vaccination, resulting in enhanced immune response through APCs recruitment and activation [233, 296]. Moreover, PβAEs mannosylation used for DNA complexation resulted in improved gene delivery and processing upon enhanced mannose-mediated APCs uptake [297]. Based on these literature suggestions, two different approaches were designed. First, a soluble β-glucan (produced from yeast-derived β-glucan particles (GPs)) was added to the homopolymers prior pDNA complexation to be incorporated in the Pol and enable interaction with immune cells as part of the delivery system. Although both soluble and particulate β-glucans bind to Dectin-1 receptor, only the latter activates the downstream signaling [224]. Second, the particulate GPs *per se*, well characterized for phagocytic targeted delivery and adjuvant properties [229, 242, 243] were added to the Pol. As far as we know, this is the first time that a PDMAEMA:PβAE:β-glucan-based gene delivery nanosystems were characterized and tested for a pDNA vaccination strategy.

3.2. Materials and methods

3.2.1. Materials

pCMV.Luc and pCMV.GFP (plasmids encoding luciferase (Luc) or green fluorescent protein (GFP)) (Vical, San Diego, CA, USA) were amplified in *E. coli* strain DH 5α and purified using QIAGEN Plasmid Giga Kit (Hilden, Germany). The purified pDNA was dissolved in Mili-Q water and its concentration and purity assessed by UV spectrophotometry by measuring the absorbance at 260/280 nm. pCMV-S (plasmid encoding the HBsAg) and the HBsAg (purity > 98 % by SDS-Page tested in ELISA with anti-HBsAg antibodies), subtype adw, a virus-like-particle, with an approximate size of 25 nm, was from Aldevron (Fargo, ND, USA). CpG oligodeoxynucleotide ODN 1826 (CpG) was from InvivoGen (California, USA). SYBR™ Safe DNA Gel Stain and Alamar Blue® were from ThermoFisher Scientific Inc (Massachussets, USA). *Saccharomyces cerevisiae* was kindly donated by AB MAURI (Mauripan, Moita, Portugal). Cell culture reagents,

lipopolysaccharide (LPS), concavalin A (ConA) and polyethylenimine (PEI) were from Sigma-Aldrich (Sigma–Aldrich, MO, USA). *DC*™ protein assay kit (Bio-Rad, Hercules, CA, USA), Image-iT™ LIVE Plasma Membrane Nuclear Labeling Kit (Hoechst 33342, Alexa Alexa Fluor™ 594, Life Technologies Corporation, Paisley, UK), Label IT® Tracker™ Intracellular Nucleic Acid Localization Kit, Cy®5 (Mirus Bio LLC, WI, USA) were used according manufacturer's instructions. IgG HRP was from Bethyl Laboratories (Montgomery, TX, USA). IL-4 or IFN-γ and IL-17 ELISA kits from Peprotech (Rocky Hill, NJ, USA). All the other used reagents were of analytical grade.

3.2.2. Polymeric nanosystem preparation

3.2.2.1. Synthesis of poly[2-(dimethylamino)ethyl methacrylate] and poly(β-amino ester)

Poly[2-(dimethylamino)ethylmethacrylate] (PDMAEMA) and poly(β-amino ester) (PβAE) synthesis and physicochemical characterization were performed as previously described by our group [295, 298].

3.2.2.2. Production of particulate β-glucan - GPs

GPs were produced from *Saccharomyces cerevisiae* by successive alkaline and acidic treatments which hydrolyses the outer cell wall and intracellular components as described by Soto and Ostroff [243] with minor modifications, resulting in hollow porous yeast cell walls mainly composed of β-glucans. Briefly, 20 g of *Saccharomyces cerevisiae* were suspended in 200 mL of NaOH 1 M and heating to 85 °C for 1 h, under rotational stirring. The insoluble material containing the yeast cell walls was collected by centrifugation at 2000 x *g* for 10 min. This procedure was repeated three times, with the third time just for 10 min. Then, the insoluble material was suspended in 200 mL of Mili-Q water and the pH brought to 4-5 with HCl and heated to 75 °C for 1 h. After that, the insoluble material was recovered again by centrifugation and washed three times in 200 mL of Mili-Q water, three times with 40 mL of isopropanol and twice with 40 mL of acetone and let dry at RT°.

3.2.2.3. Production of soluble β-glucan from GPs

Soluble β-glucan (Glu) was produced from GPs based on a method [299] using an acidic solvent and elevated temperature and pressure with some modifications. Briefly, 0.8 g of milled GPs (2 x 20 min, 2888 x *g*, ULTRA-TURRAX® Tube Drive, IKA, NC, USA) were added to 70 mL of acidic solvent (acetate buffer pH 3.6: 0.62 g sodium acetate, 5.24 mL glacial acetic acid to 1 L final volume). The GPs suspension was homogenized under magnetic stirring for 30 min and placed in a 250 mL Schott glass bottle and heated to 122 °C at 1 bar (autoclave) for 40 min. The resultant suspension was centrifuged 10 min at 5000 x *g* to separate the soluble (supernatant) from the insoluble β-glucan (pellet). If there was still insoluble β-glucan on the supernatant, it was re-centrifuged in new tubes. After that, the supernatant was vacuum filtered (0.45 µm nylon filter) resulting in nearly 50 mL of filtrate which was further precipitated with 125 mL ethanol 96 % and homogenized under magnetic stirring for 15 min. The suspension was centrifuged for 15 min at 1600 x *g*, and the pellet freeze-dried using a Labconco freeze-dryer (77530, Kansas City, USA). The Fourier transform infrared spectroscopy (FTIR) spectrum of the resultant soluble β-glucan (Glu) was recorded using a Jasco FT/IR-420 spectrometer associated with an ATR horizontal reflexion (MiracleTM, PIKE Technologies) (Figure 3.1). The instrument operated with a resolution 2 cm-1 and 30 scans were collected for each sample. Spectra were recorded between 650 cm-1 and 4000 cm-1.

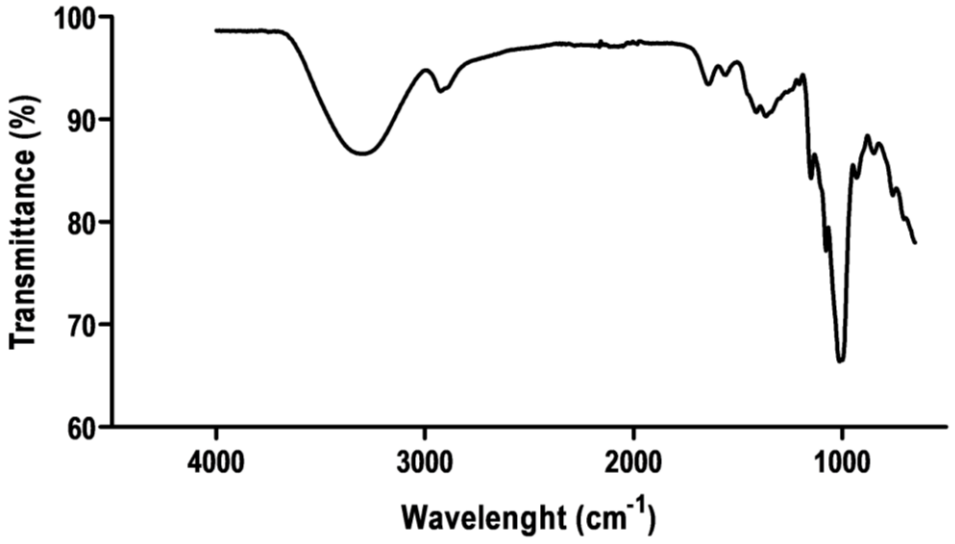

Figure 3.1. FTIR spectra of soluble glucan produced.

3.2.2.4. Preparation of Pol with or without β-glucan

Polymers were mixed (in a ratio of 1PDMAEMA:4PβAE and hereinafter designated by “PolyMix”) and dissolved in Milli-Q water at different concentrations as shown in table 3.1. The PolyMix was mixed with different volumes of pCMV.Luc at different concentrations resulting, consequently, in different polymer:DNA (+/-) charge ratios. The mixture was incubated for 15 min at room temperature (RT°) and Pol were used immediately. For Pol prepared with β-glucan the procedure was slightly modified. Glu was incorporated in Pol formation replacing 50 µL of the Mili-Q water used by a 0.8 % (w/v) Glu solution (Table 3.1) while GPs were suspended in formulation after Pol formation to a final concentration equivalent to Glu.

Table 3.1. Conditions tested to evaluate the effect of different PolyMix, pDNA and Glu conditions on the resultant Pol properties, respecting a final volume of 200 µL in water.

Condition	PolyMix			Glu 0.8 %	pDNA			Polymer:pDNA
	Vol. (µL)	[ ] (mg/mL)	Mass (µg)	Vol. (µL)	Vol. (µL)	[ ] (µg/mL)	Mass (µg)	Charge Ratio (+/-)
1[#]	27.95	3	84	---	40	100	4	25:1
1Glu				50				
2	27.95	30	840	---	80	500	40	25:1
2Glu				50				
3	27.95	30	840	---	120	500	60	17:1
3Glu				50				
4	27.95	25	699	---	120	375	45	19:1
4Glu				50				
5*	27.95	25	699	---	80	750	60	13:1
6	27.95	20	560	---	120	333	40	17:1
6Glu				50				
7*	27.5	20	560	---	80	666	53	13:1
8[$]	27.95	15	420	---	120	250	30	17:1
8Glu				50				
9	27.95	15	420	---	80	500	40	13:1
9Glu				50				

*[#] control condition previously described [295]; * condition excluded as a result of huge flocculate (precipitate) formation; [$] this condition was not excluded, but small flocculation was observed. PolyMix, PDMAEMA and PβAE mixture; Glu, soluble β-glucan; pDNA, plasmid DNA. Vol., volume.*

Envisioning *in vivo* vaccine formulation composition per mouse, Pol corresponding to the condition 4 (Table 3.1) were adjusted to a final pDNA mass of 40 µg in combination or not with 400 µg of β-glucan adjuvant (Glu or GPs) and 10 µg of CpG solution. All the

conditions were summarized in table 3.2 and were used from now on for all the further experiments.

Table 3.2. Vaccine formulation designs, composed by Pol in combination or not with the adjuvants: soluble β-glucan (Glu), particulate β-Glucan (GPs) and CpG ODN.

Formulations	PolyMix 25 mg/mL	Glu 0.8 %	pDNA 375 µg/mL	CpG 3.75 µg/µL	GPs
Pol	24.95 µL	---	107 µL	---	---
GluPol	24.95 µL	50 µL	107 µL	---	---
GluPol + CpG	24.95 µL	50 µL	107 µL	2.66 µL	---
GPsPol	24.95 µL	---	107 µL	---	400 µg

These formulations were adjusted from the condition 4 (Table 1) and correspond to a final volume of 200 µL containing a final pDNA mass of 40 µg for an in vivo administration per mouse. The same procedure was used for formulation production for in vitro studies, further diluted according to the pDNA amount used per well, described in appropriate materials and methods sections. PolyMix, PDMAEMA and PβAE mixture; Glu, soluble β-glucan; pDNA, plasmid DNA, CpG, CpG oligodeoxynucleotide; GPs, particulate β-glucan; Pol, PDMAEMA/PβAE-based polyplexes.

3.2.3. Size and zeta potential

Size and zeta potential measurements were performed immediately after Pol preparation using a Zetasizer Nano-ZS (Malvern Instruments Ltd., UK). Particle size was evaluated by dynamic light scattering (DLS) at 25 °C and backward scattering angle of 173°. Average hydrodynamic particle size average (z-average) was determined with Zetasizer 7.02 software. zeta potential measurements were performed using a coupled laser Doppler electrophoresis and determined using a Smoluchovski model.

3.2.4. Gel retardation assay

Pol stability was evaluated by agarose gel electrophoresis. 10 µL of Pol aliquots, corresponding to 1.5 µg of pDNA, were mixed with 2 µL of loading buffer containing bromophenol blue and glycerol. 6 µL were loaded and separated on a 0.75 % agarose gel in TBE solution (89 mM Tris-buffer (pH 8.6), 89 mM boric acid, 2.5 mM EDTA), containing SYBR™ Safe DNA Gel Stain in a proportion of 1:10000 (v/v), at a constant voltage of 100 V

for 45 min (horizontal DNA electrophoresis System, Bio-Rad, Hercules, CA, USA). DNA bands were visualized using a UV-transilluminator (UVITEC Cambridge, Cambridge, UK). The control was always naked pDNA.

3.2.5. *In vitro* transfection

3.2.5.1. Cell culture

Pol biological activity was evaluated in COS-7 (african green monkey kidney fibroblast-like) and RAW 264.7 (macrophage, Abelson murine leukemia virus transformed) cell lines (ATCC, USA). Cells were maintained at 37 °C and 5 % CO_2, in DMEM, supplemented with 10 % heat-inactivated FBS (unless stated FBS free medium), 1 % PenStrep and 10 mM Hepes. COS-7 cells DMEM was high glucose supplemented with 12 mM sodium bicarbonate, while RAW 264.7 cells DMEM was supplemented with 3.7 g/L sodium bicarbonate. COS-7 cells were detached by treatment with 0.5 % trypsin solution while RAW 264.7 cells with a cell scraper or cell dissociation medium (NaCl 8 g/L, Na_2HPO_4 1.16 g/L, KH_2PO_4 0.2 g/L, EDTA 0.16 g/L).

3.2.5.2. Luciferase expression

Transfection experiments were conducted as previously described [267, 295]. COS-7 or RAW 264.7 cells were seeded in 48-well plates at a density of $2x10^4$ or $6x10^4$ cells/well, respectively. After 24 h of incubation, the medium was replaced by serum-free medium and Pol or PEI-based polyplexes (PEIPol) (branched, Mw 25,000 $g.mol^{-1}$, at a 25:1 N/P charge ratio, as previously described [295]) formulations added in a concentration corresponding to 1 µg of pCMV.Luc/well in a final volume of 500 µL (2 µg/mL). After 4 h incubation the serum-free medium containing the formulations was replaced by complete medium and cells were incubated for additional 44 h. Then, cells were washed with phosphate buffer saline pH 7.4 (PBS) and 100 or 75 µL (COS-7 cells and RAW 264.7, respectively) of lysis buffer (1 mM DTT, 1 mM EDTA, 25 mM Tris-phosphate, pH 7.8, 8 mM $MgCl_2$, 15 % glycerol, 1 % (v/v) Triton X-100) were added to each well. Lysate luciferase activity was evaluated by measuring the relative light units (RLU) in a microplate reader (Synergy HT, Biotek, USA) and normalized against total protein content, measured by *DC*™ protein assay kit, using a bovine serum albumin solution as standard.

3.2.5.3. GFP expression

Transfection experiments involving GFP expression were conducted as described above for RAW 264.7 cells, using polyplexes prepared with the pCMV.GFP instead. GFP gene expression was evaluated by laser scanning confocal microscopy (LSCM) (Zeiss LSM 510 META, Carl Zeiss, Oberkochen, Germany). Cells were plated at a cell density of $24x10^4$ cells/well in 12-well plates over glass coverslips and Pol corresponding to 2 or 3 μg of pCMV.GFP were added per well in a final volume of 1 mL (2 μg/mL or 3 μg/mL). After 48 h incubation, cells were washed twice with PBS and detached with 250 μL of dissociation medium followed by 500 μL of cold medium addition to each well. After that, cells were washed twice with PBS (by centrifuging 5 min at 450 x *g* at 4 °C) and fixed with 4 % formaldehyde in PBS for 15 min at 37 °C. The nucleus and cell membrane were labeled using Image-iT™ LIVE Plasma Membrane and Nuclear Labeling Kit, according manufacturer's instructions. After labeling, cells were washed twice with PBS and the coverslips mounted in microscope slides with DAKO mounting medium, and further examined under the LSCM.

3.2.6. Cell viability

Cell viability was evaluated using a modified Alamar Blue Assay®, 47 h post-transfection with Pol prepared with pCMV.Luc, as previously described [295]. Briefly, 47 h post-transfection cells were incubated with 0.3 mL of 10 % (v/v) Alamar Blue dye in complete DMEM medium, prepared from a 0.1 mg/mL stock solution of Alamar Blue. After 1 h incubation at 37 °C, 180 μL of the supernatant were collected from each well and transferred to 96-well plate. The absorbance (abs) at 570 and 600 nm was measured in a SPECTRAmax PLUS 384 spectrophotometer (Molecular Devices, USA). Cell viability (as a percentage of untreated control cells) was calculated according to the formula (Eq. 3.1):

$$Cell\ viabilty\ (\%) = \frac{(\mathrm{Abs570} - \mathrm{Abs600})\ \mathrm{of\ treated\ cells\ x\ 100}}{(\mathrm{Abs570} - \mathrm{Abs600})\ \mathrm{of\ control\ cells}} \quad (\mathrm{Eq.\ 3.1})$$

RAW 264.7 cell viability, after incubation with suitable formulations for *in vivo* studies containing pCMV.Luc concentrations ranging from 0.75 to 6 μg/mL, was also performed the same way to determine the non-toxic Pol working range.

3.2.7. Uptake in RAW 264.7 macrophages

For the uptake experiments, RAW 264.7 cells were plated and treated as stated above for GFP transfection studies (section 3.2.5.3) and analyzed by LSCM, but only using 2 µg of pDNA/well (2 µg/mL). Here, Pol were prepared with Cy5 labeled pCMV.Luc according to manufacturer's instructions, with or without β-glucan adjuvants (GluPol or GPsPol), to evaluate internalization following 4 or 48 h incubation.

3.2.8. Mice vaccination

Seven to eight-week old female C57BL/6 mice were obtained from Charles River Laboratories (Barcelona, Spain), acclimated for 1 week and maintained in the local animal house facility, with free access to food and water and 12 h light/dark cycle. Animal studies were approved (ORBEA_50_2013/27092013) and carried out in accordance with institutional ethical guidelines and with National (Dec. No. 113/2013) and International (2010/63/EU Directive) legislation. Formulations used in vaccination groups are listed in figure 3.1. All vaccines were administered in Mili-Q water through the subcutaneous (SC) route and mice were sacrifices on day 56 by cervical dislocation. Non-vaccinated mice (Naïve, n=3) were used as a control group.

3.2.8.1. Blood collection

Blood samples were collected by submandibular venipuncture with an animal lancet to microcentrifuge tubes, 14 days after each immunization and immediately before the next boost. The blood coagulated over 6 h and was further centrifuged for 10 min at 4500 x *g*, for serum collection. The resultant supernatant was carefully transferred to another microcentrifuge tube and stored at −20 °C until further analysis.

3.2.8.1.1. Serum immunoglobulins

The determination of HBsAg-specific serum IgG titers was performed by ELISA as previously by our group [210]. Briefly, 100 µL of 1 µg/mL HBsAg in solution (50 mM sodium carbonate/bicarbonate, pH 9.6) were used for coating of a high-binding 96-well plates (Nunc MaxiSorp™ flat-bottom, Thermo Fisher Scientific Inc., Waltham, MA, USA). After an ON incubation, plates were washed five times with PBS-T and blocked with 1 % BSA in PBS-T for 1 h at 37 °C. After washing, 100 µL of serial dilutions of serum samples,

starting at 1:64, were added to the wells and incubated for 2 h at 37 °C. Following washing, 100 µL of HRP conjugated goat anti-mouse IgG (1:10000), IgG1 (1:20000), IgG2c (1:5000) and IgG3 (1:2500) antibody solutions in PBS-T were added and incubated for 30 min at 37 °C. After that, the detection was performed with 100 µL of a substrate OPD solution (5 mg OPD to 10 mL citrate buffer and 10 µL H_2O_2) incubation for 10 min at RT° in the dark. Reaction was stopped with 50 µL of 1 M H_2SO_4 and absorbance was determined at 492 nm. The serum IgG titers were presented as the end-point titer, which is the antilog of the last log 2 dilution for which the optical density (OD) was at least two-fold higher than the value of the naive sample equally diluted. The log 2 endpoint titers were used to normalize the data and equalize variability and then statistically analysed.

3.2.8.2. Spleen cells cytokine production after HBsAg restimulation

Individual mice spleen cell suspensions were prepared [273] and restimulated with the HBsAg [267] as previously described, without erythrocytes lysis. Spleens were collected on day 56 and a single cell suspension was prepared using a 70 µm cell strainer. Cells were washed three times centrifuging for 10 min at 218 x *g* and resuspending in cell culture media (RPMI 1640, 10 % FBS, 20 mM HEPES, 1 % PenStrep, 0.1 % 2-mercaptoethanol, 1 % NaOH 1 M, 1 % sodium pyruvate, 1 % MEM non-essential amino acids, 2 % MEM amino acids). Then, 50 µL of the cell suspension were plated at a density of $1x10^7$ cells/ mL in 96-well plate and 150 µL of media, either alone or containing HBsAg, Con A or LPS as positive controls (final concentrations of 6.25 µg/mL, 1 µg/mL and 5 µg/mL respectively), were added to the cells. The plates were incubated at 37 °C for 48 h to induce cytokine production by antigen-specific T cells and the supernatants collected and stored at −80 °C until further analysis. IFN-γ, IL-4 and IL-17 cytokines were determined using Peprotech murine development ELISA kits, according to manufacturer's instructions.

3.2.9. Statistical analysis

Results are expressed as mean ± standard error of the mean (SEM). Statistical analysis was performed by GraphPad Prism v 5.03 (GraphPad Software Inc., La Jolla, CA, USA). Comparisons between two samples were done using Student's t-test and multiple

comparisons by ANOVA, followed by Tukey's post-test. A value of $p<0.05$ was considered statistically significant.

3.3. Results and discussion

The present work aimed to develop a DNA vaccine against the hepatitis B virus. For that, PDMAEMA:PβAE-based polyplexes (Pol) developed by our group [295] were used as the vector for the pDNA encoding the HBsAg (pCMV-S) in combination or not with β-glucan as an additional adjuvant. New Pol preparations were tested for more concentrated formulations when compared with our previous work, envisioning a SC administration of 40 μg of pCMV-S. This pCMV-S dose was chosen based on previous results obtained following a SC vaccination with only 20 μg of pDNA per dose, even though using a different nanosystem [300].

3.3.1. Pol transfection efficiency is preserved (GluPol) or enhanced (GPsPol) in the presence of β-glucan.

Several PolyMix:pCMV.Luc charge ratios resulting from different PolyMix and pDNA solutions conditions were tested for optimal physicochemical properties and biological activity, originating the nine conditions showed in table 3.1. Condition 1 represented the starting point previously developed. Some conditions were immediately excluded due to Pol flocculation and sedimentation, which happened for higher pDNA concentrations (above 500 μg/mL – conditions 5 and 7). The remaining conditions proceeded for additional Glu incorporation and further characterization (Figure 3.2). The excellent Pol capacity to condense pCMV.Luc, previously reported for condition 1 [295, 298], was maintained in the new conditions, demonstrated through the electrophoretic mobility profile of the pDNA in agarose gel (Figure 3.2A). No free pDNA migration was observed including in the presence of Glu, meaning that it did not affect Pol formation. Expectedly, all conditions resulted in positively charged Pol with a surface charge between +30 mV and +41 mV (Figure 3.3B), due to the high quantity of cationic polymers compared to pDNA. In some cases, although not statistically significant (most notorious in condition 3) it was observed that Glu association into the formulation (GluPol) has slightly decrease zeta potential from +36 mV to +30 mV. This is consistent with the contribution of β-glucan neutral charge to Pol surface properties. Regarding Pol size, mean diameters between

135 nm and 320 nm were measured (Figure 3.2B), and differences were mostly related to formulation conditions. Although the addition of Glu did not influence mean diameter, a modest increase in polydispersity index (PDI) was observed in most Glu conditions.

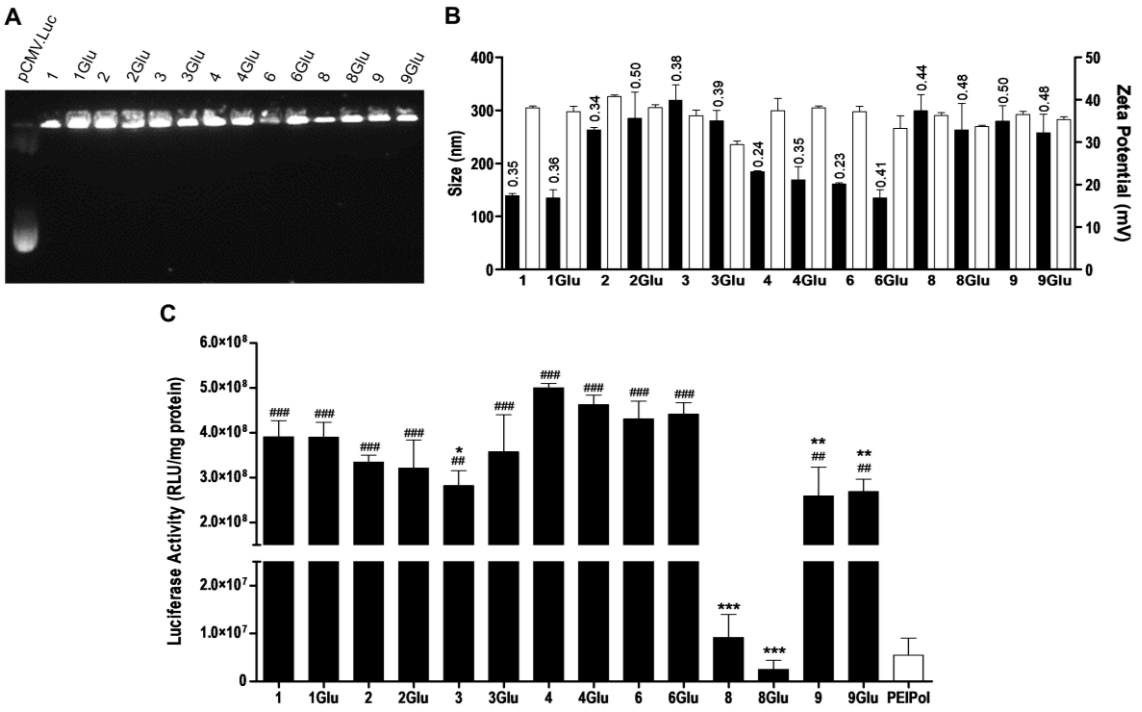

Figure 3.2. Effect of PolyMix, pDNA amount and the presence of soluble β-glucan "Glu" in Pol physicochemical properties and transfection activity. The results represent nine different conditions of polyplex preparation in the presence or not of the soluble β-glucan (Glu) (Table 3.1). (**A**) Capacity to complex pCMV.Luc evaluated through agarose gel electrophoresis. (**B**) Size (■, left Y axis, polydispersity index above each bar) and zeta potential (□, right Y axis). (**C**) Transfection activity in COS-7 cells, where 1 µg of pCMV.Luc (2 µg/ mL) complexed either with the PolyMix (PβAE and PDMAEMA polymer mixture) or the PEI as a positive control (PEIPol), were incubated 4 h with the cells and the luciferase activity (RLU/mg protein) evaluated after 48 h. Data are representative of three independent experiments and are presented as mean ± SEM. ** denotes statistical differences between condition 4 and the other conditions at p<0.05, ** p<0.01 and *** p<0.001; # denotes statistical differences between the positive control PEIPol and all the formulations at p<0.05, ## p<0.01, and ### p<0.001.*

To investigate the transfection ability of all conditions, we chose the COS-7 cell line, widely recognized as an adequate choice for transfection experiments with pDNA. Figure 3.2C data showed that all formulations, except condition 8, resulted in much higher luciferase gene expression, when compared with the positive control PEIPol, a well-known polymer-based gene delivery vector ($p<0.01$; $p<0.001$), which is a remarkable

result. Concerning to condition 8, the transfection result demonstrated that this condition was as good as the positive control and that the other conditions were even better. The observed lower biological activity could be explained due to the formation of tiny flocs observed when pDNA was added to the PolyMix (although not reflected in mean size, since the tiny flocs easily sedimented during DLS measurements). This condition was not readily excluded as the flocculation did not occur at the same extent as in conditions 5 and 7. Crossing these results with physicochemical characterization, it was observed that smaller Pol (conditions 1, 4 and 6) seemed to promoted a higher luciferase gene expression, when compared to larger Pol (conditions 2, 3, 8 and 9), even for the same polymer:DNA ratio (Figure 3.2C). Interestingly, although the differences in charge ratios of conditions 1, 4 and 6 they share the common feature of a mean diameter inferior to 200 nm and superior transfection capacity which suggests that polyplex size can play a crucial role in the expression of the carried gene. Effectively, other physicochemical properties such as positive surface charge is generally recognized as a desirable feature to increase particle-cell interactions with the negatively charged cell membrane, influencing uptake efficiency, endosomal escape and intracellular localization, improving biological activity [301, 302]. To note that Glu incorporation into PolyMix (PDMAEMA and PβAE) did not significantly interfere with the high transfection capacity (Figure 3.2C) of the Pol-based nanosystems prepared under the conditions described in table 3.1. Overall, condition 4 was the one that resulted in higher biological activity in comparison with remaining conditions (Figure 3.2C) and was therefore selected for subsequent studies including vaccination studies.

To evaluate that the excellent transfection activity of condition 4 will be preserved after pDNA adjustments and incorporation of additional adjuvants used in final vaccine formulation designs (Table 3.3), it was mandatory to perform new characterization studies showed in figure 3.3. The presence of either Glu, CpG or GPs did not affect Pol capacity to condense pDNA (Figure 3.3A). Size was similar for all vaccine designs (≈ 180 nm), except the one containing 2-4 µm sized GPs, that contributed to the increased whole formulation mean diameter (Figure 3.3B). Zeta potential values were also affected by GPs neutral charge that contributed to decreased whole formulation surface charge when compared to the Pol formulation ($p<0.001$). To note that this value represents the mean

of two individually peaks observed during DLS measurements corresponding to either highly positive Pol or neutral GPs. No differences were observed in Pol size related to Glu incorporation or CpG addition. Although not statistically significant, when compared to Pol formulation, Glu incorporation resulted in decreased surface charge, from +41 mV to +38 mV, suggesting the presence of Glu on Pol surface. Consistently, the contribution of Glu neutral charge may hide some positive groups of PDMAEMA and PβAE polymers resulting in a modest decrease of zeta potential. CpG addition to GluPol formulation resulted in a significantly decrease in the surface charge to +36 mV when compared to Pol formulation ($p<0.05$) probably due to the combined surface localization of both Glu and CpG. The combination of synthetic CpG with Glu in one of the formulations (GluPol + CpG) was justified by the fact that CpG has been proved to be an excellent immunopotentiator, able to modulate the immune response to a balanced Th1/Th2 immune response, already tested in vaccination studies with HBsAg [145, 188, 208]) The fact that although the same amount of Glu and GPs was used as a β-glucan adjuvant (400 μg) and the zeta potential has suggested that the Glu was also localized on Pol surface (GluPol), it was not possible to estimate the exact amount of Glu on Pol surface, an essential aspect to observe the immunomodulatory effect explained by the activation of Dectin-1 receptor [224]. Unmethylated CpG motifs are also present in pDNA backbone and stimulate innate immune responses via toll-like receptor (TLR)9 recognition by APCs [269]. Furthermore, figure 3.3C shows that the excellent transfection activity evaluated in COS-7 cells was preserved in the presence of the additional GPs and CpG. Luciferase gene expression was 150-fold higher for Pol, GluPol and GPsPol + CpG ($p<0.05$) and 250-fold higher for GPsPol ($p<0.01$) than that observed for the positive control. Moreover, vaccine formulations containing GPs, the transfection activity was higher than Pol “alone” ($p<0.05$). Moreover, in agreement with a previous report [295], no substantial cytotoxicity was observed (Figure 3.2D), as the cell viability was ≥70 %.

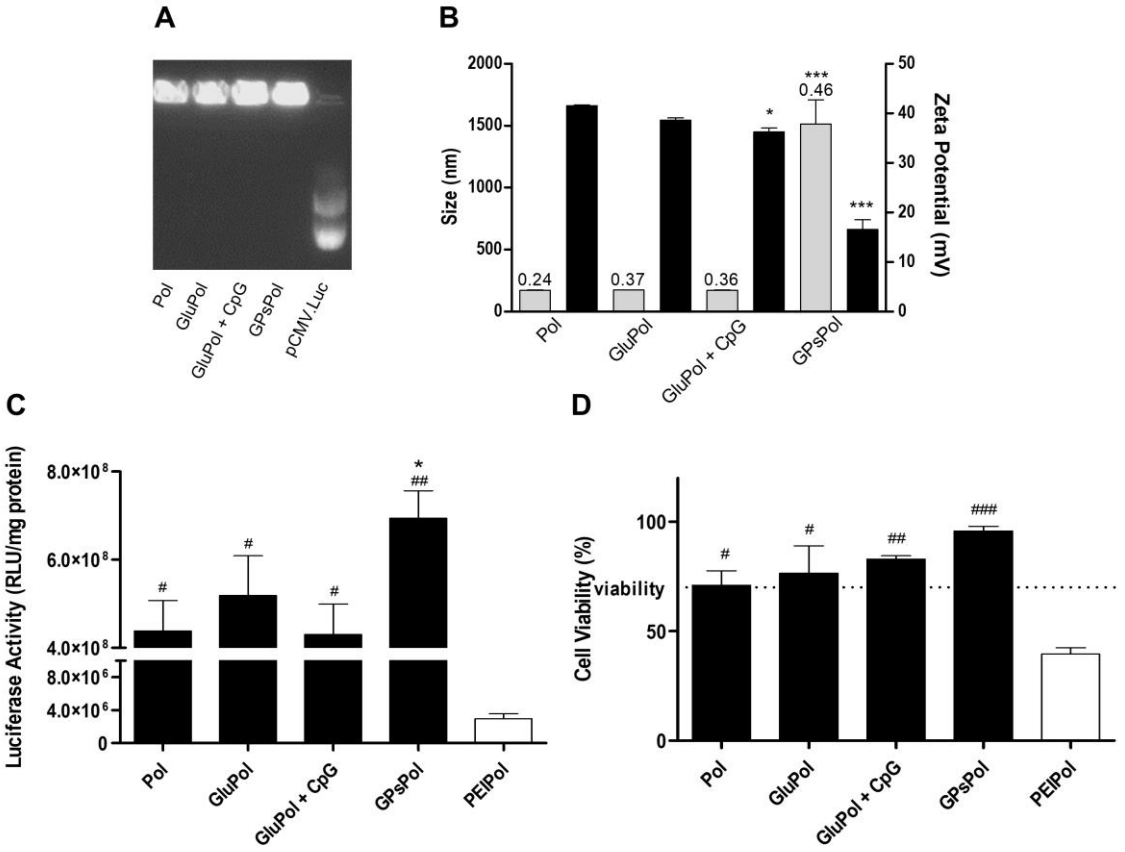

Figure 3.3. Vaccine formulation properties and transfection activity in COS-7 cells. (**A**) capacity to complex pCMV.Luc evaluated through agarose gel electrophoresis; (**B**) size (■, left Y axis, polydispersity index above each bar) and zeta potential (■, right Y axis); (**C**) transfection activity in COS-7 cells, where 1 µg of pCMV.Luc (2 µg/mL) complexed with the PolyMix (PβAE and PDMAEMA polymer mixture - Pol) in the presence of soluble β-glucan (GluPol) or combined with particulate β-glucan (GPsPol), or complexed with the PEI as a positive control (PEIPol) were incubated 4 h with the cells and luciferase activity evaluated after 48 h (RLU/mg protein). (**D**) Correspondent cell viability evaluated by an Alamar Blue® assay and expressed as % of the untreated control cells. The results represent three independent experiments and data expressed as mean ± SEM. ** p<0.05 and *** at p<0.001 denote statistical differences between Pol and the other formulations (GluPol, GluPol + CpG and GPsPol); # p<0.05, ## p<0.01, and ### at p<0.001 denote statistical differences between the positive control PEIPol and all the formulations.*

3.3.2. Particulate β-glucan (GPs) enhances Pol transfection activity in RAW 264.7 macrophages.

APCs activation could be a good strategy to improve transfection efficiency in immune cells and consequently the development of an effective immune response following pDNA vaccination. In that context, it was decided to evaluate if the presence of β-glucan, a Dectin-1 ligand, would have any impact on polyplex biological activity in immune cells. RAW 264.7 macrophage cell line, widely used to explore particle

immunomodulatory effects, was selected for that purpose [158, 303]. First, as it was not tested before, the Pol cytotoxicity profile correspondent to pCMV.Luc concentrations from 0.75 μg/mL to 6 μg/mL was evaluated in these cells and the results were presented in figure 3.4A. Non-toxic Pol working range was up to 3 μg/mL of pDNA as shown by the relative viability reaching 70 % of the control. Luciferase expression data showed a transgene expression 85 to 115-fold higher than that observed with the positive control ($p<0.001$) (Figure 3.4B). Furthermore, GPsPol also resulted in a statistically higher luciferase gene expression than only Pol ($p<0.01$), indicating a benefic and promising effect of GPs in the Pol-mediated gene expression (observed both in COS-7 and RAW 264.7 cells). Here we hypothesized that this improved transfection capacity could be due to enhanced pDNA delivery by GPs to the cells resulting in increased expression of the transgene. β-glucans (Glu and GPs) bind to Dectin-1 receptor, widely expressed in APCs, which can interfere with pDNA delivery to that cells.

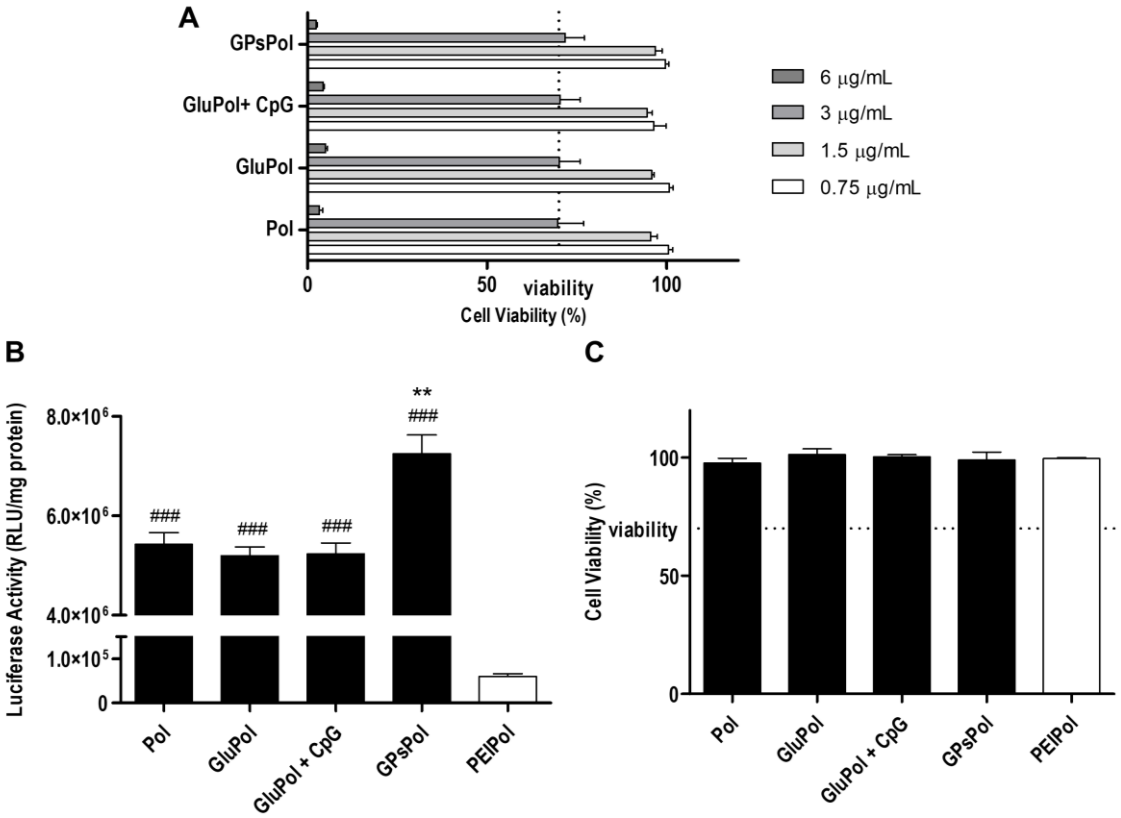

Figure 3.4. Vaccine formulation viability profile and transfection activity in RAW 264.7 macrophages. (**A**) cell viability in concentrations of complexed pCMV.Luc ranging from 0.75 to 6 μg/mL, evaluated by a Alamar Blue® assay expressed as percentage of untreated control cells. (**B**) Transfection activity in RAW 264.7 macrophages, where 1 μg of pCMV.Luc (2 μg/mL) complexed with the PolyMix (PβAE and PDMAEMA polymer mixture - Pol) in the presence of soluble β-glucan (GluPol) or combined with particulate β-glucan (GPsPol), or complexed with the PEI as a positive control (PEIPol), were incubated with cells for 4 h and luciferase activity (RLU/mg protein) evaluated after 48 h. (**C**) cell viability (evaluated as in (A)) correspondent to transfection activity presented in (B). The results represent three independent experiments and data is expressed as mean ± SEM. ** p<0.05 denotes statistical differences between Pol and the other formulations (GluPol, GluPol + CpG and GPsPol); # p<0.05 and ## p<0.01 denote statistical differences between the positive control PEIPol and all the vaccine formulations.*

Cell uptake studies were performed to figure out the hypothesis formulated in the previous section. Previously, we observed that Pol were internalized mainly by clathrin-mediated endocytic pathway [295]. However, GPs could influence the cell internalization process and, consequently, Pol transfection activity. The confocal microscopy results (Figure 3.5A) clearly showed that after 4 h of incubation a substantial amount of Pol, of all tested formulations, were observed inside the cells (red fluorescence of Cy5 labeled

pDNA – Figure 3.5A a-c). Nevertheless, similar internalization efficiency was observed for all formulations, independently of GPs presence, suggesting that as the transfection activity is very high for all the formulations, this method did not demonstrate sufficient sensibility to visualize the differences observed on luciferase transfection studies. After 48 h of incubation (Figure 3.5A d-f) less pDNA could be seen inside the cells, probably due to its incorporation into the nucleus. Bright field images are also shown to provide cell membrane morphology perception (Figure 3.5A g-l). This data correlates with previous experiments of our group in a lung epithelial cell line using chitosan nanoparticles as the pDNA vector [267]. With same purpose to have images illustrating the effect of β-glucan association to Pol (GluPol and GPsPol) on transfection efficiency, a new transfection study with RAW 264.7 macrophages was performed using GFP as reporter gene and confocal microscopy to visualize the result. The images obtained (Figure 3.5B) showed that only few cells express the transgene, following 48 h incubation with either 2 μg/mL (Figure 3.5B a-c) or 3 μg/mL (Figure 3.5B d-f) of pCMV.GFP containing Pol. Moreover, the results using 2 μg/mL of pDNA per well, corresponding to same pDNA concentration used in luciferase gene expression studies, indicate that not all cells that internalized the polyplexes expressed the transgene, since Cy5 labeled pCMV.Luc was seen inside almost every cell following 4 h of uptake (Figure 3.5A) while much less cells seemed to have expressed the GFP (Figure 3.5B d-f). Importantly, the low RAW 264.7 cell transfection rate observed is not necessarily related with a poor adjuvant effect on immune cells *in vivo*. In fact, some authors reported that even though only a small proportion of DCs were transfected with pDNA a generalized maturation of untransfected DCs occurred [88], revealing that even low transfection rates might exert a global effect for the vaccine efficacy. Regarding GluPol, although no biological differences were seen *in vitro*, we cannot exclude the possibility that a targeting effect recruiting APCs *in vivo* would occur. All in all, these data together with the good transfection results observed supported the decision to evaluate the formulations through the SC route in a vaccination study.

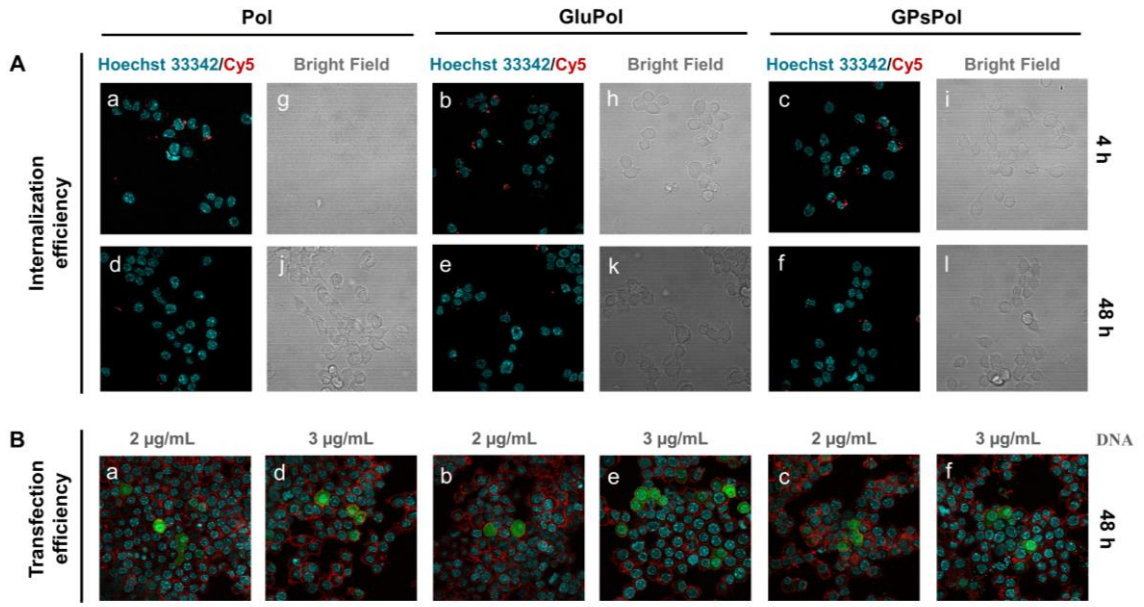

Figure 3.5. Effect of β-glucan on Pol internalization and transfection efficiency in RAW 264.7 assessed by confocal microscopy. Polyplex conditions were prepared by pDNA complexation with the PolyMix (PβAE and PDMAEMA polymer mixture - Pol) in the presence of soluble β-glucan (GluPol) or combined with particulate β-glucan (GPsPol). (**A**) Polyplex internalization following incubation with the cells for 4 h (a-c, g-i) or 48 h (d-f, j-l) (pDNA at 2 µg/mL). The images show merged channels of cell nucleus (Hoechst 33342, in blue) and polyplex (Cy5 labeled pCMV.Luc, in red) (a-f) and the bright field to show the cells (g-l). (**B**) Transfection efficiency of polyplex incubated with the cells for 4 h and evaluated after 48 h (pCMV.GFP, 2 µg/mL (a-c) or 3 µg/mL (d-f)). Confocal microscopy images show merged channels representative of nucleus (Hoechst 33342, in blue), cell membrane (Alexa Fluor™ 594, in red) and GFP expression (in green) (a-f).

3.3.3. The results of vaccination studies are not correlated with the outstanding transfection results.

All vaccine formulations were described, characterized and tested *in vivo,* and the results were illustrated in figure 3.6. Size and zeta potential results of vaccine formulations with pCMV-S (Figure 3.6A) were similar to those observed with pCMV.Luc for *in vitro* studies (Figure 3.3B). Four subcutaneous administrations of 40 µg of pCMV-S each, with 14 days interval between doses, resulted in 40 % responder mice with serum antigen-specific antibodies detectable 14 days after the last boost (day 56 – Figure 3.6C). To note that serum anti-HBsAg IgG titers were considerably lower than expected, considering the excellent transfection results obtained *in vitro*, and also considerably lower than previously observed with vaccine formulations using the HBsAg protein antigen [188, 189, 300, 304]. No significant differences were observed between groups.

Additionally, no HBsAg-specific cell-based immune responses were observed following HBsAg recall of vaccinated mice spleen cells (Figure 3.6D). The detected levels of IL-4, IL-17 and IFN-γ were extremely low and comparable to the Naïve group where no vaccine was administered. In fact, the low number of responder mice with very low antibody titers and the absence of signs concerning to cell-mediated immunity observed in all groups do not allowed to draw strong conclusions regarding the several immunopotentiators tested with polyplexes. In fact, the problem was the low transfection *in vivo* and since only the adaptive immune response was evaluated, the effect of the adjuvants was hidden.

A

Groups	pCMV-S (μg)	Adjuvant (μg)	Size (nm)	PDI	Zeta Potential (mV)
Pol (n=5)	40	___	172.5 ± 4.4	0.23 ± 0.04	42.6 ± 0.2
GluPol (n=5)	40	Glu (400)	173.8 ± 7.4	0.34 ± 0.06	39.9 ± 1.1
GluPol + CpG (n=5)	40	Glu (400) + CpG (10)	170.4 ± 9.8	0.35 ± 0.07	37.3 ± 1.3*
GPsPol(n=5)	40	GPs (400)	1514 ± 337.5	0.47 ± 0.10	16.6 ± 3.4***

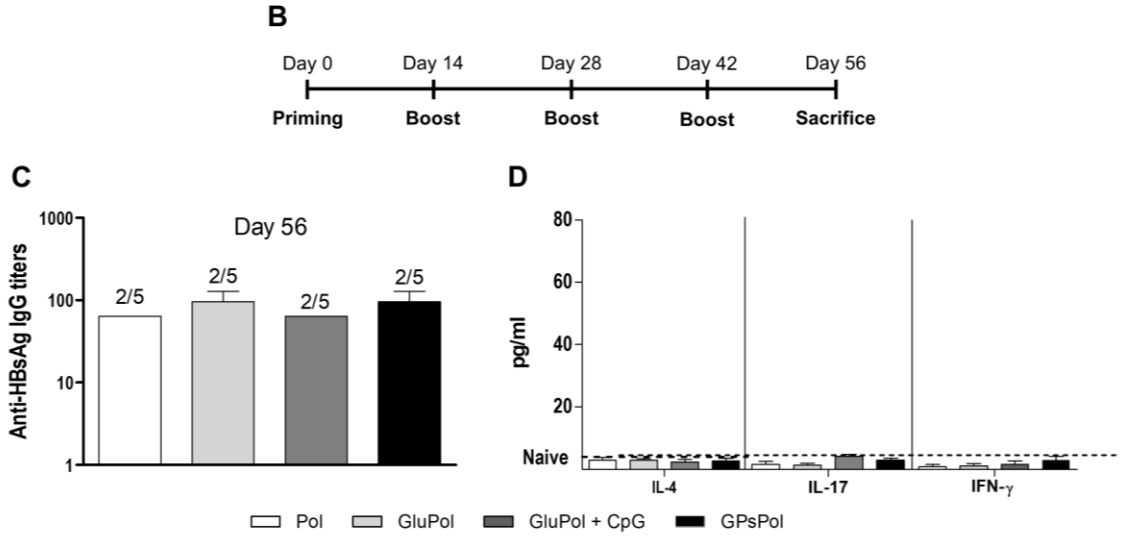

Figure 3.6. Vaccine formulation prepared with pCMV-S (plasmid DNA encoding the HBsAg) and the HBsAg-specific elicited immune response in mice. Mice were immunized with the formulations represented in (**A**) following the vaccination schedule represented in (**B**). (**C**) Serum anti-HBsAg IgG titers at day 56 (the number of responder mice is shown above each bar). The end-point titer presented is the antilog of the last log 2 dilution for which the value of OD was at least two-fold higher than that of the naive sample equally diluted. The log 2 endpoint titers were used for statistical analysis. (**D**) IL-4, IL-17 and IFN-γ levels determined by ELISA in the supernatant of mice spleen cells collected on day 56 and cultured with HBsAg for 48 h. Data are presented as mean ± SEM. ** p<0.05 and *** at p<0.001 denote statistical differences between Pol and the other formulations (GluPol; GluPol + CpG and GPsPol).*

Actually, it is widely recognized that pDNA vaccination is hard to achieve and significantly affected by several factors including the route of gene delivery, the dose and the vaccination schedule [87, 88]. The present approach was carefully designed considering all those factors and our experience with pDNA vaccination. We have recently correlated the weak antibody response observed through a subcutaneous vaccination schedule using pCMV-S condensed with chitosan/PCL nanoparticles with the low pDNA dosage (20 μg per dose) [300]. Indeed, the excellent gene delivery efficacy of previously developed PDMAEMA:PβAE-based polyplexes [295] and the present outstanding results of the polyplexes with β-glucan (GPsPol) greatly motivated the present *in vivo* study. Literature also supported the study design pointing out both PDMAEMA and PβAE polymers as great vehicles for gene delivery and β-glucan as valuable adjuvant for DNA vaccination resulting in APCs recruitment and activation [98, 233, 296]. Mannosylated-PβAEs polyplexes, a similar strategy for APCs vectorization, formulated with a pDNA encoding ovalbumin elicited humoral immune responses either by the subcutaneous or by the intraperitoneal route, without the use of an extra adjuvant [297]. PDMAEMA polyplexes formulated with pCMV-S lead to high levels of systemic immune responses following a vaccination schedule comprising a lower pDNA dosage (30 μg) by the intramuscular route [99]. Although the results of the present study revealed limited vaccine efficacy through the subcutaneous route, we cannot exclude the hypothesis that intramuscular injections can lead to better results. Some authors referred that intramuscular injection might be the best route for DNA vaccination [88]. Additionally, our group has previously demonstrated the induction of both HBsAg-specific humoral and mucosal immune responses following three intranasal administrations of 50 μg of pCMV-S complexed with chitosan-based nanoparticles [267], suggesting that pDNA vaccination can be effectively achieved by other than injectable routes. Polymer:DNA ratio can also affect transfection efficiency, as it was shown for mannosylated-PβAE polyplexes, that resulted in nearly 70 % GFP expressing RAW 264.7 cells for 200:1 ratio while less than 10 % expressed the transgene for 50:1 ratio [297]. In fact, although PDMAEMA:PβAE/DNA polyplexes induced higher transfection activity in COS-7 cells for 25:1 when compared to 50:1 charge ratio [295], we cannot exclude the possibility that it could be different for APCs *in vivo* or RAW 264.7 macrophages *in vitro* model. Therefore, this novel gene delivery nanosystem can be further optimized seeking APCs maximum transfection rate

and tested for other antigen-encoding plasmids or other vaccination routes that might lead to better *in vivo* results.

3.4. Conclusion

DNA vaccine research is often confronted with limited immunogenicity associated with poor transfection and immune tolerance. PDMAEMA and PβAE polymers used as a non-viral delivery vehicle together with additional adjuvants can be a great strategy to overcome those problems. In this study, we first proved that PDMAEMA:PβAE-based polyplexes (Pol) can be optimized for pDNA increased concentrations in order to obtain a small volume for the vaccination studies, not affecting their biological activity, making them an useful vector for mice vaccination. Then, we successfully combined two forms of β-glucan to the vaccine formulations wherein the particulate form of it (GPsPol) have enhanced Pol transfection capacity in RAW 264.7 macrophages. pCMV-S vaccination through the subcutaneous route was not effective as initially expected resulting in a 40 % HBsAg seroconversion rate, independent of β-glucan combination. DNA vaccination is exciting and significant progress has been already paved to sophisticated vaccine formulations. In that regard, the present study highlights the potential of non-viral vectors and adjuvant combination as a new design approach that might guide this research field to success.

CHAPTER 4

β-GLUCAN/CHITOSAN PARTICLES AS A NEW ADJUVANT FOR THE HEPATITIS B ANTIGEN

Abstract

The development of new vaccine adjuvants is urgently needed not only to enable new routes of vaccine administration but mostly to go beyond protective humoral immunity, often insufficient to fight infectious diseases. The association of two or more immunopotentiators or mimicking pathogen physicochemical properties are strategies that can favor powerful and more balanced Th1/Th2 immune responses. Therefore, the present work aimed to combine both chitosan and β-glucan biopolymers in the same particle, preferably with surface β-glucan localization to simulate the cell wall of some pathogens and to stimulate the immune cells expressing the Dectin-1 receptor. β-glucan/chitosan particles (GenGluChiPs) were developed through a chitosan precipitation method. The chitosan was precipitated into a β-glucan alkaline solution followed by genipin crosslink. The optimized method produced particles with a mean diameter of 837 nm for GenChiPs and 1274 nm for GenGluChiPs. β-glucan surface location was confirmed by zeta potential measurements (+24 mV for GenGluChiPs and +36 mV for GenChiPs) and zeta potential titration. These new particles showed high antigen loading efficacy and low cytotoxicity. Mice vaccination studies revealed that both GenChiPs and GenGluChiPs had an adjuvant effect for the hepatitis B surface antigen (HBsAg), with GenGluChiPs resulting in serum anti-HBsAg total IgG 16-fold higher than GenChiPs, when administered with 1.5 µg HBsAg per dose. Specifically, IgG1 subclass was 5-fold higher and IgG3 subclass was 4-fold higher for GenGluChiPs comparing to GenChiPs. Overall, the preparation method developed allowed the advantageous combination of β-glucan with chitosan, without chemical functionalization, which represents an additional step toward tailor-made adjuvants production using simple precipitation techniques.

Keywords

Chitosan, β-glucan, hepatitis B antigen, polymeric particles, vaccine adjuvants.

Graphical abstract

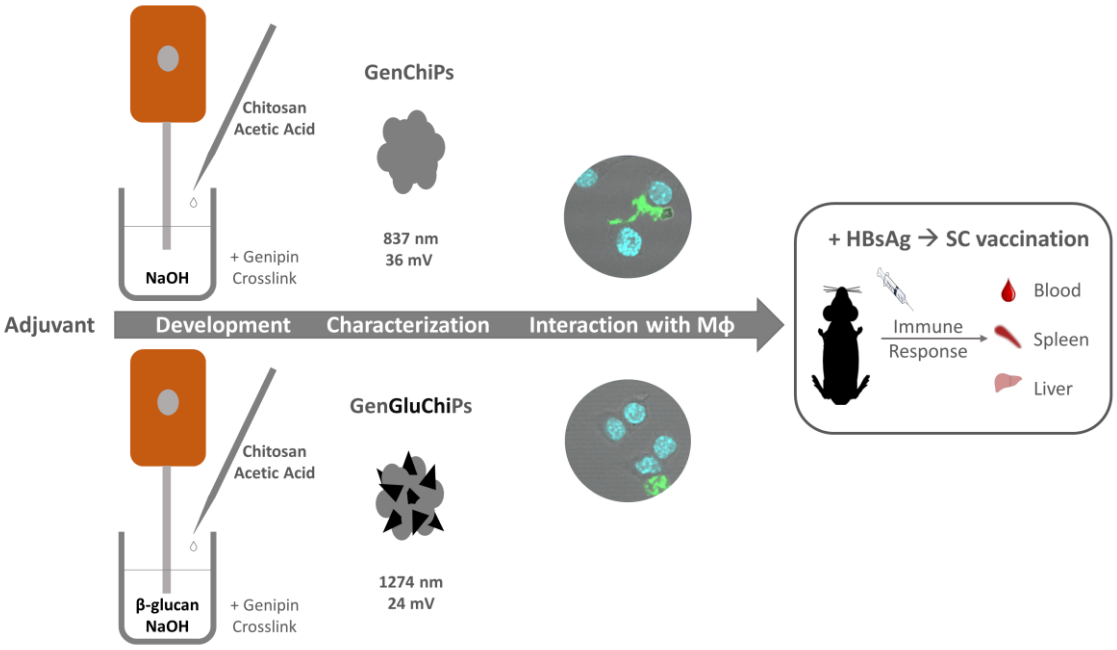

4.1. Introduction

Vaccination is one of the great successes of public health, still intangible for many infectious diseases [17]. Advancing technology allowed the development of subunit vaccines as a safer alternative to the traditional inactivated or live-attenuated [84]. However, subunit antigens (e.g. proteins, peptides or nucleic acids) are generally poorly immunogenic and require the addition of immunostimulatory agents (adjuvants) to obtain long-lasting protective immunity [19, 84, 85]. Vaccine adjuvants have multiple mechanisms of action that often include depot effect, facilitated antigen presentation, increased secretion of immunomodulatory cytokines to control T and B cells response and the ability to stimulate innate immunity and indirectly modulate adaptive immune responses [22]. Few adjuvants are currently licensed for human use, being aluminum salts (alum) the oldest and most used. The challenge is to develop new improved and safe adjuvants that will confer immunomodulatory properties, allowing vaccines to evoke other than antigen-specific antibodies, often insufficient for some infectious diseases [102]. The antigen-specific cellular immune response is rarely induced by recombinant antigens-based prophylactic vaccines and is a key-feature for the therapeutic vaccines not only for cancer but also for chronic infections diseases like the hepatitis B.

One interesting strategy is vaccine tailoring to look like pathogens, mimicking their properties responsible for immunity often including size, shape and surface molecule organization [84]. Both nano- and microparticles have been used with this aim and natural polysaccharides are potential candidates to be their main constituents due to intrinsic immunomodulatory, biocompatibility and biodegradability properties [85]. In some cases, they can act as pathogen-associated molecular patterns (PAMPs) that recognize innate immune system pattern recognition receptors (PRRs), triggering and regulating adaptive immunity [103]. Indeed, a particulate nature is a consistent principle for adjuvant design, often originating a proinflammatory environment to recruit and prolong the interaction with immune cells [108]. Moreover, the combination of PAMPs with a particulate form will definitely contribute to the potency of the vaccine adjuvant resulting in proper vaccine targeting and improved immune responses [19, 22, 84, 85, 103].

Most innate immune responses are directed against three classes of fungal cell wall glycans, recognized by dendritic cells (DCs) receptors: β-glucans, mannans, and chitin/chitosan [164]. Therefore, the aim of the present work consisted in the development of a "pathogen-like" adjuvant comprising both chitosan and β-glucan in a particulate form. Both biopolymers are well tolerated by the human body representing a safe approach with reduced side effects [19, 103]. First, chitosan is a product of chitin deacetylation widely recognized as an excelent choice for the preparation of drug delivery systems. The presence of protonated primary amine groups, especially in acidic conditions, enable the interaction with negatively charged biomolecules (e.g. protein antigens) [170]. Additionally, chitosan intrinsinc immunomodulatory properties have been associated with NRLP-3 inflammasome activation [164, 186]. Second, β-glucan surface localization was a desired feature for the new developed adjuvant. β-glucans are specifically recognized by the Dectin-1 receptor, a PRR widely expressed in macrophages and DCs, whose activation leads to the modulation of both innate and adaptive immunity, usually promoting Th17 cell differentiation [226, 227]. Although both soluble and particulate β-glucans bind to this receptor, the dowstream signaling is only activated by the latter one [224], resulting in tumor necrosis factor (TNF)-α release, the hallmark of Dectin-1 activation [231]. Consistently, curdlan was our choice for the β-glucan source as it can be solubilized in NaOH and the particulate form is a more robust activator of inflammatory response than the yeast derive β-glucan zymosan [305]. Previous results from our group showed that chitosan-based particles resulted in a predominantly HBsAg-specific Th2-biased immune response through the subcutaneous (SC) route [188, 189]. Therefore, the main intention of the present study was to understant if the addition of β-glucan would benefit the strength and the modulation of the elicited immune response towards a more balanced Th1/Th2 immune response, comparing simple chitosan particles (GenChiPs) to blend β-glucan:chitosan particles (GenGluChiPs) as adjuvants for the hepatitis B surface antigen (HBsAg). Apart from particle development, some *in vitro* assays were done to understand particle cytotoxicity to target cells as well as their ability to load and deliver model antigens.

4.2. Materials and methods

4.2.1. Materials

Chitosan (ChitoClear™ − 95 % DD and 8 cP viscosity measured in 1 % solution in 1 % acetic acid) was purchased from Primex BioChemicals AS (Avaldsnes, Norway) and purified as previously described [272]. Curdlan (Lot 60201) produced by *Alcaligenes faecalis*, the β-1,3-glucan (β-glucan) source used, was acquired from Megazyme (Bray, Ireland) and CBC Genipin from Challenge Bioproducts Co., Ltd. (Taiwan, China). The HBsAg (purity >98 % by SDS-Page tested in ELISA with anti-HBsAg antibodies), subtype adw, a virus-like-particle, with an approximate size of 25 nm, was purchased from Aldevron (Fargo, ND, USA). Bovine serum albumin (BSA, 96 % fraction V), ovalbumin (OVA, 98 %), myoglobin from equine skeletal muscle (95 % to 100 %), α-casein (>70 %), lysozyme (≥80 %), thiazolyl blue tetrazolium bromide (MTT) reagent, Dulbecco's Modified Eagle's Medium (DMEM), Roswell Park Memorial Institute (RPMI 1640), heat-inactivated fetal bovine serum (FBS), HEPES, sodium pyruvate, 5-(4,6-dichlorotriazinyl) aminofluorescein (DTAF), Lipopolysaccharide (LPS), Concavalin A, MEM amino acids, MEM non-essential amino acids and FITC-BSA (A9771) were purchased from Sigma Aldrich Corp. (MO, USA). Image-iT™ LIVE Plasma Membrane and Nuclear Labeling Kit was acquired from Life Technologies Corporation (Paisley, UK). IgG1, IgG2c, IgG3 and IgE horseradish peroxidases (HRP) were purchased to Rockland Immunochemicals Inc. (Limerick, PA, USA.). IgG HRP was obtained from Bethyl Laboratories (Montgomery, TX, USA). Goat anti-mouse HBsAg (ad/ay) HRP was acquired from Meridian, Life Science, ®Inc. (Memphis, TN, USA). Murine interferon (IFN)-γ, IL-4 and IL-17 standard ABTS ELISA development kits were acquired from PeproTech (Rocky Hill, NJ, USA). Fluorescein isothiocyanate (FITC) was purchase to Santa Cruz Biotechnology (Santa Cruz, CA, USA). DC™ Protein Assay from Bio-Rad (Hercules, CA, USA). All other chemicals and reagents used were described in methods and are of analytical grade.

4.2.2. Particle experimental design

Chitosan (GenChiPs) and β-glucan:chitosan (GenGluChiPs) particle production was based on a precipitation method followed by genipin crosslink. For particle optimization, the effect of chitosan concentration (Results and discussion - table 4.2) and genipin

maturation conditions (Results and discussion - table 4.3) were the size influencing factors evaluated. Briefly, a volume of 18 mL of several chitosan solutions (0.05, 0.025 or 0.01 % (w/v) in acetic acid 0.1 % (v/v)) were added dropwise to 18 mL of a 0.025 M NaOH solution containing or not 0.5 % (w/v) Tween™ 80 (GenChiPs), under a high-speed homogenizer (homogenizer Ystral X120, Ballrechten-Dottingen, Germany). Additionally, some of the conditions with Tween™ 80 also included 0.025 % (w/v) β-glucan in the NaOH solution (GenGluChiPs). After 1 h of maturation, the resultant particles were washed twice in 10 mL of phosphate buffered saline pH 7.4 (PBS) (centrifuging 10 min at 2000 x *g*) to remove soluble exceeding compounds. The particles were suspended again in a volume of 10 mL of 0.1 % (w/v) genipin. The optimization of the crosslink conditions was performed for three different size influencing factors summarized in table 4.3: maturation time (3 h, 6 h or overnight (ON)), buffer (PBS or Tris Buffer pH 9 (TRIS)) and temperature (4 °C or room temperature (RT°)). Size was measured after washing the particles twice with milliQ water (10 min at 720 x *g*).

For studies which required particles stained with fluorophores, part (25 %) of the chitosan was labeled with a fluorescein (FITC) and used to particle production. Chitosan was labeled as previously described [210] by mixing 35 mL of dehydrated methanol containing 25 mg of FITC to 25 mL of a 1 % (w/v) chitosan in 0.1 M acetic acid. After 3 h of reaction in the dark at RT°, the FITC labeled chitosan was precipitated with 0.2 M NaOH until pH 10 and collected following centrifugation for 30 min at 4500 x *g.* The resultant pellet was washed three times with a mixture of methanol:water (70:30, v/v). The FITC-chitosan was resuspended in 15 mL of 0.1 M acetic acid, stirred ON, and was further dialyzed in the dark against 2.5 L of distilled water for 3 days before freeze-drying (FreezeZone 6, Labconco, Kansas City, MO, US). following a method previously described by our group [272].

For *in vivo* studies, HBsAg adsorption to GenChiPs and GenGluChiPs was performed in water under mild agitation. Briefly, 1.8 µL of HBsAg stock solution at 3.95 mg/mL were added to a 700 µL of particle suspension and incubated for 30 prior vaccination (100 µL/animal). For HBsAg loading efficacy (% LE), the HBsAg was measured by a direct ELISA method, previously described by our group [304].

The loading efficacy (LE) of HBsAg was calculated by an indirect way, quantifying the unbound HBsAg remaining in the supernatant as described before [208] and represented in Eq. 4.1. HBsAg was determined by a direct ELISA method. After an ON incubation, samples were washed five times with PBS-T (PBS (phosphate buffer saline pH 7.4) containing 0.05 % Tween™ 20) and blocked with 200 µL of 1 % BSA in PBS-T for 1 h at 37 °C. HBsAg was detected using the goat anti-HBsAg HRP (1:5000 dilution) in a 30 min incubation at 37 °C followed by extensively washing and substrate OPD solution (5 mg OPD to 10 mL citrate buffer and 10 µL H_2O_2) incubation for 10 min at RT° in the dark. Reaction was stopped with 1 M H_2SO_4 and absorbance was determined at 492 nm.

4.2.3. Size, zeta potential and morphological analysis

Delsa^{TM} Nano C particle analyzer (Beckman Coulter, CA, USA) was used to measure HBsAg loaded and unloaded particle mean hydrodynamic diameter by dynamic light scattering (DLS) and zeta potential by electrophoretic light scattering (ELS). Size analyses were performed at 25 °C and scattered light collected at a 165° angle. Unloaded particles were submitted to a size and zeta potential titration measured through a wide range of pH values in water, adding NaOH or HCl for pH changes. Transmission electron microscopy (TEM) of unloaded particles suspended in Mili-Q water was performed using a JEOL JEM 1400, 120 kV (JEOL, Peabody, MA, USA), placing a drop of the sample in a mesh grid which was dried out before visualization.

4.2.4. β-glucan quantification

To assess β-glucan incorporation into GenGluChiPs, curdlan was fluorescently labeled with DTAF as previously described [274] with minor modifications. Briefly, β-glucan was solubilized at 0.025 % (w/v) in 0.1 M NaOH, vacuum filtered (0.45 µm) and added to 0.05 M sodium tetraborate in a proportion to originate the borate buffer pH 10.8. DTAF solubilized in dimethyl sulfoxide (DMSO) was added to the previous mixture in a proportion of 1:1 (w/w) DTAF:Curdlan. After an ON incubation in the dark, 96 % ethanol was added for curdlan precipitation in a proportion of 2:1. The precipitate was centrifuged 25 min at 2000 x *g*, the resultant pellet was solubilized in NaOH 0.1 M, and this process repeated until the supernatant was free of unbound DTAF. DTAF labeled β-glucan was solubilized in NaOH 0.025 M in a final concentration of 0.025 % (w/v).

GenGluChiPs were produced as described above, centrifuged and DTAF-β-glucan was measured either in the pellet or in the supernatant using a fluorescence microplate reader (Synergy HT, Biotek®) (absorption/emission 492/512 nm).

4.2.5. Protein adsorption

BSA, OVA, myoglobin, α-casein and lysozyme were incubated with GenChiPs and GenGluChiPs in Mili-Q water at a protein:particle ratio of 1:2. After 1 h of incubation the particle suspension was centrifuged at 16000 x *g* for 30 min, and the supernatant collected for unbound protein quantification with microplate DC™ Protein Assay. The protein loading efficacy (% LE) and loading capacity (% LC) of the particles was calculated as follows:

$$\text{LE } (\%) = \frac{(\text{total amount of protein } (\mu g/mL) - \text{non bound protein}(\mu g/mL))}{\text{total amount of protein}(\mu g/mL)} \times 100 \quad (\text{Eq. 4.1})$$

$$\text{LC } (\%) = \frac{(\text{total amount of protein } (\mu g/mL) - \text{non bound protein}(\mu g/mL))}{\text{weight of the particles } (\mu g/mL)} \times 100 \quad (\text{Eq. 4.2})$$

4.2.6. Cell viability

GenChiPs and GenGluChiPs cytotoxicity was evaluated using the mouse macrophage cell line RAW 264.7 (ECACC, Salisbury, UK), maintained in Dulbecco's modified Eagle medium (DMEM) supplemented with 10 mM HEPES, 3.7 g/L sodium pyruvate and 10 % of inactivated fetal bovine serum (FBS). 100 µL of a cell suspension at a density of $1x10^6$ cells/mL were seeded in 96-well plates 24 h prior the assay. Subsequently, medium was renewed and samples (GenChiPs, GenGluChiPs and Curdlan) suspended in 100 µL of culture medium were added to final concentrations ranging from 1 to 1000 µg/mL. After 24 h incubation at 37 °C and 5 % CO_2, MTT viability assay was performed. Briefly, 20 µL of MTT at 5 mg/mL in PBS were added to each well and incubated for 1.5 h, the supernatant discarded, and the formazan crystals produced by viable cells solubilized in 200 µL of DMSO. The optical density (OD) was measured at 540 nm and 630 nm as wavelength reference. The viability of control cells (culture medium) was defined as 100 % and the relative cell viability calculated using the Eq. 4.3.

$$\text{Cell viability } (\%) = \frac{\text{OD sample (540 nm) - OD sample (630 nm)}}{\text{OD control (540 nm) - OD control (630 nm)}} \text{ x } 100 \quad (\text{Eq. 4.3.})$$

4.2.7. Uptake in RAW 264.7 macrophages

RAW 264.7 cells were seeded on coverslips in 12-well plates at a density of $2.5x10^5$ and incubated ON. On the next day, cells were incubated for 2 h in a final volume of 1 mL with either FITC-BSA loaded GenChiPs and GenGluChiPs or FITC labeled GenChiPs and GenGluChiPs to achieve a final concentration of either 5 µg/mL of FITC-BSA and/or 100 µg/mL particles. Following the uptake period, cells were washed three times with PBS and fixed with 4 % formaldehyde (FA) in PBS for 15 min at 37 °C. The nucleus was labeled using Image-iT™ LIVE Plasma Membrane and Nuclear Labeling, according to manufacturer's instructions. After labeling, cells were washed twice with PBS and the coverslips mounted in microscope slides with DAKO mounting medium. Samples were examined under an inverted laser scanning confocal microscope (LSCM) (Zeiss LSM 510 META, Carl Zeiss, Oberkochen, Germany).

4.2.8. Mice vaccination

Seven to eight-week old female C57BL/6 mice were obtained from Charles River Laboratories (Barcelona, Spain), acclimated for 1 week prior to the initiation of experiments and maintained in the local animal house facility, with free access to food and water, with 12 h light/dark cycle. Animal studies were approved (ORBEA_50_2013/27092013) and carried out in accordance with institutional ethical guidelines and with National (Dec. No. 113/2013) and International (2010/63/EU Directive) legislation. Vaccination groups divided based on the use or not (No Adjuvant) of an adjuvant for different concentrations of HBsAg are listed in table 4.1. A control group where no formulation was administered (Naïve n=3) was also included in study. All particles were administered suspended in Milli-Q water through the SC route and the animals euthanized on day 28 by cervical dislocation.

Table 4.1. Vaccination groups: vaccine formulation and vaccination schedule.

Groups	**HBsAg** (/dose)	**Adjuvant** (/dose)	**Priming, Boost** (days)	**Euthanasia** (day)
Naïve (n=3)	---	---	0, 14	28
No Adjuvant (n=3)	1 μg	---		
	1.5 μg	---		
GenChiPs (n=5)	1 μg	400 μg		
	1.5 μg	400 μg		
GenGluChiPs (n=5)	1 μg	400 μg		
	1.5 μg	400 μg		

4.2.8.1. Blood collection

Blood samples were collected by submandibular venipuncture with an animal lancet to microcentrifuge tubes, 14 days after each immunization and immediately before the next boost. The blood coagulated over 6 h and was further centrifuged for 10 min at 4500 x *g*, for serum collection. The resultant supernatant was carefully transferred to another microcentrifuge tube and stored at −20 °C until further analysis.

4.2.8.1.1. Serum immunoglobulins

HBsAg-specific serum IgG1, IgG2c, IgG3 and IgE determination was performed by ELISA as previously by our group [210]. Briefly, 100 μL of 1 μg/mL HBsAg in solution (50 mM sodium carbonate/bicarbonate, pH 9.6) were used for coating of high-binding 96-well plates (Nunc MaxiSorp™ flat-bottom, Thermo Fisher Scientific Inc., Waltham, MA, USA). After an ON incubation, plates were washed five times with PBS-T and blocked with 1 % BSA in PBS-T for 1 h at 37 °C. After washing, 100 μL of serial dilutions of serum samples, starting at 1:64, were added to the wells and incubated for 2 h at 37 °C. Following washing, 100 μL of HRP conjugated goat anti-mouse IgG (1:10000), IgG1 (1:20000), IgG2c

(1:5000) and IgG3 (1:2500) antibody solutions in PBS-T were added and incubated for 30 min at 37 °C. After that, the detection was performed with 100 µL of a substrate OPD solution (5 mg OPD to 10 mL citrate buffer and 10 µL H_2O_2) incubation for 10 min at RT° in the dark. Reaction was stopped with 50 µL of 1 M H_2SO_4 and absorbance was determined at 492 nm. The serum IgG titers were presented as the end-point titer, which is the antilog of the last log 2 dilution for which the optical density (OD) was at least two-fold higher than the value of the naive sample equally diluted. The log 2 endpoint titers were used to normalize the data and equalize variability and then statistically analysed.

4.2.8.2. Spleen cells cytokine production after HBsAg restimulation

Individual mice spleen cell suspensions were prepared [273] and restimulated with the HBsAg [267] as previously described, without erythrocytes lysis. Mice were euthanized on day 28 and spleens were harvested. A single cell suspension of mice spleen cells was prepared using a 70 µm cell strainer. Cells were washed three times centrifuging for 10 min at 218 x *g* and resuspending in cell culture media (RPMI 1640, 10 % FBS, 20 mM HEPES, 1 % PenStrep, 0.1 % 2-mercaptoethanol, 1 % NaOH 1 M, 1 % sodium pyruvate, 1 % MEM non-essential amino acids, 2 % MEM amino acids). Then, 50 µL of the cell suspension were plated at a density of $1x10^7$ cells/ mL in 96-well plate and 150 µL of media, either alone or containing HBsAg, Con A or LPS as positive controls (final concentrations of 6.25 µg/mL, 1 µg/mL and 5 µg/mL, respectively), were added to the cells. The plates were incubated at 37 °C for 48 h to induce cytokine production by antigen-specific T cells and the supernatants collected and stored at −80 °C until further analysis. IFN-γ, IL-4 and IL-17 cytokines were determined using Peprotech murine development ELISA kits, according to manufacturer's instructions.

4.2.8.3. Liver tissue interstitial fluid IFN-γ

Tissue interstitial fluid (TIF) from liver was collected to ice-cold PBS as previously described [238]. Briefly, 0.25 g of 1-3 mm pieces of liver were suspended in 1 mL of ice-cold PBS and washed three times, centrifuging 3 min at 1000 x *g*, removing the supernatant. Samples were further centrifuged for 8 min at 2000 x *g* and then 30 min at 20000 x *g* at 4 °C. The resultant interstitial fluid was collect and stored at −80 °C until

further analysis. Murine IFN-γ was evaluated using a standard ABTS ELISA development kit according to provider's instructions.

4.2.9. Statistical analysis

Results were expressed as mean ± standard error of the mean (SEM). Statistical analysis was performed by GraphPad Prism v 5.03 (GraphPad Software Inc., La Jolla, CA, USA). Comparisons between two samples were done using Student's t-test and multiple comparisons by ANOVA, followed by Tukey's post-test. A value of $p<0.05$ was considered statistically significant.

4.3. Results and discussion

4.3.1. Particle size depends on chitosan concentration and genipin maturation conditions.

Size is known to be an influencing factor for enhanced immunity. Although the optimal range that will generate stronger and lasting immune responses is still unclear [108, 157], smaller particles are usually associated with more balanced Th1/Th2 immune responses [155, 157]. Therefore, several parameters were tested to achieve a homogeneous suspension of particles with a small size. As we developed a new method to produce chitosan particles based on polymer precipitation into a basic solution, to further test the outcome of β-glucan addition to the system, the optimization was performed for particles containing only chitosan. The optimized conditions that resulted in stable and reproducible chitosan particles were replicated in the presence of β-glucan in the basic solution, in the expectation that some of it could be trapped during chitosan particle formation. Chitosan particles will be then used as a reference to understand if the addition of β-glucan would benefit the modulation of the elicited antigen-specific immune response.

In that regard, the results showed in table 4.2 indicated that chitosan concentration is a critical parameter for size control of chitosan particles. Comprehensibly, the higher concentration (0.05 %) resulted in larger chitosan particles (1600 ± 99 nm, $p<0.01$) than lower chitosan concentrations of 0.025 % and 0.01 %, which resulted in particles with a size of 671 nm and 350 nm, respectively. It was also observed that the presence of the nonionic surfactant Tween™ 80 resulted in reduced particle size,

at least for the 0.025 % concentration (553 ± 27 nm, p<0.05). In this particular case, as the β-glucan would be included in particle formation in this step, the same chitosan concentration conditions were tested in the presence of β-glucan, also to validate the best conditions for GenGluChiPs. For all the chitosan concentrations tested, the inclusion of β-glucan in the NaOH solution during particle formation resulted in increased particle size (Table 4.2, p<0.01).

Table 4.2. Influence of chitosan concentration in the resultant particle size.

Chitosan conc. % (w/v)	**Tween™ 80 0.5 %** (w/v)	**β-glucan 0.025 %** (w/v)	**Size** (nm)	**PDI**	**Significance**
0.05	-	-	1600 ± 99	0.38 ± 0.07	
0.05	+	-	1468 ± 89	0.37 ± 0.09	
0.05	+	+	2345 ± 94	0.39 ± 0.09	cc
0.025	-	-	671 ± 46	0.24 ± 0.06	aa
0.025	+	-	553 ± 27	0.22 ± 0.03	b
0.025	+	+	793 ± 46	0.24 ± 0.05	cc
0.01	-	-	350 ± 56	0.29 ± 0.04	aa
0.01	+	-	286 ± 45	0.28 ± 0.03	
0.01	+	+	552 ± 44	0.29 ± 0.03	cc

*Particle size was measured by dynamic light scattering (DLS), presented as normalized intensity distribution, in the original medium of three random formulations prepared in duplicate. The chitosan concentration of 0.025 % in the presence of Tween™ 80 was the best condition to proceed for genipin crosslink. PDI, polydispersity index; conc., concentration. *p<0.05 and **p<0.01 denote statistical differences between: a, 0.05 % and the other chitosan concentrations; b, the presence and absence of Tween™ 80 and; c, the presence or absence of 0.025 % β-glucan.*

Figure 4.1 showed a detailed size distribution obtained under the conditions tested. It was clear that the conditions without β-glucan (Figure 4.1A-C) resulted in more homogeneous particle size while conditions in the presence of β-glucan (Figure 4.1D-F) originated a higher size dispersion characterized by the presence of more peaks for larger particles, that most probably corresponded to agglomerates. For 0.01 % and 0.025 % chitosan solutions, it was observed that the peak representing the majority of particle sizes measured (at least more than 50 % of cumulative intensity) (Figures 4.1A and 4.1B) slightly moved to the right (larger size) when the β-glucan was present during particle formation (Figures 4.1D and 4.1E), demonstrating that the increased mean diameter is due to a difference in the main particle population size and not only due to the presence

of agglomerates. The conditions with 0.05 % chitosan solution without (Figure 4.1C) or with β-glucan (Figure 4.1F) resulted in a particle suspension with a huge polydispersity index (Table 4.2) and because of that these conditions were excluded from the subsequent studies. On the other hand, while 0.01 % chitosan solution resulted in decreased mean diameter, which was of our interest, the truth was that the presence of huge agglomerates with sizes varying from 10 to 20 µm was a constant finding and represented about 35 % of the particle suspension (Figures 4.1A and 4.1D), conferring some problems with reproducibility. Hence, chitosan concentration of 0.025 % was the condition that allowed us to obtain particles with better physicochemical characteristics with the advantage of having a reproducible method (Figures 4.1B and 4.1E). This condition rendered particles with the smallest size distribution (PDI) with the main size population comprising at least 80 % either with or without β-glucan. Therefore, it was elected to proceed for particle crosslink methodology optimization, the last step on particle preparation protocol. Moreover, a recent study also using chitosan particles with a size of 1 µm showed favorable antigen delivery, upregulation of surface activation markers and cytokine release from macrophages when compared to 300 nm and 3 µm particles [158], consolidating the choice of that conditions whose particle size will be probably close to 1 µm after the crosslink procedure.

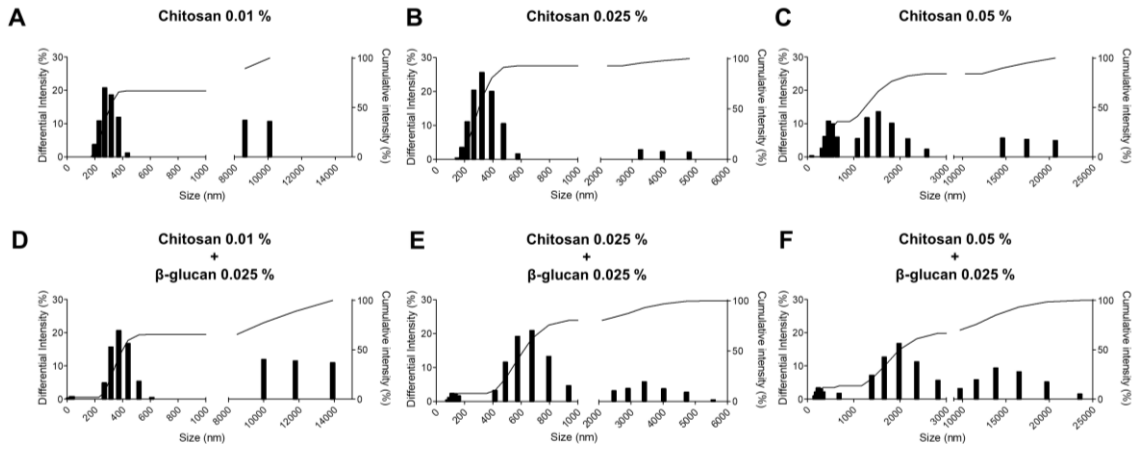

Figure 4.1. Size distribution of chitosan precipitation in the presence or not of β-glucan. Size (nm) was measured by dynamic light scattering (DLS) and is presented as differential intensity (%) and cumulative intensity (%). Different chitosan solutions with different concentrations were precipitated into a basic solution (A-C) or a basic solution containing β-glucan (D-F). The graphs show one measurement that is representative of the six measurements performed.

Several conditions were studied for genipin crosslink of chitosan particles and included the type of buffer used, the temperature and the maturation time. Among them, the most relevant factor that affected particle size was the maturation time (Table 4.3). The lowest maturation time which was 3 h (conditions 1, 4, 7 and 10) resulted in smaller particles comparing to 6 h (conditions 2, 5, 8 and 11) or ON maturation (conditions 3, 6, 9 and 12) ($p<0.01$), independent of the temperature and the buffer used. Differences between 6 h and ON maturation times were also observed for the PBS condition (4 ºC, $p<0.05$ or RT°, $p<0.01$). Temperature also had some impact on particle size. RT° maturation (conditions 4, 10 and 11) resulted in a smaller mean diameter compared to correspondent 4 ºC maturation (conditions 1 ($p<0.01$), 7 ($p<0.05$) and 8 ($p<0.01$), respectively). Lastly, differences between the type of buffer used were not so explicit, only perceived for the 3 h maturation period, with PBS buffer favoring reduced particle size (condition 1 versus 4, $p<0.01$ and condition 7 versus 11, $p<0.01$). Overall, the formulation that matched the desired particle size corresponds to the sample 4 (3 h maturation, RT°, PBS 7.4) and that condition was further applied for both GenChiPs and GenGluChiPs.

Table 4.3. Influence of genipin maturation conditions on GenChiPs particle size.

Samples	Buffer	Temperature	Time	Size (nm)	PDI	Significance
1	PBS 7.4	4 °C	3 h	1147 ± 43	0.34 ± 0.05	aa, cc, dd, ee
2	PBS 7.4	4 °C	6 h	1857 ± 150	0.54 ± 0.10	aa, b
3	PBS 7.4	4 °C	ON	2814 ± 270	0.67 ± 0.12	b, cc
4	PBS 7.4	RT°	3 h	837 ± 22	0.22 ± 0.04	aa, cc, dd, ee
5	PBS 7.4	RT°	6 h	1550 ± 68	0.43 ± 0.08	aa, bb
6	PBS 7.4	RT°	ON	2493 ± 180	0.58 ± 0.09	bb, cc
7	TRIS 9	4 °C	3 h	1446 ± 33	0.28 ± 0.06	aa, cc, d, ee
8	TRIS 9	4 °C	6 h	2219 ± 63	0.38 ± 0.07	aa, dd
9	TRIS 9	4 °C	ON	2691 ± 177	0.57 ± 0.10	cc
10	TRIS 9	RT°	3 h	1305 ± 33	0.30 ± 0.05	aa, cc, d, ee
11	TRIS 9	RT°	6 h	1651 ± 85	0.47 ± 0.09	aa, dd
12	TRIS 9	RT°	ON	2090 ± 254	0.65 ± 0.11	cc

*Size was measured by dynamic light scattering (DLS), presented as normalized intensity distribution, of particles suspended in water of three random formulations prepared in duplicate. PDI: polydispersity index. *p<0.05 and *p<0.01 denote statistical differences between: a, 3 h and 6 h; b, 6 h and ON; c, 3 h and ON; d, 4 °C and RT° and; e, PBS and Tris buffers. The best formulation found corresponded to the sample 4.*

The mean size and PDI of final GenChiPs and GenGluChiPs prepared by the optimized protocols were summarized in figure 4.2A. GenChiPs were significantly smaller than GenGluChiPs (837 nm versus 1274 nm, $p<0.01$), also confirmed by the TEM imagens and consistent with the data prior genipin crosslink (Table 4.2). Overall, the final size of both GenChiPs and GPs was a good achievement to study the immune outcome of β-glucan addition to chitosan particles. In fact, it is known that although both soluble and particulate β-glucans bind to Dectin-1 receptor, the dowstream signaling is only activated by the particulate form, which was proved using β-glucan particles in the micrometer range [224]. Concerning to PDI, and also consistent with what was previously observed before genipin crosslink (Figure 4.1), final GenChiPs exhibited a narrower size distribution (PDI 0.22) when compared to GenGluChiPs (PDI 0.35), probably due to the contribution of β-glucan to a more disperse range of particle size or particle aggregation.

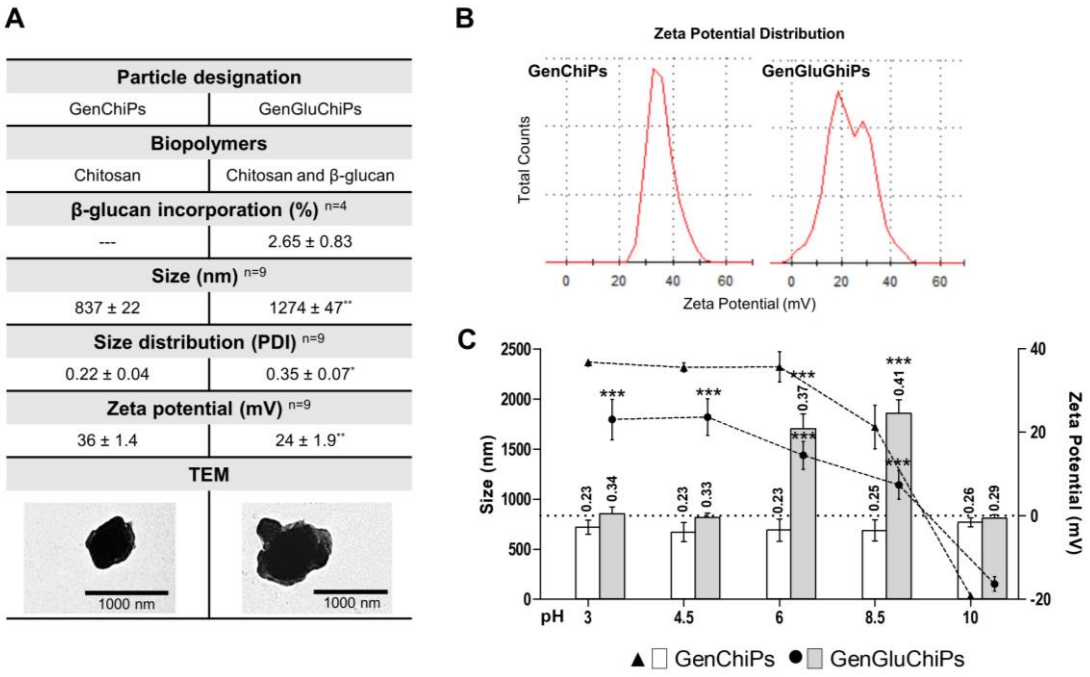

Figure 4.2. Particle physicochemical properties. (**A**) General characteristics of GenChiPs and GenGluChiPs. β-glucan incorporation (%) was evaluated for GenGluChiPs by an indirect way, tracing the amount of unbound DTAF labeled β-glucan during particle preparation. Size (nm), presented as normalized intensity distribution, size distribution (polydispersity index (PDI)) and zeta potential mean values (mV) were measured in water. Data (mean ± SEM) are representative of nine independent replicates. Size of the particles were confirmed by transmission electron microscopy (TEM). (**B**) Zeta potential distribution of both GenChiPs and GenGluChiPs. The graphs show one measurement that is representative of the six measurements performed. (**C**) Particle

size and zeta potential titration in water following acidification (HCl) or alkalinization (NaOH) for pH values ranging from 3 to 10. Size is represented by the columns and aligned with the left Y axis while zeta potential is represented by the connected dots and aligned with the right Y axis. Size PDI is presented at the top of each column. Data (mean ± SEM) are representative of three independent replicates. **** p<0.001 denote statistical differences between GenChiPs and GenGluChiPs.*

4.3.2. Zeta potential is a good indicator of β-glucan incorporation.

So, the precipitation technique developed in the present study resulted in a reproducible method that allowed the production of both GenChiPs and GenGluChiPs. Although particles with different characteristics have been obtained (GenChiPs and GenGluChiPs), which could be already an indication of the presence of β-glucan in GenGluChiPs, the main concern remained whether we assuredly succeeded in incorporating the β-glucan or not and to what extent. Therefore, we proceed to a more detailed characterization. Among the results obtained, the zeta potential and the zeta potential titration showed to be good indicators of β-glucan incorporation and may constitute a simple and good methodology to be used in futures studies as complementary to the quantitative methods.

In fact, a quantitative method was used and allowed us to determine the incorporation rate and the relative contribution of β-glucan to the overall particle composition. For that, DTAF labeled curdlan was used for GenGluChiPs preparation to facilitate the quantification of the amount β-glucan captured during particle preparation. Fluorescence analysis of both, supernatant and GenGluChiPs *per se* indicated a 2.65 ± 0.83 % incorporation rate (Figure 4.2A). This represents a 5 % contribution of β-glucan to the overall particle mass. Interestingly, when both particles were freeze-dried and weighed (before genipin crosslink and without Tween 80™) to determine the production yield per lot, a similar contribution of the β-glucan to the increased final weight of GenGluChiPs in comparison to GenChiPs was observed. More specifically, a difference in mass of about 4 % corresponded to the mass of β-glucan incorporated in chitosan particles (GenGluChiPs).

Other results suggested the incorporation of β-glucan into the particles. The zeta potential differences observed between GenChiPs and GenGluChiPs, showed in figures

4.2A and 4.2B, were a good indication. Positive charge in water was a shared feature, mostly conferred by chitosan amine group protonation in acidic to neutral solutions (pKa ≈ 6.5). Nevertheless, GenChiPs have a significantly higher zeta potential value than GenGluChiPs (+36 mV versus +24 mV, $p<0.01$), consistent with the contribution of β-glucan neutral charge to a less positive net surface charge. Moreover, figure 4.2B shows that GenChiPs have a narrower zeta potential distribution with one peak at +36 mV, while GenGluChiPs show a wider distribution with two coincident peaks at +20 mV and +30 mv that resulted in a mean zeta potential of +24 mV. This demonstrated the decreased zeta potential values were due to β-glucan incorporation in chitosan particles and not due to insoluble β-glucan present in the suspension, otherwise a peak coincident with neutral charge characteristic of this biopolymer would be present.

Finally, for a better understanding of GenChiPs and GenGluChiPs properties, a size and zeta potential titration over a pH range from 3 to 10 was performed. Once more, the zeta potential values of both GenChiPs and GenGluChiPs showed to be statistically different ($p<0.001$) from pH 3 to 8.5 (Figure 4.2C). It is known that, particle zeta potential depends on several factors such as the ionic strength and the pH of the medium and can indirectly influence particle size and PDI. Apparently, GenChiPs mean size was not affected by medium pH as it remained constant and with a narrow dispersion (PDI 0.23-0.26) through all pH values analyzed. This can be explained by the correspondent zeta potential titration curve which was never close to neutral values, favoring particle suspension stability. In other words, as GenChiPs were highly positive for pHs≤8.5 and negatively charged at pH 10 (≈ −20 mV), there was enough electrostatic repulsion among particles preventing particle aggregation. On the other side, GenGluChiPs mean diameter was highly affected by the medium pH, as an indirect consequence of particle surface charge. In more detail, GenGluChiPs had a surface charge close to neutrality for pH values of 6 and 8.5 (+12 and +7 mV, respectively) coinciding with an increment in mean size close to 2000 nm, that might reflect the formation of aggregates as a result of an insufficient repulsion forces among particles. This conclusion was also supported by the increased PDI (0.37 and 0.41, respectively) observed for those conditions. Coherently, GenGluChiPs mean diameter remained unaltered for pH≤4.5 or pH 10 conditions where they were positively (≈ +25 mV) or negatively (≈ −17 mV) charged. The β-glucan surface

localization and the resultant implications on particle properties were clearly demonstrated by the present pH titration. Overall, these results validated the successful achievement of the main goal which was the production of a particulate system composed of chitosan and β-glucan. The present work showed the possibility to combine in same particle, two polymers that do not interact to each other, using a precipitation technique. This is of great interest for particle production procedures containing β-glucans, as these polysaccharides have no functional groups with positive or negative charges and usually need to be chemically derivatized to promote interaction with other molecules [198].

4.3.3. GenChiPs and GenGluChiPs are safe and preferentially adsorb proteins with low isoelectric point.

Antigen adsorption to particle surface is a convenient loading method as it can be performed in water or any other suitable buffer, maintaining the antigen bioactivity and repetitive surface display mimicking pathogens [306]. With the intention to study the ability of both GenChiPs and GenGluChiPs to adsorb different antigens on their surface, several model proteins were used in this study. An incubation period of 1 h was fixed based on a recent report of our group showing that protein adsorption onto chitosan-based particles occurs almost instantaneously and remained unchanged overtime [189]. Five model proteins (lysozyme, myoglobin, α-casein, OVA and BSA) with different isoelectric points (IP), molecular weights (MW) and structures were tested. This study was important to predict the LE of real antigens like the hepatitis B surface antigen used in this study. The figure 4.3A showed that, although GenChiPs and GenGluChiPs were slightly different in terms of surface composition, no significant differences were observed regarding their loading capacity or antigen loading efficacy. Moreover, protein physicochemical properties were the main responsible for the differences observed for the diverse proteins. The highest LE observed corresponded to α-casein (≈ 90 %), that has the lowest IP (4.1) and thus carried the strongest negative surface charge in water favoring adsorption to the positively charged particles. Indeed, structural features of the caseins, namely highly charged N-terminal regions, may render them to form complexes with multivalent cationic macromolecules, such as chitosan [307, 308]. Next, OVA and BSA high LE (65 % and 82 %, respectively) can also be attributed to the electrostatic

interactions between the positively charged amino groups of chitosan and the negatively charged carboxyl groups of the proteins (IP 4.5 and 5.3, respectively). Although the latter proteins have the higher MW, inversely correlated with LE, the higher density of negative surface charge should be the determinant characteristic for adsorption on chitosan-based particles, as previously described [309]. Accordingly, lysozyme and myoglobin, the proteins with the highest IP (11.3 and 7.2, respectively) showed the lowest LE (≤10 %), due to the net positive charge exhibited by both particles and proteins in water. Overall, it is expected that both GenChiPs and GenGluChiPs would be a good adsorption supports for real antigens with low IP, like the HBsAg (IP 4.5), coherently with a previous study from our group with other chitosan-based particles [189]. Additionally, it was not expected that antigen adsorption efficacy would be different by the presence of surface β-glucan on chitosan particles.

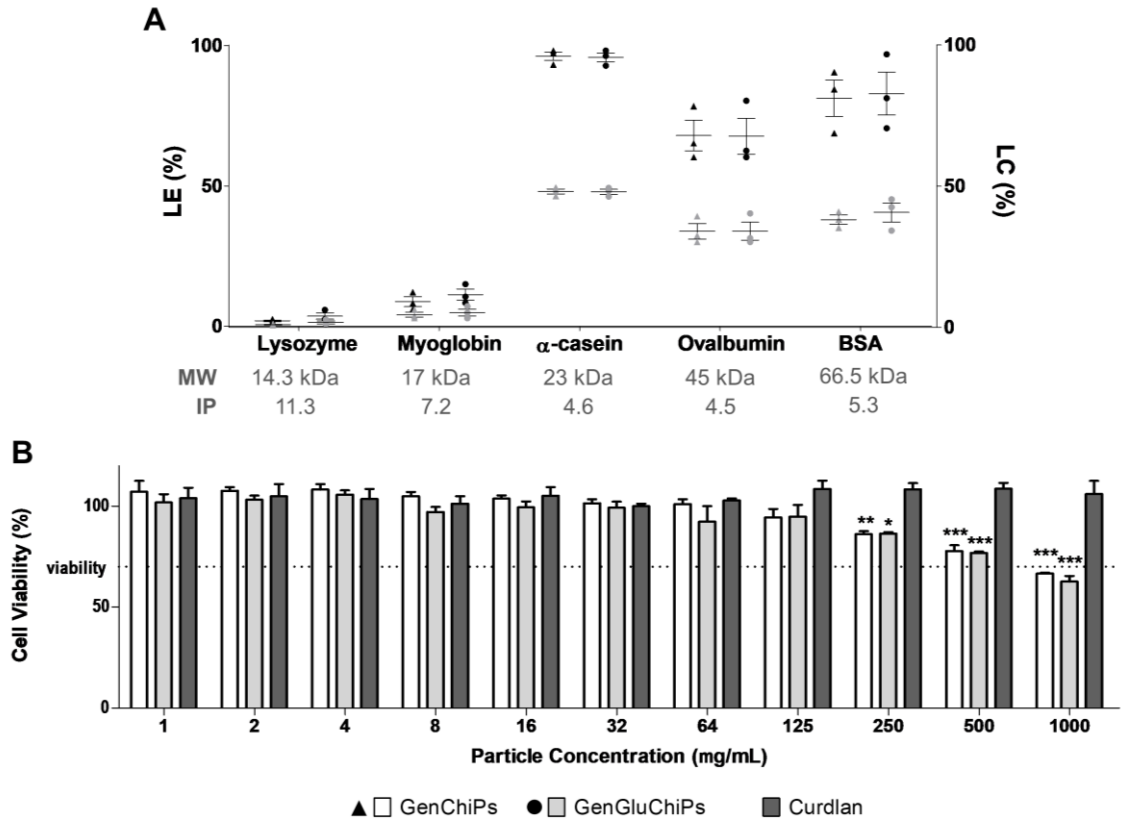

Figure 4.3. Effect of particle properties on the surface adsorption of model proteins and cytotoxicity profile in RAW 264.7 macrophages. (**A**) Particle loading efficiency (LE - %) and loading capacity (LC - %) was determined for several proteins with different molecular weights (MW) and isoelectric points (IP), through the measure of supernatant unbound protein after particle centrifugation. Proteins were adsorbed to particle surface in a protein:particle ratio of 1:2,

following 1 h incubation in water. LE is shown in black and LC is shown in grey. *BSA, bovine serum albumin.* (**B**) Cytotoxicity profile in RAW 264.7 macrophages was evaluated for a wide range of particle concentrations (1 to 1000 μg/mL), including an insoluble form of Curdlan (the β-glucan used for GenGluChiPs manufacturing), and it is shown as the % of cell viability compared to the untreated control. An MTT assay was performed after 24 h of incubation. Data (mean ± SEM) are representative of three independent experiments. ** p<0.05, ** p<0.01, and *** p<0.001 denote statistical differences between Curdlan and GenChiPs or GenGluChiPs. No statistical differences were observed between GenChiPs and GenGluChiPs.*

Rationally, the safety profile of the new adjuvants needs to be evaluated in cultured cells prior animal experiments. Once APCs are a desired immune target of the developed particulate delivery systems, RAW 264.7 cell line (murine macrophages from blood) was selected as representative of these cells to investigate the cytotoxic profile of the new GenGluChiPs. Particles shall be considered non-cytotoxic, if the relatively cell viability for the highest concentration of the sample is ≥70 % of the control group, in accordance with the international standard ISO 10993-5:2009. The cell viability of GenChiPs, GenGluChiPs and β-glucan (curdlan) (suspended in cell culture medium) were evaluated using the MTT assay following 24 h incubation and the results were depicted in figure 4.3B. Curdlan, the β-glucan used for GenGluChiPs production was also tested to have a real idea of the cytotoxicity of this constituent alone. The results (Figure 4.3B) showed that GenChiPs and GenGluChiPs, when used in cell culture with concentrations up to 500 μg/mL, resulted in cell viabilities higher than 70 % of the control. For the highest concentration used (1000 μg/mL) a slightly lower cell viability (65 %) was observed and no differences were detected between GenChiPs and GenGluChiPs. Moreover, significant differences were only detected between particles and curdlan for concentrations above 125 μg/mL. These findings indicate that chitosan rather than β-glucan constituent might be the responsible for the decreased cell viability. In fact, cationic particles cause more pronounced disruptions of plasma membrane integrity and stronger mitochondrial and lysosomal damage than neutral or anionic ones [310]. Collectively, these results provide evidence that GenChiPs and GenGluChiPs can be safely applied in mice vaccination studies due to the good biocompatibility showed over a relevant range of concentrations.

4.3.4. GenChiPs and GenGluChiPs interact with macrophage cell membrane and allow cell uptake of the adsorbed antigen.

Particle interaction with APCs is crucial for vaccines against infectious diseases to selectively deliver the antigen and trigger appropriate APCs presentation and T cell differentiation towards powerful immune responses [100]. Therefore, we investigated the ability of FITC labeled GenChiPs and GenGluChiPs to interact with RAW 264.7 macrophages, a widely used test to explore particle adjuvant effect [158, 303]. Moreover, the cell uptake of a model antigen (FITC-BSA) adsorbed on particle surface was also evaluated. The confocal microscopy images of RAW 264.7 cells following 2 h incubation with FITC labeled particles or FITC labeled BSA loaded particles were shown in figure 4.4. GenChiPs and GenGluChiPs were mostly localized near the cell membrane. It is well known and extensively described in literature that chitosan has bioadhesive properties, explained by its cationic nature which facilitates the binding to negatively charged cell membranes. On the other hand, an extensive internalization of FITC-BSA adsorbed on both particles was observed (green fluorescence on cell cytoplasm). Therefore, with 2 h incubation, the protein had to be released from the particles and enter the cell. An extended incubation period could be necessary to also observe particle internalization. Consistently, maximum antigen uptake of 1 µm-sized chitosan-based particles by RAW 264.7 cells was observed after 24 h and 48 h and reported elsewhere [158]. A previous work from our group also showed that although chitosan-based particles inside the cells was significantly higher for longer incubations, a considerable amount remained attached to the cell surface, regardless of incubation time [278]. Particle adhesion to the cell surface should facilitate continuous antigen release, that would be promptly internalized, essential condition for the development of immune responses [311]. Overall, these findings showed no significant differences between GenChiPs and GenGluChiPs, rendering both as suitable antigen delivery systems for vaccination purposes. Comprehensively, it would be difficult to see differences resulting from the surface β-glucan localization as the total incorporation of the biopolymer represented only 5 % of GenGluChiPs composition, most likely widely distributed throughout the particle not only at the surface. Coherently, although they are different particles, others have also reported no differences in particle interaction with alveolar like macrophages as a result of the presence or not of surface β-glucan [230].

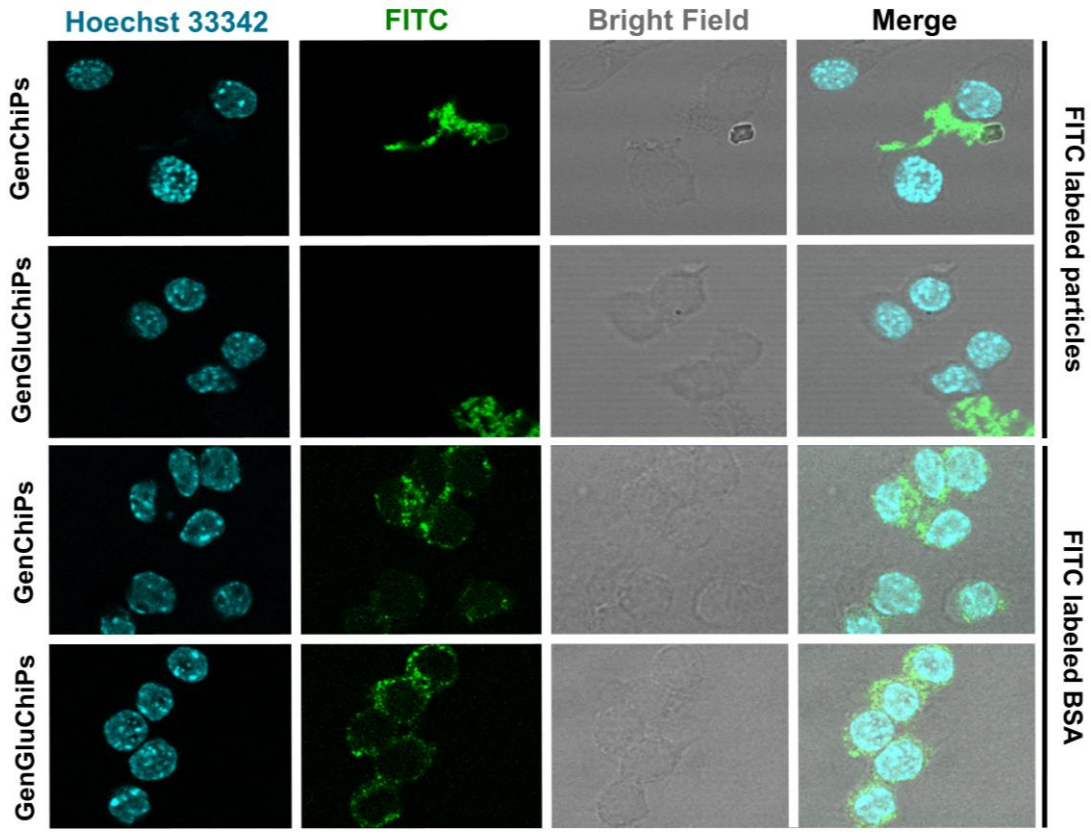

Figure 4.4. Particle interaction with RAW 264.7 macrophages and the ability to deliver a model antigen. The internalization of FITC labeled GenChiPs and GenGluChiPs or FITC labeled bovine serum albumin (BSA) adsorbed onto particle surface was evaluated 2 h after incubation at a particle concentration of 100 μg/mL and FITC-BSA concentration of 5 μg/mL. Confocal microscopy images show single and merged images of the nucleus (blue), the FITC labeled particle or BSA (green) and the cell morphology (bright field).

4.3.5. GenGluChiPs induce the highest antibody titers.

The value of nano- and microparticles as delivery vehicles for antigens has been widely demonstrated. Chitosan particles have already been validated by our group as a good adjuvant for the HBsAg by oral [145, 312], nasal [208, 267] and SC route [188, 189]. Recently, with the intention to better modulate the immune response generated, the group adopted the strategy of chitosan particle association with other compounds like C48/80 [278] and aluminum [189] or other polymers like poly-ε-caprolactone (PCL) [202, 216]. In this work, the β-glucan was associated to chitosan particles and for that a new methodology was developed not only for preparing GenGluChiPs, but also for GenChiPs that was used as a reference-control. Therefore, the main objective of the vaccination studies was the validation of GenGluChiPs as a new adjuvant for the HBsAg, the study of

the influence of the β-glucan included into chitosan particles on the quality of the immune response and the confirmation that GenChiPs, developed by a new method, were effective too. The vaccination studies showed that the inclusion of β-glucan into chitosan particles had improved its adjuvant effect and that genipin crosslink of chitosan particles, did not modify chitosan particle adjuvanticity.

Thus, to evaluate GenChiPs and GenGluChiPs ability to enhance antigen-specific immune responses, we exploit antigen dose-response through the SC route. Mice groups were divided by the presence or not (No Adjuvant) of a particulate adjuvant following vaccination schedule provided in table 4.1. The characterization of the formulations used in this vaccination study was described in table 4.4. As expected, nearly 100 % HBsAg LE was calculated for both particles, already predictable considering the similarity between HBsAg (24 kDa and IP 4.6) and the physicochemical properties of the highly loaded model proteins (Figure 4.3A). Additionally, HBsAg loading did not affect significantly the overall size and zeta potential (Table 4.4) comparing to the unloaded particles (Figure 4.2A).

Table 4.4. Vaccine formulation physicochemical properties.

Groups	**HBsAg** (μg)	**HBsAg** (LE - %)	**Size** (nm)	**PDI**	**ZP** (mV)
Naïve (n=3)	**---**	**---**	---	---	---
No Adjuvant (n=3)	1	---	---	---	---
	1.5	---	---	---	---
GenChiPs (n=5)	1	98.3 ± 1.2	850 ± 11	0.23 ± 0.04	32 ± 2.9
	1.5	98.6 ± 1.4	834 ± 24	0.23 ± 0.04	34 ± 1.4
GenGluChiPs (n=5)	1	98.0 ± 1.1	1223 ± 42**	0.36 ± 0.04*	21 ± 1.6*
	1.5	98.4 ± 1.3	1215 ± 40***	0.33 ± 0.03**	22 ± 1.6**

*LE, loading efficacy; PDI, size polydispersity index; ZP, zeta potential. * p<0.05, ** p<0.01, and *** p<0.001 denote statistical differences between GenChiPs and GenGluChiPs.*

Consistently with antigen loaded particle adjuvant mechanisms described in scientific literature, both GenChiPs and GenGluChiPs induced depot formation at the administration site, not observed for HBsAg alone (No Adjuvant). Adaptive immune responses were evaluated 14 days after each immunization (days 14 and 28) and the results were shown in figure 4.5A. Significantly higher serum HBsAg-specific antibodies were observed for both GenChiPs and GenGluChiPs, when compared to the group where "No adjuvant" was used ($p<0.05$ and $p<0.001$, respectively). This was consistently observed for both HBsAg doses tested (1 μg and 1.5 μg), and may be attributed to the ability of both particles to activate APCs, as explained elsewhere [158]. In addition to the weaker antibody production, the group vaccinated with "No Adjuvant" also took longer to mount an immune response, only detectable at day 28. Moreover, non-responder mice were observed for the lower HBsAg dose (1 μg) of the same group. The priming-boost strategy frequently results in increased antibody titers, also observed in the present study (day 14 versus day 28: GenChiPs, $p<0.05$; GenGluChiPs, $p<0.01$). Specifically, the boost of 1 μg of HBsAg loaded on GenChiPs not only resulted in increased antibodies but also increased number of responder mice. Remarkably, both GenChiPs and GenGluChiPs not only reverted the ineffectiveness of two administrations with only 1 μg of HBsAg (No Adjuvant) but also elicited HBsAg-specific IgG titers comparable to a previous study with five times higher HBsAg dose loaded in aluminum/chitosan particles [189]. Indeed, ideal adjuvants must be cheap to produce. Additionally, if they elevate the antigen-specific immune response in a way that allows antigen sparing they will contribute even more to the production of inexpensive vaccines [22]. Reasonably, 1.5 μg HBsAg dose induced even higher anti-HBsAg IgG, only for GenGluChiPs ($p<0.05$). GenGluChiPs induced 16-fold higher antibody titers than GenChiPs ($p<0.05$) for that HBsAg dose, already suggesting the revenue of β-glucan inclusion in chitosan particles. The antibody titers generated by the mice immunized with 1.5 μg HBsAg loaded GenChiPs were similar to other studies of our group following the same vaccination schedule or antigen dose and using the same [216] or higher doses of the particulate adjuvant tested (i.e. PCL/chitosan nanoparticles) [266]. That observation allowed us to conclude that the inclusion of the β-glucan into chitosan particles was by now the winning strategy.

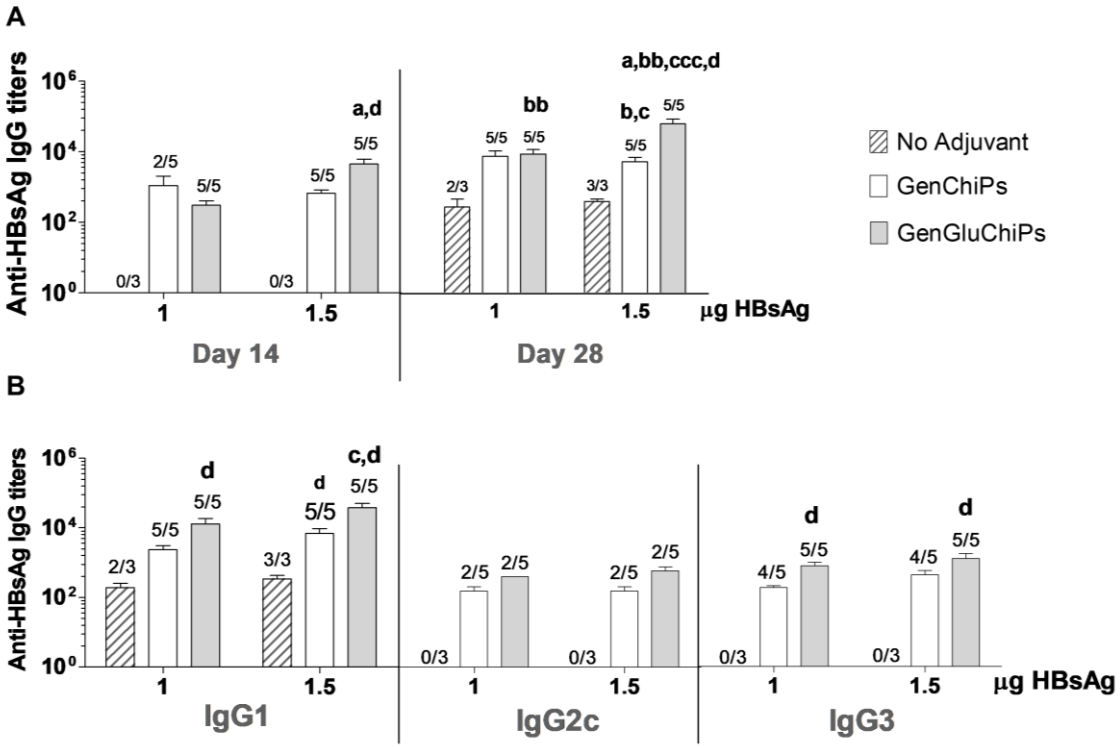

Figure 4.5. Mice serum immunoglobulins profile after vaccination with HBsAg, either alone or loaded into the particles. Vaccine formulations and the vaccination schedule were summarized in table 4.1 and their physicochemical properties on table 4.4. Two doses of either 1 or 1.5 µg of HBsAg were administered through the subcutaneous route. Serum anti-HBsAg (**A**) IgG, evaluated at days 14 and 28, and (**B**) IgG1, IgG2c and IgG3 evaluated at 28. The end-point titers presented in the figure represent the antilog of the last log 2 dilution for which the OD values were at least two-fold higher than that of the naive serum sample equally diluted. The number of mice with detectable antibodies is indicated above each bar. Data are presented as mean ± SEM. ** p<0.05, ** p<0.01 and *** p<0.001 denote statistical differences between: a, 1 and 1.5 µg HBsAg; b, day 14 and 28; c, GenChiPs or GenGluChiPs and No Adjuvant; and d, GenChiPs and GenGluChiPs.*

To understand the influence of β-glucan inclusion in GenChiPs on the quality of the immune response generated, anti-HBsAg IgG1, IgG2c and IgG3 titers were determined at day 28 (Figure 4.5B). IgG class switching may be induced when B cells are in the presence of cytokines and it is generally accepted as predictive of the T cell response generated [79]. IgG1 is associated with Th2 cells lineage typically associated with strong humoral responses effective against extracellular parasites. IgG2 and IgG3 are generally related to virus opsonization and neutralization characteristic from Th1 cells lineage associated with cell-mediated immunity particularly important against intracellular pathogens. It was observed (Figure 4.5B) that IgG1 was the predominant subclass with

higher titers observed in adjuvanted groups ($p<0.05$), mostly for GenGluChiPs when compared to GenChiPs (5-fold increase, $p<0.05$), like previous results for total IgG. Moreover, only adjuvanted groups have induced IgG2c and IgG3 subtypes, although in a lower extent than IgG1. Regarding IgG2c secretion, no differences were observed between GenChiPs and GenGluChiPs. Only IgG3 secretion was higher (4-fold increase, $p<0.05$) and detected in increased number of mice of GenGluChiPs group, suggesting the contribution of β-glucan to enhanced effector functions, namely though the complement system activation, strongly associated to this IgG subclass [313]. Regarding the anti-HBsAg IgE, an immunological parameter frequently required for adjuvant approval and commonly associated with allergic reactions, however, in the present case it was not detected at all.

The results of the HBsAg *ex vivo* stimulation of spleen cells from vaccinated mice (Figure 4.6A) allowed us to look for some antigen-specific T cell activity. No significant differences were observed between groups (including the naïve group) for antigen-specific secretion of the Th2 type cytokine IL-4 and Th1 type cytokine IFN-γ (not detected). Regarding the Th17 type cytokine, IL-17 was only detected in GenChiPs and GenGluChiPs vaccinated groups. The IL-17 has been implicated in protective cellular and memory responses, increasing immunity upon vaccination. Nevertheless, we believe that low concentrations detected will not have a significant biological relevance. Our experience with HBsAg vaccination with chitosan-based adjuvants dictates that strong HBsAg-specific cell-mediated immune response is hard to achieve [188, 189], which may also be related to the very low antigen doses used during vaccination protocols and in *ex vivo* re-stimulation. In fact, in the present study as we were interested in the possible differences between GenChiPs and GenGluChiPs regarding the antigen-specific humoral response, the antigen doses chosen were considerably low, as higher antigen doses would elicit higher antibody titers which could make those differences imperceptible. On the other side, it is known that increased antigen/adjuvant doses and number of vaccine doses affect the development of T cell responses [229]. Therefore, further studies may be designed with higher doses to specifically evaluate cell-mediated immunity. Consistently, a previous work from our group with the same vaccination schedule using HBsAg-loaded PCL/chitosan nanoparticles showed that IFN-γ and IL-17 production was statistically

significant for the highest adjuvant dose tested (four times higher) but not for the lower dose which is similar to the adjuvant dose used here [266].

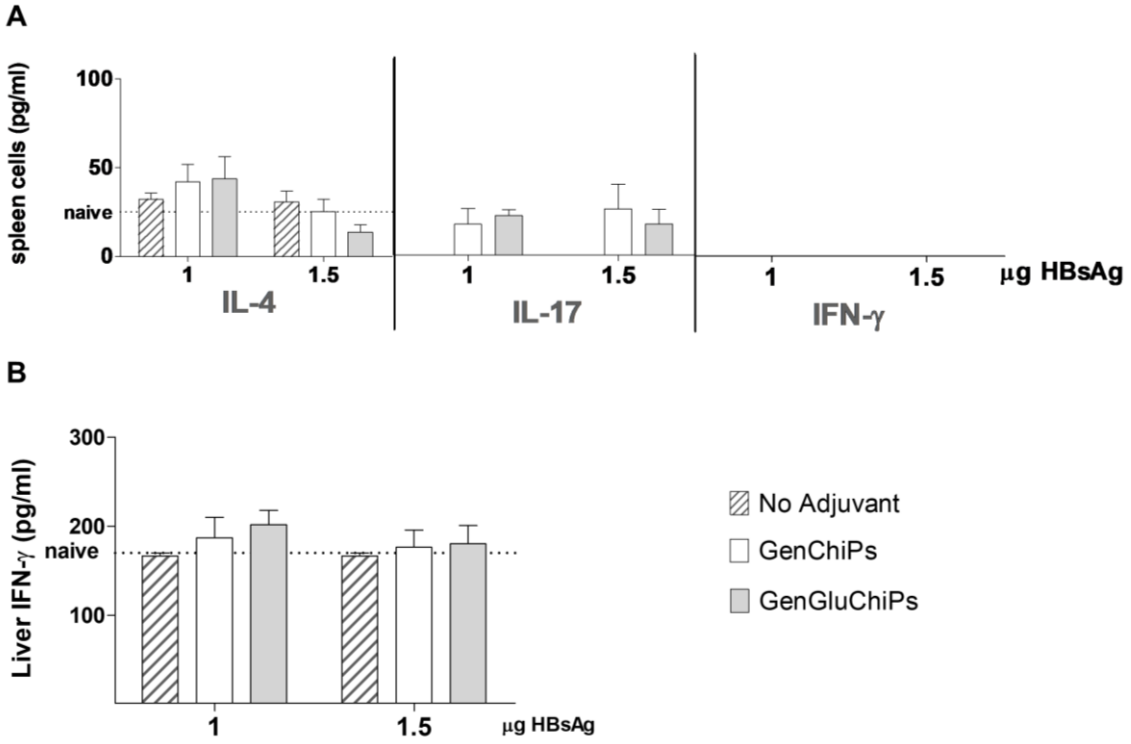

Figure 4.6. Mice spleen cells and liver interstitial fluid cytokine production after vaccination with HBsAg, either alone or loaded into the particles. Vaccine formulations and the vaccination schedule were summarized in table 4.1 and their physicochemical properties on table 4.4. Two doses of either 1 or 1.5 µg of HBsAg were administered through the subcutaneous route. (**A**) IL-4, IL-17 and IFN-γ levels were determined by ELISA in the supernatant of mice spleen cells collected on day 28 and cultures with HBsAg for 48 h. (**B**) IFN-γ production was evaluated in mice liver tissue interstitial fluid (TIF) on day 28. Data are presented as mean ± SEM.

The ability to stimulate the increase of the liver IFN-γ would be of great interest for liver-related diseases such as the chronic hepatitis B. To evaluate the liver IFN-γ production after SC administration of β-glucan-based particles in similarity to what others and we have observed after oral administration of β-glucan particles [238, 304], mice liver interstitial fluid (TIF) was assessed and the results showed in figure 4.6B. However, no differences were observed comparing the vaccinated groups to the basal IFN-γ levels of the naïve group, proving that this is indeed a peculiarity resulting from particle accumulation in the liver via the enterohepatic route only achievable through oral administrations, as previously observed [238, 304].

Overall, these results highlight the importance of the association of an adjuvant to the HBsAg to increase antibody titers and to direct the Th2-biased profile for a more balanced Th1/Th2 immune response. In fact, HBsAg self-assembles into virus-like particles (VLPs) characteristically inducing Th2-biased IgG1 subclass [314, 315]. The present study showed that both HBsAg-loaded GenChiPs and GenGluChiPs had the ability to induce a more balanced Th1/Th2-biased response, eliciting IgG2c and IgG3 subclasses, consistent with a previous report of our group with chitosan-based particles [189] and other studies with β-glucan-based particles [228, 229, 241]. The findings prove that even minor quantities of surface β-glucan can make the difference in the elicited immune response (higher antibody titers), possibly revealing the positive impact of β-glucan in *in vivo* vaccine targeting to the right cells. In fact, curdlan, the β-glucan used, is a recognized Dectin-1 agonist and a robust activator of inflammatory responses [305, 316]. Additionally, β-glucan particulate adjuvants are often associated with potent humoral immune responses [228, 229, 241]. These results may trigger further studies to gain more knowledge about the potential of this new GenGluChiPs adjuvant and to determine whether the β-glucan inclusion in chitosan particles could result in a valuable adjuvant for therapeutic vaccines. Future studies with higher antigen and adjuvant doses will be needed to fully characterize the cell-based immune response generated.

4.4. Conclusions

Natural immunostimulatory polysaccharides with inherent biocompatibility and biodegradability have been considered an optimal strategy for new vaccine adjuvants mimicking pathogen properties. The present work represents an important step for the successfully combination of two biopolymers in the same particle, basically using an easy, simple and reproducible precipitation technique. A “pathogen-like” adjuvant composed by chitosan and β-glucan was developed with β-glucan surface localization, the most important accomplishment envisioning vaccine targeting to immune cells. The combination of β-glucan with chitosan-based particles (GenGluChiPs) proved to be advantageous comparing to GenChiPs, maximizing the elicited immune response. Consistently, combining two or more immunostimulants may enhance immunogenicity due to simultaneous multiple mechanisms of action. Additionally, the possibility of antigen dose sparing provided by the present adjuvants is of pivotal importance to reduce

vaccine manufacturing costs. Future and more detailed studies on the elicited immune response would bring more knowledge about the β-glucan association to chitosan-based systems and their impact in the design of new adjuvant combinations.

CHAPTER 5

β-GLUCAN PARTICLES ARE A POWERFUL ADJUVANT FOR THE HBsAg INDUCING A CYTOKINE PROFILE ASSOCIATED WITH ANTIVIRAL IMMUNITY

Abstract

Modern vaccinology and the lack of vaccine adjuvants able to induce robust T cell responses foster the need to expand the search for more powerful adjuvants, helpful for chronic infectious diseases such as the hepatitis B. Pathogen-like particulate adjuvants are a promising approach highly influenced by their size, surface charge or chemical composition. Accordingly, the present study aimed to develop and test the adjuvant effect of β-glucan-based particles for the hepatitis B surface antigen (HBsAg). First, positively charged β-glucan/chitosan particles (GenGluChiPs) with a mean size of 1276 nm were developed by a precipitation technique. Similar chitosan-based particles (GenChiPs) were also developed and used as control. Second, neutral yeast-derived glucan particles (GPs) with a mean size of 3 μm were produced by acidic and alkaline treatment of *Saccharomyces cerevisiae*. The *in vitro* stimulation studies demonstrated that mice spleen cells responded through the production of TNF-α or RANTES, observed following the stimulation with particles containing β-glucan (GenGluChiPs and GPs) or containing chitosan (GenGluChiPs and GenChiPs), respectively. The human monocytes responded to all particles through the secretion of TNF-α. The subcutaneous vaccination studies revealed strongly increased serum HBsAg-specific IgG production for adjuvanted groups comparing to the HBsAg alone (435-fold increase for GenChiPs, 4500-fold increase for GenGluChiPs and 2500-fold increase for GPs). Additionally, the production of IgG2c and IgG3 was only found in particle adjuvanted groups. Nevertheless, only GPs elicited the secretion of HBsAg-specific Th1, Th2, Th9, Th17, Th22 and Treg related cytokines, following *ex vivo* HBsAg recall of mice spleen cells. This study proves for the first time that GPs can have a significant role against the hepatitis B virus (HBV) resulting in a cytokine release that will favor cell-mediated and antiviral immunity.

Keywords

Vaccine adjuvants, β-glucan, chitosan, polymeric particles, hepatitis B antigen.

Graphical abstract

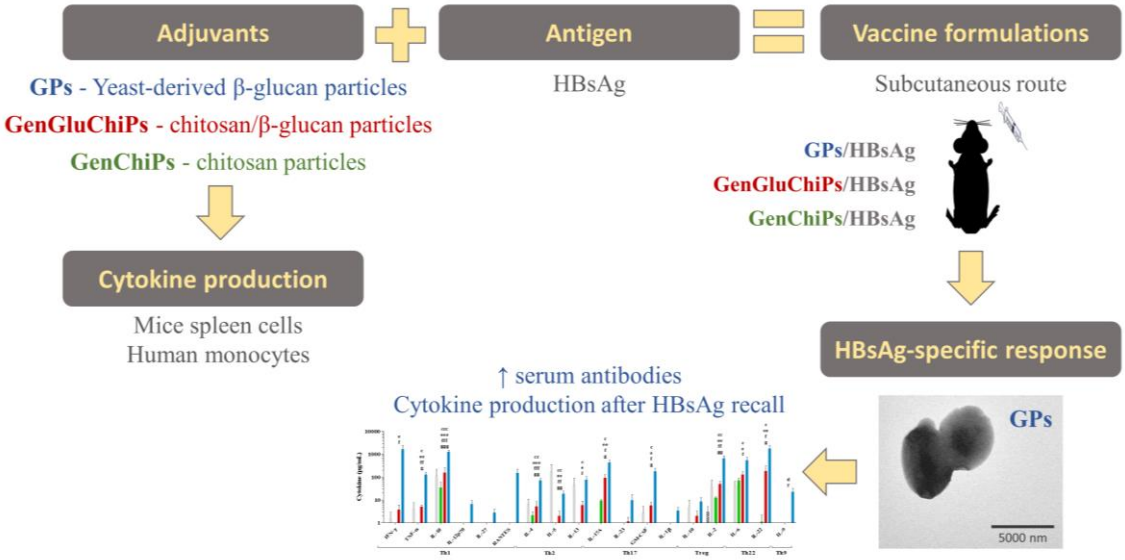

5.1. Introduction

Vaccination is the most cost-effective measure to prevent mortality [17]. Advancing technology and the desire for safer options led to the development of subunit vaccines with poorly immunogenic antigens that require the addition of immunostimulatory agents [84]. Aluminum salts mainly characterized by the generation of humoral immune response are the most commonly used adjuvants to date [102, 103]. Although the successful prophylactic vaccine application, the lack of robust T cell responses makes their use deceptive for some viral infections or therapeutic interventions. Modern vaccinology still has some challenges to solve, namely the search for better adjuvants with applicability for therapeutic vaccines against infectious diseases such as the hepatitis B, whose T cell function restoration is commonly recognized as the best immunotherapeutic approach for a functional cure [15]. Therefore, new rationally designed adjuvants are needed and must be used to modulate the desired immune response, through the stimulation of both humoral and cellular adaptive immune responses [102, 292]. Dendritic cell (DC) activation is a key factor in vaccine design for viral infections as they can orchestrate innate and adaptive immunity to induce both cytotoxic T lymphocyte (CTLs) and helper T (Th) cell differentiation, crucial for HBV-infected hepatocytes destruction [15].

Adjuvant tailoring to replicate pathogen physicochemical properties represent a promising approach [22]. Natural polysaccharides can act as pathogen-associated molecular patterns (PAMPs) and recognize innate immune system pattern recognition receptors (PRRs – e.g. toll-like receptors (TLR) and C-type lectin receptors (CLR)) enabling a promptly immune response, that may differ depending on the PRR activated [103, 231]. Interestingly, most innate immune responses are directed against fungal cell wall polysaccharides such as chitosan and β-glucan [164]. Biocompatibility and reduced side effects are additional advantageous features of those biopolymers [19, 84, 103]. β-glucans are commonly found in bacteria, fungi and yeast and are characteristically recognized by the Dectin-1 receptor (a CLR), widely expressed by immune cells like macrophages and DCs [226]. Tumor necrosis factor (TNF)-α release from macrophages is the hallmark of Dectin-1 activation, only induced by particulate β-glucans [231]. In fact, a particulate design is also strongly correlated with the generation of a pro-inflammatory

environment and immune cells recruitment [22, 85, 108]. Dectin-1 activation leads to an immune response characteristic of a Th1/Th17 differentiation [227]. On the other side, chitosan is a cationic polymer prepared by chitin deacetylation with excellent properties for controlled drug delivery and significant immunostimulatory properties, including enhanced antigen presentation to DCs and NRLP-3 inflammasome activation [158, 164, 186].

Consistently, chitosan and/or β-glucan-based particles are excellent adjuvant candidates for viral infections. The aim of the present study was to develop and test β-glucan-based "pathogen-like" adjuvants to induce hepatitis B surface antigen (HBsAg)-specific cell-mediated immune responses. Additionally, the chitosan polymer was included in the production of β-glucan/chitosan particles (GenGluChiPs) to confer the ability to adsorb negatively charged molecules (e.g. HBsAg) and complementary adjuvant properties (other than Dectin-1 signaling) to the newly developed system. Moreover, chitosan-based particles (GenChiPs) were extensively and successfully tested by our group as an adjuvant for the HBsAg [145, 184, 188, 189, 208, 216, 266, 304], however, strong cell-mediated immune responses were hardly achieved. Therefore, GenChiPs were also developed and used as a control. On the other side, the hollow porous micrometer-sized yeast-derived glucan particles (GPs) [243] were produced and tested for the first time as an adjuvant for the HBsAg. Scientific literature shows that repeated subcutaneous immunizations with GPs and model antigens are associated with cell-mediated immunity following repeated subcutaneous administrations [228, 229, 241]. Proof-of-concept *in vivo* studies were done to evaluate the vaccine efficacy with (GenChiPs, GenGluChiPs and GPs) and without the adjuvants (No Adjuvant) in the generation of humoral-mediated (antigen-specific antibodies) and cell-mediated (Th cytokines profile) immunity [292] following three subcutaneous doses. GenChiPs, GenGluChiPs and GPs induced cytokine production on mice spleen cells and human monocytes were also tested to previously predict their inherent immunodulatory properties.

5.2. Materials and methods

5.2.1. Materials

Chitosan (ChitoClear™ −95 % DD and 8 cP viscosity measured in 1 % solution in 1 % acetic acid) was purchased from Primex BioChemicals AS (Avaldsnes, Norway) and purified as previously described [272]. Curdlan (Lot 60201c) produced by *Alcaligenes faecalis*, the β-1,3-glucan (β-glucan) source used, was acquired from Megazyme (Bray, Ireland) and CBC Genipin from Challenge Bioproducts Co., Ltd. (Taiwan, China). *Saccharomyces cerevisiae* was kindly donated by AB MAURI (Mauripan, Moita, Portugal). The hepatitis B surface antigen (HBsAg) (purity >98 % by SDS-Page tested in ELISA with anti-HBsAg antibodies), subtype adw, a virus-like particle, with an approximate size of 25 nm, was purchased from Aldevron (Fargo, ND, USA). Thiazolyl blue tetrazolium bromide (MTT) reagent, *torula* yeast type IV (tRNA), Roswell Park Memorial Institute (RPMI 1640), heat-inactivated fetal bovine serum (FBS), sodium pyruvate, 5-(4,6-dichlorotriazinyl) aminofluorescein (DTAF), lipopolysaccharide (LPS), concavalin A (ConA), brefeldin A, MEM amino acids and MEM non-essential amino acids were purchased from Sigma Aldrich Corp. (MO, USA). Image-iT™ LIVE Plasma Membrane and Nuclear Labeling Kit was acquired from Life Technologies Corporation (Paisley, UK). IgG1, IgG2c, IgG3 and IgE horseradish peroxidases (HRP) were purchased to Rockland Immunochemicals Inc. (Limerick, PA, USA.). IgG HRP was obtained from Bethyl Laboratories (Montgomery, TX, USA). Goat anti-mouse HBsAg (ad/ay) HRP was acquired from Meridian, Life Science, ®Inc. (Memphis, TN, USA). Fluorescein isothiocyanate (FITC) was purchase to Santa Cruz Biotechnology (Santa Cruz, CA, USA). Th1/Th2/Th9/Th17/Th22/Treg cytokine 17-Plex Mouse ProcartaPlex™ Panel + RANTES (simplex) multiplex immunoassay (Target list: IFN-γ, IL12p70, IL-13, IL-1-β, Il-2, IL-4, IL-5, IL-6, TNF-α, GMC-CSF, Il-18, IL-10, IL-17A, Il-22, IL-23, IL-27, Il-9 and RANTES), TNF-α-PE-Cy7 (Mab11) and IL-10-PacificBlue (JES3-9D7) antibodies and sandwich ELISA kits specific for human IL-10, IL12p70, TNF-α and IL-6 from eBioscience (San Diego, CA, USA). IL-6-FITC (MQ2-13A5) and 12p40-PE (C11.5) antibodies from BD Pharmingen (BD Biosciences, San Jose, CA, USA). X-VIVO™15 culture medium, L-glutamin, HEPES, penicillin/streptomycin and PYROGENT™ Gel Clot LAL Assays (Lymulus Amebocyte Lysate - 0.125 EU/ml Sensitivity) from Lonza (Verviers Sprl, Belgium). Ultrapure LPS-SM from InvivoGen (San Diego, SA, USA). R848 from Alexis Biochemicals

(San Diego, CA, USA). Ficoll-Paque™ plus from GE Healthcare (Sweden). Magnetic CD14 MicroBeads from Miltenyi Biotech (Bergisch Gladbach, Germany). Murine interferon (IFN)-γ standard ABTS ELISA development kit from PeproTech (Rocky Hill, NJ, USA). All other chemicals and reagents used were described in methods and are of analytical grade.

5.2.2. Particle production

Particle production was done using pyrogen-free water to prepare all the solutions and also to perform the washing steps during the procedure under a laminar flow cabinet to avoid LPS contamination. After particle production a Gel Clot LAL Assay with a sensitivity of 0.125 EU/ml was performed to attest if the particles were contaminated or not. Chitosan (GenChiPs) and β-glucan/chitosan (GenGluChiPs) particle preparation was based on a precipitation method followed by genipin crosslink. A volume of 18 mL of a chitosan solution (0.025 % (w/v) in 0.1 % acetic acid (v/v)) was precipitated in an equal volume of a β-glucan solution (0.025 % (w/v) in 0.025 M NaOH containing 0.5 % (w/v) Tween™ 80) or 0.025 M NaOH solution containing 0.5 % (w/v) Tween™ 80 to either prepare GenGluChiPs or GenChiPs, respectively, under a high-speed homogenizer (homogenizer Ystral X120, Ballrechten-Dottingen, Germany). After 1 h maturation, genipin crosslink (0.1 % (w/v)) was performed in 10 mL of phosphate buffer saline (PBS) pH 7.4 during 3 h. Both GenChiPs and GenGluChiPs were centrifuged to remove exceeding genipin, washed and suspended in water for further usage. Glucan particles (GPs), hollow porous yeast cell walls mainly composed of β-glucans, were produced from *Saccharomyces cerevisiae*, by successive alkaline and acidic treatments as firstly described by Soto and Ostroff [243] with minor modifications previously reported by our group [304].

For fluorescent particle preparation, GPs were labeled with DTAF, according to Huang *et al*. [274]. Briefly, 20 mg of GPs were suspended in borate buffer pH 10.8 (49.1 mL 0.1 M NaOH + 50.9 mL 0.05 M sodium tetraborate). Then, 20 mg of DTAF were dissolved in 500 µL of dimethyl sulfoxide (DMSO), added to the GPs suspension and incubated ON under magnetic stirring in the dark. After that, the GPs suspension was extensively washed by centrifugation (10 min, 2000 x *g*) until the supernatant was clear, to eliminate the exceeding DTAF. Chitosan was labeled with FITC, as previously described

[210] and used to prepare both GenChiPs and AlgChiPs. Chitosan was labeled by mixing 35 mL of dehydrated methanol containing 25 mg of FITC to 25 mL of a 1 % (w/v) chitosan in 0.1 M acetic acid. After 3 h of reaction in the dark at RT°, the FITC labeled chitosan was precipitated with 0.2 M NaOH until pH 10 and collected following centrifugation for 30 min at 4500 x *g.* The resultant pellet was washed three times with a mixture of methanol:water (70:30, v/v). The FITC-chitosan was resuspended in 15 mL of 0.1 M acetic acid, stirred ON, and was further dialyzed in the dark against 2.5 L of distilled water for 3 days before freeze-drying (FreezeZone 6, Labconco, Kansas City, MO, US).

For *in vivo* studies, HBsAg adsorption to GenChiPs and GenGluChiPs was performed in water under mild agitation. Briefly, 2.6 µL of HBsAg stock solution at 3.95 mg/mL were added to a 700 µL of particle suspension and incubated for 30 prior vaccination (100 µL/animal). HBsAg loading in GPs was performed according to De Smet *et a*l. [249], with some modifications. Briefly, 2.8 mg of GPs were swollen with 28 µL of HBsAg in 0.9 % saline (0.375 µg/µL) for 2 h at 4 °C, allowing HBsAg diffusion into the hollow GPs cavity. GPs were frozen at -20 °C and lyophilized overnight (ON). Then, 28 µL of 25 mg/mL tRNA in TEN buffer (50 mM Tris-HCl, pH 8, 2 mM EDTA and 0.15 M NaCl) were added and incubated 30 min at 30 °C. After that, 103 µL of 10 mg/mL tRNA in TEN buffer were added and incubated 1 h at 30 °C. At the end, particles were then centrifuged (10 min at 2000 x *g*) to wash residual amounts of tRNA and suspended in 700 µL Mili-Q water for SC administration (100 µL/animal). The vaccine composition was summarized on table 5.1.

5.2.3. HBsAg loading efficacy

The loading efficacy (LE) of HBsAg was calculated by an indirect way, quantifying the unbound HBsAg remaining in the supernatant as described before [208] and represented in Eq. 5.1. HBsAg was determined by a direct ELISA method. After an ON incubation, samples were washed five times with PBS-T (PBS (phosphate buffer saline pH 7.4) containing 0.05 % Tween™ 20) and blocked with 200 µL of 1 % BSA in PBS-T for 1 h at 37 °C. HBsAg was detected using the goat anti-HBsAg HRP (1:5000 dilution) in a 30 min incubation at 37 °C followed by extensively washing and substrate OPD solution (5 mg

OPD to 10 mL citrate buffer and 10 µL H_2O_2) incubation for 10 min at RT° in the dark. Reaction was stopped with 1 M H_2SO_4 and absorbance was determined at 492 nm.

$$\text{LE (\%)} = \frac{\text{total}_{\text{HBsAg}}\ (\mu g/mL) - \text{free}_{\text{HBsAg}}\ \text{in supernatant}\ (\mu g/mL)}{\text{total}_{\text{HBsAg}}\ (\mu g/mL)} \times 100 \quad (\text{Eq. } 5.1)$$

5.2.4. Size and zeta potential

Delsa^{TM} Nano C particle analyzer (Beckman Coulter, CA, USA) was used to measure HBsAg-loaded and unloaded particles mean hydrodynamic diameter by dynamic light scattering (DLS) and zeta potential by electrophoretic light scattering (ELS). Size analyses were performed at 25 °C and scattered light collected at a 165° angle. Unloaded particles were submitted to a size and zeta potential titration measured through a wide range of pH values in water, adding NaOH or HCl for pH changes. Transmission electron microscopy (TEM) of unloaded particles suspended in Mili-Q water was performed using a JEOL JEM 1400, 120 kV (JEOL, Peabody, MA, USA), placing a drop of the sample in a mesh grid which was dried out before visualization.

5.2.5. Quantification of β-glucan incorporation

To assess β-glucan incorporation into GenGluChiPs, curdlan was fluorescently labeled with DTAF as previously described [274] with minor modifications. Briefly, β-glucan was solubilized at 0.025 % (w/v) in 0.1 M NaOH, vacuum filtered (0.45 µm) and added to 0.05 M sodium tetraborate in a proportion to originate the borate buffer pH 10.8. DTAF solubilized in dimethyl sulfoxide (DMSO) was added to the previous mixture in a proportion of 1:1 (w/w) DTAF:Curdlan. After an ON incubation in the dark, 96 % ethanol was added for curdlan precipitation in a proportion of 2:1. The precipitate was centrifuged 25 min at 2000 x *g*, the resultant pellet was solubilized in NaOH 0.1 M, and this process repeated until the supernatant was free of unbound DTAF. DTAF labeled β-glucan was solubilized in NaOH 0.025 M in a final concentration of 0.025 % (w/v). GenGluChiPs were produced as described above, centrifuged and DTAF-β-glucan was measured either in the pellet or in the supernatant using a fluorescence microplate reader (Synergy HT, Biotek®) (absorption/emission 492/512 nm).

5.2.6. Human monocyte stimulation studies

The capacity of GenChiPs, GenGluChiPs and GPs to stimulate immune cells was tested using human monocytes. Venous blood was collected from healthy individuals from Erasmus MC University Medical Center Rotterdam and a written informed consent was obtained from all participants. The peripheral blood mononuclear cells (PBMCs) were isolated by gradient density centrifugation (Ficoll-Paque™ plus). Sequentially monocytes were purified from PBMCs using magnetic CD14 MicroBeads in LS columns for positive selection (purity 95-99 %). Monocytes ($3x10^5$) were cultured overnight in 96-well plates in 250 µL of X-VIVO™15 culture medium containing penicillin/streptomycin, L-glutamin and HEPES either unstimulated or stimulated with the developed adjuvants (GenChiPs, GenGluChiPs, GPs - 200 µg/mL) or positive controls (TLR4 - Ultrapure LPS-SM - 2 ng/mL; TLR7/8 - R848 - 1 µg/mL). For intracellular cytokine staining, brefeldin-A (10 µg/mL) was added 2 h after the onset of stimulation and was present until the end. After a total of 18 h of culture, samples were fixed with 2 % formaldehyde, permeabilized with 0.5 % saponin and stained with antibodies against TNF-α-PE-Cy7, IL-6-FITC, IL-12p40-PE and IL-10-PacificBlue. Cytokine-producing monocytes were assessed by flow cytometry (FACS Canto II, BD) and analysed using FlowJo version 10.1 (Tree Star, Inc., OR, USA). For cytokine quantification, after 18 h of culture as described above, supernatants were harvested, and cytokine production determined by a sandwich ELISA kits specific for IL-10, IL-12p70, and TNF-α and IL-6. The detection limit for IL-10, IL-6 and TNF-α was 78 pg/mL and for IL-12p70 was 23 pg/mL.

5.2.7. Animal studies

Seven to eight-week old female C57BL/6 mice were obtained from Charles River Laboratories (Barcelona, Spain), acclimated for 1 week prior to the initiation of experiments and maintained in the local animal house facility, with free access to food and water, with 12 h light/dark cycle. Animal studies were approved (ORBEA_50_2013/27092013) and carried out in accordance with institutional ethical guidelines and with National (Dec. No. 113/2013) and International (2010/63/EU Directive) legislation.

5.2.7.1. *In vitro* mice spleen cell stimulation studies

GenChiPs, GenGluChiPs and GPs capacity to stimulate immune cells was achieved using a primary culture of C57BL/6 mice spleen cells, maintained in RPMI 1640 medium (10 % FBS, 20 mM HEPES, 1 % penicillin/streptomycin 0.1 % 2-mercaptoethanol, 1,1 % NaOH 1 M, 1 % sodium pyruvate, 1 % MEM non-essential amino acids, 2 % MEM amino acids). Individual mice spleen cell suspensions were prepared [273] and restimulated with the HBsAg [267] as previously described, without erythrocytes lysis. Mice were euthanized, and spleens were harvested. A single cell suspension of mice spleen cells was prepared using a 70 µm cell strainer. Cells were washed three times centrifuging for 10 min at 218 x *g* and resuspending in cell culture media. Then, 50 µL of the cell suspension at a density of $1x10^7$ cells/mL were plated in a 96-well plate and 150 µL of cell culture medium either unstimulated or stimulated with GenChiPs, GenGluChiPs or GPs was added to a final concentration of 200 µg/mL. After 48 h, the supernatants were collected, and cytokines quantified using a Th1/Th2/Th9/Th17/Th22/Treg Cytokine 17-Plex Mouse ProcartaPlex™ Panel + RANTES (simplex) multiplex immunoassay analysed using a Luminex®100™ system. The remaining cells were re-suspended in cell culture medium e proceed to an MTT viability assay with 4 h incubation. The viability of control cells (only culture medium) was defined as 100 % and the relative cell viability calculated using the following equation (Eq. 5.2):

$$\text{Cell viability (\%)} = \frac{\text{OD sample (540 nm) - OD sample (630 nm)}}{\text{OD control (540 nm) - OD control (630 nm)}} \text{ x } 100 \quad \text{(Eq. 5.2)}$$

5.2.7.2. Mice spleen cell uptake studies

For the uptake experiment, 500 µL of the spleen cell suspension at $0.25x10^7$ cells/mL were seeded on 48-well for flow cytometry (BD FACSCalibur, BD Biosciences, San Jose, CA, USA) or 24-well with poly-L-lysine coverslips for laser scanning confocal microscope (LSCM) (Zeiss LSM 510 META, Carl Zeiss, Oberkochen, Germany) analysis. Then, RPMI either with or without FITC labeled GenChiPs or GenGluChiPs and DTAF labeled GPs were added to a final particle concentration of 100 µg/mL. After 4 or 8 h incubation, cells from two wells were pooled, centrifuged for 10 min at 218 x *g* and resuspended in ice-cold PBS for further cytometry analysis. Propidium iodide (PI - 1 µL at 50 µg/mL) was used for cell death assessment and trypan blue (TB - 0.4 % in PBS) was

used to quench extracellular fluorescence. A population of 100000 cells was analyzed per sample and the results processed using CellQuestModfit LT software and presented as the frequency of fluorescent cells (%). For LSCM analysis, after 4 h of incubation, cells were fixed with 4 % formaldehyde for 15 min at 37 °C and the nucleus labeled using Image-iT™ LIVE Plasma Membrane and Nuclear Labeling Kit (Hoechst 33342) according to manufacturer's instructions. After labeling, cells were washed with PBS and the coverslips mounted in microscope slides with DAKO mounting medium.

5.2.7.3. Mice vaccination studies

Vaccination groups and schedule are listed in table 5.1. All vaccine doses were administered in water through the subcutaneous route (100 µL/dose).

Table 5.1. Vaccination groups and schedule.

Group	HBsAg (µg/dose)	Adjuvant (µg/dose)	Priming, Boost, Boost (days)	Euthanasia (day)
Naïve (n=3)	---	---	---	---
No Adjuvant (n=3)	1.5	---	0, 14, 28	42
GenChiPs (n=5)	1.5	400	0, 14, 28	42
GenGluChiPs (n=5)	1.5	400	0, 14, 28	42
GPs (n=5)	1.5	400	0, 14, 28	42

Groups were divided based on the use or not (No Adjuvant) of an adjuvant for the HBsAg.

5.2.7.3.1. Blood collection

Blood samples were collected by submandibular venipuncture with an animal lancet to microcentrifuge tubes, 14 days after each immunization and immediately before the next boost. The blood coagulated over 6 h and was further centrifuged for 10 min at 4500 x *g*, for serum collection. The resultant supernatant was carefully transferred to another microcentrifuge tube and stored at −20 °C until further analysis.

5.2.7.3.2. Serum immunoglobulins

HBsAg-specific serum IgG1, IgG2c, IgG3 and IgE determination was performed by ELISA as previously by our group [210]. Briefly, 100 µL of 1 µg/mL HBsAg in solution (50 mM sodium carbonate/bicarbonate, pH 9.6) were used for coating of high-binding 96-well plates (Nunc MaxiSorp™ flat-bottom, Thermo Fisher Scientific Inc., Waltham, MA, USA). After an ON incubation, plates were washed five times with PBS-T and blocked with 1 % BSA in PBS-T for 1 h at 37 °C. After washing, 100 µL of serial dilutions of serum samples, starting at 1:64, were added to the wells and incubated for 2 h at 37 °C. Following washing, 100 µL of HRP conjugated goat anti-mouse IgG (1:10000), IgG1 (1:20000), IgG2c (1:5000) and IgG3 (1:2500) antibody solutions in PBS-T were added and incubated for 30 min at 37 °C. After that, the detection was performed with 100 µL of a substrate OPD solution (5 mg OPD to 10 mL citrate buffer and 10 µL H_2O_2) incubation for 10 min at RT° in the dark. Reaction was stopped with 50 µL of 1 M H_2SO_4 and absorbance was determined at 492 nm. The serum IgG titers were presented as the end-point titer, which is the antilog of the last log 2 dilution for which the optical density (OD) was at least two-fold higher than the value of the naive sample equally diluted. The log 2 endpoint titers were used to normalize the data and equalize variability and then statistically analysed.

5.2.7.3.3. Spleen cell cytokine production after HBsAg restimulation

Individual mice spleen cells were collected at day 42 and treated as stated above. Then, 50 µL of the cell suspension were plated at a density of $1x10^7$ cells/ mL in 96-well plate and 150 µL of media, either alone or containing HBsAg, Con A or LPS as positive controls (final concentrations of 6.25 µg/mL, 1 µg/mL and 5 µg/mL respectively), were added to the cells. The plates were incubated at 37 °C for 48 h to induce cytokine production by antigen-specific T cells and the supernatants collected and stored at -80 °C until further analysis. IFN-γ, IL-4 and IL-17 cytokines were determined using the same multiplex immunoassay described above. For the positive controls, a pool of the splenocyte supernatant of all mice from each group was used for the multiplex assay.

5.2.8. Statistical analysis

Results were expressed as mean ± standard error of the mean (SEM). Statistical analysis was performed by GraphPad Prism v 5.03 (GraphPad Software Inc., La Jolla, CA,

USA). Comparisons between two samples were done using Mann-Whitney U test and multiple comparisons by ANOVA, followed by Tukey's post-test. A value of $p<0.05$ was considered statistically significant.

5.3. Results and discussion

Immunomodulatory properties have been claimed for β-glucans, useful for cancer treatment [317, 318] and adjuvanted vaccination [228, 229, 241, 249, 253, 319-322]. Nevertheless, their adjuvant effect for the HBsAg was scarcely evaluated to date, only tested with a synthetic form of a β-glucan oligosaccharide showing negligible effects concerning IFN-γ production [219] or with a chemically modified β-glucan showing promising increased IFN-γ+ CD4+ and CD8+ cells (curdlan sulfate) [220]. The claimed properties seem to be dependent on the β-glucan physicochemical structure as, although both soluble and particulate β-glucans bind to Dectin-1 receptor, the dowstream signaling is only activated by the latter ones [224] that results in TNF-α release [231]. Consistently, the present work aimed to develop and test particulated β-glucan-based adjuvants for the HBsAg. Apart from the yeast-derived β-glucan particles (GPs), curdlan was chosen as the β-glucan source to the newly developed system (GenGluChiPs) as the particulate form of it showed to be a more robust activator of inflammatory response than the GPs [305] and for the promsing results with HBsAg stated above. Still, as the curdlan has no charged functional groups to promote interaction with bioactive molecules, the combination with chitosan enable the HBsAg adsorption onto the particle surface. Therefore, and as mentioned before, GenChiPs were also tested as a comparison means. The physicochemical properties of HBsAg-loaded particles were summarized in table 5.2 and included size, size distribution (PDI), zeta potential (ZP), β-glucan incorporation rate and HBsAg LE. Although not represented in table 5.2, it is important to note that no significant differences were observed concerning particle size and ZP of HBsAg loaded and unloaded particles. Regarding GenChiPs and GenGluChiPs, produced using the same precipitation method, we proved that 5 % (w/w) of GenGluChiPs mass refers to β-glucan. Consistently, although both GenChiPs and GenGluChiPs were positively charged, due to the chitosan amine group protonation in acidic to neutral solutions ($pKa \approx 6.5$), the ZP values of GenGluChiPs were significantly lower than GenChiPs (+19 mV for GenGluChiPs and +27 mV for GenChiPs, $p<0.05$), also indicating a contribution of the β-glucan neutral charge to

a less positive net surface charge of the particles. Regarding their size, GenChiPs had a mean diameter of 867 nm, significantly smaller than GenGluChiPs, which had a mean diameter of 1276 nm ($p<0.01$). On the other side, the zeta potential of the GPs were close to neutrality (−5 mV) and a mean diameter of 3268 nm, generally referred to as 2-4 µm in scientific literature [240, 242, 263].

Table 5.2. HBsAg loaded particle characterization.

Particles	Size	PDI	ZP	β-glucan incorporation	HBsAg LE
	(nm)		(mV)	(%)	(%)
GenChiPs	867 ± 23	0.27 ± 0.04	+27 ± 6	---	99.1 ± 1.2
GenGluChiPs	1276 ± 46**	0.30 ± 0.05*	+19 ± 3**	2.72 ± 0.93	98.1 ± 2.1
GPs	3268 ± 425	0.39 ±0.09	-5 ± 2	---	98.5 ± 1.7

*Particles were loaded with HBsAg as described in material and methods. The size and zeta potential measurements were done with particles suspended in water. The results (mean ± SEM) are representative of three independent replicates. PDI, polydispersity index; ZP, zeta potential; LE, HBsAg loading efficiency. * and ** denote statistical differences between GenChiPs and GenGluChiPs at $p<0.05$ and $p<0.01$, respectively.*

5.3.1. Only GPs are internalized by mice spleen cells.

The spleen is the main filter for blood-borne pathogens and antigens. Additionally, this organ provides a good representation of the B and T lymphocytes of the immune system, as it has white pulp regions that resemble lymph nodes. In fact, they contain B and T cell zones and mononuclear phagocytes capable to regulate antigen-specific immune responses locally and in the whole body [323]. Moreover, a novel dendritic-like cell type capable of CD8+ T cell activation through antigen cross presentation, with subsequent induction of CTLs, was recently found in mouse spleen [324]. Apart from this, the spleen cells are easy to obtain and to culture. Therefore, splenocytes were chosen to investigate the capacity of GenChiPs, GenGluChiPs and GPs adjuvants to be internalized by those cells for antigen delivery (Figure 5.1). First, the cytotoxicity was evaluated by flow cytometry, using PI as a probe for death cells, and the results showed a non-toxicological profile for all particles in the concentration used following (PI positive cells ≈ 10 % - figure 5.1A). Figure 5.1A also demonstrated the frequency of positive cells (%) for

FITC/DTAF, following FITC labeled GenChiPs and GenGluChiPs or DTAF labeled GPs incubation. A second assay was done in the presence of TB to quench extracellular fluorescence with the intention to exclude particle adsorption to cell membrane. After 4 h or 8 h of incubation, no GenChiPs or GenGluChiPs were found inside cells and, approximately 3 % of the cells with fluorescence corresponded to GenChiPs and GenGluChiPs adsorbed on the cell surface. On the other hand, GPs were effectively internalized by the splenocytes. It was found that 30 % or 40 % of the cells had internalized the GPs after 4 h or 8 h, respectively. Moreover, GPs were not adsorbed to cell surface, as the TB addition prior analysis did not affect the frequency of FITC positive cells. Then, a different technique was used to have a visual representation of the flow cytometry results. Therefore, figure 5.1B represents the confocal microscopy images which showed that only neutrally charged GPs were seen inside the cell cytoplasm, while GenChiPs and GenGluChiPs were only found aggregated close to the cell membrane, confirming the flow cytometry analysis. These findings suggested that chitosan-based particles strongly adsorbed to the cell membrane due to their positive charge and bioadhesive properties. It is a fact that particle adhesion to cell surface is enough to facilitate antigen release and the development of an immune response [311], but higher uptake rates are usually linked to greater biological effects [325].

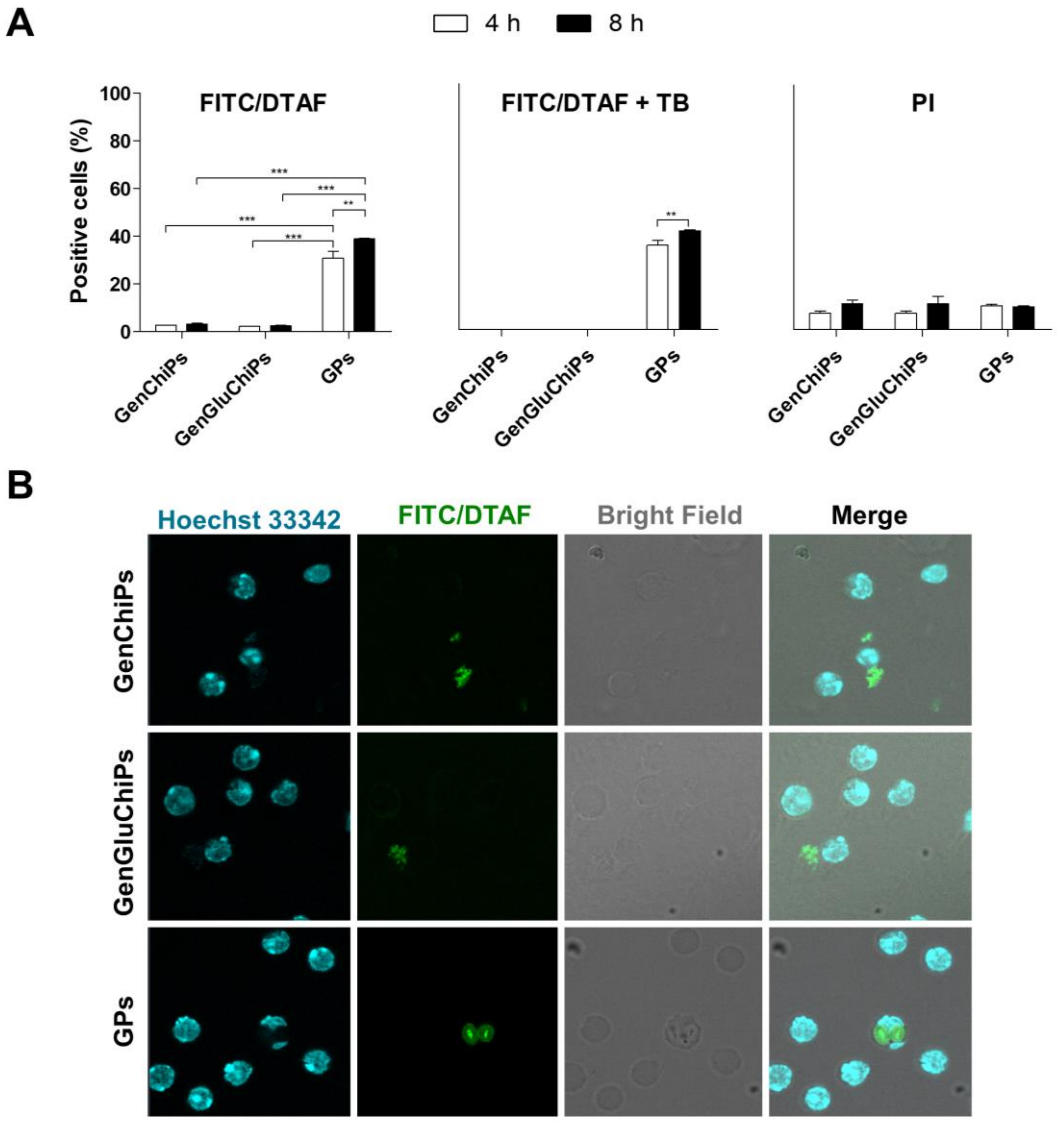

Figure 5.1. Particle internalization by mice spleen cells *in vitro*. FITC labeled GenChiPs and GenGluChiPs and DTAF labeled GPs were incubated with the cells at a particle concentration of 100 µg/mL. (**A**) The frequency of positive cells to the fluorophore used, evaluated by flow cytometry either after 4 h or 8 h of incubation. Trypan blue (TB) was used to quench extracellular fluorescence and thus assess only particle internalization rather than cell membrane adhesion. Cell death was measured by propidium iodide (PI) uptake. Data (mean ± SEM) are representative of three independent assays. *** denotes statistical differences at p<0.01 and *** at p<0.001.* (**B**) Confocal microscopy images show single and merged images of nucleus staining (blue), FITC/DTAF labeled particles (green) and the cell morphology (bright field) after 4 h incubation.

5.3.2. GenChiPs, GenGluChiPs and GPs induce a cytokine signature related to their polymeric composition.

Splenocytes were also chosen to study the impact of different particle composition in the resultant cytokine secretion. In the present study, cells were cultured with non-cytotoxic concentrations (Figure 5.2B) of GenChiPs, GenGluChiPs or GPs, as the relative cell viability for the particle concentration used was ≥70 %, considered to be non-cytotoxic in accordance with the international standard ISO 10993-5:2009. Importantly, prior the assays all particle formulations were tested for endotoxins using a LAL assay (0.125 EU/mL sensitivity) whose results were negative, to ensure that the effects were not due to LPS. Then, a total of 18 different cytokines were measured on cell culture supernatants (Table 5.3) for direct comparison between the particles and the unstimulated control (Medium).

The graph illustrated in figure 5.2A is representative of the cytokines with detectable values. TNF-α secretion induced by both GenGluChiPs and GPs was significantly higher than GenChiPs ($p<0.05$) and basal production (Medium, $p<0.01$), suggesting a specific mechanism associated to β-glucan composition. Indeed, TNF-α release following particulate β-glucan exposure is a consensual result, even using different immune cells like DCs [326, 327] and macrophages [231]. Chitosan was also reported to induce TNF-α secretion in macrophages in a different study [158]. Even though, a study comparing PLGA/chitosan shells functionalized with β-glucan found higher TNF-α levels in the alveolar like macrophages supernatant, when compared to the PLGA/chitosan shells without functionalization [230]. Our results in mice spleen cells are in agreement with that study, as the β-glucan present on GenGluChiPs induced higher TNF-α levels than GenChiPs. Likewise, only two particle types (GenChiPs and GenGluChiPs) elicited higher RANTES secretion than Medium condition ($p<0.001$), suggesting the chitosan as the responsible for the stimulation. In fact, this observation, although with different cells, is in agreement with other studies reporting that chitosan scaffolds [328] or chitosan coated beads [329] increased RANTES secretion by macrophages. The fact that chitosan-based particles are able to stimulate RANTES secretion from immune cells would be of great interest to treat viral infections, as it is associated with macrophage coactivation and, together with IFN-γ, constitute a group of

"type 1 cytokines" with the capacity to bridge innate and adaptive immune reactions [330]. Additionally, RANTES also showed a significant role in sustaining CD8+ T cell responses during a systemic chronic viral infection [331].

Table 5.3. Cytokine concentration in supernatants of spleen cells either unstimulated (Medium) or stimulated *in vitro* with the formulations (GenChiPs, GenGluChiPs or GPs) or the positive controls (LPS or ConA).

Cytokine	Medium	GenChiPs	GenGluChiPs	GPs	LPS	ConA
IFN-γ	0.0 ± 0.0	0.0 ± 0.0	0.0 ± 0.0	0.0 ± 0.0	8.3	3144.5
TNF-α	8.9 ± 3.4	42.7 ± 17.6	187.1 ± 56.3	200.0 ± 43.1	250.2	173.4
IL-18	40.1 ± 0.0	40.1 ± 0.0	90.3 ± 36.5	34.1 ± 8.4	200.3	1646.7
IL-12p70	0.0 ± 0.0	0.0 ± 0.0	0.0 ± 0.0	0.0 ± 0.0	5.2	9.7
IL-27	0.0 ± 0.0	0.0 ± 0.0	0.0 ± 0.0	0.0 ± 0.0	0.0	1.9
RANTES	56.7 ± 9.1	211.6 ± 16.3	210.0 ± 42.1	70.4 ± 10.0	729.4	351.7
IL-4	0.0 ± 0.0	0.0 ± 0.0	0.0 ± 0.0	0.0 ± 0.0	0.0	78.4
IL-5	0.0 ± 0.0	0.0 ± 0.0	0.0 ± 0.0	0.0 ± 0.0	0.0	40.4
IL-13	0.0 ± 0.0	0.0 ± 0.0	0.0 ± 0.0	0.0 ± 0.0	0.0	122.7
IL-17A	0.0 ± 0.0	0.0 ± 0.0	0.0 ± 0.0	0.0 ± 0.0	5.2	560.3
IL-23	0.0 ± 0.0	0.0 ± 0.0	0.0 ± 0.0	0.0 ± 0.0	0.0	8.3
GM-CSF	0.0 ± 0.0	0.0 ± 0.0	0.0 ± 0.0	0.0 ± 0.0	6.3	64.5
IL-1β	2.1 ± 2.4	2.2 ± 2.6	5.4 ± 1.6	1.8 ± 0.6	7.5	7.1
IL-10	2.4 ± 1.0	4.4 ± 1.0	11.2 ± 4.9	43.8 ± 5.8	128.5	34.3
IL-2	0.0 ± 0.0	0.0 ± 0.0	0.0 ± 0.0	0.0 ± 0.0	13.3	734.3
IL-6	5.4 ± 1.5	11.5 ± 4.6	26.8 ± 12.9	10.0 ± 2.1	808.0	324.7
IL-22	0.0 ± 0.0	0.0 ± 0.0	0.0 ± 0.0	0.0 ± 0.0	0.0	331.2
IL-9	0.0 ± 0.0	0.0 ± 0.0	0.0 ± 0.0	0.0 ± 0.0	0.0	28.7

Cytokine secretion of mice spleen cells either unstimulated (Medium) or stimulated with GenChiPs, GenGluChiPs or GPs at 200 µg/mL or simulated with the positive controls (LPS at 1 µg/mL or ConA at 6.25 µg/mL) for 48 h. 18 different cytokines were evaluated using a multiplex immunoassay (ProcartaPlex™). For the positive controls, a pool of the splenocyte supernatant of all mice from each group was used for the multiplex assay. Data (mean ± SEM) are representative of two independent experiments of triplicates.

Regarding IL-10, it was only significantly induced by GPs. In fact, IL-10 release resultant from particulate β-glucan but not chitosan stimulation of human PBMCs was previously observed by others [305]. On the other side, IL-10 was detected following

chitosan stimulation of PBMCs in another study [332]. Indeed, some discrepancies may exist in comparison to published data mainly related to the immune cells used and also to the particle physicochemical properties, the biopolymer source and the possible presence of contaminants (e.g. LPS), as few studies refer to that concern. The fact that GPs induced a significant secretion of both TNF-α and IL-10, a pro-inflammatory and an anti-inflammatory cytokine, was already observed by others in human PBMCs [305], that correlated this finding with the non-polarized innate immune response to fungal cell walls that seems to be induced *in vivo* to limit inflammatory pathology and promote fungal persistence. Although it was reported that particulate chitosan induced IL-1β release from mouse bone marrow derived macrophages (BMDMs) at a concentration of 500 μg/mL but not lower concentrations [329], none of the presently tested particles affected the splenocytes IL-1β secretion. The NRLP3 inflammasome activation is a two-step process that requires a priming signal, as demonstrated by Bueter *et al*., that showed increased IL-1β secretion from mouse peritoneal macrophages after LPS priming followed by chitosan suspension stimulation [333]. Actually, our research group found the same in mice bone marrow DCs (BMDCs), that required a CpG ODN priming to chitosan-based particles induce IL-β secretion, which did not happen with a single stimulus with either the particles or the CpG (data not published). IL-6 is another cytokine commonly reported to be induced by β-glucan [305, 327] or chitosan particles [158, 332], however, it was not detected in the present study after GenChiPs, GenGluChiPs or GPs splenocytes stimulation. Interestingly, LAL results were negative, and the fact that LPS control has strongly increased IL-18 and IL-6 secretion in mice spleen cells (Table 5.3) and none of the particles did, also support those results and deviate the possibility of LPS contamination.

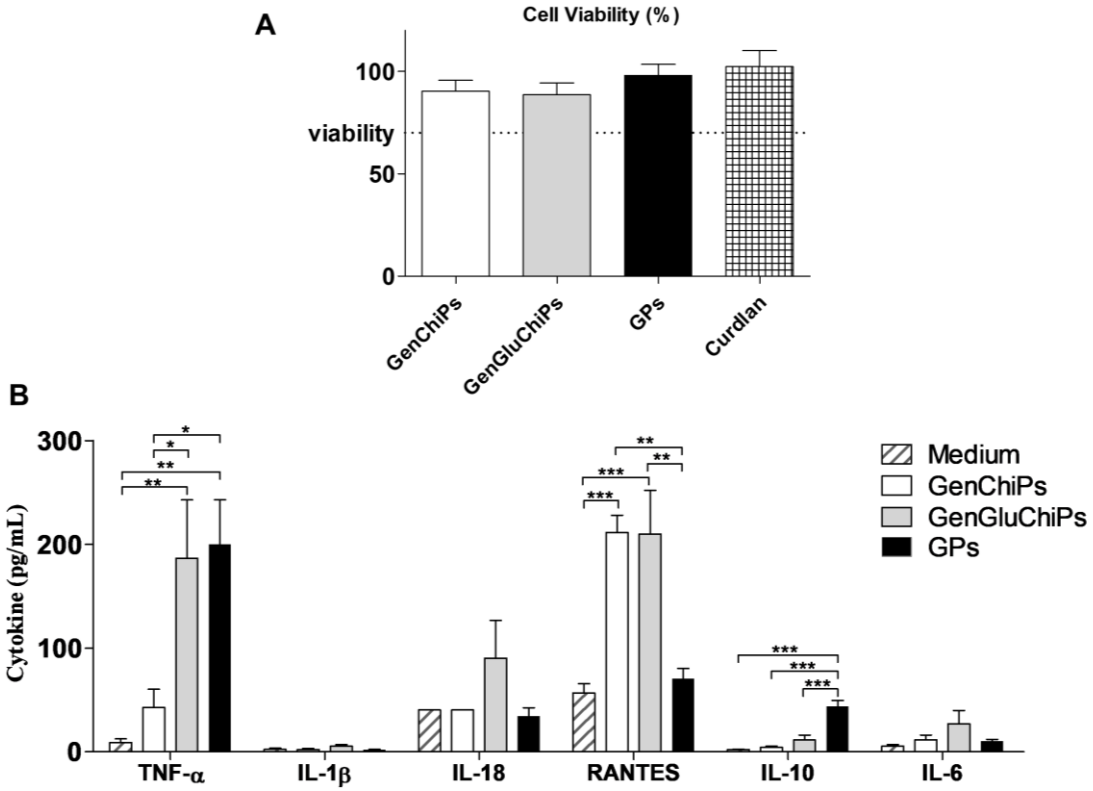

Figure 5.2. Particle induced cytokine secretion by mice spleen cells *in vitro*. (**A**) Particle cytotoxicity was evaluated by an MTT assay performed 24 h after GenChiPs, GenGluChiPs and GPs incubation at 200 μg/mL, and it is shown as the % of cell viability compared to the untreated control. (**B**) Cytokine secretion of mice spleen cells either unstimulated (Medium) or stimulated with GenChiPs, GenGluChiPs and GPs at 200 μg/mL for 48 h. 18 different cytokines were evaluated using a multiplex immunoassay (ProcartaPlex™) and all the values are shown in table 5.3. In this graph only cytokines with detectable values are represented. Data (mean ± SEM) are representative of two independent experiments of triplicates. ** denotes statistical differences at p<0.05, ** at p<0.01 and *** at p<0.001.*

To the best of our knowledge this is the first study comparing the effect of chitosan and/or β-glucan-based particles on mice spleen cells. The presence of β-glucan (GenChiPs and GPs) generating a cytokine signature that differs from chitosan (GenChiPs), suggesting the involvement of different receptors and different adjuvant mechanisms and most probably with the differences observed in the cytokine release profile (Figure 5.1).

5.3.3. GenChiPs, GenGluChiPs and GPs induce TNF-α secretion by human monocytes.

The majority of adjuvant mechanistic studies has been performed with mice cells because they offer ready access to large number of immune cells and fewer studies were performed with cells from humans. There is a big leap to trust that mouse models are applicable to humans. Therefore, we next compared the ability of GenChiPs, GenGluChiPs and GPs to induce cytokine production in monocytes isolated from human PBMCs. It is known that particulate adjuvants usually induce a local pro-inflammatory environment which results in immune cells recruitment, such as PBMCs, to the vaccine site [108]. Additionally, monocyte-derived APCs are important players in the development of adaptive immunity and are therefore a good target for vaccine design against infectious diseases [100]. The monocytes were challenged with the particles or the positive controls (LPS and R848) over 18 h and the results were represented in table 5.4.

Table 5.4. Cytokine concentrations of human monocytes either unstimulated (Medium) or stimulated with the particulate adjuvants or the positive controls.

Cytokine	Medium		LPS		R848		GenChiPs		GenGluChiPs		GPs	
	ICS	ELISA	ICS	ELISA	ICS	ELISA	ICS	ELISA	ICS	ELISA	ICS	ELISA
IL-6	1.7 ± 0.5	0.0 ± 0.0	13.9 ± 2.5	890.0 ± 263.8	20.1 ± 2.3	3973.0 ± 827.5	1.8 ± 0.3	150 ± 28.5	1.9 ± 0.6	360.0 ± 90.9	3.5 ± 0.8	98.8 ± 12.3
TNF-α	0.6 ± 0.1	0.0 ± 0.0	10.6 ± 1.3	508.5 ± 131.3	30.9 ± 3.2	3365.0 ± 710.1	6.8 ± 0.6	340.7 ± 67.9	6.7 ± 1.6	1586.2 ± 67.9	18.2 ± 1.6	348.4 ± 51.2
IL-12	0.2 ± 0.1	0.0 ± 0.0	0.4 ± 0.1	0.0 ± 0.0	4.3 ± 0.9	0.0 ± 0.0	2.7 ± 0.5	0.0 ± 0.0	1.3 ± 0.2	0.0 ± 0.0	0.1 ± 0.1	0.0 ± 0.0
IL-10	0.2 ± 0.1	0.0 ± 0.0	0.2 ± 0.1	0.0 ± 0.0	0.3 ± 0.1	0.0 ± 0.0	3.9 ± 0.5	0.0 ± 0.0	4.8 ± 1.1	0.0 ± 0.0	0.1 ± 0.1	0.0 ± 0.0

Monocytes, purified from PBMCs of healthy individuals using magnetic CD14 MicroBeads, were stimulated with 200 µg/mL GenChiPs, GenGluChiPs and GPs or stimulated with the positive controls (LPS and R848) and the cytokine production determined after an overnight incubation (18 h). The frequency of monocytes producing IL-6, TNF-α, IL-12 and IL-10 was assessed by intracellular cytokine staining (ICS) and represented as the % of positive cells evaluated by flow cytometry and the concentration in the supernatant of the same cytokines was quantified by ELISA and shown in pg/mL. Data (mean ± SEM) are representative of 10 (ICS) or 12 (ELISA) healthy individuals.

The graphs depicted in figure 5.3 only show the TNF-α, IL-6, IL-12 and IL-10 production by intracellular cytokine staining (ICS) (Figure 5.3A) or the detection in cell culture supernatant by ELISA (Figure 5.3B) from the individual monocytes either unstimulated (-) or stimulated with GenChiPs, GenGluChiPs or GPs. TNF-α production/secretion was a consistent finding observed by ICS and ELISA for all the particles, with statistically significantly higher levels ($p<0.001$) than basal production (-). The stimulation of human monocytes β-glucan receptors (e.g. Dectin-1) by glucan particles is known for a long time to induce TNF-α production [334]. Additionally, both chitosan and β-glucan-based particles have been recently reported to induce TNF-α release in PBMCs [332]. Nevertheless, chitosan induced TNF-α released by PBMCs was suggested to be mediated by the mannose receptor [305]. Overall, TNF-α, an early mediator of inflammatory responses, is of great interest for a vaccine adjuvant to recruit the immune cells to the injection site. Regarding IL-6, an inflammatory cytokine involved in Th22 and Th17 differentiation intimately associated with mucosal barriers [79], the frequency of positive cells (Figure 5.3A) did not differ between the particles and the unstimulated condition. This would be in agreement with Pattani *et al*. [335] that observed no alterations on IL-6 gene expression following PBMCs stimulation with blank chitosan particles, but contradictory to Farace *at al*. that found IL-6 up-regulated following chitosan particles stimulation of PBMCs [332]. Regarding β-glucan-based particles, Stopinsek *et al*. [305] found particulate curdlan a potent inducer of IL-6 and GPs also inducing some IL-6 secretion, contrasting from our ICS results (Figure 5.3A). As discussed before, and confirmed in this study, IL-6 is stimulated by the LPS (Table 5.4), a contaminant that can be present on biomaterials. Therefore, the negative ICS results at least confirmed that the particles might not be contaminated with LPS. On the other side, high IL-6 levels were found in the monocyte supernatant of some individuals incubated with GenChiPs (6 out of 12) and GenGluChiPs (10 out of 12) (Figure 5.3B). These unequal findings assessed by two different techniques (ICS and ELISA), confirmed that cytokine activity is a complex mechanism controlled by several factors that can result in peak or sustained secretion compromising the cytokine increase detection at a particular location and time [336]. Then, IL-12, associated to Th1 differentiation and cell-mediated immunity and IL-10, crucial in the control of immune responses through a negative feedback [62], were also monitored. The frequency of positive cells for both IL-12p70 and IL-10 was

significantly higher following GenChiPs and GenGluChiPs stimulation (Figure 5.3A). Nevertheless, the frequencies observed were significantly low and those cytokines were below the ELISA detection limit (Figure 5.3B). Oppositely, other reports correlated IL-10 and IL-12 secretion with both β-glucan and chitosan-based particles incubation with PBMCs [42, 57] or β-glucan stimulation of human DCs [50, 51, 63]. It is important to note that cytokine-consuming cells can also difficult extracellular cytokine detection and lead to misleading results, hiding momentary cytokine increases. Upon binding to a receptor, the cytokine is consumed, creating a gradient of localized cytokine niche. Increasing consumption, either by increasing the density of consuming cells or the single-cell consumption rate will lead to the decrease of cytokine niche [337].

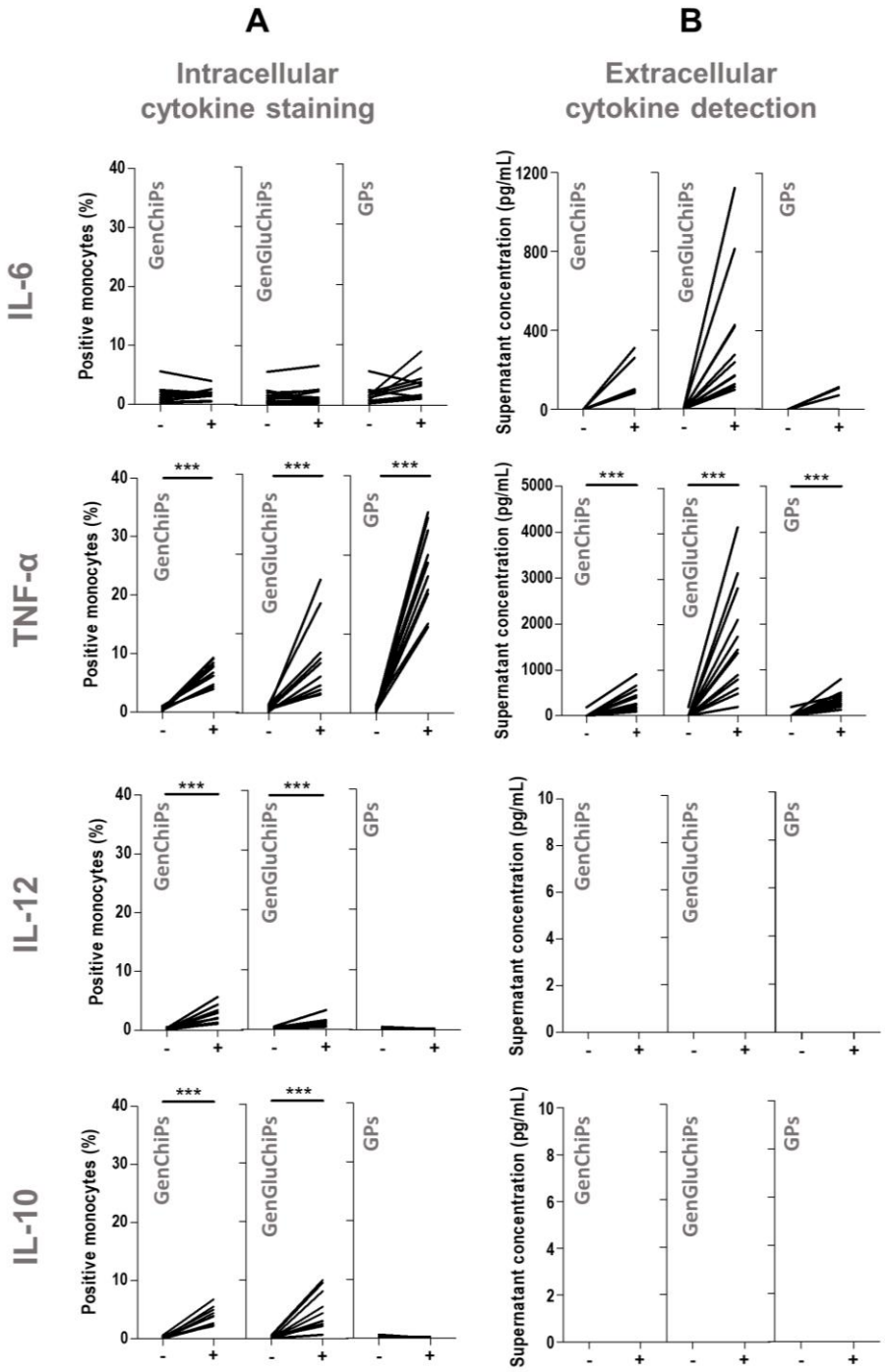

Figure 5.3. Particle induced cytokine production/secretion by human monocytes. Monocytes, purified from PBMCs of healthy individuals using magnetic CD14 MicroBeads, were stimulated with 200 µg/mL GenChiPs, GenGluChiPs and GPs and the cytokine production determined after an overnight incubation (18 h) (Table 5.4). (**A**) The frequency of monocytes producing IL-6, TNF-α, IL-12p40 and IL-10 was assessed by intracellular cytokine staining (ICS) evaluated by flow cytometry. (**B**) IL-6, TNF-α, IL-12p70 and IL-10 quantification in the supernatant was determined by ELISA. Data (mean ± SEM) are representative of 10 (A) or 12 (B) healthy individuals. **** denotes statistical differences at p<0.001.*

Overall, the impact of the three different particles in human monocytes confirmed their immunostimulatory properties. Except for the TNF-α, consistently induced by all particle compositions, the other cytokines (IL-6, IL-12 and IL-10) were mostly present following GenChiPs and GenGluChiPs stimulation. Once more, regarding some contradictory results found amongst scientific literature, it is important to keep in mind the influencing factors discussed in mice spleen cells section. Therefore, the adjuvant ability of the particles would be better understood and validated when included in a vaccine formulation with a real antigen to perform comparative vaccination studies.

5.3.4. GenChiPs, GenGluChiPs and GPs induce strong antibody production following HBsAg vaccination.

The aluminum is the adjuvant included in commercial hepatitis B vaccines, and the immune response generated is essentially mediated by antibodies. The capacity of GenChiPs, GenGluChiPs and GPs to induce HBsAg-specific humoral immune response is a good indicator of the particle's ability to function as an adjuvant. Vaccination schedule and vaccine doses are described in table 5.1 and vaccine physicochemical properties summarized in table 5.2. Briefly, three subcutaneous vaccine doses were performed with 1.5 μg of HBsAg per dose. The number of vaccine doses is known to influence the elicited immune responses and was chosen based on a study with ovalbumin loaded GPs that showed increased immunogenicity for three consecutive administrations comparing to two or just one dose [229]. To note that depot formation at the administration site, a common mechanism of vaccine adjuvants usually associated with long-lasting immune responses [22], was observed for the adjuvanted vaccine formulations tested (GenChiPs, GenGluChiPs and GPs) but not for the group with "No Adjuvant" (only HBsAg).

Serum antibodies were measured 14 days after each vaccine dose (days 14, 28 and 42) and showed in figure 5.4A. All particulate adjuvants (GenChiPs, GenGluChiPs and GPs) induced the production of HBsAg-specific IgG right after the first dose while only HBsAg (No Adjuvant) did not, demonstrating an early detected adjuvant effect. Later, serum antibodies were detected in mice from all vaccinated groups after the second and the third vaccine doses, with significantly higher endpoint-titers for all the adjuvanted groups (GenChiPs, $p<0.05$; GenGluChiPs and GPs, $p<0.001$). This can be attributed to the particle ability to enhance and activate APCs, as better explained by others [158]. Expectedly,

priming-boost strategy frequently results in increased antibody production as illustrated in figure 5.4A. Specifically, increasing endpoint-titers were detected after each boost comparing to the previous one (day 14 versus day 28 and day 28 versus day 42). Interestingly, this was most notorious for the β-glucan containing adjuvants (GenGluChiPs and GPs ($p<0.001$)). At day 42, comparing to "No Adjuvant", a remarkably 435-fold increase for GenChiPs, 4500-fold increase for GenGluChiPs and 2500-fold increase for GPs were observed for the induced IgG titers. The present vaccination schedule comprising three subcutaneous doses resulted in higher anti-HBsAg IgG endpoint-titers than previous studies from our research group with two doses of the same HBsAg dose (1.5 μg) loaded in poly-ε-caprolactone (PCL)/chitosan nanoparticles [216, 266]. Antigen dose sparing is a desired characteristic for an adjuvant. The present study provided that with all the developed particles, which resulted in increased antibody production than previously observed by our group with three and six times higher antigen dosage (HBsAg), using similar chitosan-based particles [188, 189]. This is of pivotal importance to reduce vaccine manufacturing costs, as the antigen in usually the most expensive component. Remarkably, our findings proved that the presence of β-glucan on particle composition elevated the antigen-specific humoral response, with significantly higher antibody endpoint-titers detected in GenGluChiPs ($p<0.01$) and GPs ($p<0.05$) groups when compared to GenChiPs group.

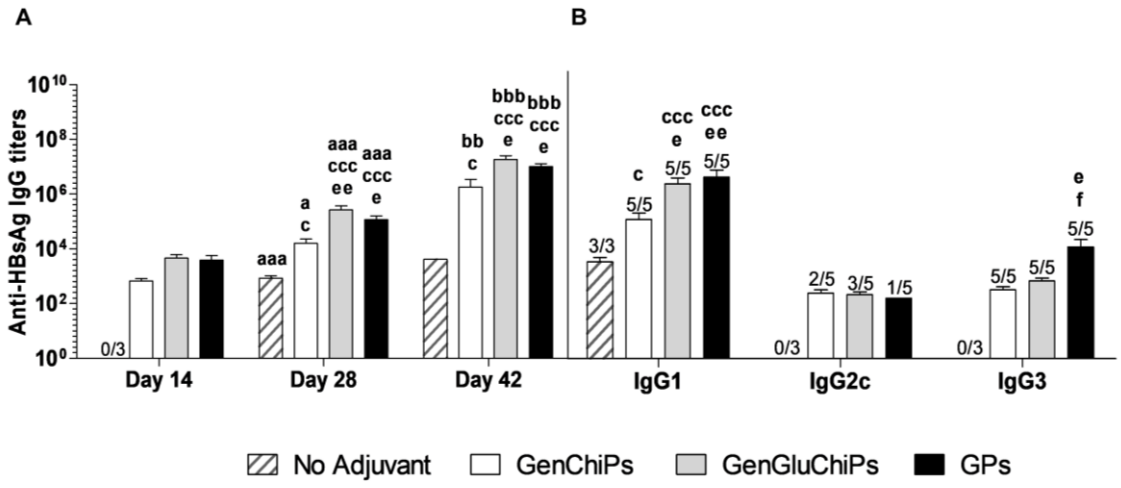

Figure 5.4. Serum HBsAg-specific immunoglobulins of vaccinated mice. Vaccine formulations and the vaccination schedule are summarized in table 5.1. Three vaccine doses of 1.5 µg HBsAg alone (No Adjuvant) or loaded in 400 µg of GenChiPs, GenGluChiPs or GPs adjuvant were administered through the subcutaneous route. Serum anti-HBsAg (**A**) IgG titers, evaluated at days 14, 28 and 42, and (**B**) IgG1, IgG2c and IgG3 titers evaluated at 42. The end-point titers presented represent the antilog of the last log 2 dilution for which the OD values were at least two-fold higher than that of the naive serum sample equally diluted. When serum antibodies were not detected in all mice, the number of responder mice is indicated above each bar. Data are presented as mean ± SEM. **p<0.05, **p<0.01 and *** p<0.001 denote statistical differences between: a, day 14 and 28; b, day 28 and 42; c, GenChiPs, GenGluChiPs or GPs and No adjuvant; d, GenChiPs and GenGluChiPs; e, GenChiPs and GPs; f, GenGluChiPs and GPs*.

5.3.5. GenChiPs, GenGluChiPs and GPs induce IgG2c and IgG3.

As the profile of an immune response for a certain antigen can be skewed by the type of adjuvant used, we decided to understand the influence of either GenChiPs, GenGluChiPs and GPs on the quality of humoral immune response generated. For that, anti-HBsAg IgG1, IgG2c and IgG3 titers were determined at day 48 (Figure 5.4B). Indeed, IgG subclass switching may be induced when B cells were in the presence of cytokines and it is generally accepted as predictive of the T cell response generated [79]. IgG1 is associated with a Th2 immune profile while IgG2 and IgG3 are associated with viral neutralization and opsonization, characteristically Th1. The group vaccinated with "No Adjuvant" only induced IgG1 production, in agreement with the fact that HBsAg self-assembles into virus-like particles (VLPs) [314] characteristically generating IgG1 subclass Th2-biased immune responses [315]. HBsAg combination with GenChiPs ($p<0.05$),

GenGluChiPs ($p<0.001$) and GPs ($p<0.001$) significantly increased IgG1 production. In similarity to the total IgG depicted in figure 5.4A, a 17-fold or 30-fold increase was observed for IgG1 production of either GenGluChiPs ($p<0.05$) or GPs ($p<0.01$), respectively, when compared to GenChiPs. Contrasting from "No Adjuvant" group, IgG2c and IgG3 were only detected in mice from adjuvanted groups (GenChiPs, GenGluChiPs and GPs). IgG3 was consistently observed among all animals, while IgG2c was only detected in the sera of some mice. Results showed that GPs induced a 15-fold or 30-fold increase of serum IgG3 than GenChiPs or GenGluChiPs ($p<0.05$), respectively. Our IgG subclass findings are in agreement with previous reports from our group with HBsAg-loaded chitosan-based particles [189, 216, 266] and to what is described in literature for repeated subcutaneous doses of GPs with model antigens [228, 229, 241]. The overall results highlight the importance of all adjuvants used to induce a broader IgG profile than the HBsAg alone (No Adjuvant), especially pronounced by the GPs vaccinated group with increased IgG3 endpoint-titers, strongly associated with the complement system activation [313]. Notably, the appearance of allergic or anaphylactic reactions following vaccination has been frequently correlated with the presence of adjuvants in vaccine formulation. Therefore, regulatory authority asks the result of the antigen-specific IgE endpoint-titers for new adjuvants. In the present study, although the high IgG endpoint-titers of adjuvanted groups, no anti-HBsAg IgE antibodies were detected.

5.3.6. GPs elicit a broad and strong HBsAg-specific cytokine production.

Then, for a better understanding of GenChiPs, GenGluChiPs and GPs adjuvant mechanism for the HBsAg, we decided to analyze the cytokine secretion from the spleen cells (day 42) after *ex vivo* restimulation with HBsAg. Usually, cytokines can act on lymphocytes and augment the immune responses of Th1 cells, favoring cell-mediated immunity or Th2 cells, favoring humoral immunity [22]. Recently five more functionally unique subsets have been described (Th9, Th17, Th22, Treg and Tfh) whose differentiation also depends on the cytokine profile of the milleu [79, 80].

In the present study, 18 different cytokines were measured on cell culture supernatant following 48 h of restimulation with HBsAg and categorized according associated Th subset (Figure 5.5A-F). First, is important to note that the graph is in

logarithmic scale to enable the illustration of all cytokine levels, however, do not tempt yourselves to take quick conclusions just by looking to the bars height. Although not presented in the graph, the mitogen ConA and LPS served as positive controls and the results are represented in table 5.5. Figures 5.5A-F showed a marked increase in the secretion of IFN-γ, TNF-α, IL-18, RANTES, IL-4, IL-5, IL-13, IL-17A, GM-CSF, IL-2, IL-6 and IL-22 in spleen cells supernatant from mice vaccinated with GPs as an adjuvant. Notably, only vaccination with GPs profoundly affected HBsAg-specific cell-mediated immunity, while the other vaccinated groups induced negligible cytokine production comparable to the Naïve group (not vaccinated). In fact, literature shows that when GPs were used as a vaccine platform for a variety of model antigens resulted in consensual strong Th1 and Th17-biased cell-mediated immune responses, frequently associated with high IFN-γ and IL-17 splenic production following antigen recall [228, 229, 241, 248]. The strong secretion of those cytokines was associated with protective immunity against the highly virulent strains *Cryptococcus neoformans* and *Criptococcus gatti* lethal challenges [248]. The truth is that although other have successfully reported IFN-γ production on vaccinated mice using HBsAg adjuvanted with poly(L-lactide acid) (PLA) nanoparticles or poly(L-lactide-coglycolide acid) (PLGA) nanoparticles modified with chitosan or its derivatives [213, 311, 338], our experience with HBsAg vaccination lead to the conclusion that strong cell-mediated immune responses with chitosan-based particles is hard to achieve with antigen doses used in our studies [188, 189]. Moreover, the results of figure 5.5 showed a 30-fold increased HBsAg-specific IFN-γ and IL-17 production than it was induced in three recent studies from our group either using PCL/chitosan nanoparticles in the same dose (400 μg) and the same HBsAg dose (1.5 μg) following two repeated administrations [216, 266] or using aluminum/chitosan particles and a higher HBsAg dose (5 μg) [189].

Table 5.5. Mice vaccination study - cytokine concentration in supernatants of spleen cells restimulated *in vitro* with HBsAg or stimulated with LPS or ConA.

Cytokine	Naïve			No Adjuvant			GenChiPs			GenGluChiPs			GPs		
	HBsAg	LPS	ConA	HBsAg	LPS	ConA	HBsAg	LPS	ConA	HBsAg	LPS	ConA	HBsAg	LPS	ConA
IFN-γ	0.1 ± 0.0	8.3	3144.5	1.5 ± 1.5	61.2	---	0.0 ± 0.0	5.37	4909.5	3.8 ± 2.2	10.5	3940.8	1683 ± 748.1	20.1	4267.5
TNF-α	0.0 ± 0.0	250.2	173.4	4.0 ± 3.7	297.2	---	1.0 ± 0.7	326.1	180.9	5.0 ± 1.0	347.4	232.6	126.6 ± 40.9	396.0	354.8
IL-18	0.0 ± 0.0	200.3	1646.7	107.8 ± 64.4	307.4	---	34.1 ± 25.4	220.2	1628.9	155.5 ± 97.67	509.7	1835.9	1258.0 ± 243.5	422.6	1977.4
IL-12p70	0.0 ± 0.0	5.2	9.7	0.1 ± 0.1	7.4	---	0.0 ± 0.0	3.4	13.1	0.1 ± 0.1	9.4	15.5	6.5 ± 2.8	11.1	19.6
IL-27	0.0 ± 0.0	0.0	1.9	0.0 ± 0.0	2.9	---	0.0 ± 0.0	0.0	2.4	0.0 ± 0.0	0.0	3.9	2.7 ± 1.2	1.9	2.9
RANTES	0.0 ± 0.0	729.4	351.7	0.0 ± 0.0	1118.1	---	1.7 ± 1.7	1249.2	421.4	0.0 ± 0.0	2225.3	521.8	150.2 ± 71.9	1075.5	599.8
IL-4	0.0 ± 0.0	0.0	78.4	6.4 ± 4.0	1.7	---	2.1 ± 0.9	2.3	84.1	5.3 ± 3.3	11.0	94.1	70.7 ± 17.5	4.8	106.9
IL-5	0.0 ± 0.0	0.0	40.4	1.9 ± 1.3	10.9	---	0.4 ± 0.2	4.4	95.8	2.0 ± 1.3	6.3	92.7	18.7 ± 5.7	7.1	318.54
IL-13	0.0 ± 0.0	0.0	122.7	0.0 ± 0.0	3.9	---	0.6 ± 0.4	3.5	168.1	5.8 ± 3.0	13.7	250.4	75.3 ± 31.1	5.2	439.5
IL-17A	0.0 ± 0.0	5.2	560.3	0.0 ± 0.0	4.8	---	9.4 ± 0.8	6.3	872.0	93.0 ± 35.1	44.9	1658.1	424.1 ± 140.1	6.2	1343.2
IL-23	0.0 ± 0.0	0.0	8.3	0.0 ± 0.0	0.0	---	0.0 ± 0.0	0.0	15.7	1.2 ± 0.6	0.0	22.9	9.5 ± 7.4	0.0	22.9
GM-CSF	0.0 ± 0.0	6.3	64.5	2.6 ± 2.6	8.7	---	0.1 ± 0.1	6.9	47.6	5.7 ± 2.5	11.7	54.9	177.0 ± 66.0	11.3	133.9
IL-1β	0.0 ± 0.0	7.5	7.1	0.3 ± 0.3	15.1	---	0.1 ± 0.1	7.5	6.2	0.5 ± 0.3	16.4	8.9	3.3 ± 1.4	14.6	14.6
IL-10	0.0 ± 0.0	128.5	34.3	4.9 ± 4.9	154.2	---	0.0 ± 0.0	194.6	56.0	2.0 ± 1.2	278.7	171.9	8.5 ± 4.0	236.7	176.2
IL-2	2.2 ± 1.6	13.3	734.3	38.7 ± 26.9	14.4	---	12.6 ± 1.0	15.3	782.4	49.4 ± 15.8	35.5	858.2	653.1 ± 209.6	19.2	1153.3
IL-6	0.0 ± 0.0	808.0	324.7	47.9 ± 15.9	1110.0	---	70.0 ± 18.5	1049.3	588.4	126.7 ± 44.6	1555.5	1019.3	444.4 ± 183.6	1761.4	1388.4
IL-22	0.0 ± 0.0	0.0	331.2	0.0 ± 0.0	44.4	---	1.1 ± 1.1	0.0	251.3	183.0 ± 122.7	90.6	601.2	1753.0 ± 618.5	27.7	902.6
IL-9	0.0 ± 0.0	0.0	28.7	0.0 ± 0.0	0.0	---	0.0 ± 0.0	0.0	64.1	0.0 ± 0.0	0.0	81.5	22.8 ± 9.4	0.0	75.1

Cytokine release of vaccinated mice spleen cells collected on day 42 and further simulated in vitro with 5 µg/mL of HBsAg or positive controls (LPS – 1 µg/mL and ConA – 6.25 µg/mL) for 48 h. 18 different cytokines were evaluated using a multiplex immunoassay (ProcartaPlex™). The results represent individual cytokine concentrations resultant from HBsAg restimulation after basal production (Medium) subtraction per mice. For the positive controls, a pool of the splenocyte supernatant of all mice from each group was used for the multiplex assay. Data are presented as mean ± SEM.

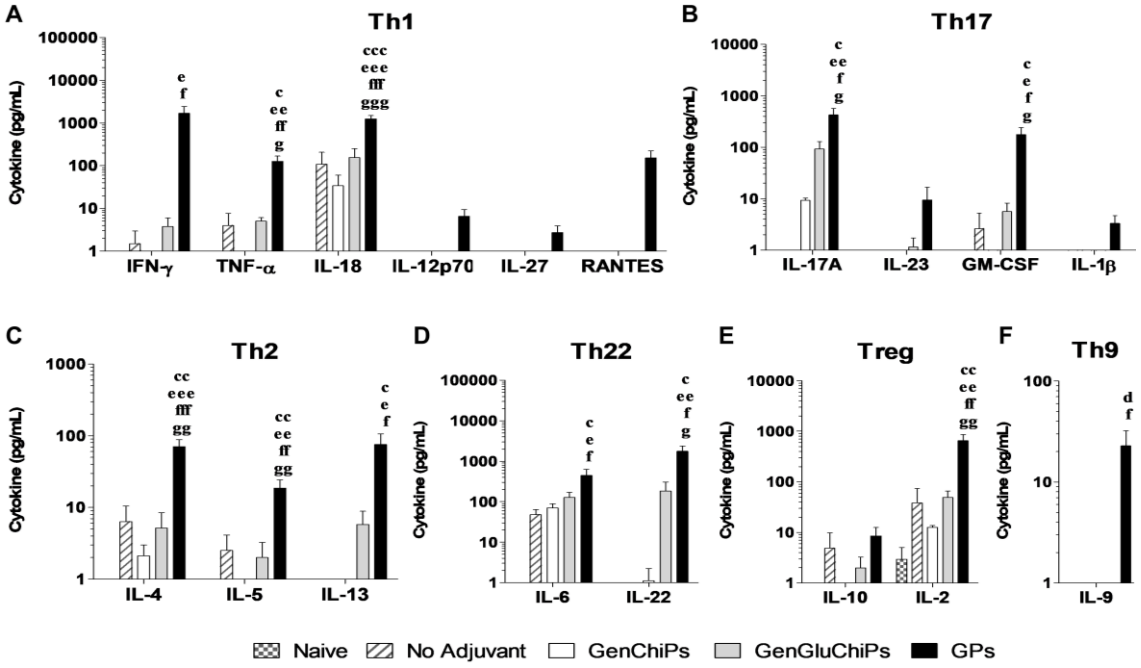

Figure 5.5. Cytokine production of vaccinated mice spleen cells after HBsAg restimulation. Vaccine formulations and the immunization schedule are summarized in table 5.1. Three vaccine doses of 1.5 µg HBsAg alone (No Adjuvant) or loaded in 400 µg of GenChiPs, GenGluChiPs or GPs adjuvant were administered through the subcutaneous route. Cytokine release of mice spleen cells collected on day 42 and further simulated *in vitro* with 5 µg/mL of HBsAg for 48 h. The results represent individual cytokine concentrations resultant from HBsAg restimulation after basal production (Medium) subtraction per mice. 18 different cytokines were evaluated using a multiplex immunoassay (ProcartaPlex™ - all the values are shown in table 5.5) and are characteristically involved in (**A**) Th1, (**B**) Th17, (**C**) Th22, (**D**) Treg and (**E**) Treg and (**F**) Th9 cell differentiation. To note that signature cytokines were associated with Th cell subsets according to Kara *et al*. (Kara, Comerford *et al*. 2014) and Raphael *et al*. (Raphael, Nalawade *et al*. 2015). For instance, cytokines such as IL-6 might be related with several T helper subsets (Th17 and Th22). Data are presented as mean ± SEM. **p<0.05, **p<0.01 and *** p<0.001 denote statistical differences between: c, GenChiPs, GenGluChiPs or GPs and No adjuvant; d, GenChiPs and GenGluChiPs; e, GenChiPs and GPs; f, GenGluChiPs and GPs and; g, GPs and Naïve*.

Overall, the present findings proved that vaccination with HBsAg-loaded GPs induced a cytokine signature embanking almost all Th cell subsets known to date: Th1 (IFN-γ, TNF-α, IL-18 and RANTES), Th2 (IL-4, IL-5 and IL-13), Th17 (IL-17A and GM-CSF), Treg (IL-2) and Th22 (IL-6 and IL-22). This may indicate that GPs could orchestrate cell-mediated cytotoxic responses against intracellular (Th1) or extracellular pathogens (Th2), mediate inflammatory responses and neutrophils phagocytic functions (Th17) and, dictate inflammatory responses at cutaneous and mucosal surfaces (Th22, although Th22 cells

are scarcely detected in mice) [79]. Regarding the need of more potent adjuvants either for low responder populations, infectious diseases or therapeutic purposes, our data gives new insights to the use HBsAg-loaded GPs as a valuable component of a future immunotherapeutic approach against the HBV. The capacity to induce a strong Th1 differentiation is usually related to enhance cytotoxic activity, crucial to the clearance of intracellular pathogens such as the HBV-infected hepatocytes. The broad cytokine production observed might also have a special role in rescuing the innate and adaptive immune exhaustion characteristic of chronic hepatitis B [339]. Moreover, HBsAg loaded GPs oral vaccination resulted in enhanced production of IFN-γ in the liver in a recent report from our group [304] and other Th1 cytokines following repeated GPs oral administrations demonstrated by others [238]. This is a peculiarity of particle accumulation in the liver via the enterohepatic route only achievable through oral administrations, consistent with no liver IFN-γ increase demonstrated after GPs subcutaneous vaccination (data not shown). Therefore, GPs oral administrations together with the subcutaneous vaccination approach of the present work could be great allies in the fight against chronic HBV.

5.4. Conclusions

Vaccination is an effective strategy to prevent infectious diseases and, depending on the type of immune response generated, can have a therapeutic applicability. Vaccine adjuvants are key components to direct immunity towards strong humoral and cell-mediated immunity. This study proved that although GenChiPs, GenGluChiPs and GPs adjuvants displayed *in vitro* immunostimulatory properties in mice spleen cells and human monocytes and demonstrated their great adjuvant effect on the generated antibody production following mice vaccination with the HBsAg, only GPs were capable to induce strong and varied HBsAg-specific cell-mediated immunity. The secretion of HBsAg-specific cytokines related with Th1, Th2, Th17, Th22 and Treg -biased immune response revealed the value of GPs as a potent adjuvant and also a possible immune-mediated antiviral component of an hepatitis B therapeutic vaccine.

CHAPTER 6

CONCLUDING REMARKS AND FUTURE PERSPECTIVES

The prospective to eliminate HBV, as a cause of public health threat, by 2030 requires new strategies for both prophylatic and therapeutic measures. Indeed, vaccination can have both a prophylactic and a therapeutic applicability for infectious diseases, depending on the type of immune response generated. Contrasting from commercially available HBsAg vaccines, a robust Th1-biased immune response, mainly dependent on the use of the right immunopotentiator, would help the exhausted CHB immune system to promote viral clearance and achieve a functional cure. In that regard, further efforts are needed to develop an adjuvant that can challenge the monopoly of aluminum salts. This, the recognized immunological potential of β-glucans and the scarcity of studies evaluating their adjuvant effect for the HBsAg, justified the main aim of the present thesis to develop and test the value of different β-glucan-based particles or β-glucan containing vaccine formulations (GPs, GluPol, GPsPol and GenChiGluPs) to address the current hepatitis B needs following several vaccination strategies.

To the best of our knowledge, this was the first time that particles containing both β-glucan and chitosan (GenGluChiPs) were produced based on a precipitation technique, representing an important step for the successfully combination in the same particle of two biopolymers that do not interact electrostatically with each other. The main driver of the choice of this technique for particle production was the development of a vaccine formulation using a simple and attractive method with the possibility of being reproducible and easy to scale up, two critical aspects for their translation into the clinic [110]. The development of a “pathogen-like” adjuvant composed by chitosan and surface localized β-glucan to activate APCs expressing Dectin-1 receptor was successfully accomplished, mostly demonstrated by the zeta potential titration of GenGluChiPs in comparison to GenChiPs. Interesting features were shown for GenGluChiPs as a delivery system for antigens with low isoelectric point showing no significant cytotoxicity *in vitro*, an important characteristic for licensing new adjuvants. Although there are natural β-glucan/chitosan complexes isolated from the cell wall of several microorganisms, newly technologically developed β-glucan/chitosan systems are scarce among the scientific literature. For immunomodulatory purposes, most of the studies that use both polymers in the same formulation, use the GPs as a carrier system for antigen/chitosan colloidal particles [229, 321, 340]. Another study used chitosan particles functionalized with β-

glucan to deliver rifampicin to human alveolar like macrophages differentiated from PBMCs-derived monocytes [230]. Other approaches include ionic and non-covalent interactions to build a β-glucan outer shell for chemotherapy purposes [341], prebiotic coating for targeted delivery to the gastrointestinal system [342], or β-glucan addition to chitosan scaffolds to enhance osteoblasts adhesion, growth and proliferation [343], mostly through a TNF-α mediated mechanism [344]. Therefore, this is the first time that non-modified natural β-glucans, including both the developed GenGluChiPs and the extensively studied GPs, were tested as an adjuvant for the HBsAg (recombinant or pDNA).

The immunodulatory properties of both β-glucan and chitosan, have been extensively explored before. Consistently, all the particulate adjuvants developed in the thesis showed *in vitro* stimulatory properties. Typically, the presence of β-glucan (GenGluChiPs and GPs) generated an immune signature that differs from chitosan (ChiPs and GenChiPs), suggesting the involvement of different receptors and mechanistic properties. Those findings already demonstrate an immunological advantage of the combination of the two biopolymers in the same adjuvant system. Aditionally, ChiPs but not GPs demonstrated the ability to induce mast cell degranulation and β-hexosaminidase release, consistent with a previous study of our group describing chitosan particles as mast cell activators [278]. This is particularly important for mucosal vaccine adjuvants, as mast cells are mainly located at the host-environment interface, ready to respond to pathogen stimulation through the release of mediators that activate innate immunity, directing immune cells (like APCs) to the site of infection and to the draining lymph nodes [277]. Another chitosan-mediated immune response was the RANTES secretion by mice spleen cells. This is of great interest for a vaccine adjuvant for viral infections, as RANTES has showed a significant role in sustaining CD8+ T cell responses during a systemic chronic viral infection [331] and has been associated with macrophages coactivation. Additionally, RANTES together with IFN-γ, constitute a group of “type 1 cytokines” with the capacity to bridge innate and adaptive immune reactions [330]. On the other side, while TNF-α secretion by mice spleen cells was associated to the presence of β-glucan on the adjuvant system (GenGluChiPs and GPs but not GenChiPs), TNF-α production/secretion by human PBMCs was a consistent finding observed either by ICS or ELISA for all GenChiPs,

GenGluChiPs and GPs. This suggests that the generation of an inflammatory environment is part of the adjuvant mechanism associated to both particles. Chitosan induced TNF-α released by PBMCs was suggested to be mediated by the mannose receptor [305]. On the other side, β-glucans are known to activate several receptors of immune cells (e.g. Dectin-1, CR3, TLR2/6), through the activation of the NF-κβ or MAPK pathways that induce the production of early proinflammatory mediators [223], benefic for the recruitment of immune cells (e.g. monocytes, macrophages, DCs) to the vaccine administration site, amplifying the immune response generated. Nevertheless, it should be carefully considered that TNF-α production may cause toxic effects increasing the risk of tissue damage at the administration site.

Regarding our attempts towards effective oral and DNA vaccine strategies, envisioning that the improved stability conferred by both formulations would benefit the developing countries, the results were not as good as expected. Usually, the best strategies from a practical point of view are the most difficult to achieve effectiveness. Coherently, few mucosal or DNA vaccines are currently licensed for human use, and promising efficient approaches are still under development. It is truth that DNA vaccine research is often confronted with limited immunogenicity, associated with poor *in vivo* transfection and immune tolerance without viral vectors [87, 88]. Nevertheless, given the design of the vaccine formulations used with β-glucan-based additional adjuvant and the excellent transfection results obtained *in vitro,* it was expected a higher vaccine efficacy *in vivo*. The hypothesis that IM injections may lead to better results cannot be excluded. Some authors refer that IM injection might be the best route for DNA vaccination [88]. Just to highlight the fact that combination of GPs with the Pol enhanced the *in vitro* transfection capacity of the system which deserves further studies to understand the mechanism involved and the potential applicability of this system to other gene-based therapies. The oral vaccination study with the HBsAg revealed the need for a SC priming prior oral boosting to induce plenty HBsAg seroconversion, as a fully oral vaccination schedule was only effective for 60 % of the mice, for both AlgChiPs and GPs adjuvants. This vaccination schedule with only one injectable dose may have a high translational potential for mass vaccination in developing countries. The requirement of multiple injectable vaccine doses difficults the implementation of a mass vaccination strategy in

those countries, mainly due to the difficulty in maintaining an uninterrupted cold chain transportation/storage to not compromising the efficacy of the vaccine and because there are few health professionals which guarantee a safe injection. Comparing to the commercialized hepatitis B vaccines, one instead of three injectable doses would facilitate immunization and reduce the risk of infections related to reuse of disposable syringes and needles. Furthermore, the detection of HBsAg-specific IgA in mucosal secretions was a proof of concept of the major advantage of mucosal vaccination. Specifically, the presence of antigen-specific IgA in vaginal mucosa achieved with AlgChiPs is particularly relevant to prevent the sexually transmitted HBV, and the detection of antigen-specific IgA in faeces for all the adjuvants tested may be important against virus transmitted through the fecal-oral route such as the hepatitis A virus, or the rotavirus and norovirus associated with grastoenteritis. The fact that the oral vaccination with GPs resulted in increased liver IFN-γ, may have a potential therapeutic applicability to CHB and it is a result of great importance obtained during this project.

To date, several strategies using particulate delivery systems for hepatitis B vaccination were tested as an improved alternative to the licensed vaccines. Particularly, strategies including chitosan particles were previously studied by our group with success through SC [188, 189, 202, 216], nasal [208, 210, 267, 278] and oral [145] routes. It is known that the HBsAg self-assembles into VLPs characteristically inducing Th2-biased IgG1 subclass through injectable routes [314, 315]. Additionally, our experience suggests that HBsAg-specific strong cellular immune responses are hard to achieve using chitosan particles with a size around 500 nm or more. Those findings triggered the desire to test the adjuvant capacity of other biopolymer-based particles, accomplished with the present thesis. The possibility of antigen dose sparing was effectively provided by all the adjuvants tested, resulting in similar antibody titers as previously observed using three or six times higher HBsAg doses [188, 189]. This is extremely important to reduce vaccine manufacturing costs as the antigen is usually the most expensive component. The expected capacity of GenChiPs and GenGluChiPs to maximize and skew the antigen-specific humoral immunity was proved by the detection of HBsAg-specific IgG2c and IgG3 subclasses, associated to opsonization and virus neutralization. This was particularly notable for GenGluChiPs, with the highest antibody titers, highlighting the importance of

β-glucan combination to the chitosan delivery system. However, only GPs were capable to induce strong and diverse HBsAg-specific cell-mediated immunity even after three repeated vaccine doses. The secretion of cytokines related with Th1, Th2, Th17, Th22 and Treg-biased immune responses by the spleen cells of vaccinated mice following HBsAg recall was only detected for mice vaccinated with HBsAg loaded GPs. These findings reveal the great value of GPs as an adjuvant for therapeutic purposes, exhibiting immunostimulatory properties greatly different from the commercial hepatitis B vaccines formulated with aluminum salts (Th2-biased immune responses). Interestingly, HBsAg-specific production of proinflammatory IFN-γ and TNF-α may confer non-cytolytic effector functions to the formulation that contribute to the non-hepatotoxic HBV cccDNA destabilization [11, 345], the hallmark of HBV persistence in CHB. Non-cytolytic effector functions could be especially relevant, as hepatocytes have been shown to be quite resilient to cell-mediated killing *in vitro* [346]. Moreover, their anti-HBV activity may be important for viral control, mainly related to the activation of CD8+ T cells and macrophages to kill both the HBV and HBV-infected hepatocytes, and also enhanced phagocytosis, antigen presentation and B cell stimulation [40]. The Th17-biased immunity is regarded as a characteristic of the immune response elicited by GPs, comprising potent inflammatory mediators involved in host defense against infectious diseases mainly through the neutrophil recruitment, particularly at mucosal sites. The IL-17 has been recently considered as a chief orchestrator of immunity, serving as an adjunct to Th1-biased immune responses [82]. Overall, GPs can be a valuable component of a future immunotherapy for hepatitis B, giving the right stimulus to promote orchestrated immune responses necessary to provide a global antiviral activity able to sense and control the infection. The strong antibody production provided has been regarded as a mean to a functional cure and, the broad cytokine production observed can have a special role in restoring CHB exhausted HBV-specific T cell populations [40, 43, 339]. The elicited Th1 antiviral protection is also a promising result for the vaccination of newborns from high viral load mothers. As the adaptive immunity requires some time to marshal, the paucity of antigen-experienced cells confers vulnerability to fast replicating pathogens and leaves newborns reliant on their sole innate immune system, equally immature [26]. Therefore, stimulation of innate immunity provides a quick first line of defense during the critical period just after newborns HBV exposure. Likewise, C-type lectin agonists (e.g. β-

glucans) were already regarded as promising early life adjuvants [26]. These findings may contribute to the development of a therapeutic HBV vaccine, or at least to guide us in that direction. Even so, some drawbacks can already be pinpointed. First, the ability of HBeAg to cross the placenta generates HBV-specific T cell tolerance that can ultimately lead to failure of immunoprophylaxis [26]. Second, the main concern of immunomodulatory therapies is the induction on uncontrolled hepatitis flares and autoimmunity [15]. Third, the fact that GPs are derived from a natural source (*Sacharomyces cerevisiae*) lead to some inherent variability that may be problematic for the regulatory requirements to approve.

To conclude, the work performed throughout this thesis encountered the main aims proposed and brought new insights into the vaccinology field. The pathogen-mimicking β-glucan/chitosan particulate delivery system was successfully developed and tested as an adjuvant. Additionally, GPs were tested for the first time as an adjuvant for the HBsAg, strongly increasing and modulating the elicited humoral and cell-mediated immunity, representing an improved alternative to licensed aluminum salts. The induction of cytokines characteristic of a Th1/Th17-biased immunity reveals the potential therapeutic effect of the formulation through the SC route. Additionally, the increased IFN-γ found in the liver following the oral vaccination schedule, suggests a coordinate effect of the combination of both SC and oral GPs/HBsAg vaccination, eliciting both HBsAg-specific immunity and localized antiviral and proinflammatory cytokines in the liver. The future perspectives of this work rely on the questions opened by the present findings. First, although no cell-mediated immunity was detected using both newly developed GenChiPs and GenGluChiPs, further studies with increased HBsAg doses would be tested. Second, heterologous prime-boost vaccination has been recently reviewed as a promising strategy for infectious diseases, more effective in the induction of cell-mediated immunity than homologous prime-boost approaches [347]. Therefore, it would be extremely interesting to study the outcome of an heterologous prime-boost regime using the Pol:pCMV.S administered through the IM route for priming, followed by SC vaccination with HBsAg loaded GPs and additional oral GPs supplementation. Third, the response of CD8+ T cells in CHB is weaker or absent against envelope antigens than the core or polymerase antigens [4]. Therefore, HBcAg-specificity can be of greater value than

HBsAg-specificity and also HBcAg is associated with a more Th1-biased immune response. The overall outcome of the present findings and the future perspectives presented may arise as an improved alternative to the heat inactivated yeast-based vaccine expressing HBV S/C/X fusion protein (GS-4774) that induced HBV-specific T cell responses in healthy volunteers but HBsAg decline and HBsAg loss were not observed in CHB patients virally suppressed on NAs or not [70, 71].

CHAPTER 7

REFERENCES

1. WHO, *Global Hepatitis Report 2017*, in *Geneva: World Health Organization*. 2017.
2. Stevens, C.E., et al., *Eradicating hepatitis B virus: The critical role of preventing perinatal transmission.* Biologicals, 2017. **50**: p. 3-19.
3. Chang, M.S. and M.H. Nguyen, *Epidemiology of hepatitis B and the role of vaccination.* Best Pract Res Clin Gastroenterol, 2017. **31**(3): p. 239-247.
4. Voiculescu, M., *How Far we are towards Eradication of HBV Infection.* J Gastrointestin Liver Dis, 2015. **24**(4): p. 473-9.
5. Schweitzer, A., et al., *Estimations of worldwide prevalence of chronic hepatitis B virus infection: a systematic review of data published between 1965 and 2013.* Lancet, 2015. **386**(10003): p. 1546-55.
6. Hsieh, C.C., et al., *Age at first establishment of chronic hepatitis B virus infection and hepatocellular carcinoma risk. A birth order study.* Am J Epidemiol, 1992. **136**(9): p. 1115-21.
7. Lewis, R., *Possible link between hepatitis B infection and gastric cancer.* Lancet Oncol, 2015. **16**(4): p. e159.
8. Valaydon, Z.S. and S.A. Locarnini, *The virological aspects of hepatitis B.* Best Pract Res Clin Gastroenterol, 2017. **31**(3): p. 257-264.
9. Dupinay, T., et al., *Discovery of naturally occurring transmissible chronic hepatitis B virus infection among Macaca fascicularis from Mauritius Island.* Hepatology, 2013. **58**(5): p. 1610-20.
10. Yan, H., et al., *Sodium taurocholate cotransporting polypeptide is a functional receptor for human hepatitis B and D virus.* Elife, 2012. **3**.
11. Allweiss, L. and M. Dandri, *The Role of cccDNA in HBV Maintenance.* Viruses, 2017. **9**(6).
12. Bruns, M., et al., *Enhancement of hepatitis B virus infection by noninfectious subviral particles.* J Virol, 1998. **72**(2): p. 1462-8.
13. Chen, M., et al., *Immune tolerance split between hepatitis B virus precore and core proteins.* J Virol, 2005. **79**(5): p. 3016-27.
14. Tsai, K.N., C.F. Kuo, and J.J. Ou, *Mechanisms of Hepatitis B Virus Persistence.* Trends Microbiol, 2018. **26**(1): p. 33-42.
15. Lok, A.S., et al., *Hepatitis B cure: From discovery to regulatory approval.* J Hepatol, 2017. **67**(4): p. 847-861.
16. Boeijen, L.L., et al., *Hepatitis B virus infection and the immune response: The big questions.* Best Pract Res Clin Gastroenterol, 2017. **31**(3): p. 265-272.
17. WHO. *Health Topics - Immunization*. 2017 [cited 2017; Available from: http://www.who.int/topics/immunization/en/.

18. Riedel, S., *Edward Jenner and the history of smallpox and vaccination.* Proc (Bayl Univ Med Cent), 2005. **18**(1): p. 21-5.
19. Karch, C.P. and P. Burkhard, *Vaccine technologies: From whole organisms to rationally designed protein assemblies.* Biochem Pharmacol, 2016. **120**: p. 1-14.
20. Mast, E.E., et al., *A comprehensive immunization strategy to eliminate transmission of hepatitis B virus infection in the United States: recommendations of the Advisory Committee on Immunization Practices (ACIP) Part II: immunization of adults.* MMWR Recomm Rep, 2006. **55**(RR-16): p. 1-33; quiz CE1-4.
21. Zampino, R., et al., *Hepatitis B virus burden in developing countries.* World J Gastroenterol, 2015. **21**(42): p. 11941-53.
22. Chauhan, N., et al., *An overview of adjuvants utilized in prophylactic vaccine formulation as immunomodulators.* Expert Rev Vaccines, 2017. **16**(5): p. 491-502.
23. Yang, J.D., et al., *Hepatocellular Carcinoma Occurs at an Earlier Age in Africans, Particularly in Association With Chronic Hepatitis B.* Am J Gastroenterol, 2015. **110**(11): p. 1629-31.
24. Nguyen, M., et al., *3 times higher healthcare cost in chronic hepatitis B patients compared to non-chronic hepatitis B controls especially those with decompensated liver disease: United States real world healthcare utilization and cost analysis*, J.o. Hepatology, Editor. 2017. p. Pages S369–S370.
25. World Health, O., *Hepatitis B vaccines: WHO position paper, July 2017 - Recommendations.* Vaccine, 2017.
26. Mohr, E. and C.A. Siegrist, *Vaccination in early life: standing up to the challenges.* Curr Opin Immunol, 2016. **41**: p. 1-8.
27. Wen, W.H., M.W. Lai, and M.H. Chang, *A review of strategies to prevent mother-to-infant transmission of hepatitis B virus infection.* Expert Rev Gastroenterol Hepatol, 2016. **10**(3): p. 317-30.
28. Mavilia, M.G. and G.Y. Wu, *Mechanisms and Prevention of Vertical Transmission in Chronic Viral Hepatitis.* J Clin Transl Hepatol, 2017. **5**(2): p. 119-129.
29. Nassal, M., *HBV cccDNA: viral persistence reservoir and key obstacle for a cure of chronic hepatitis B.* Gut, 2015. **64**(12): p. 1972-84.
30. Grossi, G., et al., *Hepatitis B virus long-term impact of antiviral therapy nucleot(s)ide analogues (NUCs).* Liver Int, 2017. **37 Suppl 1**: p. 45-51.
31. Papatheodoridis, G., et al., *Discontinuation of oral antivirals in chronic hepatitis B: A systematic review.* Hepatology, 2016. **63**(5): p. 1481-92.

32. Buster, E.H., et al., *Sustained HBeAg and HBsAg loss after long-term follow-up of HBeAg-positive patients treated with peginterferon alpha-2b.* Gastroenterology, 2008. **135**(2): p. 459-67.
33. Liu, F., et al., *Alpha-interferon suppresses hepadnavirus transcription by altering epigenetic modification of cccDNA minichromosomes.* PLoS Pathog, 2013. **9**(9): p. e1003613.
34. Allweiss, L., et al., *Immune cell responses are not required to induce substantial hepatitis B virus antigen decline during pegylated interferon-alpha administration.* J Hepatol, 2014. **60**(3): p. 500-7.
35. Bertoletti, A. and C. Ferrari, *Innate and adaptive immune responses in chronic hepatitis B virus infections: towards restoration of immune control of viral infection.* Gut, 2012. **61**(12): p. 1754-64.
36. Bertoletti, A., A.T. Tan, and S. Koh, *T-cell therapy for chronic viral hepatitis.* Cytotherapy, 2017. **19**(11): p. 1317-1324.
37. Lobaina, Y. and M.L. Michel, *Chronic hepatitis B: Immunological profile and current therapeutic vaccines in clinical trials.* Vaccine, 2017. **35**(18): p. 2308-2314.
38. Block, T.M., et al., *Chronic hepatitis B: what should be the goal for new therapies?* Antiviral Res, 2013. **98**(1): p. 27-34.
39. Lin, C.L., H.C. Yang, and J.H. Kao, *Hepatitis B virus: new therapeutic perspectives.* Liver Int, 2016. **36 Suppl 1**: p. 85-92.
40. Gehring, A.J., *New treatments to reach functional cure: Rationale and challenges for emerging immune-based therapies.* Best Pract Res Clin Gastroenterol, 2017. **31**(3): p. 337-345.
41. European Association for the Study of the Liver. Electronic address, e.e.e. and L. European Association for the Study of the, *EASL 2017 Clinical Practice Guidelines on the management of hepatitis B virus infection.* J Hepatol, 2017. **67**(2): p. 370-398.
42. Kennedy, P.T.F., et al., *Preserved T-cell function in children and young adults with immune-tolerant chronic hepatitis B.* Gastroenterology, 2012. **143**(3): p. 637-645.
43. Dawood, A., et al., *Drugs in Development for Hepatitis B.* Drugs, 2017. **77**(12): p. 1263-1280.
44. Couillin, I., et al., *Specific vaccine therapy in chronic hepatitis B: induction of T cell proliferative responses specific for envelope antigens.* J Infect Dis, 1999. **180**(1): p. 15-26.
45. Dahmen, A., et al., *Clinical and immunological efficacy of intradermal vaccine plus lamivudine with or without interleukin-2 in patients with chronic hepatitis B.* J Med Virol, 2002. **66**(4): p. 452-60.

46. Dikici, B., et al., *Failure of therapeutic vaccination using hepatitis B surface antigen vaccine in the immunotolerant phase of children with chronic hepatitis B infection.* Journal of Gastroenterology and Hepatology, 2003. **18**(2): p. 218-222.

47. Horiike, N., et al., *In vivo immunization by vaccine therapy following virus suppression by lamivudine: a novel approach for treating patients with chronic hepatitis B.* J Clin Virol, 2005. **32**(2): p. 156-61.

48. Pol, S., et al., *Efficacy and limitations of a specific immunotherapy in chronic hepatitis B.* J Hepatol, 2001. **34**(6): p. 917-21.

49. Hoa, P.T., et al., *Randomized controlled study investigating viral suppression and serological response following pre-S1/pre-S2/S vaccine therapy combined with lamivudine treatment in HBeAg-positive patients with chronic hepatitis B.* Antimicrob Agents Chemother, 2009. **53**(12): p. 5134-40.

50. Jung, M.C., et al., *Immunological monitoring during therapeutic vaccination as a prerequisite for the design of new effective therapies: induction of a vaccine-specific CD4+ T-cell proliferative response in chronic hepatitis B carriers.* Vaccine, 2002. **20**(29-30): p. 3598-612.

51. Plotkin, S.A. and W. Schaffner, *A hepatitis B vaccine with a novel adjuvant.* Vaccine, 2013. **31**(46): p. 5297-9.

52. Spellman, M. and J. Martin, *Treatment of chronic hepatitis B infection with DV-601, a therapeutic vaccine.* Journal of Hepatology, 2011. **54**((Suppl. 1)): p. S209–361.

53. Vandepapeliere, P., et al., *Therapeutic vaccination of chronic hepatitis B patients with virus suppression by antiviral therapy: a randomized, controlled study of co-administration of HBsAg/AS02 candidate vaccine and lamivudine.* Vaccine, 2007. **25**(51): p. 8585-97.

54. Akbar, S.M., et al., *A phase III clinical trial with a therapeutic vaccine containing both HBsAg and HBcAg administered via both mucosal and parenteral routes in patients with chronic hepatitis B.* Hepatology, 2013. **58**(S1): p. 647A–705A.

55. Xu, D.Z., et al., *Results of a phase III clinical trial with an HBsAg-HBIG immunogenic complex therapeutic vaccine for chronic hepatitis B patients: experiences and findings.* J Hepatol, 2013. **59**(3): p. 450-6.

56. Heathcote, J., et al., *A pilot study of the CY-1899 T-cell vaccine in subjects chronically infected with hepatitis B virus. The CY1899 T Cell Vaccine Study Group.* Hepatology, 1999. **30**(2): p. 531-6.

57. Mancini-Bourgine, M., et al., *Immunogenicity of a hepatitis B DNA vaccine administered to chronic HBV carriers.* Vaccine, 2006. **24**(21): p. 4482-9.

58. Mancini-Bourgine, M., et al., *Induction or expansion of T-cell responses by a hepatitis B DNA vaccine administered to chronic HBV carriers.* Hepatology, 2004. **40**(4): p. 874-82.

59. Yang, S.H., et al., *Correlation of antiviral T-cell responses with suppression of viral rebound in chronic hepatitis B carriers: a proof-of-concept study.* Gene Ther, 2006. **13**(14): p. 1110-7.

60. Xu, D.Z., et al., *A randomized controlled phase IIb trial of antigen-antibody immunogenic complex therapeutic vaccine in chronic hepatitis B patients.* PLoS One, 2008. **3**(7): p. e2565.

61. Luo, J., et al., *Autologus dendritic cell vaccine for chronic hepatitis B carriers: a pilot, open label, clinical trial in human volunteers.* Vaccine, 2010. **28**(13): p. 2497-504.

62. Cavenaugh, J.S., et al., *Partially randomized, non-blinded trial of DNA and MVA therapeutic vaccines based on hepatitis B virus surface protein for chronic HBV infection.* PLoS One, 2011. **6**(2): p. e14626.

63. Yang, F.Q., et al., *A pilot randomized controlled trial of dual-plasmid HBV DNA vaccine mediated by in vivo electroporation in chronic hepatitis B patients under lamivudine chemotherapy.* J Viral Hepat, 2012. **19**(8): p. 581-93.

64. Obeng-Adjei, N., et al., *Synthetic DNA immunogen encoding hepatitis B core antigen drives immune response in liver.* Cancer Gene Ther, 2012. **19**(11): p. 779-87.

65. Inovio. *Inovio's Product Pipeline*. 2015 [cited 2018 14.01.2018]; Available from: https://www.inovio.com/product-pipeline.

66. Aguilar, J.C., et al., *Development of a nasal vaccine for chronic hepatitis B infection that uses the ability of hepatitis B core antigen to stimulate a strong Th1 response against hepatitis B surface antigen.* Immunol Cell Biol, 2004. **82**(5): p. 539-46.

67. Al-Mahtab, M., et al., *Therapeutic potential of a combined hepatitis B virus surface and core antigen vaccine in patients with chronic hepatitis B.* Hepatol Int, 2013. **7**(4): p. 981-9.

68. Betancourt, A.A., et al., *Phase I clinical trial in healthy adults of a nasal vaccine candidate containing recombinant hepatitis B surface and core antigens.* Int J Infect Dis, 2007. **11**(5): p. 394-401.

69. King, T.H., et al., *A whole recombinant yeast-based therapeutic vaccine elicits HBV X, S and Core specific T cells in mice and activates human T cells recognizing epitopes linked to viral clearance.* PLoS One, 2014. **9**(7): p. e101904.

70. Gaggar, A., et al., *Safety, tolerability and immunogenicity of GS-4774, a hepatitis B virus-specific therapeutic vaccine, in healthy subjects: a randomized study.* Vaccine, 2014. **32**(39): p. 4925-31.

71. Lok, A.S., et al., *Randomized phase II study of GS-4774 as a therapeutic vaccine in virally suppressed patients with chronic hepatitis B.* J Hepatol, 2016. **65**(3): p. 509-16.
72. Fontaine, H., et al., *Anti-HBV DNA vaccination does not prevent relapse after discontinuation of analogues in the treatment of chronic hepatitis B: a randomised trial--ANRS HB02 VAC-ADN.* Gut, 2015. **64**(1): p. 139-47.
73. Yoon, S.K., et al., *Safety and immunogenicity of therapeutic DNA vaccine with antiviral drug in chronic HBV patients and its immunogenicity in mice.* Liver Int, 2015. **35**(3): p. 805-15.
74. altimmune. *HepTcell...* 2018 [cited 2018 14.01.2018]; Available from: http://www.vaxin.com/HepTcell.html.
75. Desmet, C.J. and K.J. Ishii, *Nucleic acid sensing at the interface between innate and adaptive immunity in vaccination.* Nat Rev Immunol, 2012. **12**(7): p. 479-91.
76. Netea, M.G., et al., *Innate immune memory: a paradigm shift in understanding host defense.* Nat Immunol, 2015. **16**(7): p. 675-9.
77. van Montfoort, N., E. van der Aa, and A.M. Woltman, *Understanding MHC class I presentation of viral antigens by human dendritic cells as a basis for rational design of therapeutic vaccines.* Front Immunol, 2014. **5**: p. 182.
78. McNeela, E.A. and K.H. Mills, *Manipulating the immune system: humoral versus cell-mediated immunity.* Adv Drug Deliv Rev, 2001. **51**(1-3): p. 43-54.
79. Kara, E.E., et al., *Tailored immune responses: novel effector helper T cell subsets in protective immunity.* PLoS Pathog, 2014. **10**(2): p. e1003905.
80. Raphael, I., et al., *T cell subsets and their signature cytokines in autoimmune and inflammatory diseases.* Cytokine, 2015. **74**(1): p. 5-17.
81. Lambert, P.H., M. Liu, and C.A. Siegrist, *Can successful vaccines teach us how to induce efficient protective immune responses?* Nat Med, 2005. **11**(4 Suppl): p. S54-62.
82. Veldhoen, M., *Interleukin 17 is a chief orchestrator of immunity.* Nat Immunol, 2017. **18**(6): p. 612-621.
83. Fehres, C.M., et al., *Understanding the biology of antigen cross-presentation for the design of vaccines against cancer.* Front Immunol, 2014. **5**: p. 149.
84. Moyle, P.M. and I. Toth, *Modern subunit vaccines: development, components, and research opportunities.* ChemMedChem, 2013. **8**(3): p. 360-76.
85. Cordeiro, A.S., M.J. Alonso, and M. de la Fuente, *Nanoengineering of vaccines using natural polysaccharides.* Biotechnol Adv, 2015. **33**(6 Pt 3): p. 1279-93.
86. Reed, S.G., et al., *New horizons in adjuvants for vaccine development.* Trends Immunol, 2009. **30**(1): p. 23-32.

87. Khan, K.H., *DNA vaccines: roles against diseases.* Germs, 2013. **3**(1): p. 26-35.

88. Hasson, S.S.A.A., J.K.Z. Al-Busaidi, and T.A. Sallam, *The past, current and future trends in DNA vaccine immunisations.* Asian Pacific Journal of Tropical Biomedicine, 2015. **5**(5): p. 344-353.

89. Saade, F. and N. Petrovsky, *Technologies for enhanced efficacy of DNA vaccines.* Expert Rev Vaccines, 2012. **11**(2): p. 189-209.

90. Bonam, S.R., et al., *An Overview of Novel Adjuvants Designed for Improving Vaccine Efficacy.* Trends Pharmacol Sci, 2017. **38**(9): p. 771-793.

91. Ingolotti, M., et al., *DNA vaccines for targeting bacterial infections.* Expert Rev Vaccines, 2010. **9**(7): p. 747-63.

92. Hardee, C.L., et al., *Advances in Non-Viral DNA Vectors for Gene Therapy.* Genes (Basel), 2017. **8**(2).

93. Cova, L., *Present and future DNA vaccines for chronic hepatitis B treatment.* Expert Opin Biol Ther, 2017. **17**(2): p. 185-195.

94. Zhang, M., et al., *Polymers for DNA Vaccine Delivery.* ACS Biomater Sci Eng, 2017. **3**(2): p. 108-125.

95. Yin, H., et al., *Non-viral vectors for gene-based therapy.* Nat Rev Genet, 2014. **15**(8): p. 541-55.

96. Gao, Y., et al., *Highly Branched Poly(beta-amino esters) for Non-Viral Gene Delivery: High Transfection Efficiency and Low Toxicity Achieved by Increasing Molecular Weight.* Biomacromolecules, 2016. **17**(11): p. 3640-3647.

97. Agarwal, S., et al., *PDMAEMA based gene delivery materials.* Materials Today, 2012. **15**(9): p. Materials Today.

98. Andorko, J.I., et al., *Intrinsic immunogenicity of rapidly-degradable polymers evolves during degradation.* Acta Biomater, 2016. **32**: p. 24-34.

99. Bos, G.W., et al., *Cationic polymers that enhance the performance of HbsAg DNA in vivo.* Vaccine, 2004. **23**(4): p. 460-9.

100. Qu, C., et al., *Monocyte-derived dendritic cells: targets as potent antigen-presenting cells for the design of vaccines against infectious diseases.* Int J Infect Dis, 2014. **19**: p. 1-5.

101. Ramon, G., *Sur l'augmentation anormale de l'antitoxine chez les chevaux producteurs de sérum antidiphtérique*

Bull Soc Centr Med Vet, 1925. **101**: p. 227-234.

102. Lee, S. and M.T. Nguyen, *Recent advances of vaccine adjuvants for infectious diseases.* Immune Netw, 2015. **15**(2): p. 51-7.

103. Li, P. and F. Wang, *Polysaccharides: Candidates of promising vaccine adjuvants.* Drug Discov Ther, 2015. **9**(2): p. 88-93.
104. Glenny, A.T., et al., *The antigenic value of toxoid precipitated by potassium-alum.* J. Pathol. Bacteriol., 1926. **29**: p. 38–4510.
105. Powell, B.S., A.K. Andrianov, and P.C. Fusco, *Polyionic vaccine adjuvants: another look at aluminum salts and polyelectrolytes.* Clin Exp Vaccine Res, 2015. **4**(1): p. 23-45.
106. Mohsen, M.O., et al., *Major findings and recent advances in virus-like particle (VLP)-based vaccines.* Semin Immunol, 2017. **34**: p. 123-132.
107. Cabral, G.A., et al., *Cellular and humoral immunity in guinea pigs to two major polypeptides derived from hepatitis B surface antigen.* J Gen Virol, 1978. **38**(2): p. 339-50.
108. Lebre, F., C.H. Hearnden, and E.C. Lavelle, *Modulation of Immune Responses by Particulate Materials.* Adv Mater, 2016. **28**(27): p. 5525-41.
109. Gutjahr, A., et al., *Biodegradable Polymeric Nanoparticles-Based Vaccine Adjuvants for Lymph Nodes Targeting.* Vaccines (Basel), 2016. **4**(4).
110. Sahdev, P., L.J. Ochyl, and J.J. Moon, *Biomaterials for nanoparticle vaccine delivery systems.* Pharm Res, 2014. **31**(10): p. 2563-82.
111. Mutwiri, G., et al., *Combination adjuvants: the next generation of adjuvants?* Expert Rev Vaccines, 2011. **10**(1): p. 95-107.
112. Didierlaurent, A.M., et al., *AS04, an aluminum salt- and TLR4 agonist-based adjuvant system, induces a transient localized innate immune response leading to enhanced adaptive immunity.* J Immunol, 2009. **183**(10): p. 6186-97.
113. Ilyinskii, P.O., et al., *Adjuvant-carrying synthetic vaccine particles augment the immune response to encapsulated antigen and exhibit strong local immune activation without inducing systemic cytokine release.* Vaccine, 2014. **32**(24): p. 2882-95.
114. Dalod, M., et al., *Dendritic cell maturation: functional specialization through signaling specificity and transcriptional programming.* Embo j, 2014. **33**(10): p. 1104-16.
115. Janeway, C.A., Jr., *How the immune system works to protect the host from infection: a personal view.* Proc Natl Acad Sci U S A, 2001. **98**(13): p. 7461-8.
116. Neutra, M.R. and P.A. Kozlowski, *Mucosal vaccines: the promise and the challenge.* Nat Rev Immunol, 2006. **6**(2): p. 148-58.
117. Bekiaris, V., E.K. Persson, and W.W. Agace, *Intestinal dendritic cells in the regulation of mucosal immunity.* Immunol Rev, 2014. **260**(1): p. 86-101.
118. Lamichhane, A., T. Azegami, and H. Kiyono, *The mucosal immune system for vaccine development.* Vaccine, 2014. **32**(49): p. 6711-6723.

119. Holmgren, J. and C. Czerkinsky, *Mucosal immunity and vaccines.* Nat Med, 2005. **11**(4 Suppl): p. S45-53.
120. Tokuhara, D., et al., *Secretory IgA-mediated protection against V. cholerae and heat-labile enterotoxin-producing enterotoxigenic Escherichia coli by rice-based vaccine.* Proc Natl Acad Sci U S A, 2010. **107**(19): p. 8794-9.
121. Azizi, A., et al., *Enhancing oral vaccine potency by targeting intestinal M cells.* PLoS Pathog, 2010. **6**(11): p. e1001147.
122. Czerkinsky, C. and J. Holmgren, *Mucosal Delivery Routes for Optimal Immunization: Targeting Immunity to the Right Tissues.* Mucosal Vaccines: Modern Concepts, Strategies, and Challenges, 2012. **354**: p. 1-18.
123. Shima, H., et al., *A novel mucosal vaccine targeting Peyer's patch M cells induces protective antigen-specific IgA responses.* Int Immunol, 2014. **26**(11): p. 619-25.
124. Giudice, E.L. and J.D. Campbell, *Needle-free vaccine delivery.* Adv Drug Deliv Rev, 2006. **58**(1): p. 68-89.
125. De Smet, R., L. Allais, and C.A. Cuvelier, *Recent advances in oral vaccine development: yeast-derived beta-glucan particles.* Hum Vaccin Immunother, 2014. **10**(5): p. 1309-18.
126. Kim, S.H. and Y.S. Jang, *The development of mucosal vaccines for both mucosal and systemic immune induction and the roles played by adjuvants.* Clin Exp Vaccine Res, 2017. **6**(1): p. 15-21.
127. Fievez, V., et al., *Targeting nanoparticles to M cells with non-peptidic ligands for oral vaccination.* Eur J Pharm Biopharm, 2009. **73**(1): p. 16-24.
128. Kim, S.H., K.Y. Lee, and Y.S. Jang, *Mucosal Immune System and M Cell-targeting Strategies for Oral Mucosal Vaccination.* Immune Netw, 2012. **12**(5): p. 165-75.
129. Bonnardel, J., et al., *Innate and adaptive immune functions of peyer's patch monocyte-derived cells.* Cell Rep, 2015. **11**(5): p. 770-84.
130. McGhee, J.R. and K. Fujihashi, *Inside the mucosal immune system.* PLoS Biol, 2012. **10**(9): p. e1001397.
131. Kim, S.H. and Y.S. Jang, *Antigen targeting to M cells for enhancing the efficacy of mucosal vaccines.* Exp Mol Med, 2014. **46**: p. e85.
132. Jung, C., J.P. Hugot, and F. Barreau, *Peyer's Patches: The Immune Sensors of the Intestine.* Int J Inflam, 2010. **2010**: p. 823710.
133. Montilla, N.A., et al., *Mucosal immune system: A brief review* Inmunología, 2004. **23**(2): p. 9.
134. Lycke, N.Y. and M. Bemark, *The role of Peyer's patches in synchronizing gut IgA responses.* Front Immunol, 2012. **3**: p. 329.

135. Mabbott, N.A., et al., *Microfold (M) cells: important immunosurveillance posts in the intestinal epithelium.* Mucosal Immunol, 2013. **6**(4): p. 666-77.

136. Wang, M., et al., *Roles of M cells in infection and mucosal vaccines.* Hum Vaccin Immunother, 2014. **10**(12): p. 3544-51.

137. Ohno, H., *Intestinal M cells.* J Biochem, 2016. **159**(2): p. 151-60.

138. Corthésy, B., *Multi-Faceted Functions of Secretory IgA at Mucosal Surfaces.* Frontiers in Immunology, 2013. **4**: p. 185.

139. Hooper, L.V. and A.J. Macpherson, *Immune adaptations that maintain homeostasis with the intestinal microbiota.* Nat Rev Immunol, 2010. **10**(3): p. 159-69.

140. Soares, E. and O. Borges, *Oral vaccination through Peyer's Patches: update on particle uptake.* Curr Drug Deliv, 2017.

141. Lycke, N., *Recent progress in mucosal vaccine development: potential and limitations.* Nat Rev Immunol, 2012. **12**(8): p. 592-605.

142. Rice-Ficht, A.C., et al., *Polymeric particles in vaccine delivery.* Curr Opin Microbiol, 2010. **13**(1): p. 106-12.

143. Kaur, M., et al., *Development and characterization of guar gum nanoparticles for oral immunization against tuberculosis.* Drug Deliv, 2014.

144. Lee, W.J., et al., *Efficacy of thiolated eudragit microspheres as an oral vaccine delivery system to induce mucosal immunity against enterotoxigenic Escherichia coli in mice.* Eur J Pharm Biopharm, 2012. **81**(1): p. 43-8.

145. Borges, O., et al., *Evaluation of the immune response following a short oral vaccination schedule with hepatitis B antigen encapsulated into alginate-coated chitosan nanoparticles.* Eur J Pharm Sci, 2007. **32**(4-5): p. 278-90.

146. Singh, B., et al., *Combinatorial Approach of Antigen Delivery Using M Cell-Homing Peptide and Mucoadhesive Vehicle to Enhance the Efficacy of Oral Vaccine.* Mol Pharm, 2015. **12**(11): p. 3816-28.

147. Primard, C., et al., *Traffic of poly(lactic acid) nanoparticulate vaccine vehicle from intestinal mucus to sub-epithelial immune competent cells.* Biomaterials, 2010. **31**(23): p. 6060-8.

148. Borges, O., et al., *Uptake studies in rat Peyer's patches, cytotoxicity and release studies of alginate coated chitosan nanoparticles for mucosal vaccination.* J Control Release, 2006. **114**(3): p. 348-58.

149. Garinot, M., et al., *PEGylated PLGA-based nanoparticles targeting M cells for oral vaccination.* J Control Release, 2007. **120**(3): p. 195-204.

150. Shakweh, M., et al., *Poly (lactide-co-glycolide) particles of different physicochemical properties and their uptake by peyer's patches in mice.* Eur J Pharm Biopharm, 2005. **61**(1-2): p. 1-13.

151. van der Lubben, I.M., et al., *Chitosan microparticles for oral vaccination: preparation, characterization and preliminary in vivo uptake studies in murine Peyer's patches.* Biomaterials, 2001. **22**(7): p. 687-94.

152. Joshi, G., A. Kumar, and K. Sawant, *Enhanced bioavailability and intestinal uptake of Gemcitabine HCl loaded PLGA nanoparticles after oral delivery.* Eur J Pharm Sci, 2014. **60**: p. 80-9.

153. McNeela, E.A. and E.C. Lavelle, *Recent advances in microparticle and nanoparticle delivery vehicles for mucosal vaccination.* Curr Top Microbiol Immunol, 2012. **354**: p. 75-99.

154. Shakya, A. and K. Nandakumar, *Polymers as immunological adjuvants: An update on recent developments.* J. BioSci. Biotech. , 2012. **1**(3): p. 199-210.

155. Mottram, P.L., et al., *Type 1 and 2 immunity following vaccination is influenced by nanoparticle size: formulation of a model vaccine for respiratory syncytial virus.* Mol Pharm, 2007. **4**(1): p. 73-84.

156. Shah, R.R., et al., *The impact of size on particulate vaccine adjuvants.* Nanomedicine (Lond), 2014. **9**(17): p. 2671-81.

157. Oyewumi, M.O., A. Kumar, and Z. Cui, *Nano-microparticles as immune adjuvants: correlating particle sizes and the resultant immune responses.* Expert Rev Vaccines, 2010. **9**(9): p. 1095-107.

158. Koppolu, B. and D.A. Zaharoff, *The effect of antigen encapsulation in chitosan particles on uptake, activation and presentation by antigen presenting cells.* Biomaterials, 2013. **34**(9): p. 2359-69.

159. Shima, F., T. Akagi, and M. Akashi, *Effect of Hydrophobic Side Chains in the Induction of Immune Responses by Nanoparticle Adjuvants Consisting of Amphiphilic Poly(gamma-glutamic acid).* Bioconjug Chem, 2015. **26**(5): p. 890-8.

160. Ulery, B.D., et al., *Rational design of pathogen-mimicking amphiphilic materials as nanoadjuvants.* Sci Rep, 2011. **1**: p. 198.

161. Petersen, L.K., et al., *Activation of innate immune responses in a pathogen-mimicking manner by amphiphilic polyanhydride nanoparticle adjuvants.* Biomaterials, 2011. **32**(28): p. 6815-22.

162. Fromen, C.A., et al., *Controlled analysis of nanoparticle charge on mucosal and systemic antibody responses following pulmonary immunization.* Proc Natl Acad Sci U S A, 2015. **112**(2): p. 488-93.

163. Lebre, F., C.H. Hearnden, and E.C. Lavelle, *Modulation of Immune Responses by Particulate Materials.* Adv Mater, 2016.

164. Levitz, S.M., et al., *Exploiting fungal cell wall components in vaccines.* Semin Immunopathol, 2015. **37**(2): p. 199-207.

165. Vilar, G., J. Tulla-Puche, and F. Albericio, *Polymers and drug delivery systems.* Curr Drug Deliv, 2012. **9**(4): p. 367-94.

166. Migalovich-Sheikhet, H., et al., *Novel identified receptors on mast cells.* Front Immunol, 2012. **3**: p. 238.

167. Bueter, C.L., C.A. Specht, and S.M. Levitz, *Innate sensing of chitin and chitosan.* PLoS Pathog, 2013. **9**(1): p. e1003080.

168. Vasiliev, Y.M., *Chitosan-based vaccine adjuvants: incomplete characterization complicates preclinical and clinical evaluation.* Expert Rev Vaccines, 2015. **14**(1): p. 37-53.

169. Periayah, M.H., A.S. Halim, and A.Z. Saad, *Chitosan: A Promising Marine Polysaccharide for Biomedical Research.* Pharmacogn Rev, 2016. **10**(19): p. 39-42.

170. Bernkop-Schnurch, A. and S. Dunnhaupt, *Chitosan-based drug delivery systems.* Eur J Pharm Biopharm, 2012. **81**(3): p. 463-9.

171. Jabbal-Gill, I., P. Watts, and A. Smith, *Chitosan-based delivery systems for mucosal vaccines.* Expert Opin Drug Deliv, 2012. **9**(9): p. 1051-67.

172. Artursson, P., et al., *Effect of chitosan on the permeability of monolayers of intestinal epithelial cells (Caco-2).* Pharm Res, 1994. **11**(9): p. 1358-61.

173. Sonaje, K., et al., *Opening of epithelial tight junctions and enhancement of paracellular permeation by chitosan: microscopic, ultrastructural, and computed-tomographic observations.* Mol Pharm, 2012. **9**(5): p. 1271-9.

174. Xia, Y., et al., *Chitosan-based mucosal adjuvants: Sunrise on the ocean.* Vaccine, 2015. **33**(44): p. 5997-6010.

175. Wang, S., et al., *Intranasal and oral vaccination with protein-based antigens: advantages, challenges and formulation strategies.* Protein Cell, 2015. **6**(7): p. 480-503.

176. Bucarey, S.A., et al., *Chitosan microparticles loaded with yeast-derived PCV2 virus-like particles elicit antigen-specific cellular immune response in mice after oral administration.* Virol J, 2014. **11**: p. 149.

177. Garcia-Fuentes, M. and M.J. Alonso, *Chitosan-based drug nanocarriers: where do we stand?* J Control Release, 2012. **161**(2): p. 496-504.

178. Lebre, F., et al., *Progress towards a needle-free hepatitis B vaccine.* Pharm Res, 2011. **28**(5): p. 986-1012.

179. Picola, I.P.D., et al., *Effect of ionic strength solution on the stability of chitosan–DNA nanoparticles.* Journal of Experimental Nanoscience, 2012. **8**(5): p. 703-716.
180. Amaduzzi, F., et al., *Chitosan-DNA complexes: charge inversion and DNA condensation.* Colloids Surf B Biointerfaces, 2014. **114**: p. 1-10.
181. Azuma, K., et al., *Anticancer and anti-inflammatory properties of chitin and chitosan oligosaccharides.* J Funct Biomater, 2015. **6**(1): p. 33-49.
182. Kerch, G., *The potential of chitosan and its derivatives in prevention and treatment of age-related diseases.* Mar Drugs, 2015. **13**(4): p. 2158-82.
183. Calvo, P., et al., *Chitosan and chitosan/ethylene oxide-propylene oxide block copolymer nanoparticles as novel carriers for proteins and vaccines.* Pharm Res, 1997. **14**(10): p. 1431-6.
184. Borges, O., et al., *Induction of lymphocytes activated marker CD69 following exposure to chitosan and alginate biopolymers.* Int J Pharm, 2007. **337**(1-2): p. 254-64.
185. Bakhru, S.H., et al., *Oral delivery of proteins by biodegradable nanoparticles.* Adv Drug Deliv Rev, 2013. **65**(6): p. 811-21.
186. Neumann, S., et al., *Activation of the NLRP3 inflammasome is not a feature of all particulate vaccine adjuvants.* Immunol Cell Biol, 2014. **92**(6): p. 535-42.
187. Carroll, E.C., et al., *The Vaccine Adjuvant Chitosan Promotes Cellular Immunity via DNA Sensor cGAS-STING-Dependent Induction of Type I Interferons.* Immunity, 2016. **44**(3): p. 597-608.
188. Borges, O., et al., *Alginate coated chitosan nanoparticles are an effective subcutaneous adjuvant for hepatitis B surface antigen.* Int Immunopharmacol, 2008. **8**(13-14): p. 1773-80.
189. Lebre, F., et al., *Association of chitosan and aluminium as a new adjuvant strategy for improved vaccination.* Int J Pharm, 2017. **527**(1-2): p. 103-114.
190. Tafaghodi, M., et al., *Hepatitis B surface antigen nanoparticles coated with chitosan and trimethyl chitosan: Impact of formulation on physicochemical and immunological characteristics.* Vaccine, 2012. **30**(36): p. 5341-8.
191. Lugade, A.A., et al., *Single low-dose un-adjuvanted HBsAg nanoparticle vaccine elicits robust, durable immunity.* Nanomedicine, 2013. **9**(7): p. 923-34.
192. Premaletha, K., et al., *Formulation, characterization and optimization of hepatitis B surface antigen (HBsAg)-loaded chitosan microspheres for oral delivery.* Pharm Dev Technol, 2012. **17**(2): p. 251-8.

193. Verma, A.K., et al., *Vitamin B12 Grafted Layer-by-Layer Liposomes Bearing HBsAg Facilitate Oral Immunization: Effect of Modulated Biomechanical Properties.* Mol Pharm, 2016. **13**(7): p. 2531-42.

194. Huo, Z., et al., *Induction of protective serum meningococcal bactericidal and diphtheria-neutralizing antibodies and mucosal immunoglobulin A in volunteers by nasal insufflations of the Neisseria meningitidis serogroup C polysaccharide-CRM197 conjugate vaccine mixed with chitosan.* Infect Immun, 2005. **73**(12): p. 8256-65.

195. Atmar, R.L., et al., *Norovirus vaccine against experimental human Norwalk Virus illness.* N Engl J Med, 2011. **365**(23): p. 2178-87.

196. Neimert-Andersson, T., et al., *Evaluation of safety and efficacy as an adjuvant for the chitosan-based vaccine delivery vehicle ViscoGel in a single-blind randomised Phase I/IIa clinical trial.* Vaccine, 2014. **32**(45): p. 5967-74.

197. Goodridge, H.S., A.J. Wolf, and D.M. Underhill, *Beta-glucan recognition by the innate immune system.* Immunol Rev, 2009. **230**(1): p. 38-50.

198. Wang, Q., et al., *beta-Glucans: Relationships between Modification, Conformation and Functional Activities.* Molecules, 2017. **22**(2).

199. Sonck, E., et al., *Varying effects of different beta-glucans on the maturation of porcine monocyte-derived dendritic cells.* Clin Vaccine Immunol, 2011. **18**(9): p. 1441-6.

200. Zheng, X., et al., *Alginate-chitosan-PLGA composite microspheres enabling single-shot hepatitis B vaccination.* AAPS J, 2010. **12**(4): p. 519-24.

201. Pandit, S., et al., *Enhancement of immune response of HBsAg loaded poly (L-lactic acid) microspheres against hepatitis B through incorporation of alum and chitosan.* J Microencapsul, 2007. **24**(6): p. 539-52.

202. Jesus, S., et al., *Adjuvant Activity of Poly-epsilon-caprolactone/Chitosan Nanoparticles Characterized by Mast Cell Activation and IFN-gamma and IL-17 Production.* Mol Pharm, 2018. **15**(1): p. 72-82.

203. Chen, X., et al., *Enhanced humoral and cell-mediated immune responses generated by cationic polymer-coated PLA microspheres with adsorbed HBsAg.* Mol Pharm, 2014. **11**(6): p. 1772-84.

204. Sivakumar, S.M., et al., *Immunopotentiation of hepatitis B vaccine using biodegradable polymers as an adjuvant.* J Microbiol Immunol Infect, 2010. **43**(4): p. 265-70.

205. Wang, H., et al., *Single dose HBsAg CS-gamma-PGA nanogels induce potent protective immune responses against HBV infection.* Eur J Pharm Biopharm, 2017.

206. Prego, C., et al., *Chitosan-based nanoparticles for improving immunization against hepatitis B infection.* Vaccine, 2010. **28**(14): p. 2607-14.

207. Dai, X., et al., *Co-delivery of polyinosinic:polycytidylic acid and flagellin by poly(lactic-co-glycolic acid) MPs synergistically enhances immune response elicited by intranasally delivered hepatitis B surface antigen.* Int J Nanomedicine, 2017. **12**: p. 6617-6632.

208. Borges, O., et al., *Immune response by nasal delivery of hepatitis B surface antigen and codelivery of a CpG ODN in alginate coated chitosan nanoparticles.* Eur J Pharm Biopharm, 2008. **69**(2): p. 405-16.

209. Pawar, D., et al., *Evaluation of mucoadhesive PLGA microparticles for nasal immunization.* AAPS J, 2010. **12**(2): p. 130-7.

210. Jesus, S., et al., *Immune response elicited by an intranasally delivered HBsAg low-dose adsorbed to poly-epsilon-caprolactone based nanoparticles.* Int J Pharm, 2016. **504**(1-2): p. 59-69.

211. Li, Z., et al., *Surface-functionalized, pH-responsive poly(lactic-co-glycolic acid)-based microparticles for intranasal vaccine delivery: Effect of surface modification with chitosan and mannan.* Eur J Pharm Biopharm, 2016. **109**: p. 24-34.

212. Farhadian, A., N.M. Dounighi, and M. Avadi, *Enteric trimethyl chitosan nanoparticles containing hepatitis B surface antigen for oral delivery.* Hum Vaccin Immunother, 2015. **11**(12): p. 2811-8.

213. Pawar, D., et al., *Development and characterization of surface modified PLGA nanoparticles for nasal vaccine delivery: effect of mucoadhesive coating on antigen uptake and immune adjuvant activity.* Eur J Pharm Biopharm, 2013. **85**(3 Pt A): p. 550-9.

214. Subbiah, R., et al., *N,N,N-Trimethyl chitosan nanoparticles for controlled intranasal delivery of HBV surface antigen.* Carbohydr Polym, 2012. **89**(4): p. 1289-97.

215. Mangal, S., et al., *Pharmaceutical and immunological evaluation of mucoadhesive nanoparticles based delivery system(s) administered intranasally.* Vaccine, 2011. **29**(31): p. 4953-62.

216. Jesus, S., et al., *Poly--caprolactone/chitosan nanoparticles provide strong adjuvant effect for hepatitis B antigen.* Nanomedicine (Lond), 2017. **12**(19): p. 2335-2348.

217. Bhowmik, T., et al., *Oral delivery of microparticles containing plasmid DNA encoding hepatitis-B surface antigen.* J Drug Target, 2012. **20**(4): p. 364-71.

218. Khatri, K., et al., *Plasmid DNA loaded chitosan nanoparticles for nasal mucosal immunization against hepatitis B.* Int J Pharm, 2008. **354**(1-2): p. 235-41.

219. Dong, S.F., et al., *Specific immune response to HBsAg is enhanced by beta-glucan oligosaccharide containing an alpha-(1-->3)-linked bond and biased towards M2/Th2.* Int Immunopharmacol, 2007. **7**(6): p. 725-33.

220. Li, P., et al., *Effect and mechanisms of curdlan sulfate on inhibiting HBV infection and acting as an HB vaccine adjuvant.* Carbohydr Polym, 2014. **110**: p. 446-55.

221. Shan, J., et al., *An alpha-glucan isolated from root of Isatis Indigotica, its structure and adjuvant activity.* Glycoconj J, 2014. **31**(4): p. 317-26.

222. Devi, K.S., et al., *Heteroglucan-dendrimer glycoconjugate: a modulated construct with augmented immune responses and signaling phenomena.* Biochim Biophys Acta, 2014. **1840**(9): p. 2794-805.

223. Chan, G.C., W.K. Chan, and D.M. Sze, *The effects of beta-glucan on human immune and cancer cells.* J Hematol Oncol, 2009. **2**: p. 25.

224. Goodridge, H.S., et al., *Activation of the innate immune receptor Dectin-1 upon formation of a 'phagocytic synapse'.* Nature, 2011. **472**(7344): p. 471-5.

225. Lipinski, T., et al., *Enhanced immunogenicity of a tricomponent mannan tetanus toxoid conjugate vaccine targeted to dendritic cells via Dectin-1 by incorporating beta-glucan.* J Immunol, 2013. **190**(8): p. 4116-28.

226. Willment, J.A., et al., *The human beta-glucan receptor is widely expressed and functionally equivalent to murine Dectin-1 on primary cells.* Eur J Immunol, 2005. **35**(5): p. 1539-47.

227. Carter, R.W., et al., *Preferential induction of CD4+ T cell responses through in vivo targeting of antigen to dendritic cell-associated C-type lectin-1.* J Immunol, 2006. **177**(4): p. 2276-84.

228. Huang, H., et al., *Robust stimulation of humoral and cellular immune responses following vaccination with antigen-loaded beta-glucan particles.* MBio, 2010. **1**(3).

229. Huang, H., et al., *Characterization and optimization of the glucan particle-based vaccine platform.* Clin Vaccine Immunol, 2013. **20**(10): p. 1585-91.

230. Dube, A., et al., *Multimodal nanoparticles that provide immunomodulation and intracellular drug delivery for infectious diseases.* Nanomedicine, 2014. **10**(4): p. 831-8.

231. Tam, J.M., et al., *Use of fungal derived polysaccharide-conjugated particles to probe Dectin-1 responses in innate immunity.* Integr Biol (Camb), 2012. **4**(2): p. 220-7.

232. Elder, M.J., et al., *beta-Glucan Size Controls Dectin-1-Mediated Immune Responses in Human Dendritic Cells by Regulating IL-1beta Production.* Front Immunol, 2017. **8**: p. 791.

233. Wang, J., et al., *beta-Glucan oligosaccharide enhances CD8(+) T cells immune response induced by a DNA vaccine encoding hepatitis B virus core antigen.* J Biomed Biotechnol, 2010. **2010**: p. 645213.

234. Demir, M., et al., *The Effect of -Glucan on the Antibody Response to Hepatitis B Vaccination in Chronic Renal Failure Patients.* BANTAO Journal, 2007. **5**(1): p. 10-12.

235. Ruwei, W., et al. *IMMUNE-ASSIST™ RESEARCH SUMMARY - CLINICAL TRIAL REPORT ON TREATMENT OF CHRONIC HEPATITIS B USING IMMUNE-ASSIST™ BRAND DIETARY SUPPLEMENT AS ADJUNCT WITH LAMIVUDINE [EPIVIR™]*. 2002 [cited 2018 21.01.2018].
236. Hsu, C.H., et al., *The mushroom Agaricus blazei Murill extract normalizes liver function in patients with chronic hepatitis B.* J Altern Complement Med, 2008. **14**(3): p. 299-301.
237. He, M., et al., *Mushroom lectin overcomes hepatitis B virus tolerance via TLR6 signaling.* Sci Rep, 2017. **7**(1): p. 5814.
238. Yu, X., et al., *Oral administered particulate yeast-derived glucan promotes hepatitis B virus clearance in a hydrodynamic injection mouse model.* PLoS One, 2015. **10**(4): p. e0123559.
239. Ostroff, G.R., *A particulate delivery system comprising an extracted yeast cell wall comprising beta-glucan and a payload trapping molecule.* 2005: United States of America.
240. Aouadi, M., et al., *Orally delivered siRNA targeting macrophage Map4k4 suppresses systemic inflammation.* Nature, 2009. **458**(7242): p. 1180-4.
241. Huang, H., et al., *Relative contributions of dectin-1 and complement to immune responses to particulate beta-glucans.* J Immunol, 2012. **189**(1): p. 312-7.
242. Soto, E.R., et al., *Glucan particles for macrophage targeted delivery of nanoparticles.* J Drug Deliv, 2012. **2012**: p. 143524.
243. Soto, E.R. and G.R. Ostroff, *Characterization of multilayered nanoparticles encapsulated in yeast cell wall particles for DNA delivery.* Bioconjug Chem, 2008. **19**(4): p. 840-8.
244. Soto, E. and G.R. Ostroff, *Oral macrophage targeted gene delivery sytem* NSTI-Nanotech, 2007. **2**.
245. Li, B., et al., *Yeast glucan particles activate murine resident macrophages to secrete proinflammatory cytokines via MyD88- and Syk kinase-dependent pathways.* Clin Immunol, 2007. **124**(2): p. 170-81.
246. Soto, E.R., et al., *Targeted Delivery of Glucan Particle Encapsulated Gallium Nanoparticles Inhibits HIV Growth in Human Macrophages.* J Drug Deliv, 2016. **2016**: p. 8520629.
247. Yanase, N., et al., *OVA-bound nanoparticles induce OVA-specific IgG1, IgG2a, and IgG2b responses with low IgE synthesis.* Vaccine, 2014. **32**(45): p. 5918-24.
248. Specht, C.A., et al., *Protection against Experimental Cryptococcosis following Vaccination with Glucan Particles Containing Cryptococcus Alkaline Extracts.* MBio, 2015. **6**(6): p. e01905-15.
249. De Smet, R., et al., *beta-Glucan microparticles are good candidates for mucosal antigen delivery in oral vaccination.* J Control Release, 2013. **172**(3): p. 671-8.
250. Zhang, X., et al., *In situ self-assembly of peptides in glucan particles for macrophage-targeted oral delivery.* Journal of Materials Chemistry B, 2014. **2**: p. 5882-5890.

251. Hong, F., et al., *Mechanism by which orally administered beta-1,3-glucans enhance the tumoricidal activity of antitumor monoclonal antibodies in murine tumor models.* J Immunol, 2004. **173**(2): p. 797-806.
252. Specht, C.A., et al., *Protection against Experimental Cryptococcosis following Vaccination with Glucan Particles Containing Cryptococcus Alkaline Extracts.* Mbio, 2015. **6**(6).
253. Berner, V.K., et al., *Microparticulate beta-glucan vaccine conjugates phagocytized by dendritic cells activate both naive CD4 and CD8 T cells in vitro.* Cell Immunol, 2015. **298**(1-2): p. 104-14.
254. King, T.H., et al., *Construction and Immunogenicity Testing of Whole Recombinant Yeast-Based T-Cell Vaccines.* Methods Mol Biol, 2016. **1404**: p. 529-45.
255. WHO. *Hepatitis B Fact Sheet*. 2017 [cited 2017 03/07/2017]; Available from: http://www.who.int/mediacentre/factsheets/fs204/en/.
256. Kochhar, S., et al., *Introducing new vaccines in developing countries.* Expert Rev Vaccines, 2013. **12**(12): p. 1465-78.
257. Poonam, P., *The biology of oral tolerance and issues related to oral vaccine design.* Curr Pharm Des, 2007. **13**(19): p. 2001-7.
258. Gupta, P.N., et al., *M-cell targeted biodegradable PLGA nanoparticles for oral immunization against hepatitis B.* Journal of Drug Targeting, 2007. **15**(10): p. 701-713.
259. Mishra, N., et al., *Lectin anchored PLGA nanoparticles for oral mucosal immunization against hepatitis B.* Journal of Drug Targeting, 2011. **19**(1): p. 67-78.
260. Dinda, A.K., et al., *Novel nanocarrier for oral Hepatitis B vaccine.* Vaccine, 2016. **34**(27): p. 3076-81.
261. Soto, E. and G.R. Ostroff. *Oral Macrophage Mediated Gene Delivery System*. in *NSTI Nanotech 2007 Technical Proceedings*. 2007.
262. Taylor, P.R., et al., *The beta-glucan receptor, dectin-1, is predominantly expressed on the surface of cells of the monocyte/macrophage and neutrophil lineages.* J Immunol, 2002. **169**(7): p. 3876-82.
263. Tesz, G.J., et al., *Glucan particles for selective delivery of siRNA to phagocytic cells in mice.* Biochem J, 2011. **436**(2): p. 351-62.
264. Shah, A., et al., *beta-Glucan as an encapsulating agent: Effect on probiotic survival in simulated gastrointestinal tract.* Int J Biol Macromol, 2016. **82**: p. 217-22.
265. Baert, K., et al., *beta-glucan microparticles targeted to epithelial APN as oral antigen delivery system.* J Control Release, 2015. **220**(Pt A): p. 149-59.

266. Jesus, S., et al., *Adjuvant Activity of Poly-epsilon-caprolactone/Chitosan Nanoparticles Characterized by Mast Cell Activation and IFN-gamma and IL-17 Production.* Mol Pharm, 2017.

267. Lebre, F., et al., *Intranasal Administration of Novel Chitosan Nanoparticle/DNA Complexes Induces Antibody Response to Hepatitis B Surface Antigen in Mice.* Mol Pharm, 2016. **13**(2): p. 472-82.

268. Li, X.Y., et al., *Preparation of alginate coated chitosan microparticles for vaccine delivery.* Bmc Biotechnology, 2008. **8**.

269. Vollmer, J. and A.M. Krieg, *Immunotherapeutic applications of CpG oligodeoxynucleotide TLR9 agonists.* Adv Drug Deliv Rev, 2009. **61**(3): p. 195-204.

270. Bode, C., et al., *CpG DNA as a vaccine adjuvant.* Expert Rev Vaccines, 2011. **10**(4): p. 499-511.

271. Wernersson, S. and G. Pejler, *Mast cell secretory granules: armed for battle.* Nat Rev Immunol, 2014. **14**(7): p. 478-94.

272. Jesus, S., G. Borchard, and O. Borges, *Freeze Dried Chitosan/ Poly-ε-Caprolactone and Poly-ε-Caprolactone Nanoparticles: Evaluation of their Potential as DNA and Antigen Delivery Systems.* Journal of Genetic Syndromes & Gene Therapy, 2013.

273. Jesus, S., E. Soares, and O. Borges, *Poly-epsilon-caprolactone/Chitosan and Chitosan Particles: Two Recombinant Antigen Delivery Systems for Intranasal Vaccination.* Methods Mol Biol, 2016. **1404**: p. 697-713.

274. Huang, H., et al., *Distinct patterns of dendritic cell cytokine release stimulated by fungal beta-glucans and toll-like receptor agonists.* Infect Immun, 2009. **77**(5): p. 1774-81.

275. Staats, H.F., et al., *A Mast Cell Degranulation Screening Assay for the Identification of Novel Mast Cell Activating Agents.* Medchemcomm, 2013. **4**(1).

276. Urb, M. and D.C. Sheppard, *The role of mast cells in the defence against pathogens.* PLoS Pathog, 2012. **8**(4): p. e1002619.

277. McLachlan, J.B., et al., *Mast cell activators: a new class of highly effective vaccine adjuvants.* Nat Med, 2008. **14**(5): p. 536-41.

278. Bento, D., et al., *Development of a novel adjuvanted nasal vaccine: C48/80 associated with chitosan nanoparticles as a path to enhance mucosal immunity.* Eur J Pharm Biopharm, 2015. **93**: p. 149-64.

279. Farrugia, B.L., et al., *The localisation of inflammatory cells and expression of associated proteoglycans in response to implanted chitosan.* Biomaterials, 2014. **35**(5): p. 1462-77.

280. Voa, T.-S., et al., *Protective effect of chitosan oligosaccharides against FcεRI-mediated RBL-2H3 mast cell activation.* Process Biochemistry, 2012. **47**(2): p. 327-330.

281. Ferry, X., et al., *G protein-dependent activation of mast cell by peptides and basic secretagogues.* Peptides, 2002. **23**(8): p. 1507-15.

282. Chablani, L., S.A. Tawde, and M.J. D'Souza, *Spray-dried microparticles: a potential vehicle for oral delivery of vaccines.* J Microencapsul, 2012. **29**(4): p. 388-97.

283. Fujkuyama, Y., et al., *Novel vaccine development strategies for inducing mucosal immunity.* Expert Rev Vaccines, 2012. **11**(3): p. 367-79.

284. Hayden, C.A., et al., *Bioencapsulation of the hepatitis B surface antigen and its use as an effective oral immunogen.* Vaccine, 2012. **30**(19): p. 2937-2942.

285. Hayden, C.A., et al., *Supercritical fluid extraction provides an enhancement to the immune response for orally-delivered hepatitis B surface antigen.* Vaccine, 2014. **32**(11): p. 1240-1246.

286. Mahdavi, M., et al., *Oral administration of synthetic selenium nanoparticles induced robust Th1 cytokine pattern after HBs antigen vaccination in mouse model.* J Infect Public Health, 2016.

287. Hayden, C.A., et al., *Oral delivery of wafers made from HBsAg-expressing maize germ induces long-term immunological systemic and mucosal responses.* Vaccine, 2015. **33**(25): p. 2881-2886.

288. Wang, W. and M. Singh, *Selection of Adjuvants for Enhanced Vaccine Potency.* World Journal of Vaccines, 2011. **1**: p. 33-78.

289. Demoulins, T., P. Milona, and K.C. McCullough, *Alginate-coated chitosan nanogels differentially modulate class-A and class-B CpG-ODN targeting of dendritic cells and intracellular delivery.* Nanomedicine, 2014.

290. Tajiri, K. and Y. Shimizu, *Unsolved problems and future perspectives of hepatitis B virus vaccination.* World J Gastroenterol, 2015. **21**(23): p. 7074-83.

291. World Health Organization. *Hepatitis B Fact Sheet*. 2017 [cited 2017 23/08/2017]; Available from: http://www.who.int/mediacentre/factsheets/fs204/en/.

292. World Health Organization, *WHO Expert Committee on Biological Standardization*. 2013, WHO Technical Report Series.

293. Lynn, D.M. and R. Langer, *Degradable Poly(β-amino esters): Synthesis, Characterization, and Self-Assembly with Plasmid DNA.* Journal of american chemical society, 2000. **122**(44): p. 10761–10768.

294. Synatschke, C.V., et al., *Influence of polymer architecture and molecular weight of poly(2-(dimethylamino)ethyl methacrylate) polycations on transfection efficiency and cell viability in gene delivery.* Biomacromolecules, 2011. **12**(12): p. 4247-55.

295. Santo, D., et al., *Combination of PDMAEMA and PbetaAE results in a strong and synergistic transfection activity.* Biomacromolecules, 2017.
296. Ara, Y., et al., *Zymosan enhances the immune response to DNA vaccine for human immunodeficiency virus type-1 through the activation of complement system.* Immunology, 2001. **103**(1): p. 98-105.
297. Jones, C.H., et al., *Mannosylated poly(beta-amino esters) for targeted antigen presenting cell immune modulation.* Biomaterials, 2015. **37**: p. 333-44.
298. Cordeiro, R.A., et al., *High transfection efficiency promoted by tailor-made cationic tri-block copolymer-based nanoparticles.* Acta Biomater, 2017. **47**: p. 113-123.
299. Cox, D.J., *Particulate-soluble glucan preparation*. 2016, Google Patents.
300. Jesus, S., et al., *Poly--caprolactone/chitosan nanoparticles provide strong adjuvant effect for hepatitis B antigen.* Nanomedicine (Lond), 2017.
301. Zhao, L., et al., *Nanoparticle vaccines.* Vaccine, 2014. **32**(3): p. 327-37.
302. Shang, L., K. Nienhaus, and G.U. Nienhaus, *Engineered nanoparticles interacting with cells: size matters.* J Nanobiotechnology, 2014. **12**: p. 5.
303. Akagi, T., F. Shima, and M. Akashi, *Intracellular degradation and distribution of protein-encapsulated amphiphilic poly(amino acid) nanoparticles.* Biomaterials, 2011. **32**(21): p. 4959-67.
304. Soares, E., S. Jesus, and O. Borges, *Oral hepatitis B vaccine: chitosan or glucan based delivery systems for efficient HBsAg immunization following subcutaneous priming.* Int J Pharm, 2017. **535**(1-2): p. 261-271.
305. Stopinsek, S., et al., *Fungal cell wall agents suppress the innate inflammatory cytokine responses of human peripheral blood mononuclear cells challenged with lipopolysaccharide in vitro.* Int Immunopharmacol, 2011. **11**(8): p. 939-47.
306. Smith, D.M., J.K. Simon, and J.R. Baker, Jr., *Applications of nanotechnology for immunology.* Nat Rev Immunol, 2013. **13**(8): p. 592-605.
307. Anal, A.K., et al., *Preparation and characterization of nanoparticles formed by chitosan-caseinate interactions.* Colloids Surf B Biointerfaces, 2008. **64**(1): p. 104-10.
308. Elzoghby, A.O., W.S. El-Fotoh, and N.A. Elgindy, *Casein-based formulations as promising controlled release drug delivery systems.* J Control Release, 2011. **153**(3): p. 206-16.
309. Koppolu, B.P., et al., *Controlling chitosan-based encapsulation for protein and vaccine delivery.* Biomaterials, 2014. **35**(14): p. 4382-9.
310. Gustafson, H.H., et al., *Nanoparticle Uptake: The Phagocyte Problem.* Nano Today, 2015. **10**(4): p. 487-510.

311. Kanchan, V. and A.K. Panda, *Interactions of antigen-loaded polylactide particles with macrophages and their correlation with the immune response.* Biomaterials, 2007. **28**(35): p. 5344-57.

312. Soares, E., S. Jesus, and O. Borges, *Oral hepatitis B vaccine: chitosan or glucan based delivery systems for efficient HBsAg immunization following subcutaneous priming.* Int J Pharm, 2018. **535**(1-2): p. 261-271.

313. Vidarsson, G., G. Dekkers, and T. Rispens, *IgG subclasses and allotypes: from structure to effector functions.* Front Immunol, 2014. **5**: p. 520.

314. Roldao, A., et al., *Virus-like particles in vaccine development.* Expert Rev Vaccines, 2010. **9**(10): p. 1149-76.

315. Visciano, M.L., et al., *Effects of adjuvants on IgG subclasses elicited by virus-like particles.* J Transl Med, 2012. **10**: p. 4.

316. Zhu, C.C., et al., *Dectin-1 agonist curdlan modulates innate immunity to Aspergillus fumigatus in human corneal epithelial cells.* Int J Ophthalmol, 2015. **8**(4): p. 690-6.

317. Liu, J., et al., *Combined yeast-derived beta-glucan with anti-tumor monoclonal antibody for cancer immunotherapy.* Exp Mol Pathol, 2009. **86**(3): p. 208-14.

318. Yan, J., D.J. Allendorf, and B. Brandley, *Yeast whole glucan particle (WGP) beta-glucan in conjunction with antitumour monoclonal antibodies to treat cancer.* Expert Opin Biol Ther, 2005. **5**(5): p. 691-702.

319. Baert, K., et al., *Duality of beta-glucan microparticles: antigen carrier and immunostimulants.* Int J Nanomedicine, 2016. **11**: p. 2463-9.

320. Tipper, D.J. and E. Szomolanyi-Tsuda, *Scaffolded Antigens in Yeast Cell Particle Vaccines Provide Protection against Systemic Polyoma Virus Infection.* J Immunol Res, 2016. **2016**: p. 2743292.

321. Yang, Z., et al., *A novel antigen delivery system induces strong humoral and CTL immune responses.* Biomaterials, 2017. **134**: p. 51-63.

322. Clemons, K.V., et al., *Whole glucan particles as a vaccine against murine aspergillosis.* J Med Microbiol, 2014. **63**(Pt 12): p. 1750-9.

323. Bronte, V. and M.J. Pittet, *The spleen in local and systemic regulation of immunity.* Immunity, 2013. **39**(5): p. 806-18.

324. Hey, Y.Y., B. Quah, and H.C. O'Neill, *Antigen presenting capacity of murine splenic myeloid cells.* BMC Immunol, 2017. **18**(1): p. 4.

325. Frohlich, E., *The role of surface charge in cellular uptake and cytotoxicity of medical nanoparticles.* Int J Nanomedicine, 2012. **7**: p. 5577-91.

326. Cardone, M., et al., *Interleukin-1 and interferon-gamma orchestrate beta-glucan-activated human dendritic cell programming via IkappaB-zeta modulation.* PLoS One, 2014. **9**(12): p. e114516.

327. Qi, C., et al., *Differential pathways regulating innate and adaptive antitumor immune responses by particulate and soluble yeast-derived beta-glucans.* Blood, 2011. **117**(25): p. 6825-36.

328. Caires, H.R., et al., *Macrophage interactions with polylactic acid and chitosan scaffolds lead to improved recruitment of human mesenchymal stem/stromal cells: a comprehensive study with different immune cells.* J R Soc Interface, 2016. **13**(122).

329. Guzman-Morales, J., et al., *Biodegradable chitosan particles induce chemokine release and negligible arginase-1 activity compared to IL-4 in murine bone marrow-derived macrophages.* Biochem Biophys Res Commun, 2011. **405**(4): p. 538-44.

330. Dorner, B.G., et al., *MIP-1alpha, MIP-1beta, RANTES, and ATAC/lymphotactin function together with IFN-gamma as type 1 cytokines.* Proc Natl Acad Sci U S A, 2002. **99**(9): p. 6181-6.

331. Crawford, A., et al., *A role for the chemokine RANTES in regulating CD8 T cell responses during chronic viral infection.* PLoS Pathog, 2011. **7**(7): p. e1002098.

332. Farace, C., et al., *Immune cell impact of three differently coated lipid nanocapsules: pluronic, chitosan and polyethylene glycol.* Sci Rep, 2016. **6**: p. 18423.

333. Bueter, C.L., et al., *Spectrum and mechanisms of inflammasome activation by chitosan.* J Immunol, 2014. **192**(12): p. 5943-51.

334. Abel, G. and J.K. Czop, *Stimulation of human monocyte beta-glucan receptors by glucan particles induces production of TNF-alpha and IL-1 beta.* Int J Immunopharmacol, 1992. **14**(8): p. 1363-73.

335. Pattani, A., et al., *Immunological effects and membrane interactions of chitosan nanoparticles.* Mol Pharm, 2009. **6**(2): p. 345-52.

336. Duitman, E.H., Z. Orinska, and S. Bulfone-Paus, *Mechanisms of cytokine secretion: a portfolio of distinct pathways allows flexibility in cytokine activity.* Eur J Cell Biol, 2011. **90**(6-7): p. 476-83.

337. Oyler-Yaniv, A., et al., *A Tunable Diffusion-Consumption Mechanism of Cytokine Propagation Enables Plasticity in Cell-to-Cell Communication in the Immune System.* Immunity, 2017. **46**(4): p. 609-620.

338. Thomas, C., et al., *Aerosolized PLA and PLGA nanoparticles enhance humoral, mucosal and cytokine responses to hepatitis B vaccine.* Mol Pharm, 2011. **8**(2): p. 405-15.

339. Ghasemi, F., et al., *Current progress in the development of therapeutic vaccines for chronic hepatitis B virus infection.* Iran J Basic Med Sci, 2016. **19**(7): p. 692-704.

340. Yu, M., et al., *Specifically targeted delivery of protein to phagocytic macrophages.* Int J Nanomedicine, 2015. **10**: p. 1743-57.

341. Singh, P.K., et al., *1, 3beta-Glucan anchored, paclitaxel loaded chitosan nanocarrier endows enhanced hemocompatibility with efficient anti-glioblastoma stem cells therapy.* Carbohydr Polym, 2018. **180**: p. 365-375.

342. Yucel Falco, C., et al., *Design of a potentially prebiotic and responsive encapsulation material for probiotic bacteria based on chitosan and sulfated beta-glucan.* J Colloid Interface Sci, 2017. **487**: p. 97-106.

343. Przekora, A. and G. Ginalska, *Addition of 1,3-beta-D-glucan to chitosan-based composites enhances osteoblast adhesion, growth, and proliferation.* Int J Biol Macromol, 2014. **70**: p. 474-81.

344. Przekora, A. and G. Ginalska, *Chitosan/beta-1,3-glucan/hydroxyapatite bone scaffold enhances osteogenic differentiation through TNF-alpha-mediated mechanism.* Mater Sci Eng C Mater Biol Appl, 2017. **73**: p. 225-233.

345. Lucifora, J., et al., *Specific and nonhepatotoxic degradation of nuclear hepatitis B virus cccDNA.* Science, 2014. **343**(6176): p. 1221-8.

346. Kafrouni, M.I., G.R. Brown, and D.L. Thiele, *Virally infected hepatocytes are resistant to perforin-dependent CTL effector mechanisms.* J Immunol, 2001. **167**(3): p. 1566-74.

347. Kardani, K., A. Bolhassani, and S. Shahbazi, *Prime-boost vaccine strategy against viral infections: Mechanisms and benefits.* Vaccine, 2016. **34**(4): p. 413-423.